

LOUGHBOROUGH  
UNIVERSITY OF TECHNOLOGY  
LIBRARY

AUTHOR/FILING TITLE

RAYMOND, E A

ACCESSION/COPY NO

040015520

VOL NO.

CLASS MARK

ARCHIVES  
COPY

FOR REFERENCE ONLY

040015520 6





AN ASSESSMENT OF THE  
INFORMATION TRANSFER PROCESS  
FOR EMBOSSED HOLOGRAPHIC  
ELEMENTS

BY

ELIZABETH A RAYMOND

A Doctoral Thesis submitted  
in partial fulfilment of the  
requirements for the award of  
Doctor of Philosophy  
of the  
Loughborough University  
of Technology

JULY 1989

Department of Mechanical  
Engineering

© by Elizabeth A Raymond, 1989

Loughborough University  
of Technology Library

Date Jun 90

Class

Acc  
No 040015520



*To John*  
*With Love and Thanks*

\*\*\*\*\*

*To my parents,*  
*Daphne and Peter*

AN ASSESSMENT OF THE INFORMATION TRANSFER PROCESS  
FOR EMBOSSED HOLOGRAPHIC ELEMENTS

ABSTRACT

Embossed holographic elements, such as diffraction gratings, display holograms and optical discs are now firmly established as mass replicated items. The embossed hologram has evolved from its original form recorded in emulsion on glass plate to present day images stamped into plastic. The process of obtaining a holographic image in plastic requires several stages of information transfer: first a surface relief image must be recorded into emulsion; next a metal replica must be made; finally the embossed plastic image is produced. A detailed analysis of the information transfer process has been undertaken and is described.

Techniques are discussed which are currently used for the production of embossed holograms from origination to display copy images. Analysis of the information transfer process is made by the use of diffraction gratings which facilitate quantitative assessment. Optical and surface finish techniques used to quantify the change in surface relief information for each stage are described. The optimization of methods of material exposure and processing has been studied in order to achieve repeatable results and this is discussed. Electroplating techniques are explained for the production of metal replicas of the surface relief pattern and a modification of a hand operated platen printer is described which allows control of the variables important in the embossing of different thermoplastics. The levels of distortion of surface pattern were assessed and compared at each stage of the information transfer process. Results identify areas of loss by profile assessment and diffraction efficiency measurement.

### ACKNOWLEDGEMENTS

I would like to thank the many friends and colleagues who have helped me in this work. I am thankful to my supervisor Mr.B.Bergquist and Director of Research Professor J.Dent for help and guidance. In particular my thanks go to Professor Jim Hewitt for his time and comments.

I thank members of the Optical Engineering Group. The making and mending skills of Vic Roulstone, Steve Penney and Terry West! Remembrance is paid to Mick Bramley, whose photoresist spinner will always be a delight to use. David Kerr, Fernando Mendoza Santoya and Paul Montgomery have all contributed to this work and I thank them for their time and effort. Thanks also to Margaret and Ken in the Photographic Section.

I am indebted to the Department of Mechanical Engineering, in particular Professor Gordan Wray for his help and financial assistance during a difficult period. My thanks also to the University for their support throughout this work.

I thank John Tyrer for his love, help and support in bringing this thesis to a successful conclusion. Thanks for being there.

# ASSESSMENT OF THE INFORMATION TRANSFER PROCESS FOR EMBOSSED HOLOGRAPHIC ELEMENTS

## CONTENTS

	Page No.
Abstract ... ..	(i)
Acknowledgment ... ..	(ii)
Contents ... ..	(iii)
Introduction ... ..	1
 <b>CHAPTER 1: CRITICAL REVIEW</b>	
1.0 Introduction ... ..	7
1.1 Diffraction Gratings ... ..	7
1.2 Hologram Replication ... ..	8
1.3 Photosensitive Materials ... ..	9
1.4 Electroforming and Embossing ... ..	11
1.5 Summary ... ..	15
 <b>CHAPTER 2: IMAGE RECORDING AND OPTICAL COPYING</b>	
2.0 Introduction ... ..	16
2.1 Holograms and Diffraction Gratings ... ..	17
2.2 Diffraction Efficiency ... ..	23
2.3 Experimental Detail - Image Recording ... ..	29
2.4 Optical Copying ... ..	37
2.5 Experimental Detail-White Light Rainbow Hologram	38
2.6 Alternative Copy Routes for White Light Holograms	43
2.7 Experimental Detail- Contact Printing Techniques	52
2.8 Summary ... ..	56
 <b>CHAPTER 3: SELECTION OF SURFACE RELIEF MATERIAL FOR OPTICAL COPYING</b>	
3.0 Introduction ... ..	58
3.1 Selection of Surface Relief Materials .. ..	58
3.2 History of Photoresists ... ..	62
3.3 Negative Resists ... ..	66

3.4	Positive Resists	...	...	...	...	69
3.5	Bartolini Model for Resist Characterisation					73
3.6	Photoresist Characteristics	...	...	...		80
3.7	Experimental Detail and Results	...	...			91
3.8	Discussion of Results	...	...	...		114
CHAPTER 4:	MEASUREMENT OF SURFACE RELIEF PATTERN AND DIFFRACTION EFFICIENCY					
4.0	Introduction	...	...	...	...	116
4.1	Measurement of Groove Depth and Profile	...				117
4.2	Scanning Electron Microscopy	...	...	...		118
4.3	Optical Microscopy	...	...	...	...	123
4.4	Talysurf Instrument	...	...	...	...	135
4.5	Measurement of Diffraction Efficiency	..	...			140
4.6	Discussion and Conclusions	...	...	...		146
CHAPTER 5:	REPLICATION OF SURFACE DETAIL BY ELECTROFORMING TECHNIQUES					
5.0	Introduction	...	...	...	...	147
5.1	Electroforming Process - First Conductive Layer					149
5.2	Vacuum Evaporation of Silver	...	...	...		150
5.3	Electroless Deposition of Nickel	...	...			154
5.4	Chemical Reduction of Silver	...	...	...		157
5.5	Electroforming the Conductive Layer - Deposition by Electrolysis	...	...	...		160
5.6	Experimental Detail and Results	...	...			170
5.7	Discussion and Conclusions	...	...	...		179
CHAPTER 6:	EMBOSSING OF METAL REPLICAS INTO PLASTIC FILM					
6.0	Introduction	...	...	...	...	181
6.1	Plastics for Embossing	...	...	...	...	184
6.2	The Nature of Embossing	...	...	...	...	188
6.3	Experimental Detail and Results	...	...			195
6.4	Discussion and Conclusions	...	...	...		209

<b>CHAPTER 7:</b>	<b>EXPERIMENTAL RESULTS AND ANALYSIS</b>	
7.0	Introduction ... ..	218
7.1	Review of the Information Transfer Process ...	219
7.2	Experimental Detail ... ..	221
7.3	Summary ... ..	239
 <b>CHAPTER 8:</b>	 <b>DISCUSSION AND CONCLUSIONS</b>	
8.0	Introduction ... ..	240
8.1	Accuracy of Electroforming ... ..	240
8.2	Accuracy of Embossing ... ..	245
8.3	Further Work ... ..	251
 <b>REFERENCES</b>	 ... ..	 252
 <b>APPENDICES:</b>		
Appendix 1:	Mathematical Description of the Holographic Recording Process ... ..	256
Appendix 2:	Diffraction Gratings, Wave Propagation ...	261
Appendix 3:	Positive Photoresist, Formulation, Image Models	269
Appendix 4:	Electroforming ... ..	282
Appendix 5:	Embossing ... ..	287

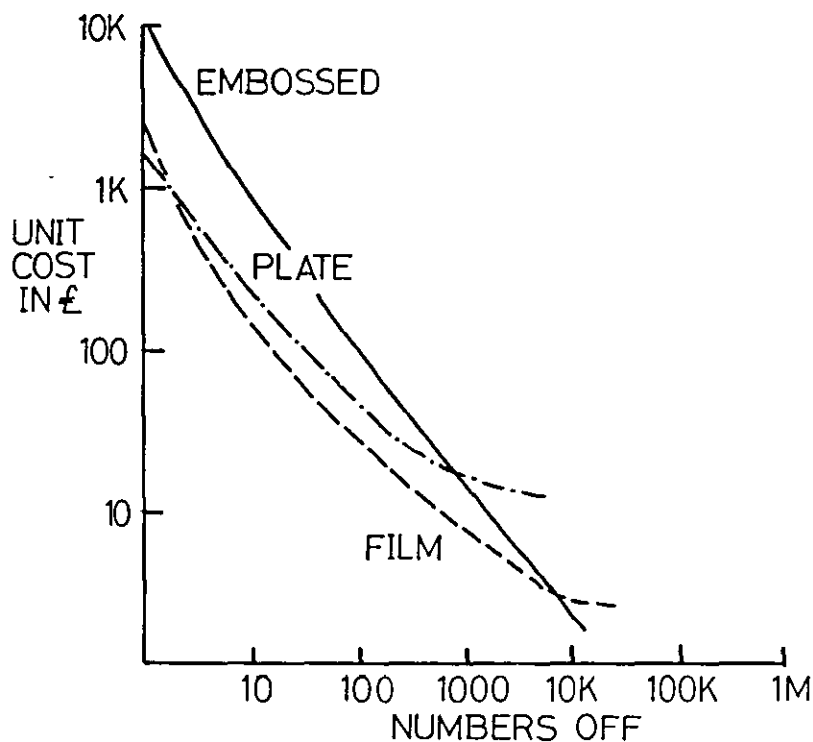
## INTRODUCTION

Holographic images are becoming increasingly familiar, appearing in journals, engineering laboratories, art galleries, on credit cards and even toys. The ability to record and display images in three dimensions is an exciting prospect for scientists, engineers, advertisers, surgeons and artists alike. The type of hologram available includes large format, laser-lit holograms, holograms lit by small white light sources and metallic-like holograms found on credit cards or book covers. This latter hologram, known as an embossed hologram, is the type of hologram most suited to low cost, mass replication for inclusion in magazines, technical journals etc. The production of such holograms requires the interaction of many different technologies and processes. The study of the entire process through each individual stage has provided the basis for the work in this thesis.

Denis Gabor is accredited with the invention of holography and the means by which to record and replay the third dimension that distinguishes holography from photography. The phenomenon of interference between direct and reflected wavefronts produces a unique "interference pattern" that Gabor realised could yield three dimensional information about an object. Holography was an apt title for the discovery, 'holos', from the Greek, meaning whole, 'graphos' to write or record, hence recording the complete and total information about an object.

Holography was initially confined to engineering and physics laboratories which had suitable light sources, producing holograms on glass substrates that could only be viewed with a laser source. As improvements in laser sources and holographic techniques were made, holography was recognised as a potential tool for many applications - holographic interferometry, multiple image recording, vibration studies, object deformation studies, etc. The emergence of display holograms for galleries and exhibitions is more recent. The mid 1960's

produced holograms viewable by white light sources instead of lasers, coloured images by chemical treatments, true colour holograms, 'rainbow' holograms with bands of colour, 360° holograms with animated images and latterly metallic holograms transferred to book covers and magazines by printing techniques. The majority of display holograms are recorded into silver halide emulsions on either glass or film substrates. The emulsion is stable, sufficiently fine grained and sensitive enough to record the interfering wavefronts. However, large numbers of silver halide holograms can be time consuming to produce requiring wet chemistry processing and finishing operations. The embossed hologram was developed to met the demand for mass replication of images with the minimum of processing and handling stages. The process of producing embossed holograms becomes cost effective only when large number are involved. Graph 1) below illustrates the unit cost per number off for plate, film and embossed holograms.



Graph 1) Unit Cost for Plate, Film and Embossed Holograms



The possibility of including holograms in point of sale displays and mass circulation literature has seen the development of a type of hologram that can be mass replicated by printing techniques without the need for individual wet chemistry, handling or finishing stages. Despite these apparent advantages, the production of embossed holograms requires individual areas of technology that must be rigidly controlled to produce quality holograms. The process involves optical and mechanical copying stages that introduce distortion and change to the original image or element. The quantitative assessment of the accuracy and efficiency of these transfer stages has been the objective of this research. No quantitative feedback system has been reported that considers the overall transfer process in the production of embossed elements.

This work has identified and studied the individual stages involved in the production of an embossed holographic element and applied the results to improving the overall accuracy and efficiency of the process. The sequence involves many copying stages in which losses or distortions occur, these variables have been defined and quantified.

The information transfer process can be considered in a number of different stages as illustrated in Figure a).

These stages are;

1. The recording and optical copying of a surface pattern or profile for the transfer of information.
2. The production of a metal replica of the surface pattern by electroforming techniques.
3. The embossing of the metal replica of the surface pattern into thermoplastic material.

A brief description of these stages and the contents of chapters is given in the following pages.

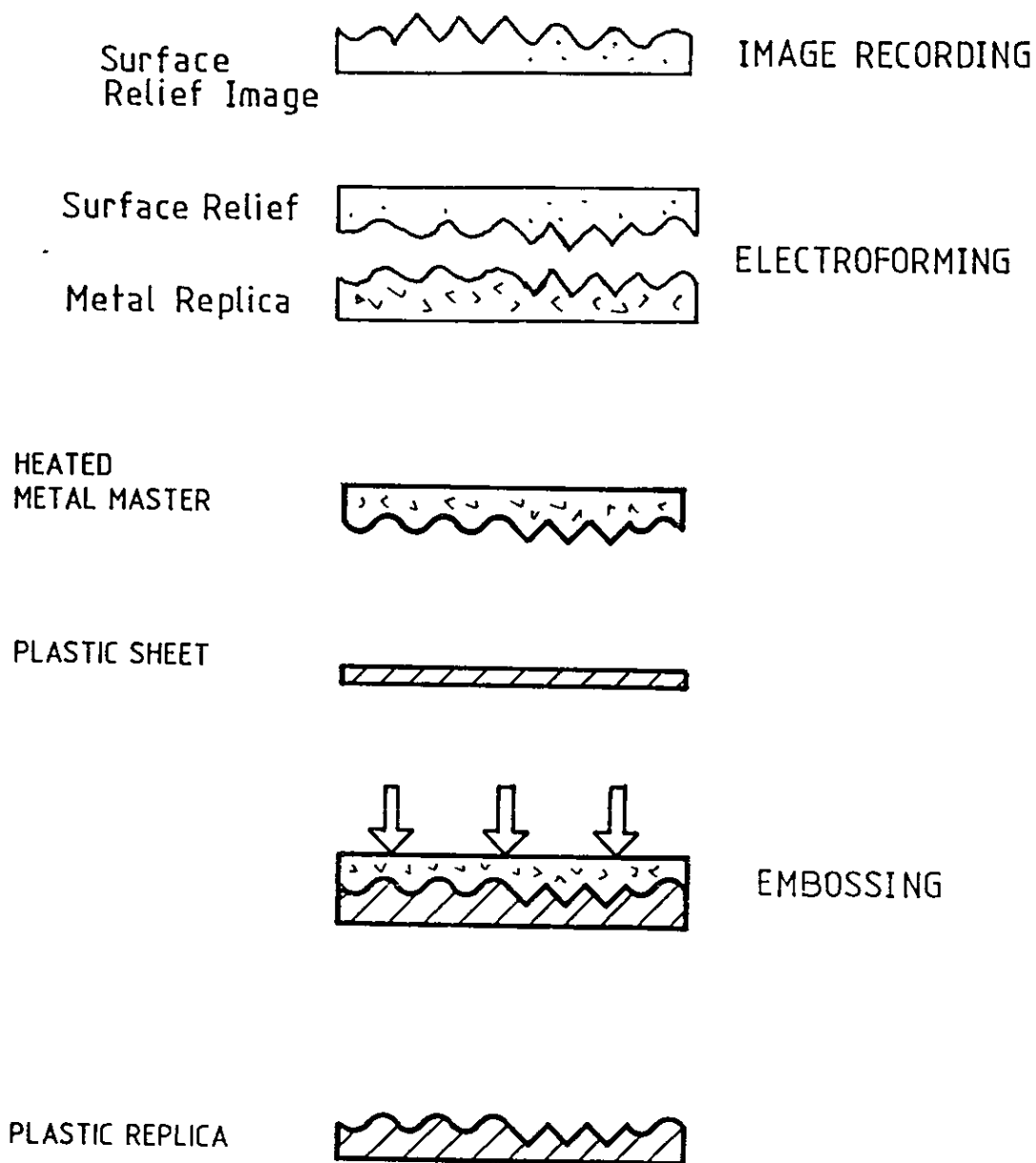


Figure a) Overall Scheme of the Information Transfer Process  
for the Production of Embossed Optical Elements

Chapter 1 - CRITICAL REVIEW presents a review of the literature studied in this thesis.

Chapter 2 - IMAGE RECORDING AND OPTICAL COPYING. The image recording and optical copying of the surface relief pattern is detailed. Alternative methods for producing the surface relief hologram are presented and experimental details given.

Chapter 3 - SELECTION OF SURFACE RELIEF MATERIAL FOR OPTICAL COPYING. The transfer process relies upon the production of a surface relief image and a number photosensitive materials capable of giving surface detail are discussed. Photoresist is identified as the ideal material and the chapter considers theoretical and experimental aspects of positive photoresist.

Chapter 4 - MEASUREMENT OF SURFACE RELIEF PATTERN AND DIFFRACTION EFFICIENCY. The surface relief pattern carries the information through the optical and mechanical copying stages of the embossing process. Measurement of the surface pattern at each copying stages allows quantitative analysis of the cycle. The measurement of diffraction efficiency determines accuracy and quality of the copying process.

Chapter 5 - REPLICATION OF SURFACE RELIEF PATTERN BY ELECTROFORMING TECHNIQUES. The original surface relief pattern is reproduced in metal by electroforming techniques to produce multiple, durable metallic copies which are used to stamp into plastic. Experimental details of equipment and bath formulations are given and results of electroformed gratings presented.

Chapter 6 - EMBOSsing OF METAL REPLICAS INTO PLASTIC FILM. The metal copy of the surface relief pattern is used as the embossing stamper. The process of embossing is described and theoretical and experimental detail for the embossing of the holograms and gratings is given.

Chapter 7 - EXPERIMENTAL RESULTS. The results from experimental work are presented from each stage of the copying process. Surface profile traces and efficiency curves are used to study the accuracy of the process.

Chapter 8 - DISCUSSION AND CONCLUSIONS. Conclusions drawn from the experimental work are presented. The accuracy and efficiency of the information transfer process is detailed. Further Work addresses the

areas of the transfer process that would benefit from continued investigation.

Appendix 1 presents a mathematical description of the holographic recording process.

Appendix 2 details the theoretical and optical properties of diffraction gratings as used in this study.

Appendix 3 describes the composition of positive resists and proposed image formation models.

Appendix 4 discusses the metal distribution and accuracy of electroforming.

Appendix 5 presents a brief description of properties of thermoplastics important in the study of embossing.

## CHAPTER 1

### CRITICAL REVIEW

#### 1.0 Introduction

The embossed hologram is firmly established in the market place; every credit card displays one. Literature discussing the production of embossed holograms is less widely available. The technologies and processes used for embossed holograms are separate areas that have been applied to a quite different field - holography. Consequently, the literature review has covered a number of topics; diffraction gratings - the basis of the hologram, photosensitive materials in which to record gratings, electroforming - the art of reproducing patterns and details in metal form, embossing - the stamping of patterns into plastic. Each of these topics is used in the production of embossed holograms and needs to be considered on an individual basis before applying the technology to the overall scheme of embossed holograms. Since the embossed hologram is essentially a complex diffraction grating generated by interference of laser light wavefronts to produce a pattern that is copied into a plastic medium, the literature review starts with a discussion of the importance of early diffraction gratings and how the need to replicate such patterns has always been of interest.

#### 1.1 Diffraction Gratings

Since the 1800's diffraction gratings have been important in the sciences of physics and spectroscopy. Diffraction gratings change or 'diffract' a wavefront striking the surface and produce diffracted orders. The original diffraction gratings were hand produced, extremely delicate, unique specimens. As the demand for gratings increased automated manufacture was sought and diffraction gratings were 'ruled', literally scratched, into metal blanks. Such 'masters' were expensive

one-offs, each individually ruled with the errors and inaccuracy associated with the ruling machinery. Hence the interest and desire to be able to mass replicate from one master. The possibility of replicating such elements was investigated as early as 1947, before the manufacture of optical elements such as flats, mirrors and prisms was totally perfected. In a paper by Jarrel [1] mention is made of a patent filed in 1947 by J.U. White et al describing a method of making replica optical elements by depositing a greasy "parting" layer onto the master, followed by evaporated aluminium, approximately 0.1 $\mu$ m thickness. The aluminised master is coated with a thin layer of plastic, 'laminac' or epoxy and backed with a replica blank. After several hours the plastic polymerizes and the replica is separated from the master grating. Similar work had been undertaken using electroforming techniques applied to metal or glass substrates [2]. Replicas from gelatin substrates were reported by G. Dew [3] in 1956, copies being made using glass-based mixtures. The work is one of the few to give details of damage to masters, the number of replications possible and efficiency measurements. Replicas were widely used in place of original gratings, however, recent advances in the production of interference gratings, (produced by interfering light beams) have resulted in perfect, cost effective master gratings, readily and easily manufactured reducing (but not eliminating) the need for replicas.

### 1.2 Hologram Replication

Commercial replication of holograms is more recent, spurned initially by the production of higher quality images available with the development of the off-axis holographic techniques [4]. The early copy methods concentrated on "contact printing" of holograms onto silver halide copy material. F.Harris [5] describes the early techniques of using high pressure mercury lamps to expose holograms held in intimate contact with a copy plate by means of vacuum printing frames. Harris is the first to mention the "venetian blind" effect whereby the orientation of the interference planes within the hologram

to the exposing beam must be considered to avoid obscuring detail. Landry [6] studied the effects of contact copying parameters, orientation of the plates to the exposing beam and separation between original and copy plate. Using laser beams instead of mercury arc lamps offers greater coherence properties allowing reduced intimate contact between the plates. In this way Landry was able to obtain copies made at orientations not easily copied using the mercury arc techniques of Harris. Palais [7] suggested the copying of gratings by contact printing to improve upon the efficiency of the original. The measure of efficiency of gratings is more straightforward than for holograms but the idea of improving upon efficiency of the original is mentioned in later work.

### 1.3 Photosensitive Materials

With the development in copying techniques attention was turned to different copy materials, silver halide was well tested but could not produce sufficient surface relief information needed for replication. Photoresist was identified as a material suitable for hologram copying because its image recording mechanism results in a surface profile. Puech [8] offers a theoretical explanation of contact printing and shows reconstructed holographic images from both silver halide master and photo-resist replica. Puech studies the replica by measuring diffraction efficiency (the amount of light diffracted into a spectral order for a given input intensity) and claims increased efficiency of  $\times 10$  of replica over original. However, the replica is a phase hologram and the original an amplitude hologram. Phase holograms are inherently more efficient than amplitude holograms (by at least a factor of 4) because of the way in which the hologram is reconstructed. The work of Nakajima et al [9] investigates the optical properties and characteristics of copied phase holograms using diffraction efficiencies and similarly claims  $\times 10$  to  $\times 16$  increased efficiency. A novel approach using contact printing is reported by Nakano [10]. In an effort to overcome the need for a vacuum frame, photoresist is

coated onto film and rolled onto a heated original hologram. The combination of pressure and heat is designed to remove air bubbles and ensure intimate contact between plates. After exposure the plastic copy is "peeled" from the original for development. No mention is made of the likely distortions that would occur by heating of original hologram to the temperatures suggested nor the effect of having to peel resist from the original. The technique is almost a one-stage embossing method, the final stage in the production of embossed plastic holograms.

The use of photoresist as a holographic recording medium is discussed by Beesley and Castledine [11]. Their treatment of the subject concerns experimental technique, in particular a pre-exposure stage to reduce exposure times caused by low sensitivity of photoresist to wavelengths greater than 350nm. The major discussion of photoresist properties and parameters for holographic recording is found to be that by Bartolini [12]. The development of a theoretical model for positive photoresist exposure characteristics is verified by the experimental techniques related to interference gratings. The work reported by Bartolini has provided the basis for photoresist characterisation undertaken in this study whereby high emphasis is placed upon controlling the parameters of the initial surface relief pattern. The measurements of properties were made using Shipley AZ1350 resist and the 441.6nm output for a He-Cd laser. Norman and Singh [13] traced the experiments of Bartolini and extended them to the then new Shipley AZ1350J resist using Ar and Kr ion laser lines between 457.9nm and 488nm. The work uses the model proposed by Bartolini to characterise the spectral sensitivity and linearity of the new resist. Other models proposed by Neureuther and Dill [14], Dill et al [15] and Kim et al [16] are not based upon experimental techniques and consequently have proven difficult to verify.



#### 1.4 Electroforming and Embossing

The step from the single photoresist to mass replication by embossing is a logical one. Techniques of electroforming as previously applied to grating replication can be used on photoresist. This yields a metal copy with surface relief detail that can be used as hard wearing 'masters' to stamp, or emboss the detail into a plastic copy.

In a review paper by Burns [17] the process from master hologram ( $H_1$ ), transfer technique, photoresist replica, electroforming and embossing is outlined. Figures for resist thickness, exposure parameters, plating solutions and plastic substrate details are reported but the important optical and physical characteristics of the copies are not studied. No attempt is made to quantify the overall information transfer process. Iwata [18] gives figures on properties of a photoresist hologram and its replica. More accurately it describes point object holograms, ie. two beam interference gratings. The replica was made using epoxy resin, nickel plated to produce a metal mould used as the embossing master. Diffraction efficiencies of the replica are less than for the original, attributed to the fact that "deep grooves can not be accurately copied". The measurements made on groove depth compare  $0.75\mu\text{m}$  original with  $0.45\mu\text{m}$  of the replica. Values of SNR (signal-to-noise-ratio) and efficiency for a hologram of a diffusely illuminated object are given. The efficiency of the replica is almost one third that of the original. The reason for this loss of efficiency for the hologram as opposed to the grating is given by the fact that the hologram has a more complicated fringe pattern and is thus more difficult to reproduce by replication. Reference to efficiency and relief depth is made by Bartolini et al [19] in respect to embossed hologram motion pictures for television playback. Photoresist relief images of Fraunhofer type holograms are metallized and embossed into plastic tape. Bartolini reports on the limits of efficiency given the non-linear response of the recording medium. The exposure parameters

encountered for studies undertaken result in an efficiency of only 3% requiring a valley to peak depth in relief pattern of  $0.1\mu\text{m}$  for the values of 633nm wavelength of light and a refractive index of photoresist of  $n=1.4$ . Claims are made that studies using a scanning electron microscope confirm the depth experimentally - thus the process for replicating relief phase holograms must be capable of yielding a resolution of  $0.1\mu\text{m}$  in depth and less than  $1\mu\text{m}$  along a surface. These results are not expanded upon nor supported by accompanying photomicrographs but this reference is the first to quantify a relief pattern depth and relate it to diffraction efficiency. No references to a "feedback" system have been found relating the initial resist depth to efficiency nor relating the depth of copies and their efficiency.

Much literature exists dealing with refinements of experimental techniques in terms of exposure and development parameters, processing latitude, groove profile formation and specific details will be referred to throughout the text. As for photoresist characterisation the main source of data has come from references [12,13]. The area of metal deposition and electroforming prior to embossing is less well documented. One reason for this may be the commercial nature of the process, little experimental detail is given over and above solution make-up or perhaps foil thickness [17].

The study of stress in electrodeposits is documented in an early paper by Hammond [20]. The work discusses the stresses in electrodeposits as a feature of solution composition and operating parameters. In particular the measurement of stress is well reported with reference to experiments as early as 1877, indicating that the problem has always been encountered but not necessarily solved. The stresses in electroforms is considered by McKinney and Bartle [21]. Interested in replicated gratings for high energy lasers and spectroscopy work, the authors found that epoxy replica techniques lacked the necessary

accuracy, durability and high thermal conductivity necessary for short high energy laser pulses. Mention is made of the "residual stresses" in the electroform, giving surface deformation of many fringes upon separation of the original from the electroform. It is reported that stress which accumulates in the nickel can be avoided by electroforming to a thickness of 120 $\mu$ m only. How this factor is determined is not reported.

More recent still with direct application is the work in the area of electroforming for video and optical disc manufacture. Wearmouth and Bishop [22] concerned with video disc stampers compare stress and hardness of deposits for two commercially available nickel plating baths. Nickel is the most commonly used for electroforming and the composition of bath make-up is well formulated and tested. The addition of organic brighteners to the composition is believed to affect the roughness of the surface finish. The work of Wearmouth and Bishop shows a linear relationship between the deposited stress and the addition of the brighteners (butyne - diol) and compares stress values for increasing deposit thicknesses upto 50 $\mu$ m. The typical thicknesses for the stampers however is reported as 250-300 $\mu$ m. The conclusions reached suggest that the solution with the additional brighteners offered advantages in deposit hardness and residual stresses and may be used in preference to the traditional sulphamate solutions. Similar mention is made to the use of brighteners by Legierse [23] in considering the electroforming process for optical disc systems. Legierse discusses all aspects of the replication of discs from master recording, electroforming through to injection moulding of discs with mention of internal stress, flatness and roughness of the electroform. Although reaching no conclusions on the nature of stresses or the means to reduce them, the work is the most applicable and informative to the work in this study. Of similar importance and interest is a paper discussing the accuracy of detail reproduction by one-off electroforms [24]. The application in this

instance appears to be the dental profession and the use of elastomeric impression mould mandrels. Conclusions reached upon the study of the electroforming process suggests that "infilling" of detail occurs. The difference with the procedure used however is the use of metallising powders directly onto the elastomer original to render the surface conductive prior to electroforming. It would appear that this process is normal for such applications. A liquid containing colloidal silver and silver powders is physically burnished onto the surface of the original. The authors suggest that the spherical nature of the silver particles used in this manner results in poorer dimensional accuracy than when using flat, flaky powders. These conclusions may also be relevant to the deposition of the initial conductive layer for gratings. The dimensions under study in the paper ranged from  $6\mu\text{m}$  to  $1\mu\text{m}$  and the authors suggest accuracy of 0.1% was possible.

The final stage of the process is the embossing of the metal copy of the electroformed original. Embossing is not a new technique but its application in holography is novel, though becoming more commonplace with the advent of the credit card hologram. The work by Bartolini [19] already mentioned, is concerned with producing embossed holographic motion pictures intended for television playback. The required relief depth in the photoresist resist is calculated at  $0.1\mu\text{m}$  and less than  $0.1\mu\text{m}$  surface resolution. The embossing process used for all these types of applications is governed by four parameters; type of plastic, temperature of embossing, duration of embossing (dwell time) and pressure of embossing. Bartolini describes a roller embossing process of master and plastic passing through heated rollers. Details of the above four factors are not given but in a later paper [25] are discussed more fully. A series of papers by the authors Gale and Knop [26,27,28] consider the embossing process for the production of black and white and colour images from relief grating structures. The papers report no significant differences in replica and original but is not quantitative. The last reference considered on the area of embossing

is one mentioned previously, that by Burns [17]. The section on embossing considers all current market place techniques including hot foil stamping. Although comparisons are drawn between embossing methods, little experimental detail in terms of embossing parameters are given.

### 1.5 Summary

A wealth of references is available on the individual areas of holography, electroforming, embossing and replication but very few consider the entire process. None offer a quantitative assessment of the losses or distortions that occur throughout the information transfer process. Here we attempt an insight into each individual stage of the process, to identify and quantify the changes that occur and to assess the overall sequence defined as the Information Transfer Process.

## CHAPTER 2

### IMAGE RECORDING AND OPTICAL COPYING

#### 2.0 Introduction

The assessment of the transfer function for embossed elements relies upon transfer of information or images through optical and mechanical copying processes as illustrated in Figure 2.1. Image recording and optical copying is the first stage of the transfer process.

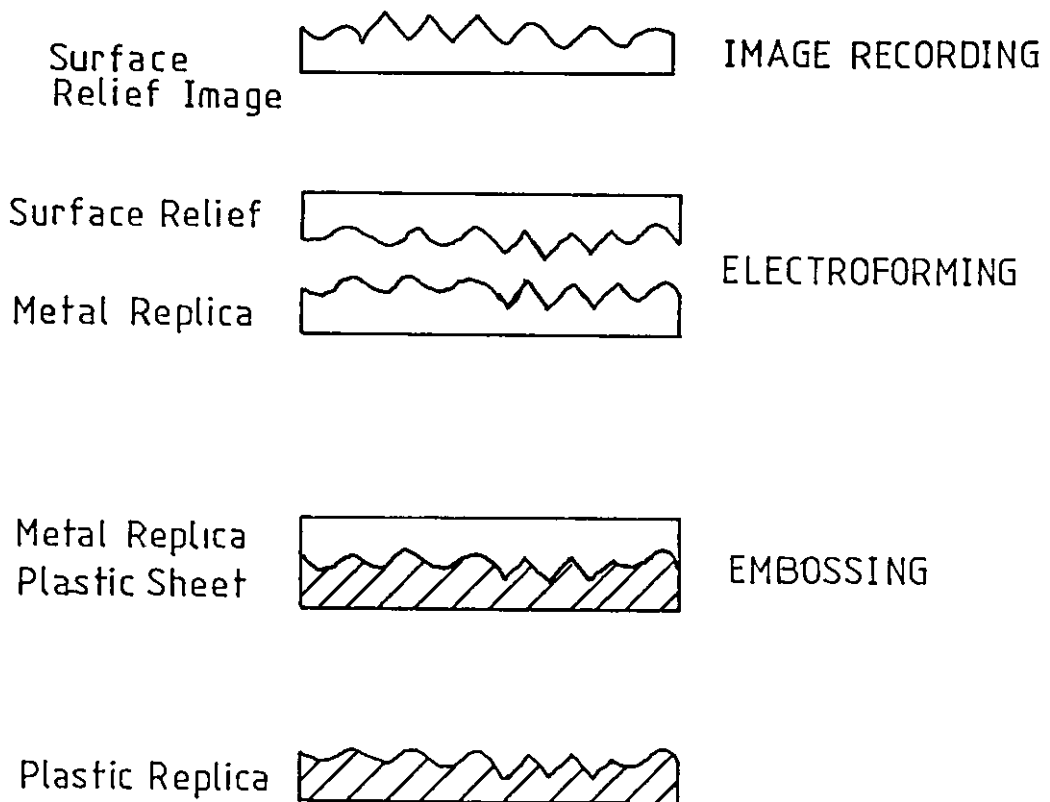


Figure 2.1 Overall Scheme for the Information Transfer Process

The majority of display holograms seen in galleries are produced by a two stage copying process much as prints are generated from negatives. From a 'master' transmission hologram (effectively the 'negative'), multiple 'prints' can be copied to produce a variety of different holograms in different photosensitive materials. Different optical copy techniques include direct transfer or contact printing methods using laser and non-laser sources. Theoretical and experimental detail for each copying regime is presented including the merits of each system. This two stage optical copying process is used in this study for producing copies that possess surface relief detail. The surface relief pattern then becomes the information 'carrier' through the embossing sequence which must withstand mechanical copying stages. In order to quantify the information transfer process, the surface relief pattern must be measured in order to assess the accuracy and efficiency of the copying stages.

This chapter details the recording of diffraction gratings and holograms and explains the need to produce simplified, uniform surface information for quantitative analysis. A mathematical description of the holographic recording process is presented in Appendix 1. Appendix 2 describes the optical properties of diffraction gratings. The experimental detail of recording diffraction gratings and holograms is given before considering the optical copying of the 'master' to produce white light copy holograms.

### 2.1. Holograms and Diffraction Gratings

The theory of 'wavefront reconstruction' or holography, was proposed by Denis Gabor working in 1948 to improve the resolution of images from electron microscopes. Gabor had suggested that interfering wavefronts could produce "interference patterns" unique to the object being recorded and that a three dimensional image of that object could be replayed from the record of the unfocussed diffraction pattern. Gabor was limited in his work by lack of suitable light sources, he had

recognised the need for a coherent light source with sufficient intensity and was restricted to mercury arc lamps for his own experimentation. Additionally, Gabor made images of transparent objects in a similar fashion to shadowgraphs, making re-illumination and viewing of the hologram difficult. Figure 2.2 illustrates the nature of light from some sources to show the limitations of the mercury arc output compared to the monochromatic, coherent output from the laser. Also illustrated is the on-axis recording arrangement used by Gabor.

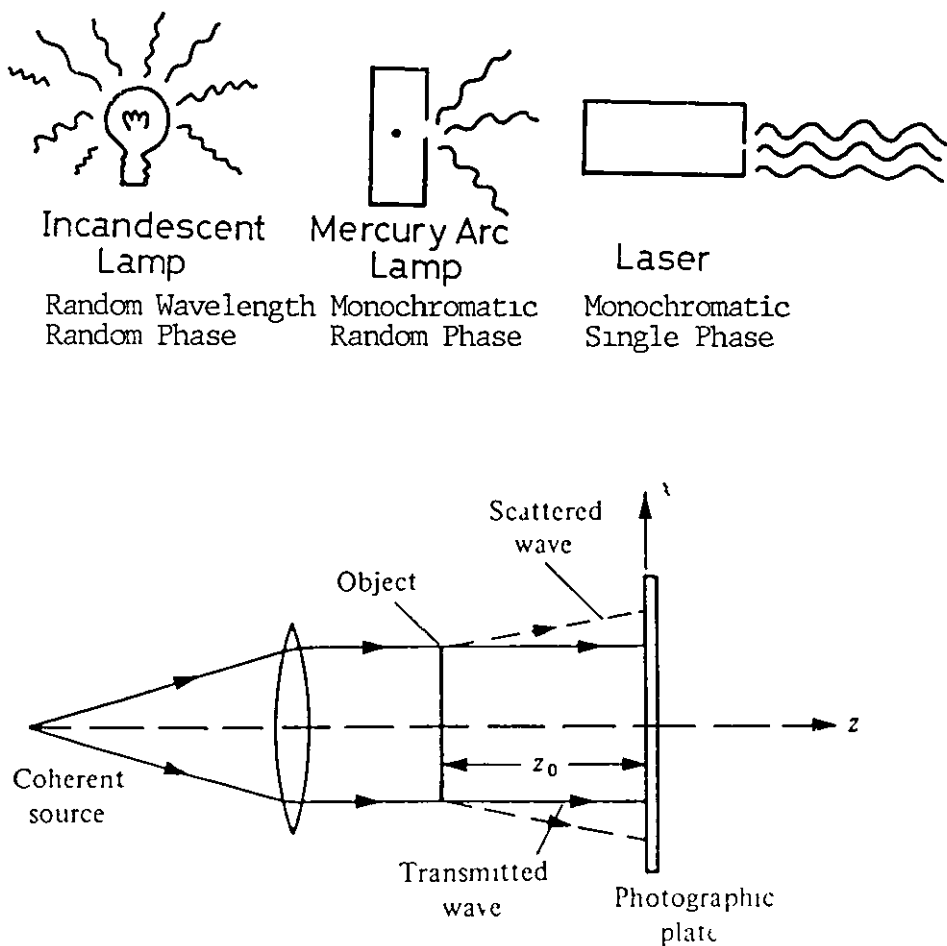


Figure 2.2 Light Sources and the On-Axis Gabor Arrangement



Not until the 1960's with the invention of the laser did holography find further advancement. Leith and Upatneiks used an off-axis arrangement to record and replay holograms, which combined with the advantages of a laser source produced holograms of objects in three dimensions that were sharp, bright and clearly visible. The arrangement for off-axis recording is illustrated in Figure 2.3

Another type of hologram was demonstrated at about the same time by Yuris Denisyuk in the Soviet Union. Using reflected light, he successfully produced a three dimensional image of an object by recording wavefront interference throughout the volume of a photographic emulsion. The advantage of this type of hologram is that it can be viewed in white light unlike the previous two examples of holograms that must be replayed with the original recording source. The arrangement for Denisyuk holograms is shown in Figure 2.4

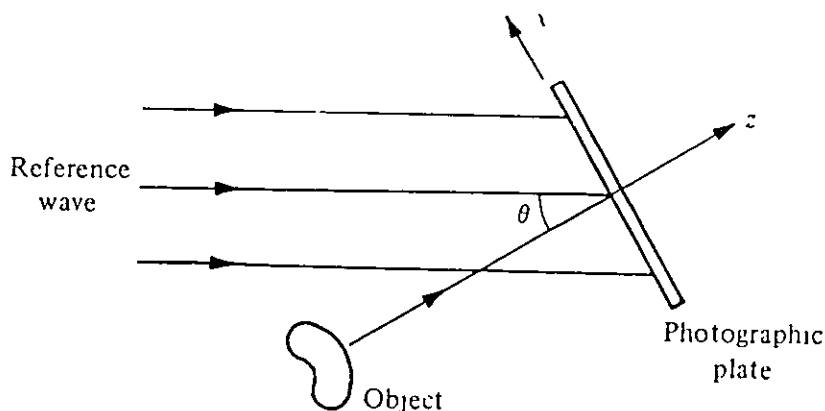


Figure 2.3 Off-Axis Recording Arrangement

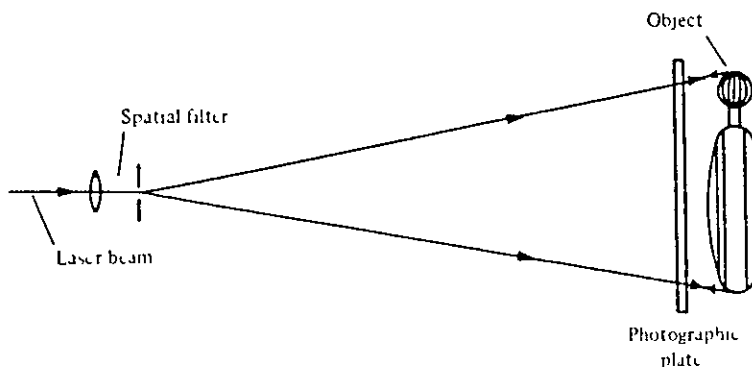


Figure 2.4 Denisyuk Recording Arrangement

A photograph only records the intensity of light using a lens to gather light diverging from each object point and focus it onto the film plane. No phase relationship exists between the incident wavefronts. Holography records both the amplitude and phase information from an object. The object wave is made to interfere with a second, phase-related reference wave introduced from the split laser beam. (Holography is a two beam recording process, see Figures 2.3, 2.4, two wavefronts interfere in each regime.) The two interfering wavefronts must be coherent for the relative phase between object and reference wave to remain constant in time. This produces a definite effect upon the intensity distribution of the resulting interference pattern and is recorded by a photosensitive emulsion. This pattern contains information on both phase and amplitude of the diffracted wavefronts. These original wavefronts can be reconstructed (hence "wavefront reconstruction") by replaying the developed hologram with the reference wavefront. Just as the reference wave was used to encode phase information of the object, so it can be used to recreate the object wavefront as if the object was still there. A mathematical description of the process will be found in Appendix 1.

The interference patterns recorded in a hologram are extremely complicated and no regular feature or pattern could be identified as relating directly to the object used in the hologram. However, if two coherent wavefronts interfere without an object present, interference patterns still result and produce a 'diffraction grating'. At the points of constructive and destructive interference bright and dark bands appear respectively and the surface pattern appears as a uniform and regular array of lines or troughs. Plates 1 and 2 show photomicrographs of the surface of a hologram and a diffraction grating. The recording regimes are illustrated in Figure 2.5.

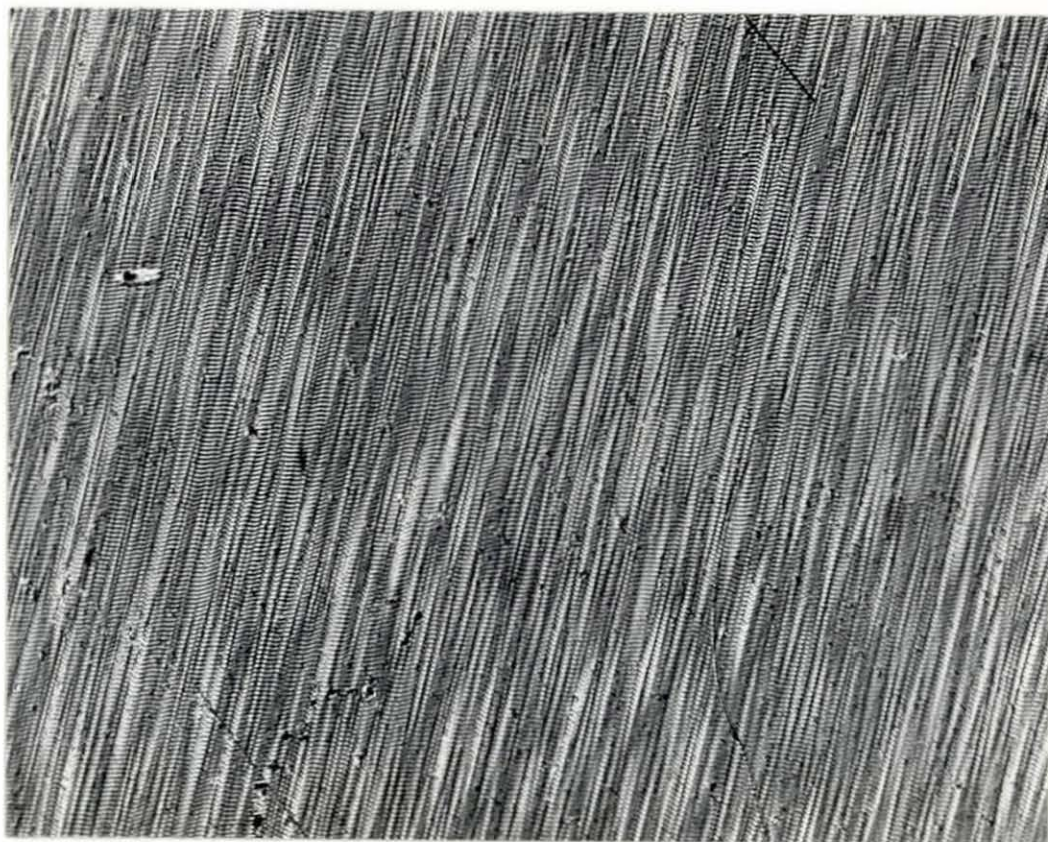


Plate 1. Photomicrograph of the Surface of a Hologram

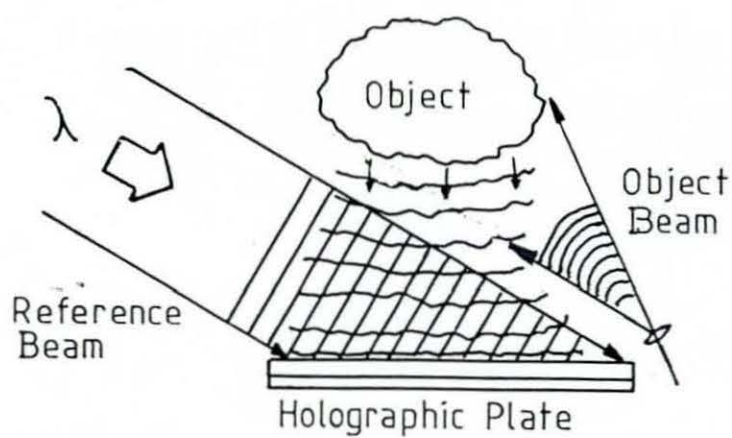


Figure 2.5 a). Recording Regime for an Off-Axis Hologram

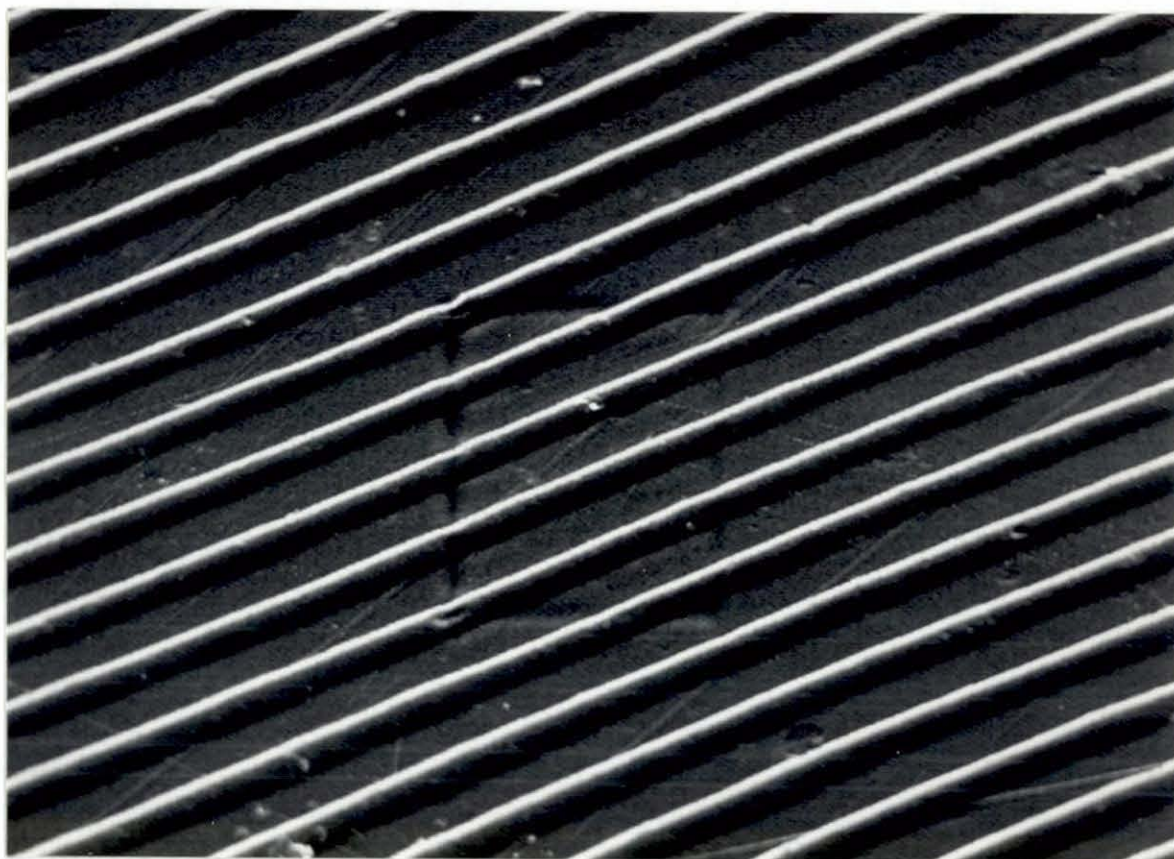


Plate 2. Photomicrograph of the Surface of a Diffraction Grating

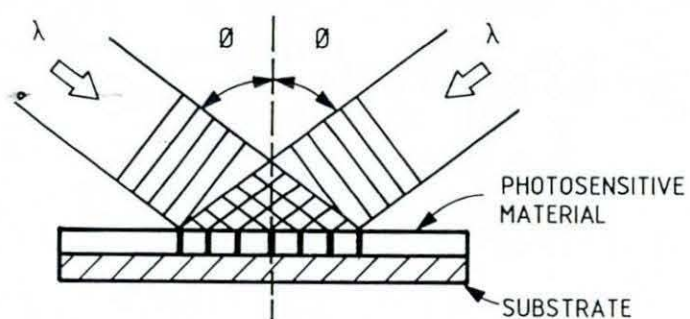


Figure 2.5 b) Recording Regime for a Diffraction Grating

Whilst holograms and gratings are similar in most respects they are not identical since the hologram does not necessarily have a regular surface structure. A holographer may describe a diffraction grating as a simple hologram, whilst a spectroscopist may describe a hologram as a complex grating.

The transfer of surface detail through each stage of the embossing process is the key to identifying losses or changes that affect final image quality. To undertake quantitative study a simple grating pattern was chosen, providing a vehicle of known dimensions at each stage through the process. Using a hologram with a far more complicated surface pattern would not improve the study but only introduce more optical information. By producing gratings of varying spacings and depths, as would be found in a holographic pattern, the transfer process for the hologram can be modelled. Two important features of the surface pattern have been studied at each stage of the process, these are; groove profile and diffraction efficiency. Groove profile is the nature and shape of the groove generated from the interfering wavefronts. It influences the way light striking the surface of a grating is split into different orders and reflected from that surface. Diffraction efficiency of a grating is a measure of how much light is split into the orders for a given intensity and angle of incidence.

Appendix 2 presents the history, optical properties and theoretical description of wave propagation and diffraction gratings.

## 2.2 Diffraction Efficiency

A diffraction grating, described in this context is a one-dimensional array, a regular form of parallel, equispaced lines or grooves diffracting a propagated wave into spectral orders. Figure 2.6 illustrates the action of a diffraction grating. The grating changes the direction of the propagation as a function of the spacing, or period, of the grooves and the incident wavelength of light.



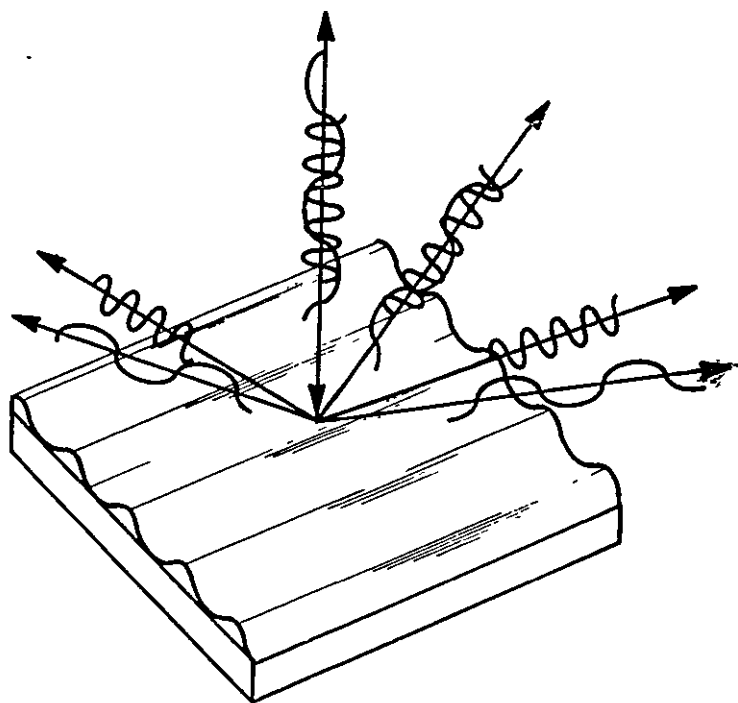


Figure 2 6 The Action of a Diffraction Grating - Production of Spectral Orders

Diffraction efficiency of a grating is a measure of how much light is split into the diffracted orders. Diffraction efficiency expressed as a single percentage is a very inaccurate figure unless parameters such as the measured angle of incidence, polarisation and wavelength of light are quoted, especially when considering that gratings may operate from soft X-ray to far IR regions. An accurate measure of efficiency is important for spectroscopists and grating manufacturers.

Two expressions of efficiency are commonly used; ABSOLUTE EFFICIENCY, the percentage of incident light diffracted into the required order. Influencing factors are groove shape and reflectance of the material on which the grating is made. RELATIVE OR GROOVE EFFICIENCY, only groove profile is important since a reference mirror and not the

reflectance of the grating material is used to determine reflected intensity of light. Relative efficiencies should always be higher than absolute efficiencies. Relative efficiency is a measure used by grating manufacturers to determine accuracy of groove profile. For complete characterisation of gratings, profile and efficiency are interlinked and should be determined.

A number of factors influence the measurement of efficiency and the way in which it is calculated. The wavelength of light used, the angle of incidence of light, the reflectance of the surface, the polarization vector of light, (horizontal or vertically polarized laser light can be used), the optical arrangement for measurement of incident and diffracted beams. The 'Littrow' configuration allows incident and diffracted beams to return along the same axis. When quoting efficiency values all of these parameters should also be expressed but rarely are.

Efficiency curves for ideal gratings would show smooth variations from one wavelength to another. Often however, ridges or troughs are seen, described as Wood's anomalies [29]. These anomalies appear as rapid changes in efficiency for just small changes in wavelength or angle of incidence. In order to illustrate anomalies many data points are necessary, measurement by laser is useful in this respect because point interrogation of the surface is possible reducing the chance of missing an anomaly. Figure 2.7 illustrates a 'typical' grating diffraction efficiency curve and shows how an anomaly may be missed if insufficient points are read.

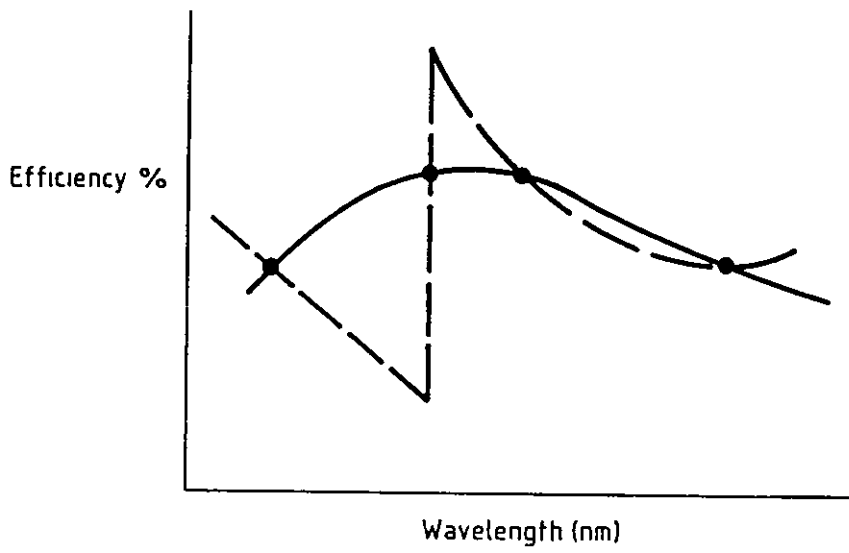


Figure 2.7 Diffraction Efficiency Versus Wavelength  
The Broken Line Represents a Grating Anomaly

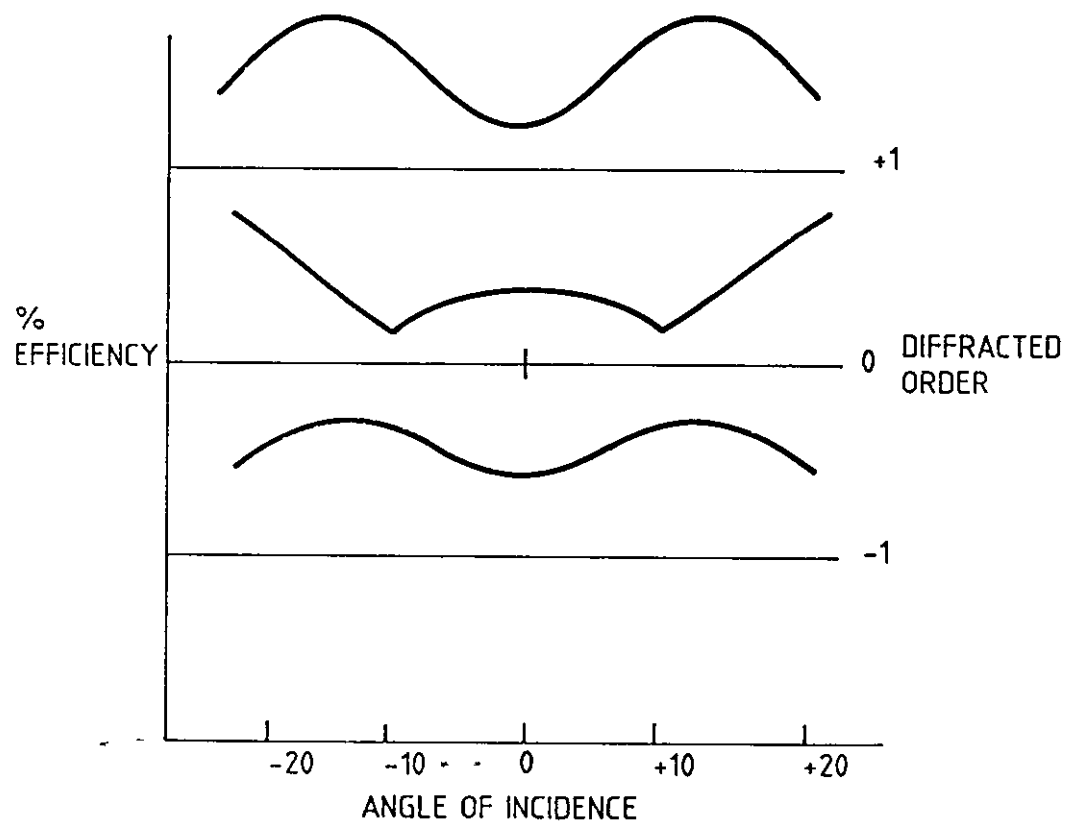


Figure 2.8 Example of Variations in Diffraction Efficiency  
for Diffracted Orders



It is not necessary to describe in detail the nature of the anomalies and how they affect grating theory. However, the loss of energy in one order is accounted for in other orders and sudden fluctuations may be seen in higher orders. Figure 2.8 illustrates this phenomenon. Anomalies are more pronounced when the S polarization of light is used (the electric vector being perpendicular to groove profile). Hutley [29] presents a detailed account of grating theory and anomalies for a wide variety of diffraction gratings.

Diffraction efficiency has not been used to determine groove depth of the gratings but primarily as a quantitative technique to evaluate distortions that occur in the transfer process. It can not be ignored however that groove profile of the gratings has an effect on the calculated diffraction efficiency. It is believed that the quality of gratings produced, having sinusoidal profiles, does not limit the usefulness of the diffraction efficiency measurements. Several workers have attempted to define the relationship between groove profile and diffraction efficiency. Brainin et al [30] described studies made on transparent holographic gratings and found that deviation from a sinusoidal profile shape exerted a strong influence on diffraction efficiency and hence the relationship with groove depth. They concluded, for determination of groove depth from measurement of diffraction efficiency, that grating frequency, polarisation of incident light and actual profile shape data was necessary. If the shape of profile was ignored errors of up to 20% could arise in the determination of groove depth. Efficiency measurements of gratings produced are included in Chapter 7.

The measurement of hologram diffraction efficiency should apply the same criteria as for diffraction gratings. The complex nature of the surface of the hologram does not produce distinct spectral orders that can be measured in the same way as for gratings. Holograms are often only considered 'efficient' by how bright they appear, strictly a

measure of brightness. Often the only criteria applied to holography is the subjective measure of brightness. The measurement of luminance (measure of light emitted from a surface) is possible and can be used to provide an objective assessment if critical illumination and viewing requirements are met. This would be a more useful standard for assessing holographic quality than is currently seen but factors such as image content, sharpness, depth of field or image blurr still determine the quality of a hologram.

For the experimental work undertaken in this study both holograms and diffraction gratings were produced. The following section details the recording of a laser transmission or 'master' hologram and the recording of the white light copies produced from the 'master' hologram. The optical arrangements and experimental details are also given for the diffraction gratings recorded.

## 2.3 Experimental Detail - Image Recording

### 2.3.1 Laser Transmission 'Master'

A mathematical description of the holographic recording process and the generation of real and virtual images is presented in Appendix 1. Figure 2.9 illustrates a basic optical layout for the recording of the master hologram. The laser beam is directed onto a shutter mechanism to control exposure times on the holographic plate. The beam splitter produces two beams, one of which is directed onto the object via a steering mirror through a spatial filter assembly to expand and clean the beam. The object may be lit with more than one light to remove shadows, add highlights, etc. The second beam from the beam splitter is also expanded and cleaned and falls directly onto the holographic plate, this is the reference beam. In the region of the holographic plate, interference occurs between the reflected object beam and the direct reference beam. The holographic plate records the resultant interference pattern.

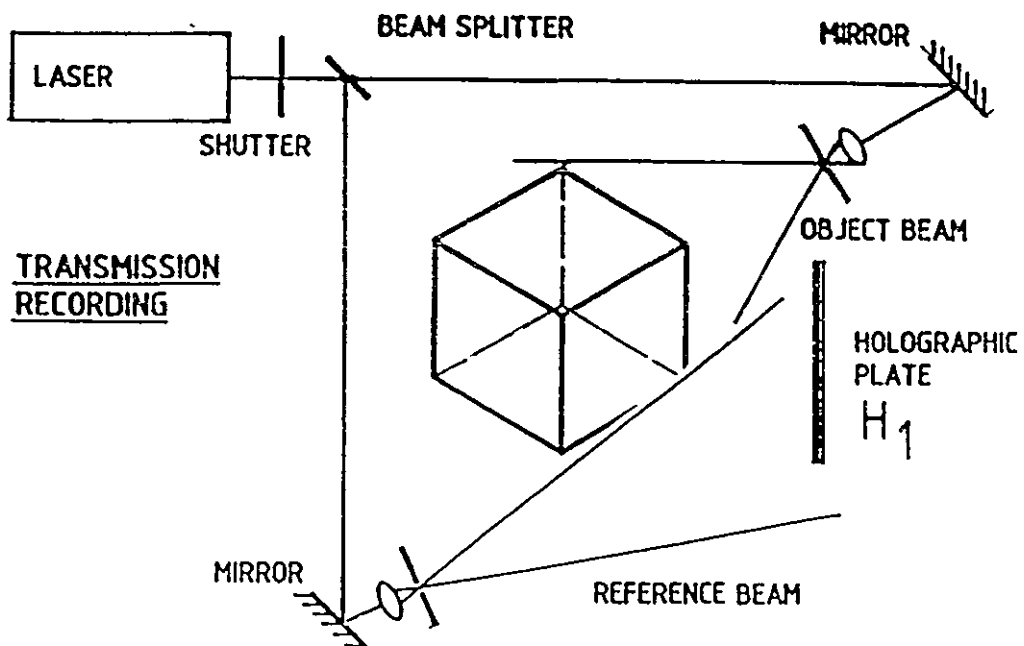


Figure 2.9 Transmission Recording of a 'Master' Hologram

Processing the holographic plate produces a metallic silver image that can be fixed and bleached to give a stable photographic record of the interference pattern. The holographic image can not be observed until wavefront reconstruction occurs by placing the master hologram back into the plate holder in its original recording position. The object beam is blocked off and only the reference beam illuminates the plate. The observer can then look 'through' the plate to the original object position and will see the holographic image of the object. The image will be a 1:1 recording with the same position and illumination as when the object was recorded. Figure 2.10 illustrates this arrangement.

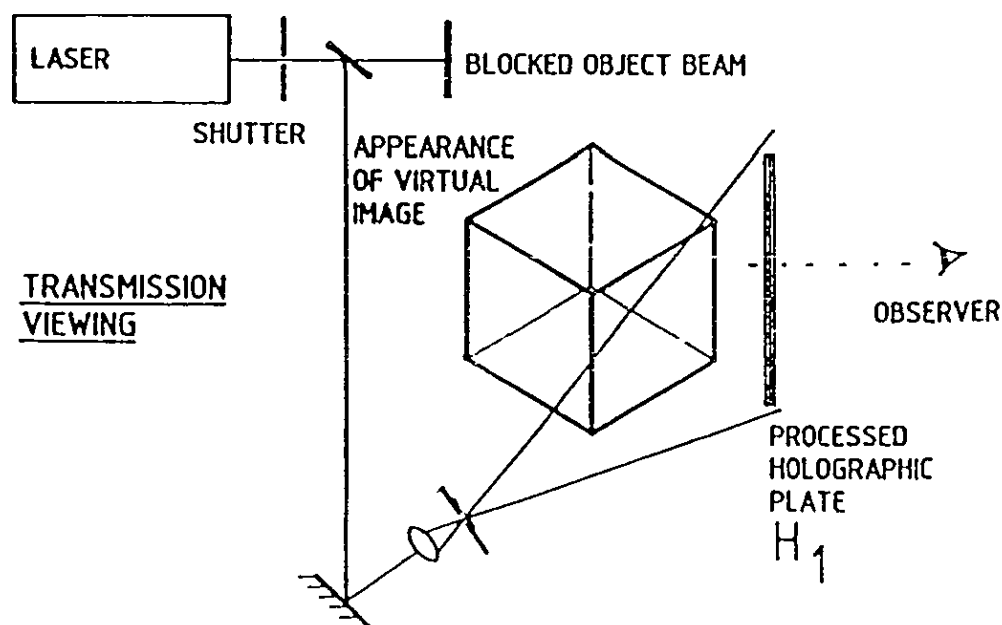


Figure 2.10 Viewing A Transmission, 'Master' Hologram

In viewing the hologram as illustrated in Figure 2.10 the observer is seeing the virtual image as it appears behind the holographic plate. The mathematical description of the process (Appendix 1) shows that the hologram can produce a second 'real' image whereby the image of the object appears to be projected out in front of the holographic plate. This is achieved by illuminating the plate with the conjugate of the original reference beam and this arrangement is used for the recording of white light copy holograms. The 'master' hologram can be viewed in monochromatic sources (of suitable wavelength) but would not replay satisfactorily in white light. The broad spectral output of a white light source produces many blurred images from each wavelength reconstructing the object wavefront at different angles to the original giving colour smear and a blurred image.

The experimental hologram was of a small brooch. The subject was ideal in many respects, it was small with shallow depth and fine detail, it could be easily mounted and remain stable during exposure. The experimental arrangement was similar to that shown in Figure 2.9. The object was mounted onto black cloth in front of the plate holder. It was illuminated by a single overhead expanded beam which adequately lit the subject without harsh shadows or highlights. The collimated reference beam illuminated the holographic plate situated in the holder. The master hologram was recorded on Ilford blue/green sensitive plate using the 457nm output from an Argon ion laser.

Recording details are tabulated below;

Plate	Reference - Object Beams		Exposure Time	Development
	$\mu\text{w}/\text{cm}^2$		secs	
Ilford Blue/Green Sensitive	0.8	0.1	4	Ilford SP678 2 mins.
				Ilford Hypam 2 mins.
				Ferric Nitrate Bleach
				till clear
				Wash, dry.

### Observations

An acceptable master hologram, 'clean' with little scatter and noise. This master hologram was subsequently copied to produce a white light transmission display copy, the experimental details will be found in Section 2.5

### 2.3.2 Diffraction Gratings

The diffraction gratings produced allowed quantitative assessment of the simplified, uniform surface pattern. Groove depth and diffraction efficiency could be more easily measured than for the complex nature of holographic images. The basic requirement for the generation of interference fringes has been illustrated in Figure 2.5. The initial optical arrangement used for grating manufacture is shown in Figure 2.11.

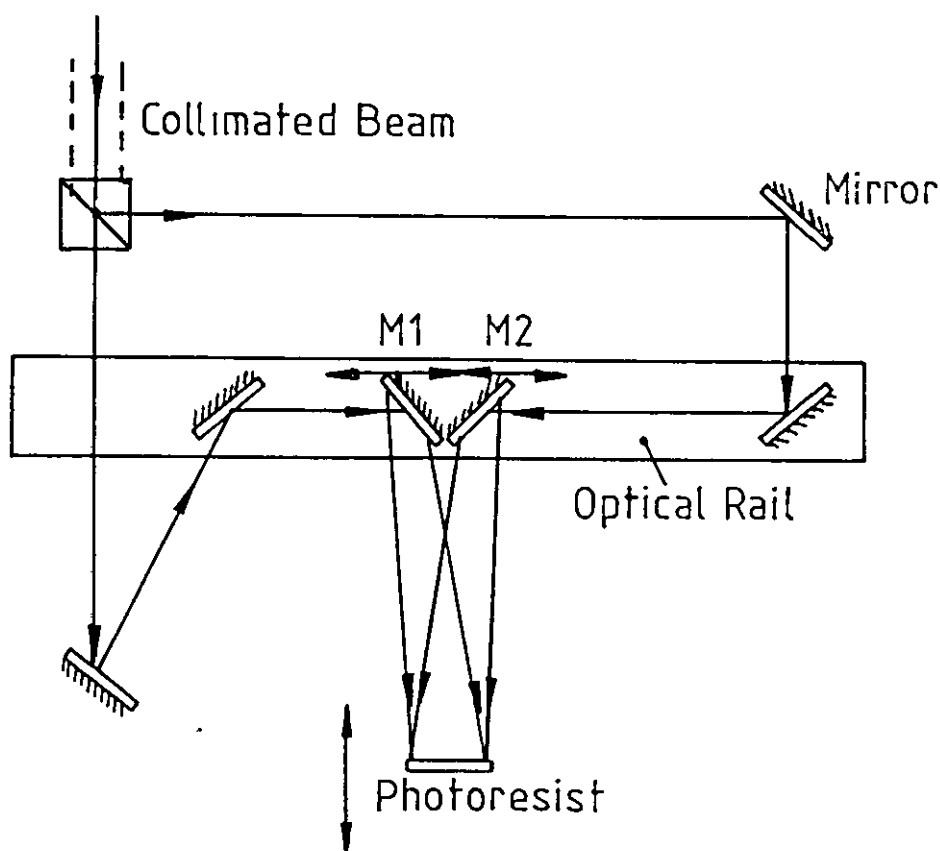


Figure 2.11 Initial Optical Arrangement  
for the Recording of Diffraction Gratings

It was necessary to produce gratings with different line spacings and rotation of mirrors  $M_1$  and  $M_2$  allowed the collimated laser beams to interfere on the plate from different angles. The position of the plate holder facilitated variable frequency recordings. This arrangement worked satisfactorily for both silver halide and photoresist materials. The arrangement was inefficient however due to the high number of optical components and the number of reflective surfaces each path traced was not matched. The path length of each beam was identical but the transmitted beam was reflected from only three surfaces whilst the beam reflected at the beam splitter traversed four optical surfaces.

It was felt that the quality of the gratings could be improved if each beam encountered the same number of reflective surfaces. A second optical arrangement was devised that greatly reduced the number of optics in the system, used the same number of reflective surfaces and allowed a range of frequencies of grating to be recorded. The layout is illustrated in Figure 2.12

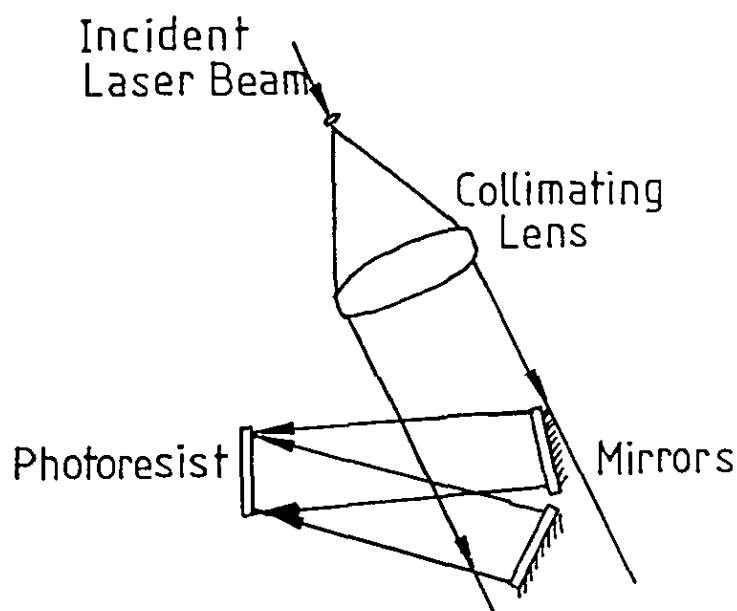


Figure 2.12 Final Optical Arrangement  
for the Recording of Diffraction Gratings

Diffraction gratings were initially recorded in silver halide material to assess the optical arrangement and quality of gratings. The gratings were also used for surface profile and groove depth measurements and the measurement of diffraction efficiency.

Three series of diffraction gratings were recorded in photoresist for the study of the embossing sequence to quantify variation in groove depth and diffraction efficiency. From the original photoresist gratings, metal replicas were taken, measured and assessed before being used to emboss plastic copies which were similarly measured and assessed. Previous trials determined the optimum exposure and development parameters and the core conditions tabulated below are for the three series used in this work.

Photosensitive Material: Shipley AZ1450B Positive Photoresist  
 Substrate: Glass, Self Spun Coating 1 $\mu$ m thickness  
 Baking: 93°C, 25 minutes  
 Development: Shipley, AZ303, 20°C, 1 minute  
 (Dilution as detailed below)

GRATING	INCIDENT POWER	EXPOSURE	$\text{mJ/cm}^2$
100 1/mm	mW/cm <sup>2</sup>	secs	
SERIES 1			
1+4 Developer Dilution			
1a1	0.3	10	3
1a2	0.3	20	6
1a3	0.3	40	12
1a4	0.3	60	18
1b1	0.3	80	24
1b2	0.3	100	30
1b3	0.3	120	36
1b4	0.3	140	42



GRATING	INCIDENT POWER	EXPOSURE	$\text{mJ/cm}^2$
100 1/mm	mW/cm <sup>2</sup>	secs	
SERIES 2			
1+5 Developer Dilution			
2a1	0.3	30	9
2a2	0.3	60	18
2a3	0.3	90	27
2a4	0.3	120	36
2b1	0.3	150	45
2b2	0.3	180	54
2b3	0.3	210	63
2b4	0.3	240	72
2c1	0.3	270	81
2c2	0.3	300	90
2c3	0.3	330	99
2c4	0.3	360	108
SERIES 3			
1+6 Developer Dilution			
3a1	0.3	120	36
3a2	0.3	180	54
3a3	0.3	240	72
3a4	0.3	270	81
3b1	0.3	300	90
3b2	0.3	330	99
3b3	0.3	360	108
3b4	0.3	420	126

The above series of gratings were recorded at 100 lines per millimetre for simplified assessment of surface profile and depth by microscope and surface finish instruments. The gratings were examined by optical microscope for defects or distortions. Plate 3 shows a photomicrograph of the surface finish of a diffraction grating recorded in photoresist.

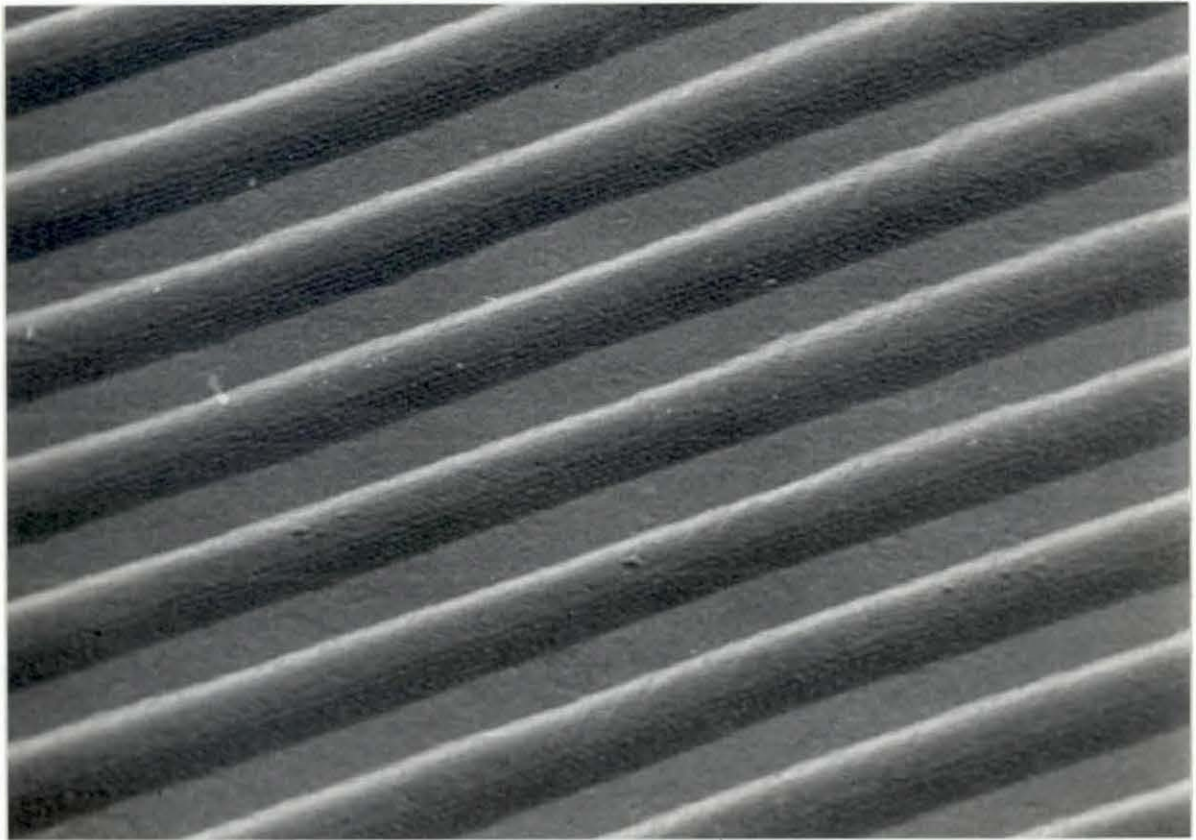


Plate 3. Photomicrograph of the Surface of a Diffraction Grating

## 2.4 Optical Copying

The previous section described the recording of a laser transmission 'master' hologram and diffraction gratings. The master hologram can be used to produce two different types of white light display holograms, reflection or 'rainbow' copies. The latter is used in the manufacture of embossed holograms. The master hologram is a photographic record of interference patterns within the volume of a photosensitive emulsion. The white light copy hologram can be recorded such that the interference pattern is produced as a relief profile of micro peaks and troughs over the emulsion surface. A surface relief pattern capable of reproducing three dimensional holographic images is essential to producing embossed holograms by printing techniques. The surface pattern, if sufficiently prominent and stable, "carries" the holographic information through the embossing sequence and contains the necessary information to replay an image viewable in white light.

This section details the recording of rainbow holograms and some alternative holographic copying techniques. Production of white light holograms by direct, interferometric recording requires the same interferometric and environmental stability criteria as for recording the master hologram. Using silver halide materials with their relatively high sensitivity presents few problems but alternative materials, such as photoresist which is used to enhance the surface relief pattern requires increased laser output and greater environmental stability due to reduced sensitivity of the material. To overcome this, alternative methods of reproducing holograms into a surface relief material have been developed. In a similar fashion as lithographic and photomask images are produced by ultra-violet exposure of contacting negative and plate, a silver halide hologram can be contact copied into photoresist to produce a copy with a surface relief pattern capable of being embossed.

The following section presents the experimental detail for the recording of a white light, 'rainbow' hologram before considering the alternative copy techniques.

### 2.5 Experimental Detail - White Light 'Rainbow' Hologram

Appendix 1 details the properties of a master hologram and the generation of a real and virtual image. The real image can be projected from the hologram by using a conjugate reference to illuminate the master hologram. Figure 2.13 illustrates the recording sequence for a rainbow hologram.

It will be observed from Figure 2.13 c) that the master hologram is masked with a narrow horizontal slit in the copying process. This technique developed by Benton [31] removes the vertical parallax information from the image. The slit across the master determines a number of features; image sharpness, image blurr and noise of the reconstructed image. Loss of vertical parallax is acceptable since depth perception relies mostly upon horizontal parallax. By masking the master a copy can be recorded, viewable in white light producing a sharp, bright image with a good depth of field. Recording the hologram without masking the master produces a copy viewable in white light but limited to only a few centimetres depth of field. The image reconstructs but with blurred edges and colour bands.

The second holographic plate is placed in the plane of the real image as seen in Figure 2.13 d). The position of the plate determines the depth of projected image that appears to stand out from or behind the copy. The projected real image serves as the object beam and the new reference beam is introduced at an angle to the plate.

Replaying the image with a diverging white light source projects a real image of the slit towards the observer. The light diffracted from the holographic copy passes through this slit pupil. Using a white light source the image of the slit is dispersed in the vertical plane to form a continuous spectrum. Moving the head up and down whilst viewing the hologram shows a spread of red, green and blue colours across the

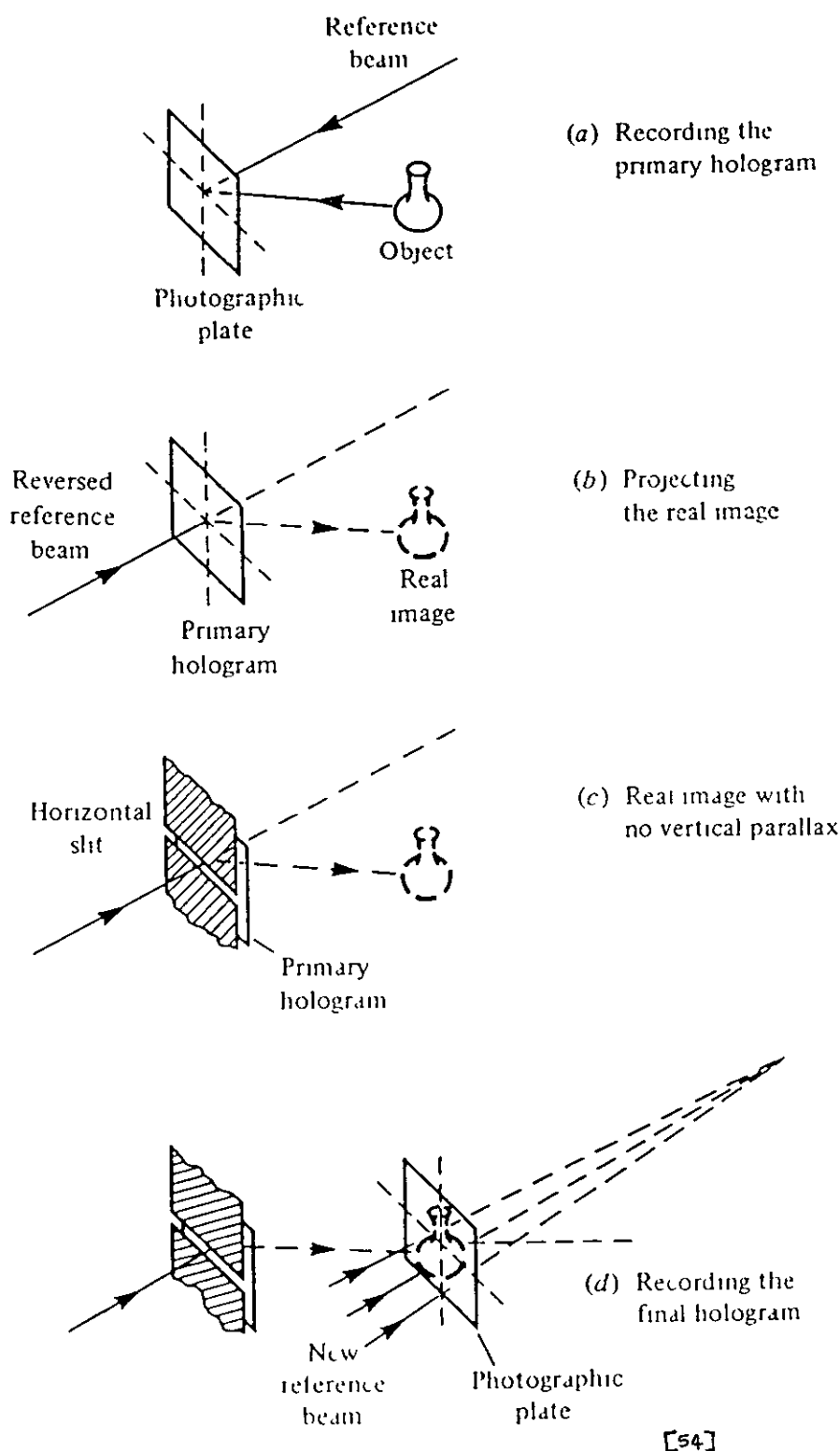


Figure 2.13 Recording Sequence for a Rainbow Hologram

image. The hologram can be viewed in transmission or mirror backed to allow viewing by reflection as is more often the case. The viewing of a 'rainbow' hologram and the production of the real slit is illustrated in Figure 2.14.

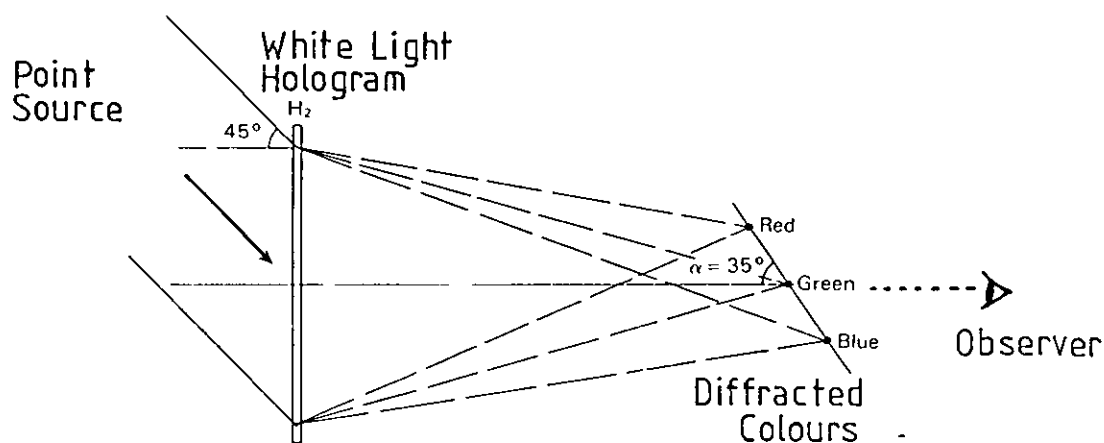


Figure 2.14 Viewing a 'Rainbow' Hologram

The photosensitive material used to record the copy hologram is not restricted to silver halide material. The intention is to produce a white light copy that has a pronounced surface relief pattern capable of withstanding the subsequent physical copying processes. The recording mechanism of photoresist produces a surface relief pattern. Photoresist may be used to record a 'rainbow' copy hologram if the following requirements can be met;

1. A laser output of 350-488 nm of suitable power and single line frequency.
2. A stable, interferometric environment for long periods of time - (exposures may be >30 minutes).

The advantages of this direct recording are;

1. A one step process from master to surface relief hologram is achieved..
2. Recording master and copy hologram at the same wavelength (350-488nm) avoids image distortion.
3. Reduced handling stages result in less physical damage to the surface relief copy, eg. fingerprints, scratches.

#### 2.5.1 Silver Halide Copy Hologram

The master hologram of the small brooch, was used in the optical arrangement as illustrated in Figure 2.13. The conjugate of the original reference beam was used to illuminate the master plate to project the real image into the plane of the second holographic plate, Figure 2.13 b). A slit was placed across the master hologram illuminated with a stripe of laser light from a cylindrical lens. This was more efficient than using a large diameter collimated beam to illuminate only a small slit of the hologram. The new reference beam was directed onto the copy plate from 45° overhead which slightly overfilled the copy plate. The second copy plate was positioned in the plane of the real image such that the image was partly behind and partly in front of the plate, Figure 2.13 d). Stiffening braces and magnetic supports were necessary to provide a stable environment during long exposure periods.

Experimental details are given below:

Photosensitive material:	Ilford Blue/Green Sensitive Plate
Beam Ratios:	Reference beam 4.2 $\mu\text{W}/\text{cm}^2$
	Object beam 0.6 $\mu\text{W}/\text{cm}^2$ 7:1
Exposure:	4 seconds
Development:	Ilford SP678C developer, 2 mins
	Ilford Hypam Fixer, 2 mins
	Ferric Nitrate Bleach clear
	Wash, dry.

### Observations

A clean and bright white light image with low noise and good detail. The hologram in silver halide was made to prove the stability of the transfer rig and produce an acceptable copy for comparison with the image in photoresist. The silver halide hologram was recorded at 457nm to match the original mastering wavelength and avoid image distortions, this explains the low power output and long exposure times. Normal transfer at 514nm into silver halide would require 1/2-1 second exposure times.

### 2.5.2 Photoresist Copy Hologram

The same optical arrangement was used for copying into photoresist as for the silver halide copy. The image plane was identical and only the plate holder changed to accommodate the smaller plate format. Additional bracing was found necessary to overcome movement in the system. A small enclosure was used around the plate holder to reduce air movement effects during the long exposure times. Details are given below,

Photosensitive material:	Shipley AZ1450B Positive Photoresist
Substrate:	Glass, self spun layer, 1 $\mu$ m
Beam Ratios:	Reference beam 4.2 $\mu$ W/cm <sup>2</sup> Object beam 0.6 $\mu$ W/cm <sup>2</sup> 7:1
Exposure:	30 minutes
Development:	Shipley AZ303 developer, 1 minute, 20°C, 1+5 dilution.

### Observations

Maintaining interferometric stability over the long exposure times was difficult and some holograms had movement fringes across them. Other white light copies were not as bright as expected due to movement during exposure. Additional bracing and screening overcame these problems. These white light holograms served as the first stage for the transfer process and were subsequently electroformed and embossed.



## 2.6 Alternative Copy Routes for White Light Holograms

It was described earlier that alternative copying techniques had been developed to overcome the laser and environmental constraints that copying directly into photoresist could introduce. This section will consider some alternative methods of contact printing using laser and non-laser sources. Figure 2.15 illustrates the possible routes by which a master silver halide hologram can be used to produce a white light copy with surface relief detail.

Referring to Figure 2.15 two distinct routes have been identified both starting from the master silver halide hologram. The distinction between the methods is as follows;

Route 1, 1a - copy hologram made directly into a photosensitive material to produce a white light hologram, a 'direct transfer' requiring interferometric stability.

Route 2 - silver halide white light hologram used to contact copy into a surface relief material, 'indirect transfer' involving one or more stages.

The broken lines on Figure 2.15 are further options, not discussed in detail as routes 1 and 2 have been experimentally verified. They are included in the figure as it is known that attempts have been made to follow these routes.

The production of a white light 'rainbow' hologram using the projected real image has been described. (Route 1,1a Figure 2.15) This technique for producing a surface relief copy hologram is possible only with suitable high power laser output and environmental stability. Alternative copying methods designed to overcome these requirements have been developed that use a silver halide copy as the 'mask' for contact printing methods.

### 2.6.1 Contact Printing Techniques

Direct transfer from a master hologram into photoresist requires access to larger laser outputs of suitable wavelength, suitable optics and

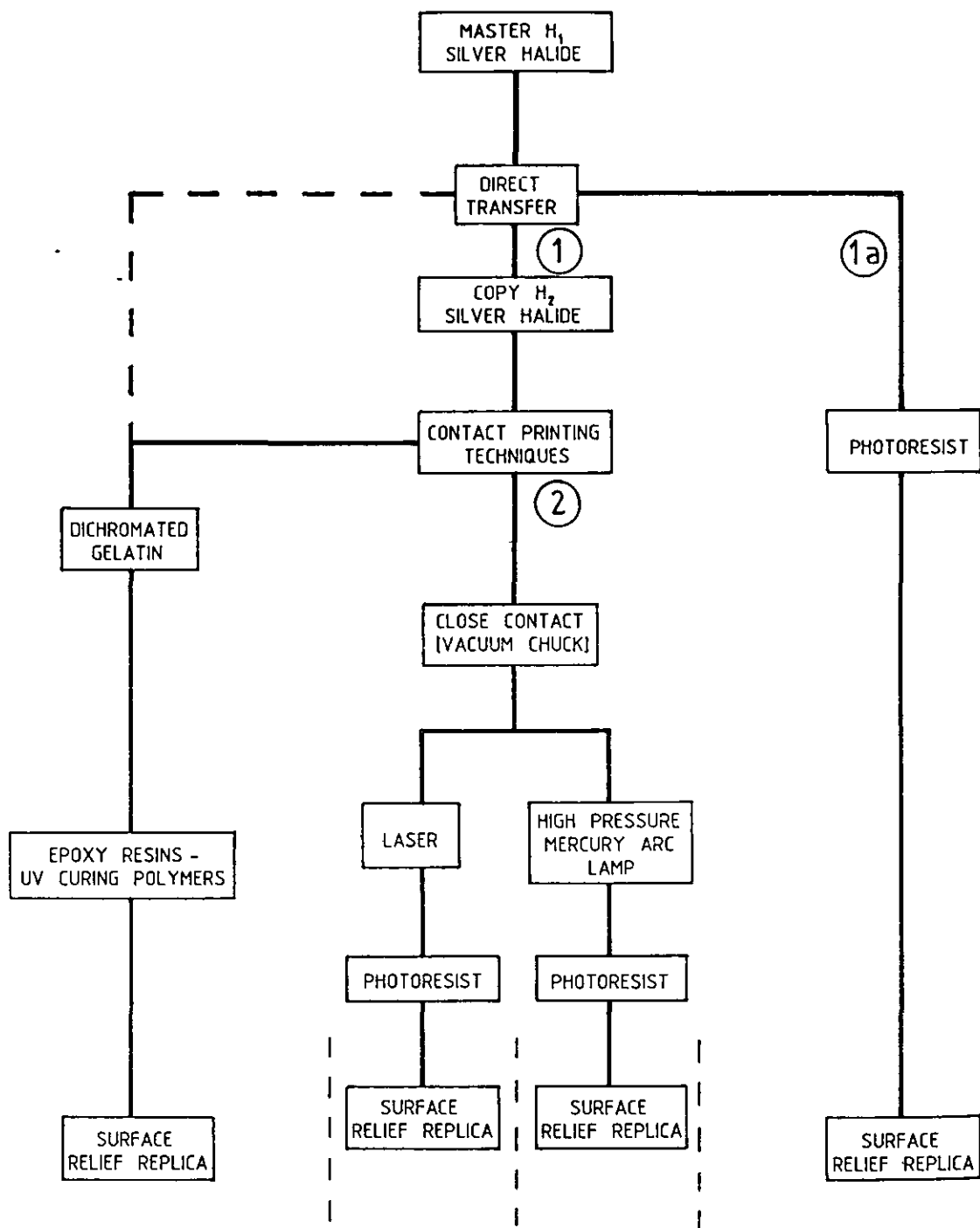


Figure 2.15 Transfer Routes to Produce  
A Surface Relief Image

environmental stability. If these requirements can not be met a silver halide 'rainbow' hologram can still be copied to produce a surface relief replica. Route 2, Figure 2.15.

The intermediate silver halide hologram is made using holographic copy techniques of 'rainbow' holography as detailed. The advantages of this method are;

1. The increased sensitivity of silver halide materials over photoresist allows reduced exposure times and use of smaller laser outputs.
2. The white light copies produced in this way are highly efficient, bright images with low noise and image distortion.

The disadvantages are;

1. Silver halide material produces limited surface relief detail. The gelatin substrate would not withstand the physical and mechanical copying processes for the embossing sequence.
2. Copying into silver halide followed by transfer into surface relief material involves additional processing and handling stages.
2. Images recorded in silver halide at 514nm and transferred into photoresist at 350-488nm suffer image distortion.

Transfer into photoresist, better suited for subsequent stages, is achieved by contact printing techniques. The white light copy and photoresist plate are held together and exposed to radiation of 350-488nm, (useful sensitivity range of photoresist). Holographic information is transferred by diffraction through the silver halide copy. The exposed photoresist softens (positive working resist) and is removed by development leaving unexposed areas in tact. This produces a copy of the silver halide hologram in photoresist in the form of a surface relief pattern. The sensitivity range of photoresist allows different sources to be used as the exposing radiation;

- 1) Contact printing using vacuum frame and high pressure mercury arc lamps.

- 11) Contact printing using lasers with suitable output wavelengths.

### 2.6.2 Theory of Vacuum Frame Printing

Work in this area has been reported by several workers [5,6,10,18] and as early as 1952 [32]. Rogers described the copying process as the production of a Gabor type hologram of a transparency - where the original hologram acts as a transparency through which light is diffracted and the interference pattern copied.

Harris et al [5], acknowledged the need for a high resolution copying system, without the use of lenses and was the first to mention the shadowing or "Venetian blind" effect. The finite thickness of the hologram fringes require the hologram to be orientated with respect to the copying beam so as not to shadow the fringes. To best achieve this, contact printing methods holding hologram and copy material in intimate contact are necessary. Harris used high pressure mercury arc lamps and ensured that the light source subtended only a small angle. The holograms used for copying had fringe separations of  $1.6\mu\text{m}$  and  $3.2\mu\text{m}$ , intimate contact between the hologram and copy plate was achieved by use of a commercial vacuum printing frame. The copy plate records the original interference pattern from the white light hologram by diffraction through the silver halide emulsion. Despite being copied in this fashion the hologram that results still appears as a positive image, the phase information of the copy is reversed but this does not affect the visual image.

### 2.6.3 Contact Printing by Non-Laser Source - Mercury Arc Lamp

The intimate contact required between hologram and copy plate is most easily achieved by vacuum printing frames. Such intimate contact may produce interference fringes such as Newtons rings caused by the air/glass interface which can be overcome by index matching fluids, such as xylene. The holographic information is copied by diffraction of light through the hologram. The nature of the exposing light source is important in that it should be monochromatic to avoid image blurring and have some degree of coherence to overcome unwanted diffraction effects that may occur between the hologram and copy plate.

Consider Figure 2.16. The white light silver halide hologram,  $H_2$ , is placed in intimate contact with the copy plate, CP. For diffraction effects between  $H_2$  and copy plate, CP, to be ignored the separation,  $p$ , must be less than the wavelength of radiation used to illuminate the copy assembly. Considering the wavelength from a filtered mercury arc source may be 350nm, such a separation is very difficult to achieve without the use of vacuum printing frames. In order to accurately copy the hologram the complex amplitudes of the interference pattern must be recorded. This can be done if the degree of coherence of the illuminating source is sufficient to produce high visibility interference fringes between the undiffracted and diffracted light over the surface of the the copy plate, CP. The coherence properties of a mercury arc lamp differ from those of a laser source with a high degree of spatial and temporal coherence. High coherence sources are essential for recording interferometric fringe patterns.

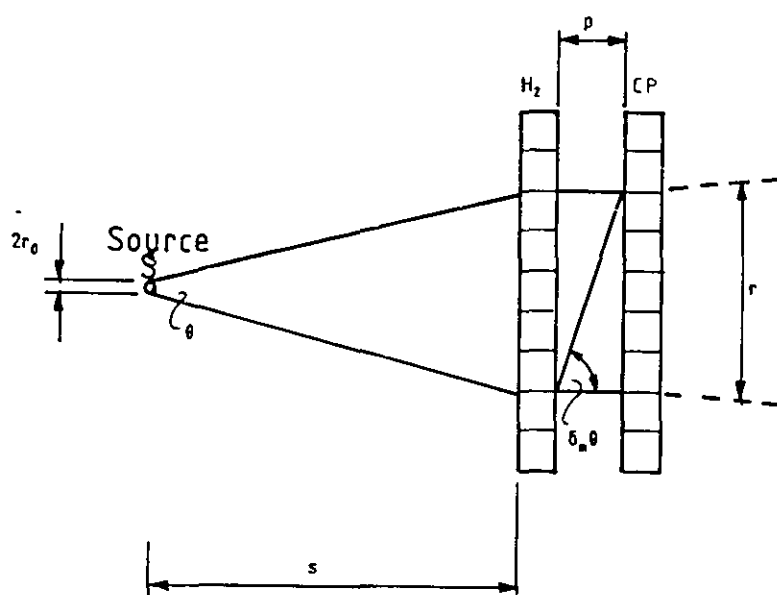


Figure 2.16 Contact Printing A Hologram

The factors which determine the degree of spatial coherence needed in the source are considered below to explain why non-laser sources can be used to replicate holograms.[33].

If  $\delta_m \theta$  is the maximum angle at which light is diffracted and is normally incident ( $i=0$ ) from source S over the surface of H<sub>2</sub>, then diffraction of normally incident light is given by;

$$d \sin \delta_m \theta = \lambda \quad \text{.....1}$$

where d is the smallest fringe spacing recorded in the hologram, H<sub>2</sub> and  $\lambda$  is the wavelength of light used. The light source S, as in Figure 2.16 must have a high degree of spatial coherence over a cone whose angle is

$$\theta = \frac{r}{S} = \frac{p \tan \delta_m \theta}{S} \quad \text{.....2}$$

if all of the diffracted light is to interfere at H<sub>2</sub> with the undiffracted light.

Spatial coherence of a source is a function of the product  $\theta r_0$ , where  $\theta$  is given by equation 2, and  $r_0$  is the radius of the source S. In practical terms with nearly all sources,  $\theta$  is so small that any source with moderate radius  $r_0$  has sufficient power and sufficient spatial coherence to record the hologram,  $H_2$ , into a copy plate. Hence a mercury arc lamp, a line source with a possible power output of hundreds of watts can be used to replicate holograms.

The temporal coherence of a mercury arc source must also be sufficient to correctly replicate the hologram,  $H_2$ , into a surface relief material on the copy plate. The coherence length  $\Delta L_H$  of the source S must exceed the maximum optical path difference between diffracted and undiffracted light. (The same is true for all holographic recording regimes whereby path lengths of the interferometer must always be less than or equal to the coherence length of the source.)

From Figure 2.16, the path difference is  $[p/(\cos \delta_m \theta)] - p$ , the coherence length,  $\Delta L_H$ , must therefore be;

$$\Delta L_H > \frac{p(1 - \cos \delta_m \theta)}{\cos \delta_m \theta}$$

or

$$p < \frac{\cos \delta_m \theta}{1 - \cos \delta_m \theta} \Delta L_H \quad \dots\dots\dots 3$$

Holograms formed in a photographic emulsion are considered plane when  $\delta_m \theta$  is small, so that we can approximate  $\sin \delta_m \theta$  by  $\delta_m \theta$  and may set  $\cos \delta_m \theta \approx \lambda/d$  so that from equation 3, we have;

$$p < \Delta L_H [2(d/\lambda)^2 - 1] \quad \dots\dots\dots 4$$

This expression gives the separation necessary to achieve correct replication from a white light hologram using any source. Taking a mercury arc lamp as an example, a high pressure source may have a coherence length of approximately 0.2mm at a wavelength of 435nm. For a

plane hologram,  $d/\lambda$  can be taken as 3 [33]. From equation 4, this would require a plate separation  $p$ , of less than 3.4mm which is easily possible with vacuum printing frames.

This example has shown that it is possible to replicate white light holograms by contact printing techniques using non-laser sources which reduce the constraints of excessive exposure times and interferometric stability. Coherence properties of the chosen source can be calculated to ensure that experimental regimes can be met. The merits of using non-laser sources are summarised in Table A.

#### 2.4.4 Contact Printing Using Laser Sources

The second source of radiation suitable to expose the assembly of hologram and copy plate is the laser. Exposure of photoresist at 456 nm and 488 nm is possible using an argon-ion laser. Exposure times are increased by the low output powers at these wavelengths but stability for contact printing systems is less critical and longer exposure times do not present a problem.

The laser output offers increased coherence lengths over that of a mercury arc lamp. This reduces the need for intimate contact as explained previously and copies can be made without vacuum frames. The mechanism for contact printing is the same as for non-laser sources, by diffraction through the original hologram. Table A compares non-laser and laser based contact printing techniques.



Non-laser source	Laser source
eg. High Pressure Mercury Arc Lamp	eg. Argon Ion Laser
Specialised units with high power output at 350nm (peak resist sensitivity).	Possible outputs of 457-488nm.
Limited coherence properties dictate use of vacuum printing frames.	High coherence properties even in blue wavelengths.
	Limited power output at peak resist sensitivity (Argon ion laser).
Multi-line output unless narrow band filtered.	Single wavelength output.
Limited optical arrangements when using specialised units.	Unlimited optical arrangements possible.
Initial unit cost, £10K. High pressure lamp, replacement cost, £5K. Minimum running/maintenance cost.	Initial unit cost, £40K. Replacement laser tube cost, £8K. High running/maintenance cost.
Unit restricted to contact copying.	Laser available for holoram/grating recording.

Table A Merits of Laser and Non-Laser Sources for Contact Printing

## 2.7 Experimental Detail - Contact Printing Techniques

### 2.7.1 Contact Printing by Non-laser source - Mercury Arc Lamp

The loan of a 200W Oriel Mercury arc lamp and vacuum chuck substrate holder made it possible to conduct a number of contact printing transfers. The optical arrangement is illustrated in Figure 2.17

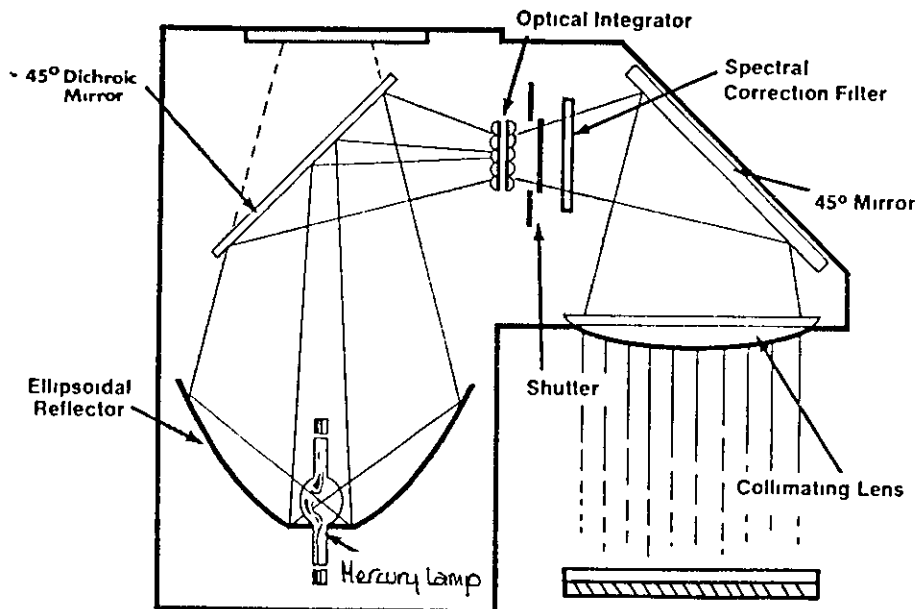


Figure 2.17 Contact Printing Using High Pressure Mercury Arc Unit

A six inch collimated beam of light was directed at normal incidence to the hologram and copy plate assembly. The all-lines output of the lamp was  $36\mu\text{W}/\text{cm}^2$ . The original hologram used in early trials was a white light 'rainbow' hologram of a metal cube with resolution chart and fine detail. The hologram was considered visually 'bright' and

clean. The copy plate assembly was held by the vacuum chuck, with the photoresist copy plate the silver halide hologram, emulsion to emulsion. When the vacuum was applied to the chuck interference fringes between the two plates appeared and changed as vacuum pressure was varied, the plates could not be separated until the vacuum was released.

Initial trials were made using the all-line output of the lamp. Experimental details are given below:

Photosensitive material:	Copy Plate - Shipley AZ1450B Photoresist
Substrate:	3"square glass, self spun resist, 1 $\mu$ m
Baking:	95°C, 25 minutes
Exposure time:	3-5 seconds all-line output at 36 $\mu$ W/cm <sup>2</sup> 2-3 minutes 350nm output at 13 $\mu$ W/cm <sup>2</sup>
Development:	Shipley AZ303, 20°C, 30 seconds, 1+5 dilution.

Initial copies showed interference fringes between hologram and copy plate. To overcome this index matching fluids such as xylene, liquid paraffin and collodion solutions were tried. It was found that xylene gave the best results but complete elimination of fringes was dependant upon thickness and quantity of index matching fluid used. If the plate assembly was left too long before exposure, the fluid would seep from the sides leaving a void in the middle of the copy assembly and large circular fringes would transfer to the copy hologram where the fluid had escaped. The use of an all-line output also added to interference fringe problems and a 350nm narrow band filter was used in the mercury arc lamp to overcome this. The lamp output dropped by almost a third and exposure times for the photoresist plate had to be increased accordingly. The improvement in image brightness was immediate and the use of index matching fluid, namely xylene continued. The images were not free of all fringe patterns but almost entire and bright images were achieved by contact copy using vacuum frame.

The experiments in this series demonstrated results were possible by contact printing a silver halide hologram onto a photoresist copy plate. The original hologram could equally well be copied into silver halide if a surface relief hologram is not required. Use of a matt backing on the copy plate improved the contrast of images and reduced internal reflections arising from the back surface of the copy plate. The technique could be applied to mass replication of 'rainbow' holograms if necessary although direct transfer would be recommended to reduce handling and wear upon the original. Transferring into photoresist material is greatly facilitated by this technique however due to shorter exposure times and reduced interferometric stability requirements.

#### 2.7.2 Contact Printing by Laser Source

The advantage of using a laser source instead of a mercury arc lamp is the increase in coherence length. This increased coherence reduces the need for intimate contact between hologram and copy plate. The same problems of interference fringes can be eliminated by index matching fluids and backing the copy plate. The optical arrangement used is illustrated in Figure 2.18

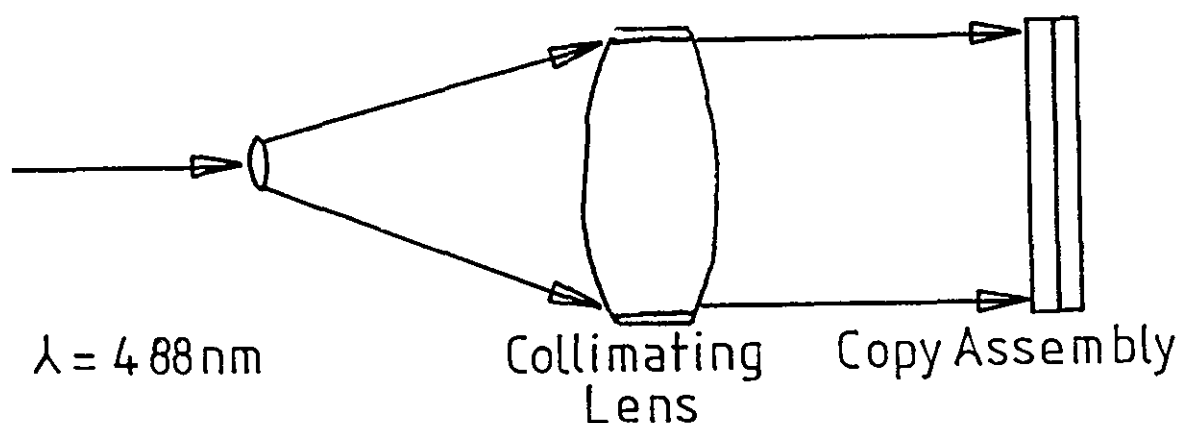


Figure 2.18 Contact Printing Using a Laser Source

The collimated laser beam illuminated the copy plate assembly of photoresist and copy plate. The angle of incidence of the illuminating beam could be easily varied but was directed normal to the assembly. The two glass plates were held upright within a frame holder and sealed together at the edges using opaque tape. The tape also prevented any stray illumination from scattering within the edges of the plate assembly.

The drawback of this technique was the introduction of additional handling stages which despite clean conditions and the use of cotton gloves could not prevent dust and dirt settling between the plates. The process also transferred all marks from the original silver halide to the photoresist by diffraction around any marks. Consequently the original plate had to be scrupulously clean and dust free to produce quality transfers.

The experimental details are given below;

Photosensitive material:	Copy Plate - Shipley AZ1450B Photoresist
Substrate:	3"square glass, self spun resist, 1 $\mu$ m
Baking:	95°C, 25 minutes
Exposure:	15 minutes at 457nm, at 13 $\mu$ w/cm <sup>2</sup>
Development:	Shipley AZ303 developer, 20°C, 1 minute, 1+5 dilution.

Observations These contact copying techniques offered advantages over direct, interferometric transfer regimes by reducing the requirement for environmental stability. Transfers could be obtained quickly and easily with no operator skill necessary once the initial silver halide hologram had been produced. Purpose built mercury arc systems with vacuum frame assemblies, automatic timers, loading mechanisms etc. are ideal for mass replication of small format plates. The added advantage of the laser over the mercury arc lamp was the reduced constraint for intimate contact due to increased source coherence. The initial outlay and running costs of the laser as opposed to the mercury arc unit should not be overlooked. Merits are summarised in Table A.

## 2.8 Summary

This chapter has considered the first stages of the Information Transfer Process, that of image recording and optical copying. The production of laser transmission holograms and the white light copies taken from the 'master' have been detailed. The recording of the diffraction gratings used in this study has also been outlined. The essential feature of this first stage is the production of information in the form of surface relief detail. This surface pattern then undergoes physical and mechanical copying stages to produce a surface detail in plastic with the same clarity and accuracy as that recorded in the initial stages. The alternative copying techniques using laser and non-laser sources for contact printing have been presented. These methods overcome the need for large laser outputs and environmental stability but are not without disadvantages. The theoretical and experimental detail for the holograms recorded by contact printing have been given

No difference in the nature of the surface relief pattern produced from direct, interferometric transfer or contact printing techniques has been found in the study undertaken. Scanning electron and optical microscopy investigations have shown that both techniques produce a distinct surface relief pattern, the depth of which has been sufficiently pronounced to allow metal and plastic replicas to be produced.

Conclusions drawn from the experimental results are as follows:

- Contact copy holograms of equal visual "brightness" as the original hologram have been produced by non-laser and laser sources contact printing methods.
- Vacuum chuck copy assembly was essential to overcome interference fringes when using a non-laser source.
- Index matching fluids eliminated interference fringes arising between the copy plate assembly.
- The reduction in exposure times for non-laser sources and ease of copying process was valuable especially when numerous copies were

required.

- The contact copy process transferred dirt and marks from the original hologram despite clean handling conditions.

The following chapter will consider the choice and importance of the photosensitive material used to record the surface relief pattern. A number of materials are considered and a detailed theoretical and experimental analysis of the material used to record the series of diffraction gratings assessed in this work is presented.

## CHAPTER 3

### SELECTION OF SURFACE RELIEF MATERIAL FOR OPTICAL COPYING

#### 3.0 Introduction

The previous chapter described the recording of a 'master' hologram and white light copy holograms and alternative copy methods. The purpose of the first stage of the recording process is to produce an image that possesses surface relief detail. The importance of this image is that it becomes the information "carrier" through the embossing sequence and must withstand the rigours of physical and mechanical processes during the copy stages. One suitable material for recording surface relief images is photoresist but it is not the only choice. This chapter will briefly describe alternative materials for surface relief copying and give reasons for the selection of photoresist as the most appropriate material.

The characterisation and properties of the photoresist material used for recording the gratings and holograms in this work has provided a large area of experimentation. This chapter considers both positive and negative acting resist, concentrating on the positive resist used in this study. The formulation of resists is discussed and image formation models presented. The chapter also describes the experimental characteristics in terms of coating substrates, exposure and development and handling.

#### 3.1 Selection of Surface Relief Materials

The replication of a holographic element using printing techniques is dependent upon the transfer of surface relief detail through each stage of the process. The image intended for copying must therefore be recorded in a material capable of generating surface relief detail.



The requirements of such a material are;

1. It should possess good surface relief characteristics.
2. It should have a high sensitivity to exposing radiation.
3. It should show no image distortion or noise from scattered light.
4. It should reproduce an image with high efficiency.
5. It should be easy to prepare, process, handle and store.

The materials identified as fulfilling some or all of the above requirements are;

1. Dichromated gelatin.
2. Ultra-violet curing polymers and epoxy resins.
3. Photoresist.

### 3.1.1 Dichromated Gelatin

Colloid layers sensitised with chromates (di-chromated gelatin) are an important type of imaging system forming the basis of many photographic and photomechanical processes. It has been known since the 1830's that ultra-violet or blue light can cause gelatin molecules to cross-link when there is a small amount of dichromate present in the gelatin. Dichromates alone are not photosensitive but in the presence of oxidizable organic compounds are decomposed by exposure to initiate the photo-chemical process. Although not fully understood the overall reaction of reduction of chromates to chromium oxide may be summarised as follows;



The chromium oxide is thought to react with the polar part of the gelatin substrate and cause cross-linking of the gelatin molecules (tanning) resulting in local hardening in areas of exposure. Photocrosslinking reactions involve radiation-induced cross-linking of polymer chains by one of two means. Firstly by radiation sensitive cross-linking agents incorporated into the polymer matrix (as for dichromated gelatin). Secondly, by the use of polymers which have photocrosslinkable groups attached to the polymer chain (polymeric

diazo compounds). The effect of photocrosslinking renders insoluble the exposed areas by the action of photodimerization. This leads to a three dimensional insoluble network as a result of multiple dimerization reactions within the gelatin substrate. The use of photosensitizers to extend the spectral sensitivity of the polymer also enhances the effect of photocrosslinking. The extremely high spatial resolution of dichromated gelatin results from the molecular scale of the imaging mechanism - at most a few dichromate ions and the adjacent gelatin molecules. This feature is important in holography when a resolution of  $>4000$  l/mm may be required.

Dichromated gelatin can be made to render surface relief detail. In graphic arts and printing it is typically used as a negative 'resist' whereby unexposed image areas remain soluble and are washed away by alcohol. The areas exposed to light undergo cross-linking and local hardening and become insoluble, these areas remain after processing to form the relief image. This relief image can then be dyed, contacted onto another gelatin layer to transfer the dye and produce a colour image. Three such images in yellow, magenta and cyan form the basis for colour printing in cinematography and relief image printing. Dichromated gelatin is extremely sensitive to moisture and heat and is not a very stable medium. Holograms must be hermetically sealed against moisture for long term storage. The physical and mechanical copying stages in the production of an embossed hologram such as electroforming in wet chemistry would totally destroy the image and surface relief detail.

The application of dichromated gelatin to holography has been well reported by Meyerhofer [34]. Some characteristics and properties are summarised in Table B.

### 3.1.2 UV Curing Polymers and Epoxy Resins

The use of polymers and epoxy resins are a further intermediate stage that can be used to produce a surface relief copy from an original not suitable for the electroforming process. Most often they have been used in conjunction with dichromated gelatin but references to the

usage of epoxy resins for replicating ruled gratings and optical elements are known as early as 1947 [1,3]. Epoxy resins are prepared as two part mixtures applied over the surface of the element, polymers that harden upon exposure to ultra violet light can similarly be applied over the surface and exposed under small lamp units. Once hardened the polymer can be separated from the original surface, often damaging it in the process. A similar technique is used in the preparation of replicas for electron microscopy. Solvents are used to 'mould' a plastic sheet over a surface such that the plastic replica is used in the instrument and not the original.

The problem in using such materials for replicating holographic surface relief information is the resolution required of the copy material. Line spacings of  $>4000$  l/mm may be typical for a transmission holographic recording and epoxy resins or polymers would not be capable of reproducing such line spacings. In addition the information may have a groove profile or depth that can not be accurately reproduced. Curran and Shankoff [35] claim replicas of gratings made from dichromated gelatin with periods  $>5\mu\text{m}$  copied using "Plexiglass" sheet. This method is essentially an embossing technique whereby the sheet is heated and applied under pressure, allowed to soften to conform to the original gratings, cooled and removed. Large period gratings,  $>5\mu\text{m}$ , replicate sufficiently to replay with at least 50% of the original efficiency, smaller periods,  $0.5\mu\text{m}$  show markedly reduced efficiency, to only a few percent of the original. The nature of dichromated gelatin suggests that factors such as pressure and temperature as applied to the surface are extremely critical factors. In a similar fashion, the application of solvents to 'mould' plastics to a grating structure, or the use of epoxy resins is difficult.

Characteristics of polymers and resins are summarised in Table B.

### 3.1.3 Photoresist

Photoresists are light sensitive organic materials capable of yielding surface relief detail by exposure and development. Both positive and negative acting resists are available whereby exposed areas become

soluble and are dissolved away by development (positive resist) or unexposed areas become soluble and are removed by development (negative resist)

The characteristics and properties of photoresist are summarised in Table B.

Photoresist is the most suitable material for the production of a surface relief copy and has been used extensively in this work. A detailed discussion of photoresist is presented in later sections.

#### 3.1.4 Summary

A brief consideration of two alternative materials to photoresist has been given using dichromated gelatin or epoxy resins/polymers. Both techniques have been investigated by other workers [35,36,37]. The advantages of photoresist as summarised in Table B make it the most obvious choice for the production of a surface relief copy. The remainder of this chapter will discuss photoresist in detail.

### 3.2 History of Photoresists

Modern photoresists and current photoetching processes have evolved from technology developed in the printing industry. As early as 1852, W.F.Talbot patented a photoetching process using dichromate sensitised gelatin plates. Ferric chloride solution etched patterns into copper that could be used for printing plates.

Natural organic colloids such as starch, protein, and carbohydrates are all capable of sensitization by dichromates. To produce relief images and act as a photoresist the material has to be capable of sensitization, possess chemical resistance and film forming properties, adhere to suitable substrates and be water soluble in the unexposed or unhardened state in order to be easily applied and developed. Dichromate sensitized resists are generally negative acting - exposed areas harden and become insoluble - and were in use before positive acting resists. A comparison of negative and positive acting resists is

Table B. Comparison of Materials for the Production of  
a Surface Relief Image

	MATERIAL	EXPOSURE	DEVELOPMENT	RESOLVING POWER	STABILITY
DICHROMATED GELATIN (DCG)	Fresh material prepared for each use. Limited shelf life. Temperature, humidity sensitive.	Dye sensitised to red, and blue/green sensitive	Series of water/alcohol baths. Extremely temp. critical.	> 5000 l/mm	Extremely temperature & humidity sensitive. Must be sealed against environment. Would not withstand electro-forming process.
POLYMERS / UV CURING RESINS	Applied over DCG or silver halide original.	Ultra-violet exposure hardening. (Requires surface relief pattern to copy from).	After curing period replica is separated from original.	< 2500 l/mm	Stable to environment, would withstand electro-forming process.
PHOTO- RESIST	Stock material available in range of thicknesses. Can coat own substrates if req.	350-488nm. Direct exposure/contact copy.	Alkali based developer. Automatic spray, flood development techniques.	> 4000 l/mm	Excellent stability & line accuracy. No swelling for positive resist. Would withstand electro-forming process.
SILVER HALIDE	Stock bought material. Film or plate stock.	red, green and blue sensitive	Photographic developer. Proprietary formulations available. Immersion, tank development techniques.	3000 l/mm	Emulsion sensitive to moisture, would swell and distort image in electroforming process.

made in Figure 3.1. Positive and negative acting resists share common features in that they are essentially a film forming resin dissolved in a solvent system.

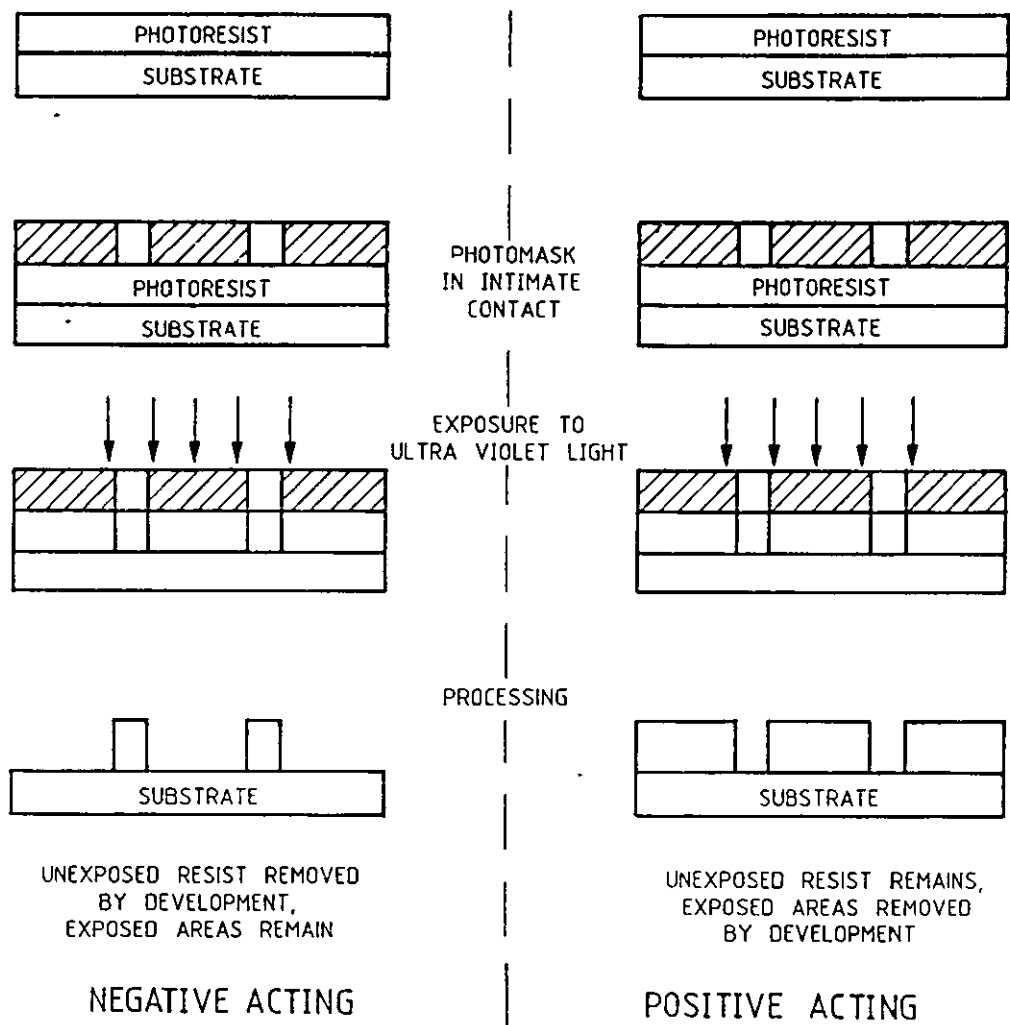


Figure 3.1 Negative and Positive Working Photoresist

• Positive acting resists are more recent - although the photosensitizers used in them were in use in diazo processes in the 1890's. Diazo systems are photochemical, non-silver imaging processes still widely used, being simple and economic to use, producing direct positive copies

Diazo systems are based on diazonium compounds and have two essential features for photo-imaging;

- a) the diazonium compound can be decomposed by radiation,
- b) the un-decomposed diazonium compound can couple with colour formers to produce a stable image.

Modern types of resists are based upon cinnamic acid derivatives, which are intrinsically photosensitive compounds and offer advantages over the dichromate system such as extended shelf life and improved resolution. Originally used in the graphic arts for producing lithographic plates they were recognized as suitable materials by which to form positive images. Cinnamic acid and its derivatives were mixed with natural film forming gums and resins to prevent the cinnamate compound from crystallizing. During the 1940's and 1950's much study of cinnamates was carried out and typically cinnamoyl chloride was used to react with polymeric materials to form light-sensitive esters and ketones possessing high molecular weight, good solvency and excellent film-forming properties. The introduction of the KPR resin, cinnamate ester of polyvinyl alcohol, by Kodak in 1953 was the beginning of the trend with over 40 new photoresists introduced to serve the rapidly expanding electronics industry over the following 17-20 years.

The unique properties of accurately reproducing chemically resistant images on metal and oxide surfaces have made photoresist the premiere material in the electronics industry. The history of their usage can be traced in the Figure 3.2

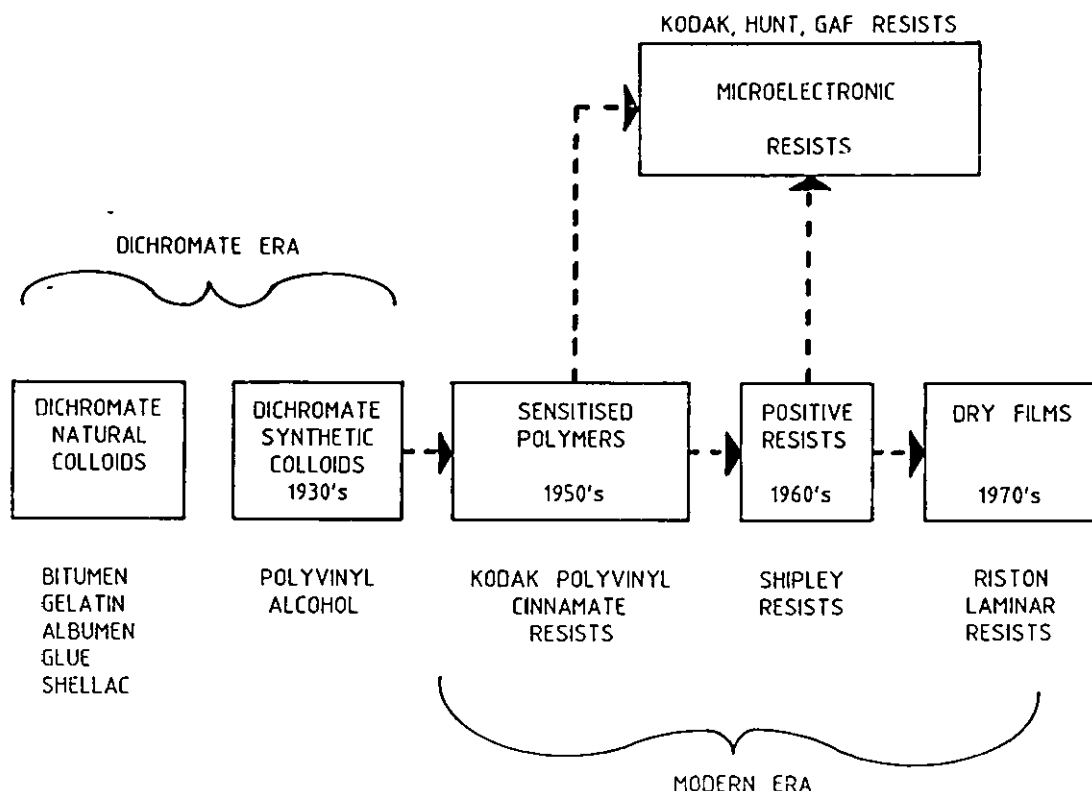


Figure 3.2 The History of Photoresists

### 3.3 Negative Resist

Negative acting resists are characterised by high chemical resistance, good image reproduction qualities and low cost.

Resins for negative resists must be capable of insolubilization by reaction with sensitizers activated by absorbed light energy in the process of exposure. All modern resists have resins that possess "chemical unsaturation". This relates to a chemical bond between two carbon atoms through shared electron pairs in the same molecule. Upon activation the one electron pair can be shared by carbon atoms of adjacent polymer molecules which are similarly unsaturated. The sharing of an electron pair by carbon atoms in adjacent polymer molecules is referred to as 'cross-linking' and has a profound effect



on the physical properties of coatings in which it occurs. Cross-linking increases the hardness, chemical resistance and adhesion to the substrate. It is this property of 'cross-linking' that causes the exposed areas of the negative resist to become hardened and rendered insoluble. Figure 3.3 The process involves chain propagating reactions induced by the absorption of radiation and sets up an interconnected three-dimensional network within the structure of the resist. As a result of this network the exposed areas are sufficiently polymerized so as to lose their solvency and the exposed areas remain after exposure and development. The unexposed areas that remain as linear polymers keep their solvency and are removed in the developer.

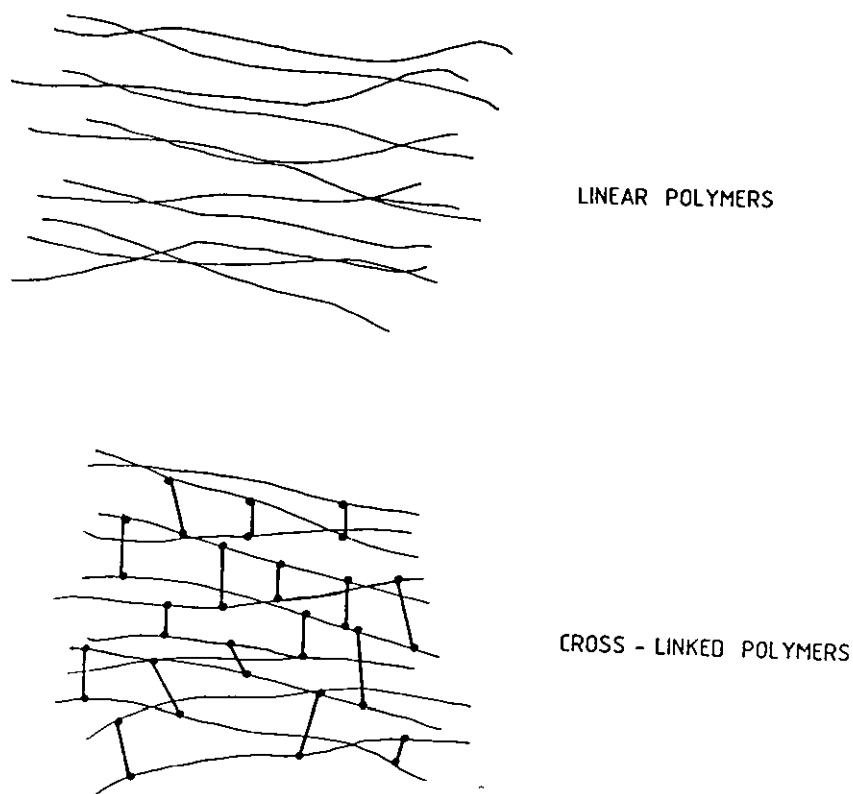


Figure 3.3 Linear and Cross-Linked Polymers

The polymers commonly used in negative resists are linear polymers such as vinyl or polyvinyl compounds. These polymers are only held by secondary forces weaker than electron bonds, bonds which are easily broken by heating - ie. the absorption of thermal energy, the process by which melting occurs. If the polymers have a photo-cross-linkable group attached, polymerisation may occur upon exposure and produce a stronger, more brittle structure with greater thermal and chemical resistance. Such a compound would not melt, the bonds would rupture upon heating to form new lower molecular weight compounds. The process of cross-linking is enhanced by including photosensitizers in the emulsion make-up. These also extend the spectral sensitivity of the polymer to cover a greater range of wavelengths and typically involve aromatic nitro and ketone compounds.

The main disadvantage of negative resists in holography is the need for good adhesion to the substrate. The unexposed areas of resist are removed by development whilst the exposed areas are hardened by the action of photo-cross-linking and remain upon the substrate. To ensure good adhesion, sufficient exposure is necessary and the exposure required to achieve this adhesion may actually exceed the desired holographic exposure for quality holograms. If the hologram consisted of very fine lines of photoresist these could either detach from the substrate due to insufficient exposure, or be inaccurate by the over-exposure necessary to ensure good adhesion. This problem would not arise from positive resist due the different mechanism of image formation. The exposure of negative acting resists is a critical parameter (more so than for positive resist) the development of which requires solvents such as xylene or cyclohexanone solutions which necessitate adequate precautions for safe working such as ventilation and skin coverage. A further drawback of negative resists for holography is that the developer, whilst capable of dissolving unexposed areas is also absorbed by the exposed areas so causing swelling of the resist. This swelling causes image distortion and is obviously undesirable.

### 3.4 Positive Resist

Positive resists, yield extremely accurate images, the development of which is more straightforward than for negative resists, using mildly alkaline solutions rather than xylene based solvents. In addition, no swelling of the emulsion occurs accounting for the greater image accuracy. The resist is stripped by aqueous solution, important for cleaning and re-processing since the optically flat substrates are expensive to produce and typically re-used. The composition of positive resist is essentially the same as that for negative resist, a resin system with sensitizers, solvents and additives. The mechanism of image formation however is totally different from that for negative resist. Whilst photo-crosslinking and polymerisation accounts for the hardening of negative resists and it would be logical to assume that some type of de-polymerisation occurs in positive resists to soften exposed areas. Detailed composition of positive resist and proposed image formation models are presented in Appendix 3. An outline of the image formation mechanism is given before considering the image formation model proposed by Bartolini and the experimental used to study this model

#### 3.4.1 Image Formation Mechanism

The sensitizers used in positive resist are most usually diazo oxide or orthoquinone diazide derivatives. The sensitizer reacts with absorbed radiation to result in a change in the solubility of the composition from solvent-soluble to water-soluble. The sensitizer does not react with the resin in the composition; consequently the sensitizer is a prime constituent and present in high proportions.

In reacting with the absorbed radiation, quinone diazides undergo major physical changes. [38] A new compound is formed as a result of rearrangement of the ring structure containing the nitrogen and oxygen. Along with the new compound nitrogen is evolved. This physical reaction is illustrated in Figure 3.4

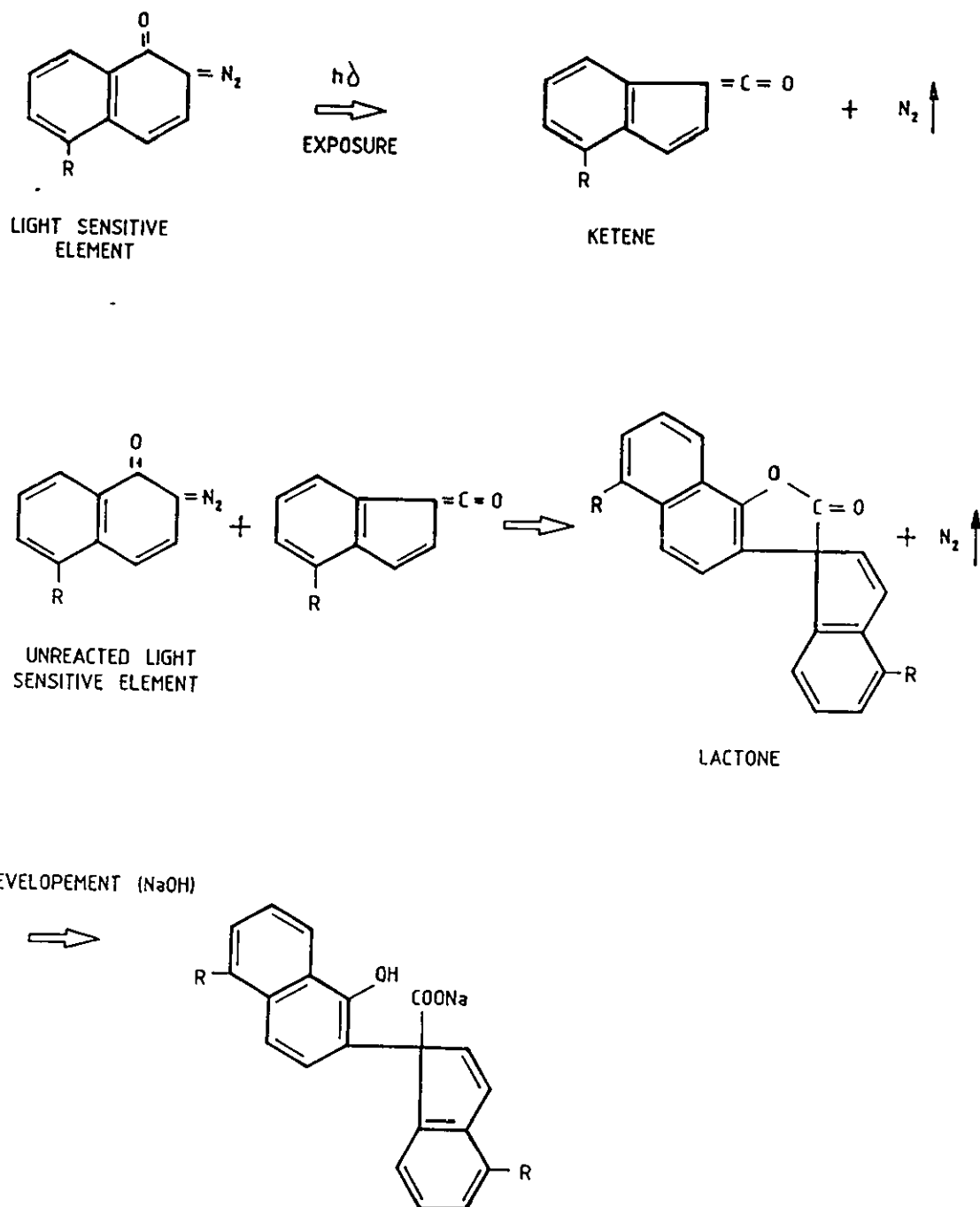


Figure 3.4 Reaction of the Light Sensitive Element  
with Absorbed Radiation

The process begins with the re-arrangement of the ring structure by the absorption of radiation to produce a ketene. Levine [39] studied several positive resists by infra red spectroscopy to determine the nature of the photochemical structures. Results suggested the presence of 1,2 and 1,3 benzo- and naphthoquinone diazide groups. Such groups readily undergo re-arrangement. The reaction, known as the Wolff re-arrangement results in the loss of nitrogen from the diazo carbon and the carbonyl to the former diazo carbon. This produces a ketene which hydrates readily to form a carboxylic acid.

This type of photochemically induced re-arrangement producing a carboxyl group renders the molecule soluble in aqueous alkali solutions, corresponding to the behaviour observed in positive photoresists. The presence of ketenes during exposure has been difficult to confirm because they react so rapidly. Nitrogen is evolved in this reaction. It was suggested by Levine [39] that the ketene reacts with the remaining light sensitive elements not affected by exposure. This reaction occurs downwards through the thickness of the coating, suggesting that the first stage is a surface layer reaction. The result of the unreacted element and the ketene reaction is the evolution of nitrogen with the formation of a lactone. Lactones are ring compounds having hydroxyl groups at the end opposite a carboxylic acid group. Development in alkaline solution, (NaOH) breaks the lactone ring to produce a carboxylic acid group salt.

In summary, the reaction which results in image formation involves the conversion of the functional groups within the sensitizer changing it from a hydrophobic diazide to a group soluble in dilute aqueous alkaline solutions. This occurs by means of neutralization and salt formation. It should be stated that the precise mechanism of image formation is not fully understood. The interpretation by Levine differs from that of other workers, who whilst agreeing with the formation of ketones believe they react with water present in the emulsion to produce carboxylic acid groups. The developing solution (NaOH) then neutralizes the acid groups. For this reaction to occur it is necessary to have moisture ( $H_2O$ ) present within the emulsion for the

ketene to react with. The baking cycles given to pre-exposed resists are designed to evaporate excess solvents and moisture so this mechanism is not generally accepted.

The positive resist used for this work was Shipley AZ1350B, the appearance of which suggests a novolak resin based in a xylene solvent system. The range of the Shipley 1450 series resists varies in viscosity and solids content (for use at different spin coating speeds) but offers identical imaging characteristics.

#### 3.4.2 Summary

The history and applications of photoresists have been outlined and the composition of positive and negative photoresists compared. The advantages of positive resist offering increased accuracy and adhesion, no swelling and ease of development makes it ideally suited for applications ranging from micro-electronics to holographic recording.

The following section will detail an image formation model proposed by Bartolini that has been used in the experimental work undertaken in this study.

### 3.5 Bartolini Model for Characterisation of Positive Photoresist

Appendix 3 details models proposed for the image formation of positive resist. From those models, that by Bartolini was developed to consider the experimental aspects of image formation. The following section expands the model proposed by Bartolini [40] and includes experimental parameters determined in the theory.

The prime characteristic of photoresist material is the change in layer thickness  $\Delta d$ , caused by an exposure  $E$ . The relationship between  $\Delta d$  and  $E$  can be found by considering the Lambert Law whereby equal paths in the same absorbing medium absorb equal fractions of the light that enters. Hence at a depth,  $dx$  the intensity may be reduced from  $I$  to  $I - dI$ . Lamberts law states that  $dI/I$  is the same for all elementary paths of length  $dx$ ,

$$\frac{dI}{I} = -K \cdot dx \quad \dots\dots\dots 1$$

where  $K$  is constant term known as the absorption coefficient.

$$\log I = -Kx + c \quad \text{where } c = \text{a constant}$$

If  $I = I_0$  at  $x=0$ ,  $c = \log I_0$  and

$$I = I_0 \cdot e^{-Kx} \quad \dots\dots\dots 2$$

Applying this to the exposure of photoresist, the constant K can be defined in terms of absorption cross section of the molecule and density of the absorbing molecules, hence at a depth x (cm);

$$I(x) = I_0 \exp(-\alpha N_1 x) \quad \text{.....3}$$

where  $I_0$  = intensity of light irradiance on resist surface (mW/cm<sup>2</sup>)

-  $\alpha$  = absorption cross section of molecule (cm<sup>2</sup>)

$N_1$  = density of absorbing molecules (cm<sup>-3</sup>)

If the photoresist layer is thin, a few micrometers, the percent absorption will be small and the number of photons N (cm<sup>-2</sup>.sec<sup>-1</sup>) available for absorption throughout the material is expressed by;

$$N = I_0/h\nu$$

$h$  = Planck's constant

$$(6.23 \times 10^{-31} \text{ mJ.s})$$

$\nu$  = frequency of light (s<sup>-1</sup>)

By equating the time t, rate of decrease of unabsorbed (unexposed) molecules,  $-dN_1(t)/dt$  with the rate of creation of absorbed (exposed) molecules, for a small absorption only,  $I(x)I_0$ .

$$-\frac{dN_1(t)}{dt} = n_q I_0/h \alpha N_1(t) \quad \text{.....4}$$

Photoresist (as with silver halide systems) is not a totally efficient system and so not all of the absorbing molecules react accordingly, i.e. become excited when absorbing a photon. Hence, quantum efficiency,  $n_q$  is introduced and defined as the number of excited molecules per number of absorbed photons



Solving equation 4 for  $N_1(t)$ ;

$$N_1(t) = N_0 \exp \frac{(-n_q \alpha I_0 t)}{h\nu} \quad \text{.....5}$$

$$\text{or} \quad Du = \frac{N_1(t)}{N_0} = \exp(-\alpha_0 E) \quad \text{.....6}$$

where  $Du$  = fraction of unabsorbed (unexposed) photoresist molecules

$N_0$  = initial density of total resist molecules ( $\text{cm}^{-3}$ )

$\alpha_0 = n_q \alpha / h\nu \cong$  exposure constant for positive resist ( $\text{cm}^2 \cdot \text{mJ}^{-1}$ )

$E = I_0 t$  = photoresist exposure ( $\text{mJ}/\text{cm}^2$ )

Relating the fraction of absorbed (exposed) molecules ,  $Da$

$$Da = \frac{N_2(t)}{N_0} \quad \text{.....7}$$

where  $N_2(t)$  = density of positive molecules that have absorbed  
a photon ( $\text{cm}^{-3}$ )

then with  $Da + Du = 1$  we have;

$$\begin{aligned} Da &= 1 - Du \\ &= 1 - \exp(-\alpha_0 E) \quad \text{.....8} \end{aligned}$$

The mechanism for positive resist is believed to be one whereby exposed (absorbed) and unexposed (unabsorbed) portions are attacked by the developer but at differential rates, then the etch rate model for the thickness change,  $\Delta d$  ( $\mu\text{m}$ ) at any one point can be described by;

$$\Delta d = (D_{ar1} + D_{ur2})T \quad \text{.....9}$$

where  $r_1$  = removal etch rate of exposed molecules during development ( $\mu\text{m/s}$ )

$r_2$  = removal etch rate of <sup>un</sup>exposed molecules during development ( $\mu\text{m/s}$ )

$T$  = development time (secs)

(Effects of developer flow or agitation are not considered, refer to surface limited reactions in other models, Appendix 3.)

Substituting  $D_a$  and  $D_u$ , with  $\Delta r = (r_1 - r_2)$

$$\Delta d = T[r_1 - \Delta r \exp(-\alpha_o E)] \quad \text{.....10}$$

If no exposure were given, i.e.  $E=0$ , then  $\Delta d$  is determined purely by the removal etch rate of the unexposed molecules. With a heavy exposure,  $E$  very large,  $\Delta d \sim r_1 T$ , i.e. the material change,  $\Delta d$  is determined solely by the exposed molecules rate constant.

$$\text{If } \alpha_o E \ll 1 \text{ then } \Delta d \sim \Delta r T \alpha_o E + r_2 T \quad \text{.....11}$$

Hence the relationship between material change and exposure  $E$  has become a linear one determined by a constant term  $r_2 T$  and the exposure term  $\Delta r T \alpha_o E$ .

Appendix 3 outlines Bartolini's consideration of material and inherent non-linearity. Whilst Bartolini believed inherent non-linearity could be overcome by correct processing, the material non-linearity is effectively expressed by equation 10,

$$\Delta d = T[r_1 - \Delta r \exp(-\alpha_0 E)] \quad (10)$$

If  $\Delta d$  can be expressed by equation 11, then the material non-linearity is removed. This can only be possible if  $\alpha_0 E \ll 1$  and so a value for the constant  $\alpha_0$  is needed.

From equation 6, where  $\alpha_0$  = exposure constant,  

$$= n_q \alpha / h\nu$$

Broyde [41] has found for Az 1350 resist,

$$n_q = 3.2\% \quad \text{and} \quad \alpha = 6.25 \times 10^{-17} \text{ cm}^2$$

$$\alpha_0 = 0.5 \times 10^{-2} \text{ cm}^2 \cdot \text{mJ}^{-2}$$

With the value of  $\alpha_0$  known, the usable range of exposures is also known, which in turn can give the usable values of material thickness change  $\Delta d$ .

### 3.5.1 Experimental Considerations of Material Non-Linearity

For photoresist to be a useful recording material, the relationship between exposure  $E$  and thickness change  $\Delta d$ , should hold for parameters met in a holographic recording situation. In practice, exposure values vary considerably according to particular type of resist used and available laser power. A linear relationship between exposure and thickness change would ensure distortion and noise could be kept to a minimum and mean that any limiting factors arise from inherent non-linearities of the recording process and not material non-linearity. For this linear relationship to exist the nature of the developer must be included in any model or evaluation of a system.

All positive resist developers are alkaline solutions but vary in pH, rate of etch and activity. Typically for AZ1350 resist systems, an AZ303 developer was used and Bartolini had shown that the relationship between  $E$  and  $\Delta d$  was non-linear with this recommended developer. Use of the AZ303 developer overcomes this problem when diluted with distilled water. The dilution factor is important since a too strong solution will remove unexposed resist at too great a rate. It is known that both exposed and unexposed resist is removed by a developer but the rate at which the unexposed is removed is important in avoiding image distortion. An additional advantage of using AZ303 is the apparent increase in sensitivity of 2.5 to 1 over AZ1350.

A measure of the etch rate of a developer can be found by plotting values for exposure  $E$  versus thickness <sup>change</sup> $\Delta d$ , this is true for any one resist/developer combination as illustrated in Figure 3.5.

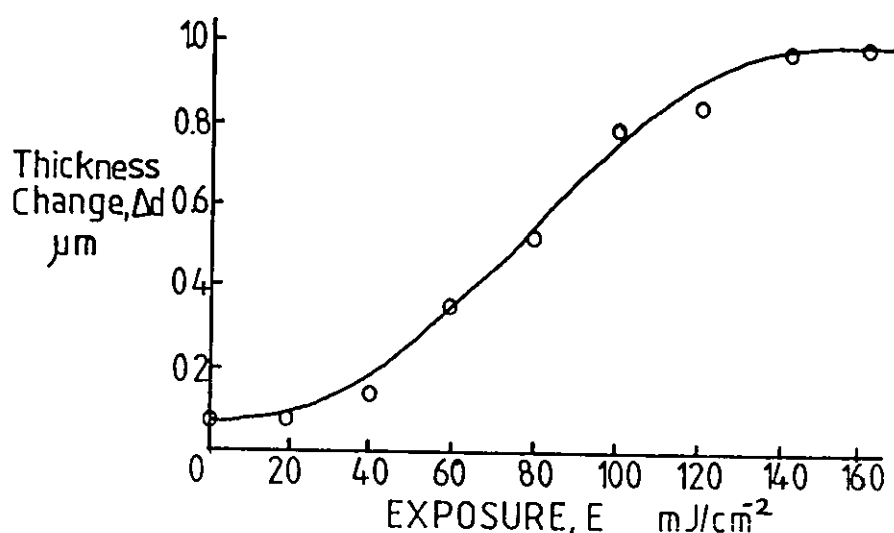


Figure 3.5 Thickness Change  $\Delta d$  Versus Exposure  $E$

Referring to the series of Bartolini equations;

$$\Delta d = T[r_1 - \Delta r \exp(-\alpha_0 E)]$$

At  $E = 0$ ,  $\Delta d = r_2 T$  hence a value for  $r_2$  is calculated by;

$$r_2 = \frac{\Delta d}{T} \quad \text{and} \quad \Delta r \alpha_0 = 0.5 \times 10 \mu\text{m.cm}^2.\text{mJ}^{-1}.\text{s}^{-1}$$

with this value,  $\Delta r$  can be calculated whereby  $\Delta r = r_1 - r_2$  (exposed etch rate - unexposed etch rate).

In knowing both these values a series of curves can be plotted to demonstrate the linearity of the relationship between  $E$  and  $\Delta d$ . This is useful in predicting the behaviour of grating profiles exposed in photoresist when, if the exposure characteristic for a specific development time  $T_1$  is known, the etch depth for any other time  $T_2$  is;

$$\Delta d(E, T_2) = (T_2/T_1) \Delta d(E, T_1) \quad \dots\dots\dots 12$$

This series of equations is used in this study to demonstrate the linear relationship between exposure and etch depth and to be able to predict grating depths for the series of experiments undertaken.

### 3.5.2 Summary

The Bartolini model for image formation is based upon preferential developer etch rates for exposed and unexposed resist. The consideration of the inherent material non-linearity is shown to be overcome by judicious choice of the development system. The experimental verification of a linear relationship between exposure and development can be demonstrated by application of the Bartolini equations.

The experimental and practical aspects of the use of photoresist will be considered in the following sections.

### 3.6 Photoresist Characteristics

The following section will detail the experimental and practical aspects of photoresist. The areas that will be discussed are as follows:

1. Substrate preparation.
2. Photoresist application.
3. Soft bake parameters.
4. Photoresist exposure.
5. Photoresist development.
6. Post bake.
7. Storage and handling.
8. Photoresist stripping.

#### 3.6.1 Substrate Preparation

The coating of photoresist onto a substrate can only be successfully achieved using a scrupulously clean substrate. Advances in the microelectronics industry and the production of VLSI chips, mean that contamination on the substrate can be greater than the surface area of the components. Consequently substrate preparation has become more refined with surfaces needing to be free from dust, grease and particulate matter.

Adhesion of the resist to the substrate is achieved by secondary forces between polymer molecules and polar sites on the substrate surface. Polymer molecules achieve maximum adhesion by close proximity through orientation around the polar sites. Contamination on the surface prevents the polymer molecules attaching themselves directly to the substrate results in pinholes, poor adhesion and reduced image accuracy.

The cleaning cycle chosen for substrates depends upon the type of contamination present on the surface; organic, particulate or metallic. Soils identified as problems in this work are listed below;

	CONTAMINATION	LIKELY CAUSE
<u>ORGANIC</u>	Oils and Greases	Contaminated cleaning solutions
	Fingerprints and sweatmarks	Personnel handling
	Resinous material	Residual photoresist
	Miscellaneous;	
	Wetting agents	Poor rinses from cleaners or photoresist strippers
<u>PARTICULATE</u>	Fibres, paper,	Personnel clothing, dirty working environment
	Abrasive particles	Abrasive, pumice cleaners
<u>METALLIC</u>	Metal oxides	Baking, heating, oxidation
	Metal salts	Poor rinsing, wet storage, perspiration

To deal with such a range of contaminants, cleaning processes typically follow three stages;

- i) General Cleaning Process - to remove the organic soils, inorganic contamination and particulate matter already on the substrate. This process removes the majority of contaminants by chemical or physical means.
- ii) Dehydration Bake - to remove moisture and volatile cleaning residues from the substrate.
- iii) Final Cleaning Process - to remove residues remaining from previous cleaning cycles immediately before the resist is applied.

The cleaning process should not replace one contamination with another consequently cleaning solutions and working environments should be of the highest standard.

The table below summarises the available cleaning methods for the removal of grease and particulate matter.

SOLVENTS/SOLVENT EMULSIONS

Excellent removal of mineral & vegetable oils, greases, waxes but not fingerprints.  
e.g. 1,1,1-trichloroethane.

SOAK CLEANERS

Degreasing agents, work by emulsification. Not as effective as solvents but do not redeposit soils and are less toxic.

ELECTROLYTIC CLEANERS

Scrubbing action of gas from electric current. Vigorous action removes particulate matter. Fast, thorough & inexpensive. Break-down of solutions often caused by evolution of gas.

ABRASIVE CLEANERS

Most common for heavy oxides & inorganic soils. Abrasive slurry, by hand or machine removes soils. Damage to substrate possible. Requires thorough & effective rinsing.

After degreasing and particulate removal the substrate is acidified prior to rinsing and drying.

Acidification Lightly soiled substrates would require solutions of 5-15 vol percent of sulphuric, hydrochloric or perchloric may be necessary. For heavier contamination an etching solution prior to acidification may be necessary.

Rinsing and Drying must be as thorough as the initial cleaning process to reduce remaining contaminants to an insignificant level. Rinse water should be free of turbidity, colourless, pH 6.5-7.5. The best rinsing method is an immersion-spray combination where the substrate is immersed in an overflowing rinse and given a final spray upon withdrawal. Drying is usually achieved compressed gasses such as air or nitrogen to force water from the surface. Use of clean environments aids in all the stages.

All the above mentioned stages are part of the General Cleaning Process. Remaining steps are Dehydration Bake and a Final Cleaning Process.



#### 3.6.1.2 Dehydration Bake

The substrate is baked before resist application to remove moisture and ensure good resist adhesion. If the substrate is allowed to cool and stand for any length of time moisture can be re-absorbed, especially with silica substrates. The substrate must be cleaned, baked, cooled briefly and resist applied in the shortest possible time. Applying resist before the sufficient cooling causes solvent evaporation and the resist sets prematurely to give uneven coatings and unpredictable results. The baking cycle can be used as a stand-alone cleaning cycle as many organic substrates decompose with sufficient baking and for once only used substrates may be all that is required.

#### 3.6.1.3 Final Cleaning Process

Contamination remaining on the substrate after the general cleaning process and dehydration bake is most typically particulate matter or vaporous materials condensed from the bake cycle. Solvents may be used immediately prior to resist coating, alternatively gas blow-offs or suction techniques may be successful. The solvents must not react with the resist in any way and should be applied to the spinning substrate to wash over it with some force followed by a high speed spin dry. Gas blow-offs and suction methods are less effective than solvents and should be applied dry and warm to avoid chilling the substrate and cause condensation on the surface.

Experimental details of the cleaning cycles used for the preparation of resist blanks will be found in Section 3.7.1

#### 3.6.1.4 Nature of the Substrate

The type of substrate used will vary according to the application. The micro-electronics industry typically uses 'wafers', circular discs of 3-4" diameter, anti-reflection coated substrates. They must be flat, ( $\lambda/4$ ) smooth, stable and not react with the chemicals as applied or used in processing. For this study, float glass blanks of various sizes, back coated to reduce scattered reflection have been used. Glass can be easily cut to size, easily cleaned and handled, is readily available and economical to buy.

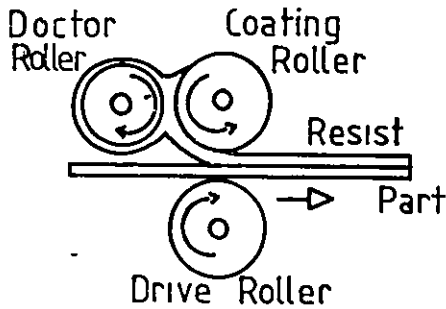
### 3.6.2 Resist Application

Having described the methods available for cleaning the substrate prior to resist application, the methods for applying the resist will be described. The quality of the final image is influenced by the uniformity and thickness of the resist coating. Factors such as soft bake times, exposure times, chemical resistance, pinholing and development time are all affected, to a greater or lesser extent by the thickness of the resist layer. All resists specify a range of coating thicknesses over which the processing conditions produce accurate results. Resist thickness should be as thick as possible to reduce the presence of pinholes, but thin enough to resolve the desired image. In general positive resists can resolve slightly more than three times the resist-film thickness, Heflinger et al [42] suggests that for submicron fabrication, the optimum thickness of the resist is one-half of the grating period. The reason for this is that standing waves occur in the layer normal to the substrate during an exposure of two co-incident parallel beams.

A number of different application methods are summarised in Figure 3.6

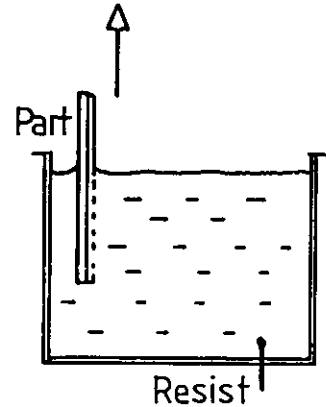
There are two variations in the application of the resist by spin coating, a) applying the resist to a stationary substrate and spinning with high acceleration or, b) applying the resist to a slowly rotating substrate and gradually increasing acceleration. The first method gives very high resist losses but very uniform coatings, the second method has lower resist losses but slightly less uniform coatings. The important feature in either technique is that to achieve good uniformity spinning is started whilst the resist is still fully liquid.

### ROLLER COATING



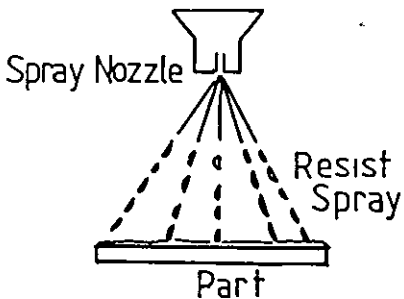
Economical in use. Uses system of rollers to spread resist.

### DIP COATING



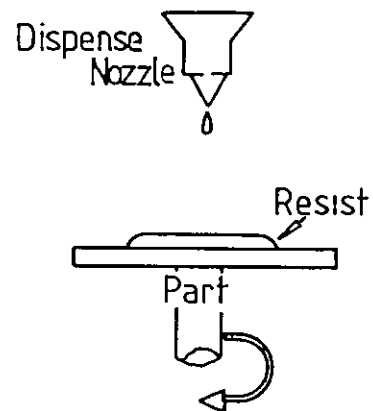
Part immersed then slowly removed. Allows double sided application "Wedge" effect occurs from vertical draining.

### SPRAY COATING



Resist applied under pressure from spray gun. Droplets flow outwards to form film. Resist thinning & solvent concentration important. Skilled operation

### SPIN/WHIRLER COATING



Most common technique. Resist applied to static or slowly rotating substrate then spun upto high speeds. High resist losses, very uniform coatings.

Figure 3.6 Photoresist Application Techniques

Elliot and Hockey [43] discuss coating uniformity by spin coating and some of the variables to be considered. A summary is presented below;

1. Nozzle position; the nozzle tip position should be in close proximity to the substrate to avoid splashing or shearing of the resist.
2. Dispense volume; the volume of resist poured onto the substrate must be sufficient to cover the entire area at the start of the high speed spin cycle.
3. Static flow spread time; a short time to allow the resist to flow out naturally under only gravity and surface tension should be allowed before spinning starts (suitable for static dispense only).
4. Spin ramp; a high acceleration ramp in conjunction with a motor warm-up period to allow the motor speed to stabilize gives repeatable results.
5. Spin velocity; higher spin speeds produce better uniformity of coating.
6. Solvent atmosphere; coating in a solvent atmosphere reduces radial striations in the spun film.
7. Resist viscosity; correct viscosity gives good uniformity and minimises edge bead.
8. Chuck characteristics; ideally the substrate is held on the spinner by a vacuum chuck, large substrates should not be used with small chucks, a minimum of vacuum should be used to avoid thickness variation at the centre.

Each type of resist used will specify an ideal viscosity and spin coating parameters to ensure repeatability.

Experimental details for the application of resist are given in Section 3.7.2. Once the photoresist has been successfully applied to a cleaned substrate, a further stage is necessary before exposure is possible.

### 3.6.3 Softbaking

1) Air drying is an important stage immediately after spinning and before softbaking. A solvent retaining skin may form over the resist because of solvents remaining in a thick coating which prevents

complete solvent evaporation of the lower layer and results in exposure sensitivity and processing variations. To prevent this skin, a 5-10 minute air dry is usually given immediately after coating.

ii) Softbaking is an essential step for positive photoresists. Its purpose is to remove most of the solvent in the resist formulation and render the resist photosensitive. Baking is done in a fresh air oven or an infra-red nitrogen belt oven and time and temperature are important variables. Too low a temperature (60°C) leaves solvents in the resist and results in an apparent increase in sensitivity. This is due to a greater attack by the developer, which removes the resist at a greater rate, but both exposed and unexposed areas. Conversely, a higher softbake temperature reduces apparent sensitivity since the resins in the formulations are hardened and reduce the development effectiveness. Hence for a fixed development time, higher softbake temperatures remove less resist. At further increased temperatures (>100°C), adhesion of the resist to the substrate is improved and as the film is hardened a greater resistance to handling damage is afforded.

Manufacturers' literature suggests optimum times and temperatures and these have been confirmed experimentally - at 90-100°C  $\pm$  2°C for 25 minutes. (Section 3.7.3) These parameters offer the best combination of differential solubility, photosensitivity, adhesion and line control.

#### 3.6.4 Exposure

Exposure of positive resists is slightly less stringent than for negative resists since resist adhesion is not dependant upon exposure. Exposure changes the affected area from a resinous surface insoluble in acids and dilute alkalies to a readily soluble chemical compound, so producing an image by differential development rates. Methods of exposure vary considerably and are application dependant but the effects of under and over-exposure are evident in all techniques.

In extreme cases underexposure will fail to produce an image. Slight underexposure results in scumming and development is not effective. Extreme overexposure will remove all the image or reduce image accuracy

by line-width removal. Some latitude is possible by underexposure and over-development methods but this is not recommended practice.

Exposure methods include, contact printing, proximity printing, refractive and reflective projection printing, electron beam and x-ray exposure. The two latter methods require e-beam and x-ray sensitive resists, increasingly used in micro-electronics applications. For repeatable results, the source characteristics must be known, eg. wavelength, output power, source stability. The methods for judging correct exposure include use of step tablets, inspection and image accuracy techniques. It is possible to fully characterise the material in a similar way to photographic materials using Hurter & Driffeld curves. In this work exposure determination has included use of step wedge and image accuracy measurements and is detailed in Section 3.7.4.

#### 3.6.5 Photoresist Development

Development of the resist can not be considered as a separate process in the characterisation of the material. An inverse relationship exists between exposure and development of the resist. The relationship is illustrated in Figure 3.7 [44]

By using high resolution photomasks, the resultant image geometries can be studied to establish the effects of development. A degree of processing latitude is found in developer type and concentration, temperature, agitation methods, exposure level and softbake conditions. The function of the developer is to remove the exposed resist at a faster rate than at which it attacks the unexposed areas. With a heavily exposed part and prolonged development too much resist may be removed, hence the need to study the latitude of the exposure/development parameters

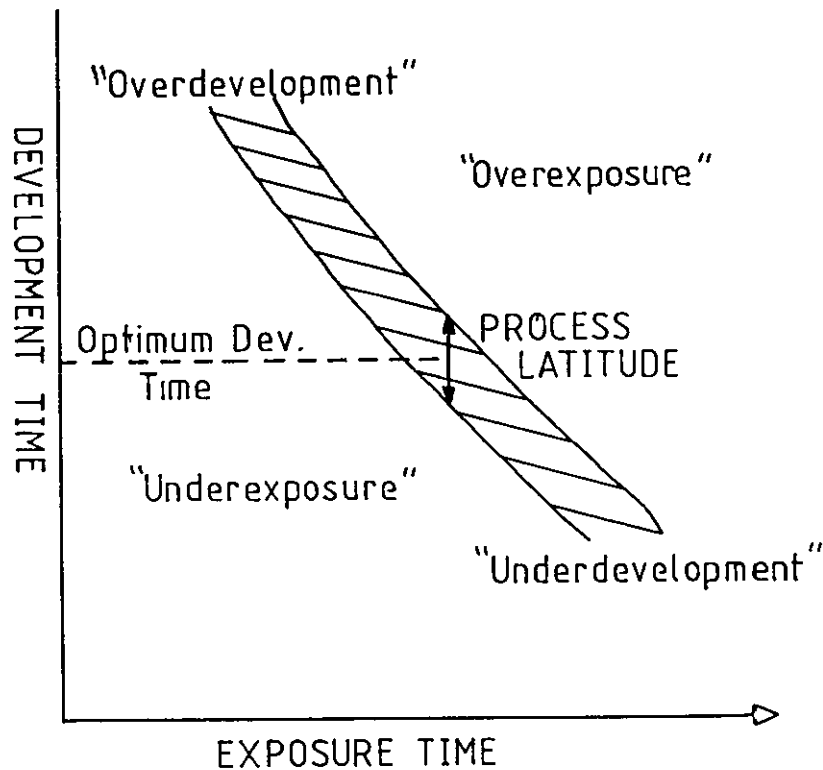


Figure 3.7 Development/Exposure Curve for Positive Photoresist

The following development methods for resist processing are possible;

- a) Immersion development can be used for batch processing where a number of substrates are processed in tanks and immersed for a fixed period. As the image formation mechanism has been described as a surface rate limited reaction, the degree of agitation control is important. It is likely that agitation effects occur as for silver halide materials if the proposed image formation mechanism is correct.
- b) Spray development can be used for both batch and in-line processes. A fine mist of developer is directed at the resist surface for a given period. Problems occur in ensuring even spray patterns and controlling temperature drop of the developer as it strikes the surface.
- c) Puddle development (Flood development) is an in-line process where the part is flooded with developer for a given period. Development is stopped by flooding with de-ionized water. Uneven resist removal is often a problem with this method. Leonard et al [45] have considered puddle development for the integrated circuit industry with its critical demands placed upon the development cycle.

For any development technique the developer must be suitable in terms of foaming, striations and activity properties. Typically, potassium or sodium hydroxide developers are used, more recently the ion-free developers claim greater image accuracy and repeatability of processing. The developer contains a source of alkalinity and a surfactant in aqueous solution in addition to buffering agents, glycol ethers and coupling agents. As the solution is used, the carboxylic acid groups produced from reaction with the sensitizer are neutralized by the alkalinity in the developer. (Absorbed CO<sub>2</sub> from the atmosphere also reduces alkalinity). Control is needed over the pH and this can be used as a indicator of developer exhaustion. Experimental details can be found in Section 3.7.5.

#### 3.6.6 Postbake

Post baking of the developed image is necessary for some applications to improve the adhesion and chemical resistance of the image making it suitable for etching or plating. Temperature control is important as positive resists may soften and flow, followed by embrittlement at high temperatures. Hence 80-120°C for 20-30 minutes is typical.

#### 3.6.7 Storage and Handling

An interesting feature of positive resists is that they retain photosensitivity after processing and this can be used in specialised applications of multi-level micro-electronics wafers. Some resists maintain good handling properties in terms of chemical resistance but others may degrade under white fluorescent lights. Storage of uncoated resist should be short term as the liquid will slowly decompose and lose photosensitivity at room temperature with the evolution of nitrogen.

#### 3.6.8 Resist Stripping

Positive resists can be easily stripped by immersion in alkaline solutions. Organic solvents such as ketones, amines or glycol ethers are also used. The majority of manufacturers produce specific removers for the product. The stripper used should not leave deposits that can not easily be removed in the substrate cleaning process.



### 3.7 Experimental Detail and Results

The properties and characteristics of photoresist have provided a major area of study in the work undertaken. Since the initial photoresist grating or hologram acts as the information carrier to be replicated and embossed it was felt that it was important to use the material to its best advantage to achieve high quality images. The following section will detail these experimental areas;

#### 3.7.1 Substrate Preparation

Extremely high quality coated substrates are available from companies such as Balzers, who supply much of the microelectronics industry. The quality of the material is guaranteed with details of pinhole counts and level of defects. The material cost is accordingly high and the cost of using such substrates for the duration of this work necessitated the use of alternative coated substrates. One alternative was self-spun plates offering a range of sizes, choice of resist type and thickness, freshly spun plates always available, cost and time saving. The drawback was the need for ultra-clean facilities to achieve any repeatable quality of coated substrate. Throughout, glass blanks, of 3mm thickness have been used as a stable, cheap and suitable material. For coating, a small unit and facility was designed, built and installed to allow self-spun plates to be produced. Before coating however, the glass blanks required thorough cleaning as detailed in section 3.6.1. The following cleaning cycles were investigated; 1) Hand abrasive cleaning.

11) Non-abrasive cleaning.

1) Hand Abrasive Cleaning; The cycle as detailed below was applied to a number of blanks [38]. After cleaning the blanks were baked, cooled and coated to inspect defect levels. The cycle was carried out in eight steps as follows

- 1) Abrasive scrub of alumina and salt solution.  
(Degreasing, heavy particulate matter removal) A slurry of alumina and salt solution was applied to the blank with finest grade polishing cloth and gently rubbed across the surface. Salt solution;
- 2) Rinse - distilled water.
- 3) Wet Brush- soft bristle brush to remove remaining slurry.
- 4) Soak clean - alkaline solution (Optional)
- 5) Rinse - distilled water.
- 6) Acid Dip - Dilute HCL 15 % vol/gall.
- 7) Rinse - deionised water.
- 8) Dry.

#### Salt Solution

Citric Acid	12g/l
Sodium Chloride	42g/l
Non-ionic wetting agent	
Pure water	1000g/l

#### Soak Cleaner

Sodium Hydroxide	20%
Sodium Carbonate	18%
Tetrasodium Phosphate	20%
Sodium Metasilicate	30%
Wetting agents	
Solution should be warmed.	
Soak period 5 minutes.	

#### Observations:

- 1) Alumina scrub - without sufficient salt solution to keep slurry very wet, physical abrasion can damage blank.
- 2)/3) Rinsing - needs to be very forceful to remove the slurry remaining on the blank. The use of the wet brush aids this but the brush can introduce further contamination
- 4) Optional soak clean - leaves slight precipitate on blank which defeats object Suggests formulation not correct.
- 5) Acid dip - pH 4.5
- 6)/7) Rinse and dry - blank remains fully wetted throughout process and water not repelled from surface making good drying difficult. Blanks drained for short period then baked at 195°C for 15 minutes.

11) Non Abrasive Cleaning; The cleaning cycle as detailed below was applied to a further set of blanks. After cleaning and drying the plates were spun with resist to check for cleanliness of the cycle.

- 1) Soak - distilled water and wetting agent.
- 2) Surface wipe - soft brush or lint free cloth.
- 3) Rinse - distilled water.
- 4) Acid dip - Dilute HCL 10%.
- 5) Rinse - deionised water.
- 6) Dry - water blow off and dehydration bake.

#### Observations:

- 1) Cold or hot water with detergent and wetting agent effective in removing slight contamination.
- 2) Rinse - the surface repels water and cannot be totally wetted.
- 3)/4) Acid dip does not effectively wet surface.
- 5)/6) Air blow-off by clean, filtered air prevents streaks.

#### Conclusions

Both cleaning cycles were applied to plates prior to coating with photoresist. Resist was applied under clean conditions to reduce new contamination after the blanks were dry and awaiting coating. The level of contamination on both sets of blanks was acceptable, mostly hair or dust particles that may be unrelated to cleaning cycle. The non-abrasive cleaning cycle was more suited to new blanks or those not previously coated with resist as it was not effective at removing streaks of resist not removed by acetone soaking. The hand abrasive cycle must be done with care to avoid abrading the surface and very thorough washing was essential to remove the slurry from the blank. In both cases the acidification dip, designed to remove metallic contamination was of little obvious benefit. The biggest factor for both methods appears to be the cleanliness of the environment and airborne contamination. Grease and fingerprints can be effectively removed by abrasive cleaning and the use of detergents.

From the methods tried a compromise method evolved for subsequent work. A gentle abrasive method using wetting agents and detergents was employed, surface rubbing was only necessary for badly marked blanks. The final thorough rinsing and removing of excess water on the surface by physical blow-off with clean air left blanks streak free and clean. Observation under yellow safe-light immediately prior to coating revealed any lightly bound surface hairs or dust that could be removed by a small suction unit with the substrate rotating at low speed on the spinner unit. Allowing the plates to air dry after coating in a clean environment prevented dust landing on the surface whilst the resist was still tacky. Obviously the purest water available should be used throughout to prevent introduction of particulate matter and deposits. Plate 4 shows a photomicrograph of a coated substrate with particulate matter beneath the resist coating. The grating period is  $\sim 10001/\text{mm}$  ( $1\mu\text{m}$ ) and the contamination covers an area of almost  $15\mu\text{m}$ . The contamination has disrupted the surface and is clearly unacceptable. Plate 5 shows a better quality surface with little evident particulate matter present.

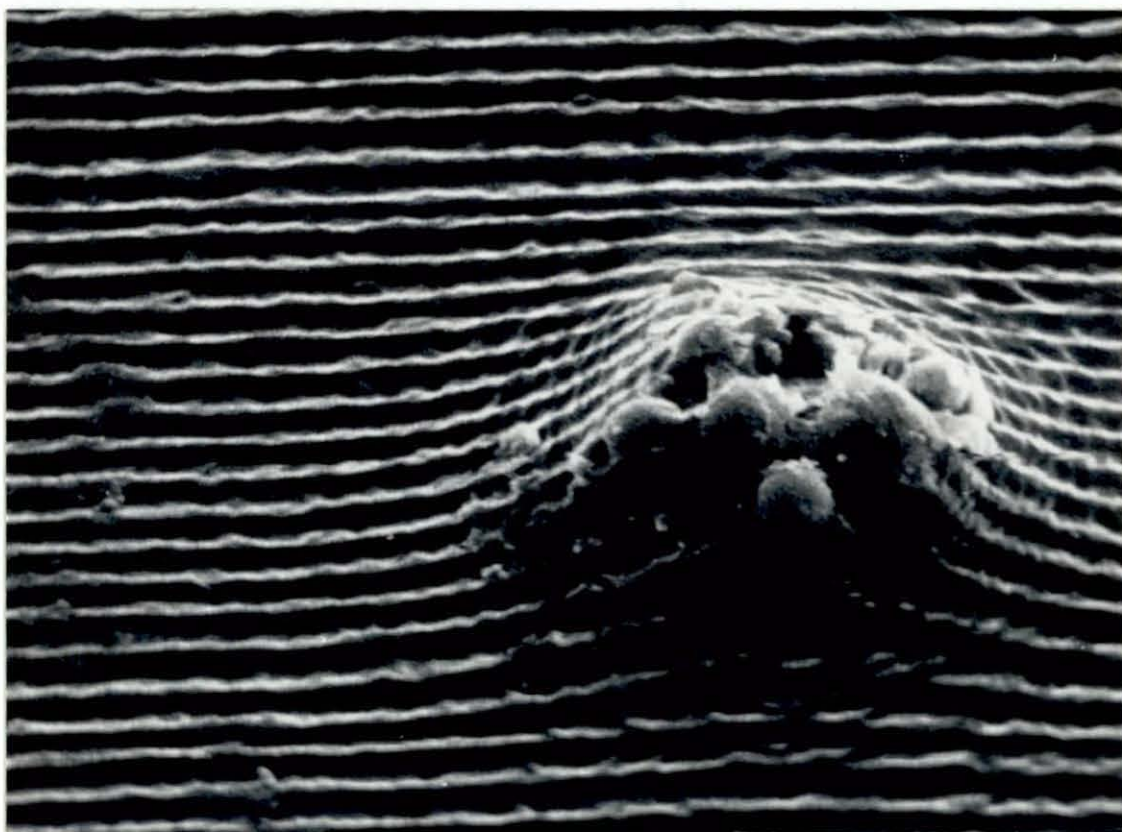


Plate 4. Photoresist Coated Over a Dirty Substrate

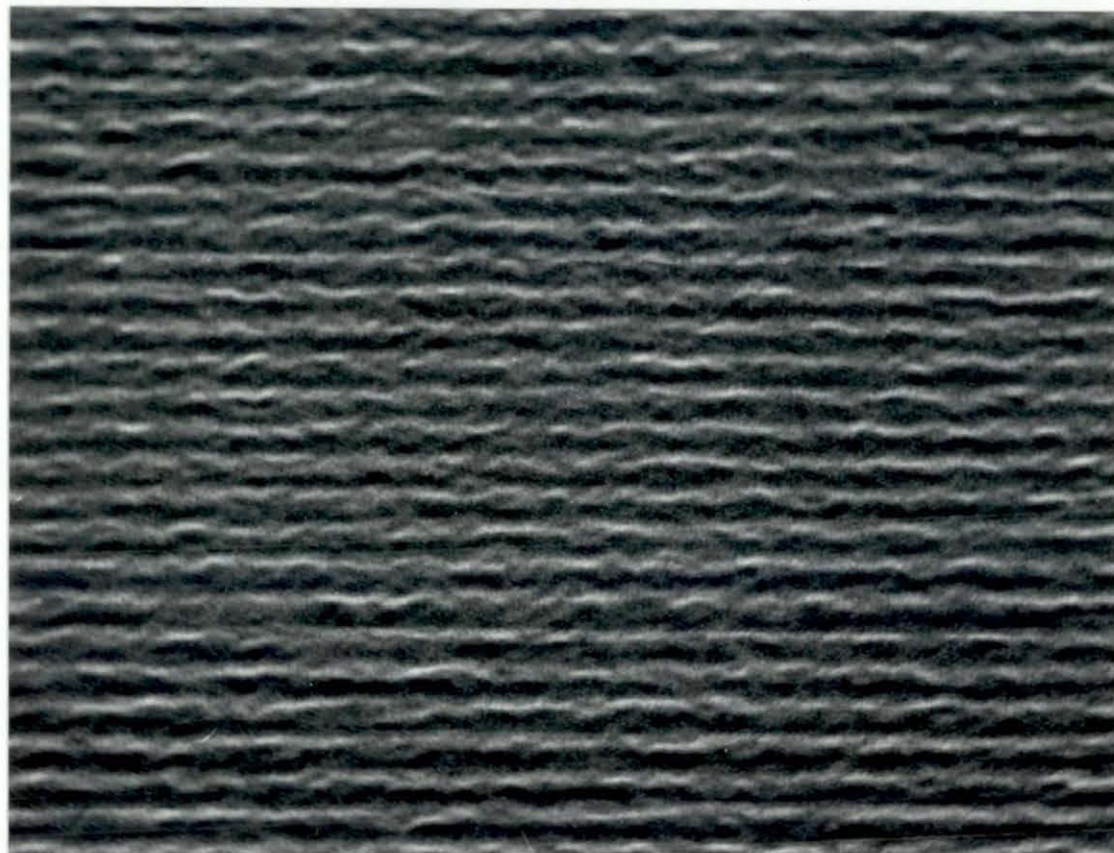


Plate 5. Photoresist Coated onto a Cleaner Substrate

### 3.7.2 Resist Application

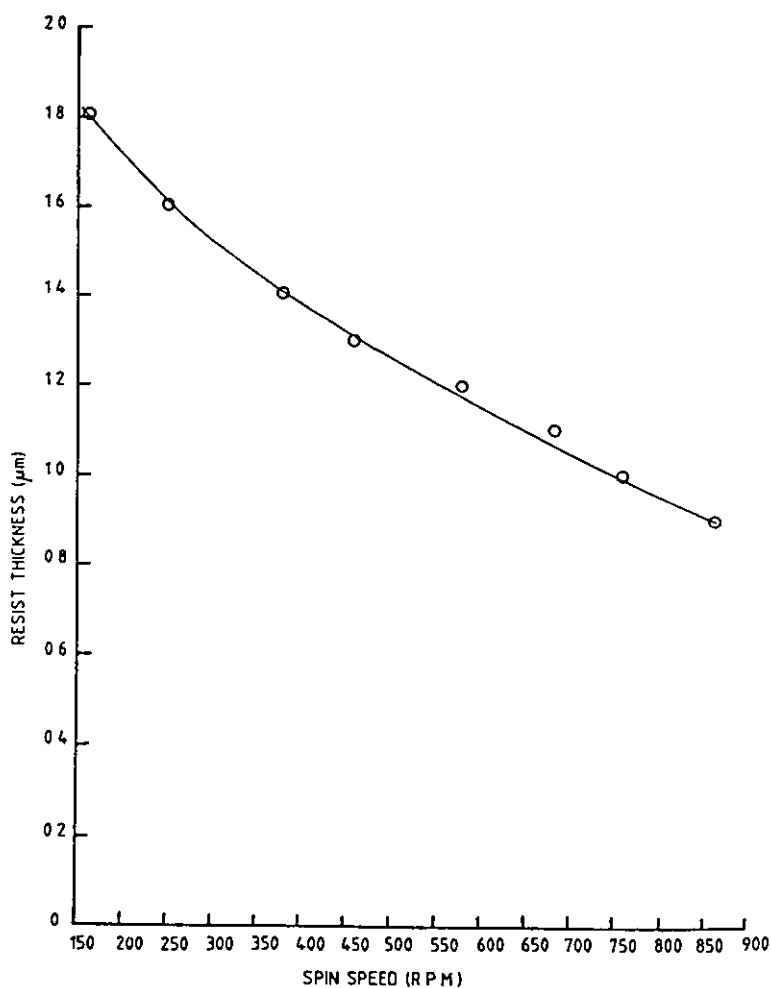
Section 3.6.2 detailed the various methods of resist application. Commercial photoresist spinners are available with very high spin speeds, controlled ramp, automatic resist dispense and development processes. The version used for this study was made from a turntable type platen and motor driven over a range of speeds. The substrate was held onto the platen by small retaining clips to ensure the blank did not fly loose whilst spinning. The resist was dispensed onto the substrate by pipette dropper and allowed a minute flow time to spread the resist out and allow the escape of any air bubbles before being driven upto spin speed. The whole unit was enclosed within a polythene frame with an extractor fan to draw fumes from the 'tent' and vent out from the laboratory environment. Safelamp conditions allowed visual inspection of the process and made it possible to monitor the cleanliness and quality of spinning. By observing the interference fringes that flow across the substrate whilst spinning as the resist thins and flows outwards it was possible to ensure flatter coatings once the interference bands stopped.

Throughout this work, Shipley AZ1450B positive working resist has been used as it was found reliable, well documented in use and easy to obtain and use. No problems were experienced with adhesion of the resist to glass provided it was thoroughly cleaned and degreased. The resist was used unthinned since the limited spin speeds available prevented thicker coatings. Whilst the spin speeds of the unit were considerably slower than recommended, (900 rpm versus 3500 rpm), the results were felt to be satisfactory and flatness of resist was assessed by Talysurf and SEM. Graph 3.8 shows the determination of thickness versus spin speed. Thickness was determined by exposing a small square area sufficiently to remove the resist in that region and measuring step height with a Talystep instrument.

### Observations

It can be seen from Graph 3.8 that a possible resist thickness of  $1.8\mu\text{m}$  spun at 150 r.p.m. could be achieved with unthinned Shipley AZ1450B resist and available spinner. The spin speed was significantly slower

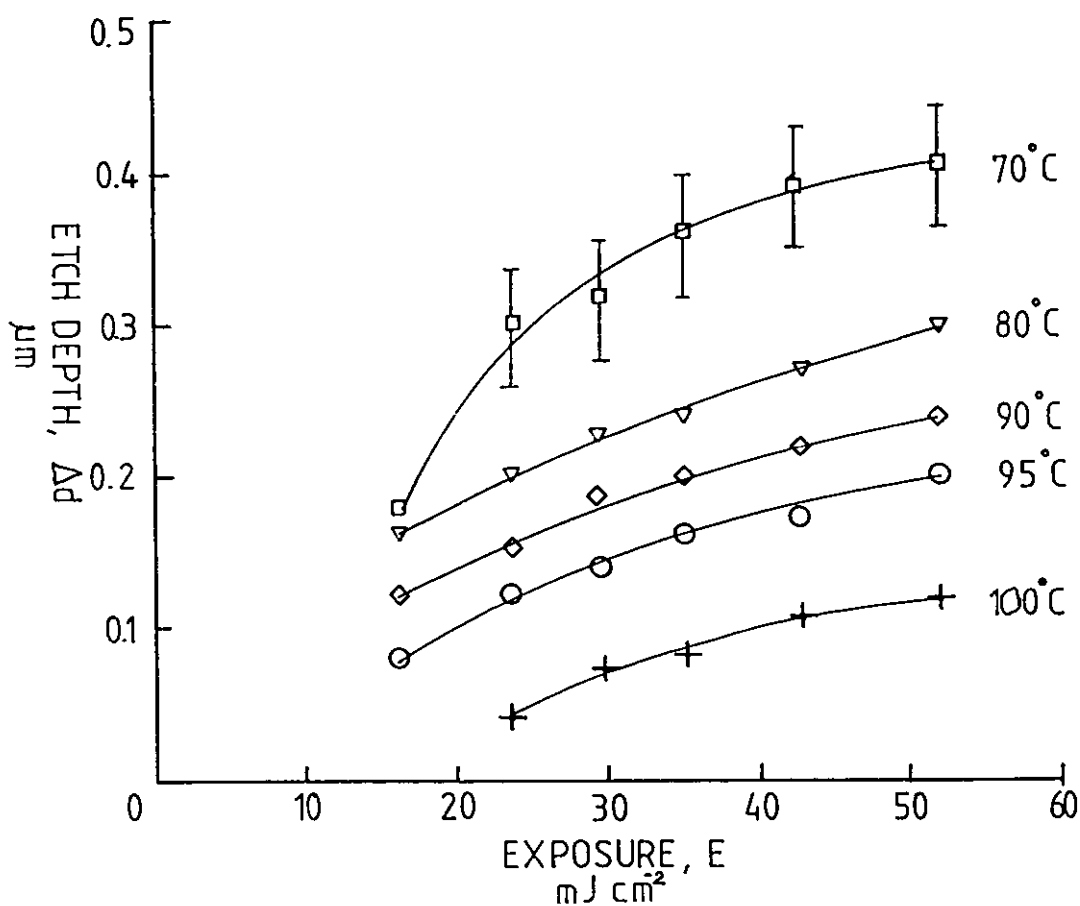
than recommended by the manufacturer and the quality of the coatings was found to vary around the edges of the substrate as would be expected from a build-up of resist at the edges. A faster spin speed of 750 r.p.m gave a resist thickness of  $1\mu\text{m}$ . This combination was used to improve evenness of coating and give adequate thickness of resist. The resist was dispensed from a pipette onto the static substrate, a period of one minute was allowed to remove air bubbles and allow the resist to flow before the spinner was turned to speed for two minutes spin time. The  $1\mu\text{m}$  thickness was found suitable for both grating and holographic images and was used consistently throughout experimental work. No variation in resist thickness was observed during studies of the substrates and images.



Graph 3.8 Resist Thickness Versus Spin Speed

### 3.7.3 Softbake

After the resist had been spun onto the substrate a five minute airdry within the clean area was given to prevent the surface skinning. The substrate was then placed into a fresh air oven for a predetermined time and temperature. The oven was cleaned regularly to try and prevent dust settling and baking onto the plates. A series of trials were conducted to consider the effect of softbaking on sensitivity and resist removal. Areas of resist were exposed through a photomask of clear and opaque areas to remove steps which could be measured for resist thickness after development. The mask areas were also used to assess image accuracy. Graph 3.9 plots the effects of softbake temperatures upon etch depths and the exposure required to achieve that depth.



Graph 3.9 Etch Depth Vs. Exposure for Different Softbake Temperatures



### Tabulation of Results - Effect of Softbake Upon Exposure Sensitivity

BAKE TEMP. °C	EXPOSURE (mJ/cm <sup>2</sup> )						
	16	22	30	35	42	52	
70	0.19	0.30	0.32	0.37	0.39	0.40	
80	0.16	0.20	0.23	0.25	0.27	0.30	
90	0.12	0.15	0.18	0.19	0.22	0.24	AV. ETCH DEPTH
95	0.08	0.14	0.14	0.16	0.18	0.20	(μm)
100	-	0.04	0.07	0.08	0.11	0.12	

### Observations

Graph 3.9 illustrates the effects of softbake sensitivity upon apparent exposure sensitivity. (Error bars are shown on the curve for 70°C to avoid confusion with the closely spaced curves of the other bake temperatures.) The results show that lower bake temperatures produce greater etch depths than higher bake temperatures for the same given exposure. This has the effect of appearing to increase sensitivity by removing more resist for a shorter exposure. In practice the lower softbake temperature leaves a higher solvent concentration remaining in the photoresist. The developer is then able to remove the resist at a faster rate but removes both exposed and unexposed areas which is undesirable. A controllable removal rate for adequate sensitivity is more desirable and the postbake temperature of 95°C for 25 minutes was chosen as a good working result. The temperature of 70°C appears to have a greater effect than the temperature range from 80-95°C. It is believed that significantly more solvent remains at this lower temperature and would result in an uncontrollably fast etch rate given that the development time was 30 seconds for a 1+4 developer dilution. At the other extreme of 100°C a very slow etch rate at lower exposures is seen and would require excessive exposures to produce even 0.5 μm thickness change. Obviously the nature of the development will affect resist removal and standard procedures must be adopted to remain consistent.

#### 3.7.4 Photoresist Exposure

Details for the recording of gratings and holograms can be found in Chapter 2. This section describes early results from the study of resist behaviour and sensitivity following the model proposed by Bartolini [40].

Bartolini stated that a linear relationship could be found between resist removal and resist exposure for a given development regime. Two important factors of this behaviour are the rate at which exposed and unexposed resist are removed by a developer. These are defined by the following expression;

$$\Delta d = T[r_1 - \Delta r \exp(-\alpha_0 E)] \quad \dots\dots\dots 1$$

where  $T$ =development time (seconds)

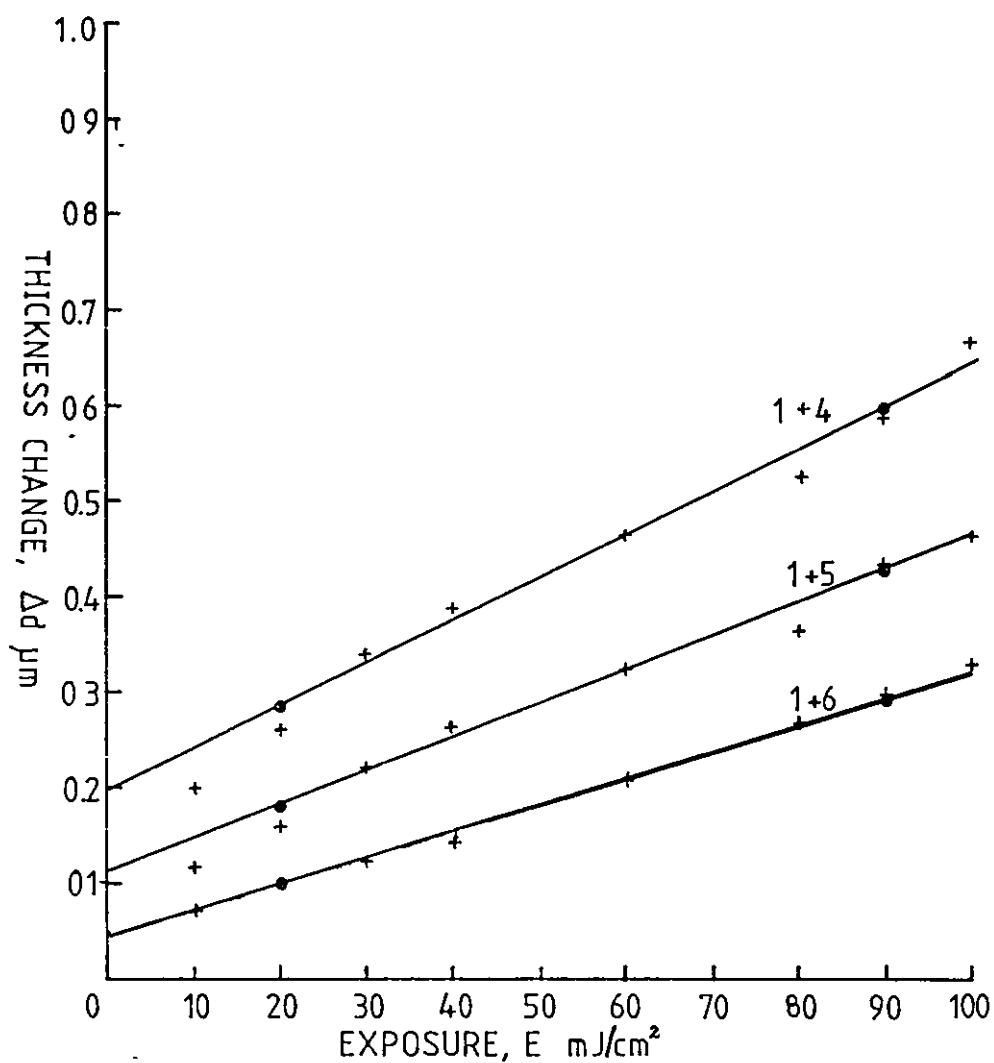
$\alpha_0$ =exposure constant

$\Delta r = r_1 - r_2$  for  $r_1$  = exposed etch rate

and  $r_2$  = unexposed etch rate

##### 3.7.4.1 Exposed Etch Rate Determination- $r_1$

A series of discrete exposures were made upon a number of photoresist plates. Each exposure was logged in terms of laser power density ( $\text{mW}/\text{cm}^2$ ) and exposure time (seconds) so that energy  $E$ , in  $\text{mJ}/\text{cm}^2$  could be calculated. The exposed plates were developed at constant time, temperature and agitation, only the developer dilution was varied. The resultant areas presented themselves as 'steps' of removed resist that could be measured by Talystep or Talysurf instruments. The plot of results is shown in Graph 3.10



Graph 3.10 Determination of Exposed Etch Rate - r<sub>1</sub>

Tabulation of results - Exposed Etch Rate Determination

EXPOSURE mJ/cm <sup>2</sup>	STEP HEIGHT μm			SLOPE Δr ∝ T			INTERCEPT r <sub>2</sub> T		
	DEVELOPER DILUTION								
	1+4	1+5	1+6	1+4	1+5	1+6	1+4	1+5	1+6
10	0.20	0.12	0.07						
20	0.26	0.16	0.10						
30	0.34	0.22	0.12						
40	0.44	0.28	0.14						
60	0.46	0.32	0.20	0.01	0.007	0.006	0.20	0.12	0.03
80	0.52	0.36	0.26						
100	0.66	0.46	0.32						

#### Observations - Exposed Etch Rate Determination, $r_1$

The results presented in Graph 3.10 illustrate the relationship between resist removed for a given exposure. The effect of developer dilution is clearly shown, in that a stronger developer, whilst removing resist in a linear fashion does so at a considerably higher rate. The graph shows good linearity of resist removal for the exposure energy using the development parameters as stated. The use of AZ303 developer was believed to improve the linearity of resist removal over that of Microposit developer [13,40]. The non-zero intercept from the 1+4 developer dilution appears higher than desirable, such etch depths could be greater than intended and hence the choice of 1+5 dilution as the optimum between linearity of resist removal and unexposed resist removal. Adjustment of developer times allows variability to be introduced in much the same way as for photographic processes, but for good reproduction of results this can not be recommended. The slope of each curve is defined as  $\Delta r \propto T$  and this relates to the parameter in the Bartolini equation, it is the linearity of this term that is important. The intercept is expressed as  $r_2 T$  and is non-zero because the developer will also remove unexposed resist whilst developing exposed areas. As long as the intercept is not too great (hence the need to determine the unexposed etch rate), the first term will remain linear. A large removal of unexposed resist will etch away overall resist thickness and cause heavily exposed areas to lose correct profile.

#### 3.7.4.2 Unexposed Etch Rate Determination- $r_2$

The rate at which unexposed resist is removed by the developer is important in reducing large resist losses that cause 'bottoming out' of heavily exposed areas. To determine the etch rate an unexposed plate was immersed into developer at a fixed depth, to remove a given area of resist, agitated for a given period and removed. This etched a step into the resist at developer level that could be measured by Talystep or Talysurf. Developer dilution was varied along with development time. Temperature and agitation were kept constant as both factors affect resist removal. Results are plotted in Graph 3.11

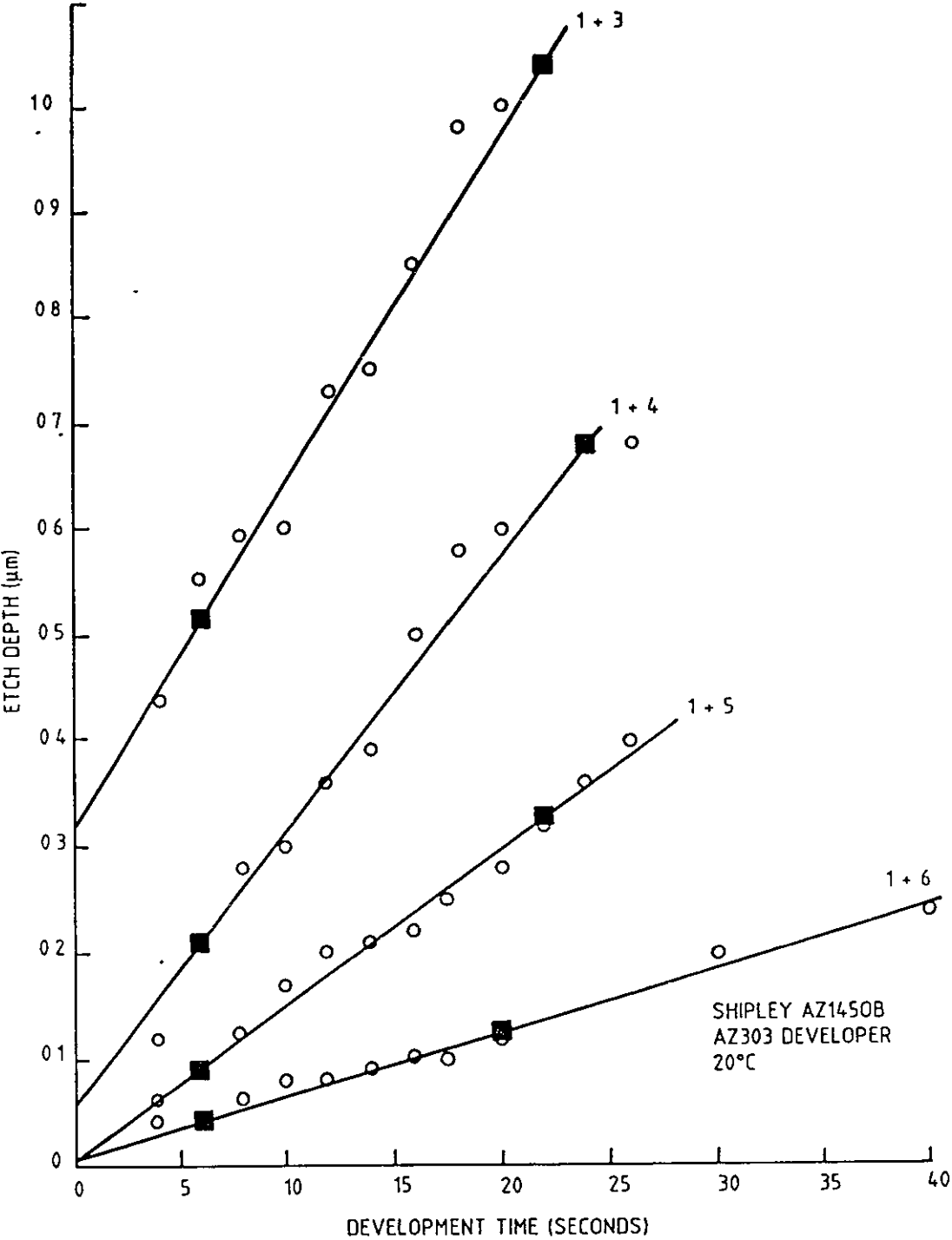
Tabulation of Results - Unexposed Etch Rate Determination.

Developer Dilution	Development Time		Step Height		r <sub>2</sub>
	seconds		μm		μm/sec
1 + 3	4	6	0.44	0.55	0.037
	8	10	0.59	0.60	
	12	14	0.73	0.75	
	16	18	0.85	0.98	
	20	22	>1.0	>1.0	
1 + 4	4	6	0.12	0.22	0.028
	8	10	0.28	0.30	
	12	14	0.36	0.44	
	16	18	0.50	0.58	
	20	22	0.61	0.65	
	24	26	0.68	0.68	
1 + 5	4	6	0.06	0.08	0.016
	8	10	0.12	0.17	
	12	14	0.20	0.21	
	16	18	0.22	0.25	
	20	22	0.28	0.32	
	24	26	0.36	0.40	
1 + 6	4	6	0.04	0.04	0.0057
	8	10	0.06	0.08	
	12	14	0.08	0.09	
	16	18	0.10	0.10	
	20		0.12		
	30		0.20		
	40		0.24		

Observations - Unexposed Etch Rate Determination, r<sub>2</sub>

Results are presented in Graph 3.11. The effect of developer dilution is clear with a marked difference between the dilutions. The 1+3 dilution is far too aggressive, removing almost 1.0μm of resist in only 20 secs, this compares with 0.11μm in the same time for the 1+6 dilution. The 1+5 dilution was chosen as the most suitable for the process showing good linearity and a removal rate that would not

require excessively long or short development times. This tallies well with the developer dilution chosen for exposed photoresist removal. In this way only areas with sufficient exposure are removed and unexposed areas are not reduced by developer action alone.



Graph 3.11 Determination of Unexposed Etch Rate - r2

### Discussion Of Etch Rate Determinations, $r_1, r_2$

These experiments have attempted to establish a linearity between the relationship of resist exposure and resist removal. The results were useful for the regime on which they were tested, that is, Shipley AZ1450B positive resist, with the development times, temperature and dilutions as stated. The extension of results to different combinations can be applied with caution and serve as useful 'pointers' in reducing experimental lead times. From the experiments undertaken the linearity using the parameters stated has been proven and can be applied to other experimental work.

The results obtained have been applied to the Bartolini equation to assess the usefulness of the expression in understanding the characteristics of photoresist behaviour. Values are taken from results using 1+5 developer dilution at 20°C for one minute.

From Bartolini;  $Ad = T[r_1 - Ar \exp(-\alpha_0 E)]$  ..... 1

Exposure constant,  $\alpha_0 = nq / hv$

where  $n$  = quantum efficiency  
 $\alpha$  = absorption cross section of resist molecule  
 $h$  = Planck's constant  $6.23 \times 10^{-3}$  mJ.s  
 $v$  = frequency of light  $6.8 \times 10^{14}$  s<sup>-1</sup>

For AZ1300 series resist, Broyde [41] found  $nq=3.2\%$  and  $\alpha=6.25 \times 10^{-7}$  such that  $\alpha_0 = 0.5 \times 10^{-2}$  cm<sup>2</sup>.mJ<sup>-1</sup>

From Graph 3.10, Slope  $\Delta r \alpha_o T = 0.007 \mu\text{m cm}^2 \text{ mJ.s}^{-1}$

$$\Delta r = \frac{0.007}{\alpha_o \cdot T}$$

where  $T = 15$  seconds

$$\alpha_o = 0.5 \times 10^{-2} \text{ cm}^2 \cdot \text{mJ}^{-1}$$

$$\Delta r = \frac{0.007}{0.5 \times 10^{-2} \times 15}$$

$$\therefore \Delta r = 0.093 \mu\text{m/s}$$

Also,  $\Delta r = r_1 - r_2$ , where  $r_2 = 0.016 \mu\text{m/s}$  (Graph 3.11)

$$0.093 = r_1 - 0.016$$

$$r_1 = 0.093 + 0.016$$

$$r_1 = 0.109 \mu\text{m/s}$$

This figure represents the rate at which exposed resist is removed for the given exposure and development sequence stated. The usefulness of this figure is found by applying it back to the original equation as follows;

To determine the exposure necessary to remove a depth of resist with a known development time using the regime above, exposure  $E$  can be found;

$$\Delta d = T[r_1 - \Delta r \exp(-\alpha_o E)] \quad (1)$$

$$\frac{\Delta d}{T} - r_1 = -\Delta r e^{-\alpha_o E} \quad (2)$$

$$\ln \frac{r_1 - \frac{\Delta d}{T}}{\Delta r} = -\alpha_o E \quad (3)$$

$$\text{Exposure } E = -\frac{1}{\alpha_o} \ln \frac{1}{\Delta r T} (r_1 T - \Delta d) \quad (4)$$



Hence, the exposure necessary to remove 0.5  $\mu\text{m}$  of resist for a 1 minute development at 1+5 developer dilution;

$$E = - \frac{1}{0.5 \times 10^{-2}} \ln \frac{1}{(0.093)^{60}} [(0.109)^{60} - 0.5] \quad (\text{from 4})$$

$$= \underline{15.84 \text{ mJ/cm}^2}$$

It must be stressed that this is valid only for the precise experimental parameters used for these tests. For each new section of work some initial trial exposures had to be made to take into consideration resist ageing, differences in bake parameters, development temperatures, all factors that are encountered in practice and that affect results. The development times given for the above series of experiments proved to be too short to control and not practical for any method other than dish development. Consequently later work found it necessary to extend development times and figures and this series of work proved helpful.

The experiments have given a practical usefulness to the model being most closely followed in this work and have shown good correlation to figures obtained by other workers using similar material and methods.

### 37.4.3 Image Accuracy Determination

The study of softbake parameters utilized a photomask in contact with the unexposed photoresist to produce step areas for measurement of etch depth versus exposure at different softbake temperatures. The images were also used to examine image accuracy versus exposure. The photomask consisted of clear and opaque areas, the dimensions of which were measured by optical microscopy giving a limiting accuracy of one eyepiece division =  $\pm 0.01\text{mm}$ . The photomask was held in close contact to the photoresist plate and illuminated with a collimated, normal incidence beam,  $\lambda=457\text{nm}$ . Different exposure times at constant intensity were given to expose areas for a known energy in  $\text{mJ}/\text{cm}^2$ . Exposures were designed to range from underexposure to overexposure to investigate effects of 'bleeding' or scumming. Development of the resist was by immersion with details as shown. Results are plotted in the form of plus and minus deviations versus Exposure E for one photomask area. Transparent areas are exposed and removed upon development, conversely for opaque areas. The size of the areas were measured and compared to that of the photomask. Plates 6 and 7 show the photomask original and a photoresist area. Diffraction effects around noise and dirt on the optics can be seen around the area.

#### Tabulation of Results - Image Accuracy

Mask Area	Exposure	Resist Dimensions	
Dimensions	$\text{mJ}/\text{cm}^2$	Opaque	Clear
Opaque 0.12mm	24	0.15	0.06
Clear 0.12mm	28	0.14	0.07
	32	0.14	0.09
	38	0.13	0.10
	42	0.12	0.10
	44	0.11	0.12
	52	0.09	0.13
	56	0.09	0.15

Accuracy limited to  $\pm 0.01\text{mm}$  (eyepiece divisions).

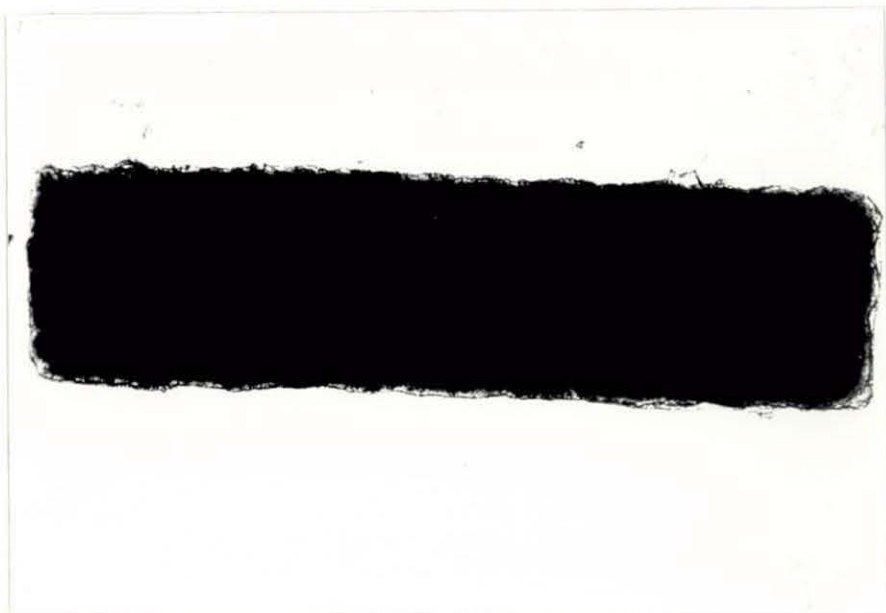


Plate 6. Area from Photomask Original

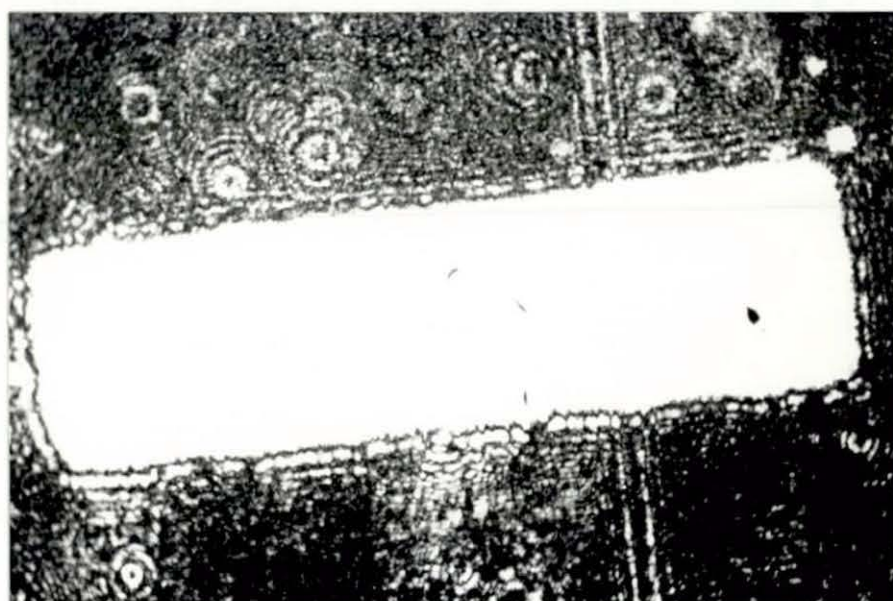
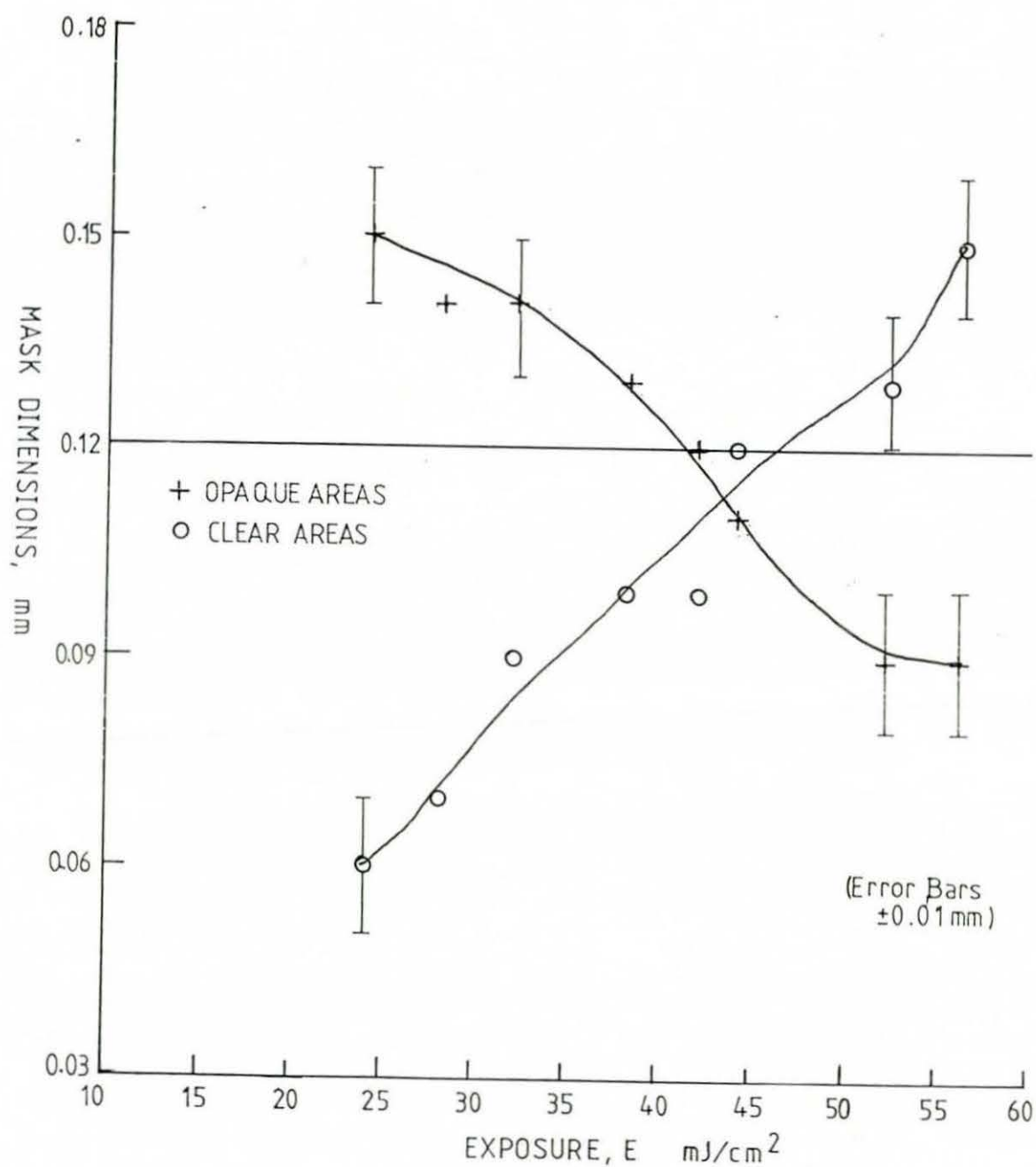


Plate 7. Area of Photoresist After Exposure to Photomask



Graph 3.12 Image Accuracy Determination

### Conclusions

Graph 3.12 plots the results from the image accuracy experiments. The results were limited by the accuracy of the optical measuring system to  $\pm 0.01\text{mm}$ . The trend from the graph is seen by the falling to minimum deviation, for both opaque and clear photomask areas for an exposure of  $44\text{mJ}/\text{cm}^2$ . The exposed resist through the clear photomask area shows reduced aperture size for underexposure and increased aperture size for overexposure. Conversely, the area under the closure, not exposed, shows increased dimensions for underexposure and reduced accuracy for overexposure. Considering the clear, aperture area, an overexposure would 'leech' around the edges of the aperture and the resist in that area would also be etched or removed by development to a greater extent than that beyond the edges of the aperture. Underexposure of the clear area would not effectively remove all of the resist within the boundaries of the aperture leaving a smaller dimension than the original. These effects would be influenced by the softbake temperature which affects line width accuracy. Consequently the data used was taken from photoresist plates baked at recommended temperatures. Plate 8 shows a loss of accuracy resulting from the 'bleeding' of the grating structure.

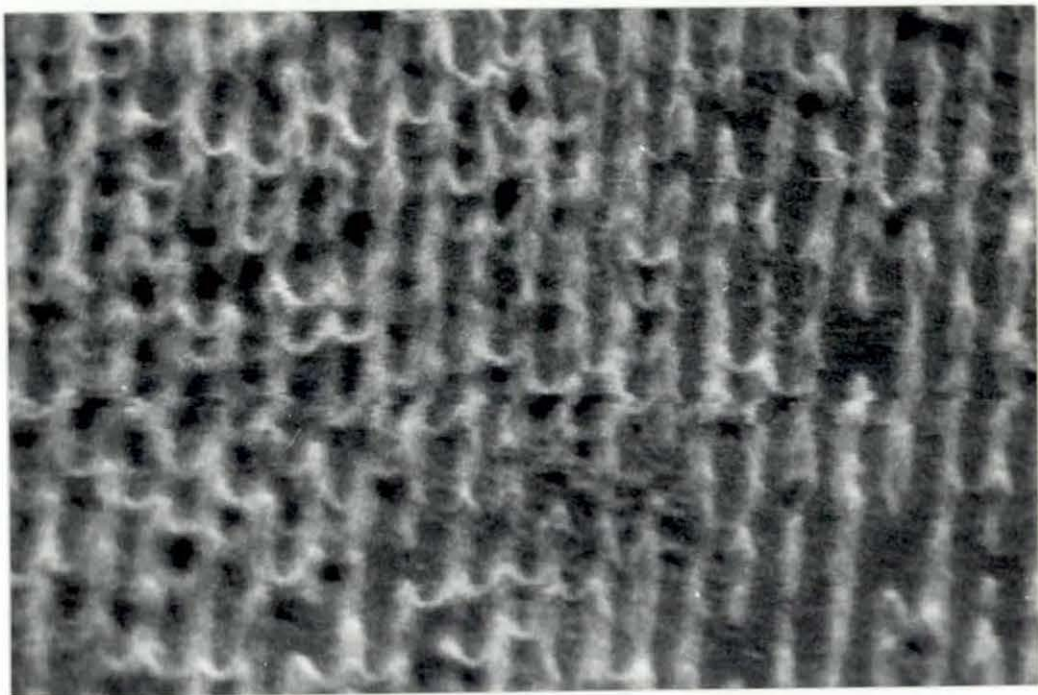


Plate 8. Loss of Image Accuracy from Line 'Bleeding'

### 3.7.5 Development Parameters

The experimental work in this area has considered primarily the methods of development not the nature of developers and their characteristics. However it should be pointed out that the developer used almost exclusively throughout this work has been AZ303 which is not a Shipley recommended developer for AZ1450B resist. A number of workers [12,13,40] have shown that this developer improves the linearity between resist exposure and removal. The recommended developer for AZ1450B resist differs considerably in total alkaline normality (0.30 versus 1.67-1.73 for AZ303) and has a different appearance in colour. Development times for the recommended developer are also considerably shorter (40-60secs versus 1-3 mins.) The 1400 series of resist and recommended developers are used in the fabrication of semiconductor devices, photomasks and micro-electronics. The AZ303 developer is recommended for use with the Microposit 111, 340 and 119 series of resist. These resists are suitable for application on all metal and metal alloy substrates and are used in photochemical machining and electroforming applications. The difficulty in using this resist is its restricted sensitivity range, peak sensitivity drops rapidly from 350nm to almost zero at 450nm and is intended ideally for use with UV lamp exposure systems. The AZ1400 series resist has extended sensitivity out to 460-480nm, making it the most suitable for laser exposure with Argon-ion lasers.

Recommended development procedures include immersion, spray and puddle. The easiest system from equipment and handling view point is the immersion technique as for many photographic applications. The exposed plate is laid flat in a small tray and completely immersed by developer, agitation is by controlled movements of the tray and after appropriate development time, the plate is lifted out, drained and rinsed in flowing water to stop development. For the majority of this work development was carried out in this way. A small tank was employed that could allow development of five or six plates at any one time, developer temperature was maintained by the use of heated water jackets and the tank used a floating lid to reduce oxidation of the developer. The plates were loaded vertically into a mount that allowed

the developer to flow evenly and without restriction across the resist face. By batch development some of the variables in terms of developer temperature, exact time and agitation could be controlled. It was important that delay times between exposure and development were minimised. Fresh batches of developer were prepared for each new series of experiments.

An alternative system of development tried in the early stages of the work was that of spray development. Spray development is most commonly used by the microelectronics industry and specialised equipment is available for such. In this instance a two way tap was connected to two tanks, one containing developer the other rinse water. A small hand spray with nozzle was fed under pressure from the tanks, directing either developer or water onto the exposed plate. Several problems were encountered. Initially the development time was short <30 seconds and switching between developer and rinse on the hand nozzle gave  $\pm 10$  seconds variability in processing times. The spray nozzle directed a mist of fresh developer onto the plate at all times which was an advantage over the immersion method but the mist employed was too coarse and the developer fell more in drops on the surface and caused blotchy and uneven removal. When attempts were made to increase the fineness of the mist the developer foamed more easily again leaving areas of poor development. The nozzle had to be directly lightly across the resist surface as a static position was found to remove more resist at the centre than at the edges of the plate. This method was used with more success in later work and results presented have been achieved by spray or immersion techniques.

#### 3.7.6 Postbaking

Postbaking of the developed image was described in Section 3.6.6 for improving chemical resistance and adhesion of the resist to the substrate. Plates that were postbaked before the electroforming process did show better adhesion to the substrate and the initial electroform could be better removed and leave the resist more in tact than without postbaking. Plates that were electroformed immediately after exposure lost the resist image when the first electroform was

removed. Whilst this was not disastrous, retention of the original image proved useful for inspecting the quality of transfer through the processes. Postbaking was carried out in a fresh air oven at 80°C for 15 minutes. It is believed that this process did not cause any 'flowing' of the resist or image distortion at this temperature.

#### 3.7.7 Storage and Handling

Processed plates were kept in sealed boxes prior to subsequent copying stages as cleanliness was important. Some handling wear and tear was unavoidable when mounting samples for the Talysurf and SEM inspections.

#### 3.7.8 Resist Stripping

Plates with processed images that were no longer needed were stripped of resist by soaking in acetone prior to the cleaning cycles being used. Substrates that showed scratches or ingrained stains were not reused and fresh glass blanks prepared.

### 3.8 Discussion of Results

The experimental detail has dealt primarily with investigation into the characteristics of the working resist. Options such as different resists, developers, exposure systems were not extensively researched as the system chosen was designed to most closely match the experimental materials and procedures used in the commercial production of embossed holographic images.

Conclusions reached from the experimentation are summarised below:

- Glass substrates have been successfully cleaned and prepared prior to resist application
- Photoresist has been spin coated onto glass substrates of various sizes using available spinner with good evenness of coating and repeatability of results.
- Softbaking parameters have been investigated to optimise resist sensitivity and resist removal. An optimum time and temperature has been identified.
- Exposure characteristics have been fully characterised with regard to



required exposure times, ideal development parameters and ideal resist removal rates. Effects of developer upon unexposed resist have been characterised and applied to experimental methods by use of the Bartolini equations.

- Image accuracy has been investigated with reference to exposure times to achieve maximum image accuracy for photomasks.
- Development parameters have been studied and different methods and regimes characterised. Fully repeatable results throughout experimental work have been achieved.
- Postbaking to improve adhesion before further processing has been successfully applied to results.
- The storage, handling and stripping of substrates for re-use has been carried out with no detrimental effects of reusing glass blanks.
- A greater understanding of the properties, characteristics and features of positive working photoresist has been gained in order to fully utilize the material to produce accurate, efficient diffraction gratings and holographic images for the purposes of this thesis.

The following chapter considers the important surface pattern features for the assessment of the Information Transfer Process. The surface relief detail recorded into photoresist is measured by optical and surface finish techniques to compare the accuracy of the original image with that produced in the physical and mechanical copying stages.

## CHAPTER 4

### MEASUREMENT OF SURFACE RELIEF PATTERN AND DIFFRACTION EFFICIENCY

#### 4.0 Introduction

The previous chapters have described the recording of the white light 'rainbow' hologram into a surface relief material and identified photoresist as the most appropriate photosensitive material. This section considers the features of the surface relief pattern and identifies measurements for quantifying the entire transfer process through each of its stages.

The essential features chosen to quantify the transfer process of the diffraction grating were groove depth and diffraction efficiency. By study of these factors at each stage through the embossed hologram cycle a better understanding of the distortions or losses of surface relief pattern could be identified. The process of transferring surface relief detail from holographic image to metal copy through into stamped plastic introduced distortions. The importance of groove profile and grating efficiency and the difficulties that arise in using holograms for measurement due to the extremely complex surface patterns have been described. The series of diffraction gratings used simplify the measurement of the transfer of information. From an understanding of the problems of accurately copying diffraction gratings through each stage of the process, the problems of copying holograms can be better appreciated.

The initial and final depth of grooves through the embossing sequence is determined. The overall scheme is illustrated in Fig 4.1

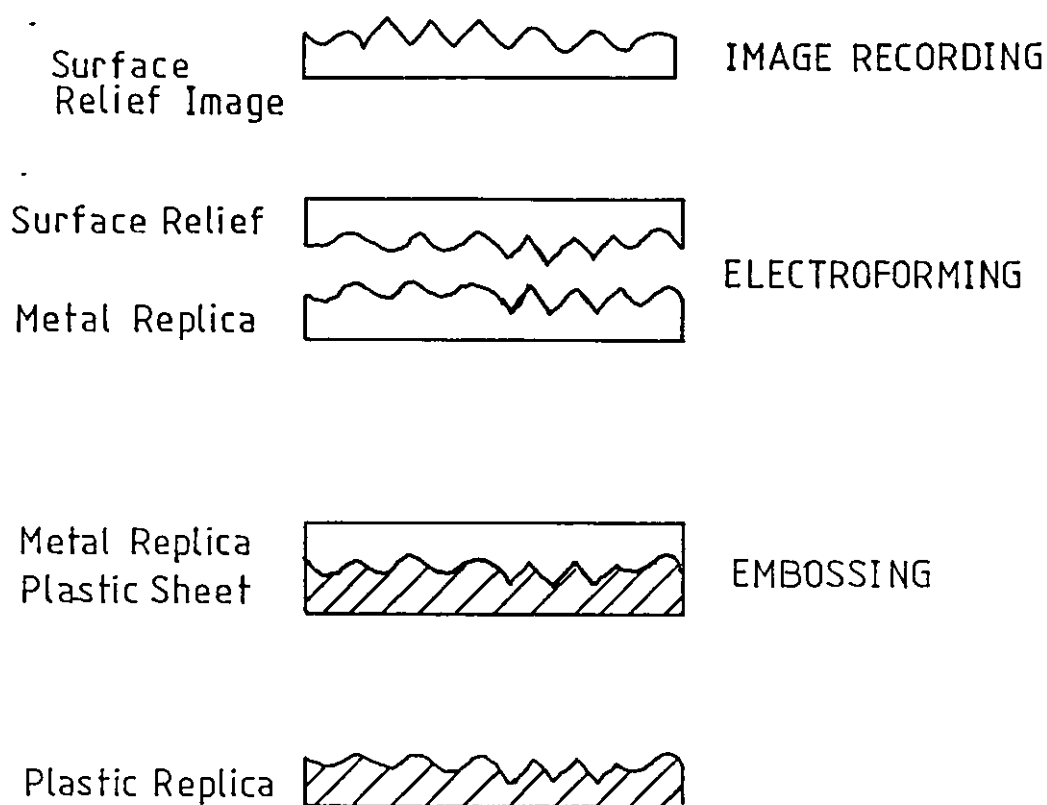


Figure 4 1 Overall Scheme of the Information Transfer Process

#### 4.1 Measurement of Groove Depth and Profile

Three techniques have been used to measure the detail of the surface relief pattern for groove depth and profile. These are, scanning electron microscopy, optical microscopy and surface finish measurements using a Talysurf instrument. The latter section of this chapter will cover the measurement of diffraction efficiency and the relationship to groove depth and profile.

A distinction should be drawn between groove profile and groove depth for the purposes of this study. Groove profile of a grating is an important factor in influencing spectroscopic properties and is as important as depth in the measure of diffraction efficiency. This work has concentrated on assessing groove depth in preference to true profile. Visualisation of groove profile is possible from some measuring techniques but is a difficult feature to accurately record. With good quality gratings recorded with two plane wavefronts intersecting at an angle, pure sinusoidal profiles should result. Less than perfect sinusoids introduce noise and scatter into the diffracted wavefronts so reducing efficiency. The depth of the groove is determined by exposure and development procedures in the recording of the interference patterns.

#### 4.2 Scanning Electron Microscopy

The scanning electron microscope (SEM) is a well established research analysis tool. The surface under study is effectively scanned by a focussed electron spot. The electrons behave like waves whose wavelength depends upon the voltage through which they are accelerated. Between 100 and 10,000V, the wavelength can lie in the region of a fraction of an angstrom unit. Magnetic and electric fields focus the electrons emitted or reflected from the surface of an object which in turn are detected by a collector. An associated electrical signal is processed and displayed upon a cathode ray tube synchronised to the scan of the electrons over the surface. In this way details not very much larger than the wavelength of the electrons can be photographed. The advantages of the SEM are an extremely large depth of field and large magnifications, typically 15K to 30K. If the object surface is conducting little or no surface preparation is necessary, (replicas may sometimes be used). Size of specimen is usually limited to 4x4". Whilst the SEM provides an excellent visual study of gratings the interpretation of the images can be difficult as it is not straightforward to assess depth or profile. For depth measurement, shadowing techniques using fibres have been developed but skilled operation and interpretation is required for unambiguous results

Figure 4.2 illustrates how interpretation of profile can be difficult if the precise tilt and viewing conditions are not known. [29]

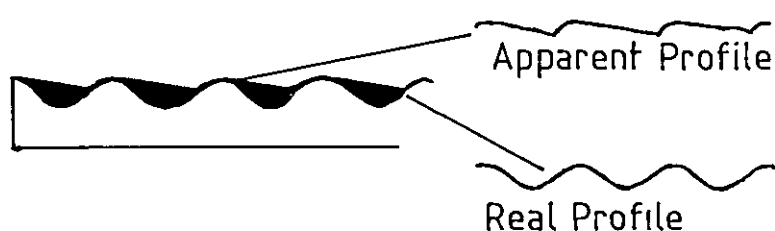


Figure 4.2 The Interpretation of Groove Profile

Plates 9 and 10 show results from SEM investigation of different grating structures. The SEM was used in this work for visual inspection of quality of surface/noise/damage more than for quantitative measurements.

A summary of merits is given below;

Advantages

Excellent visual inspection  
High magnifications possible.  
Resolution in the order of 20nm

Disadvantages

Surface preparation/replica needed.  
Skilled operator dependent.  
Ambiguity of data interpretation.  
Slow method for many samples.



Plate 9.

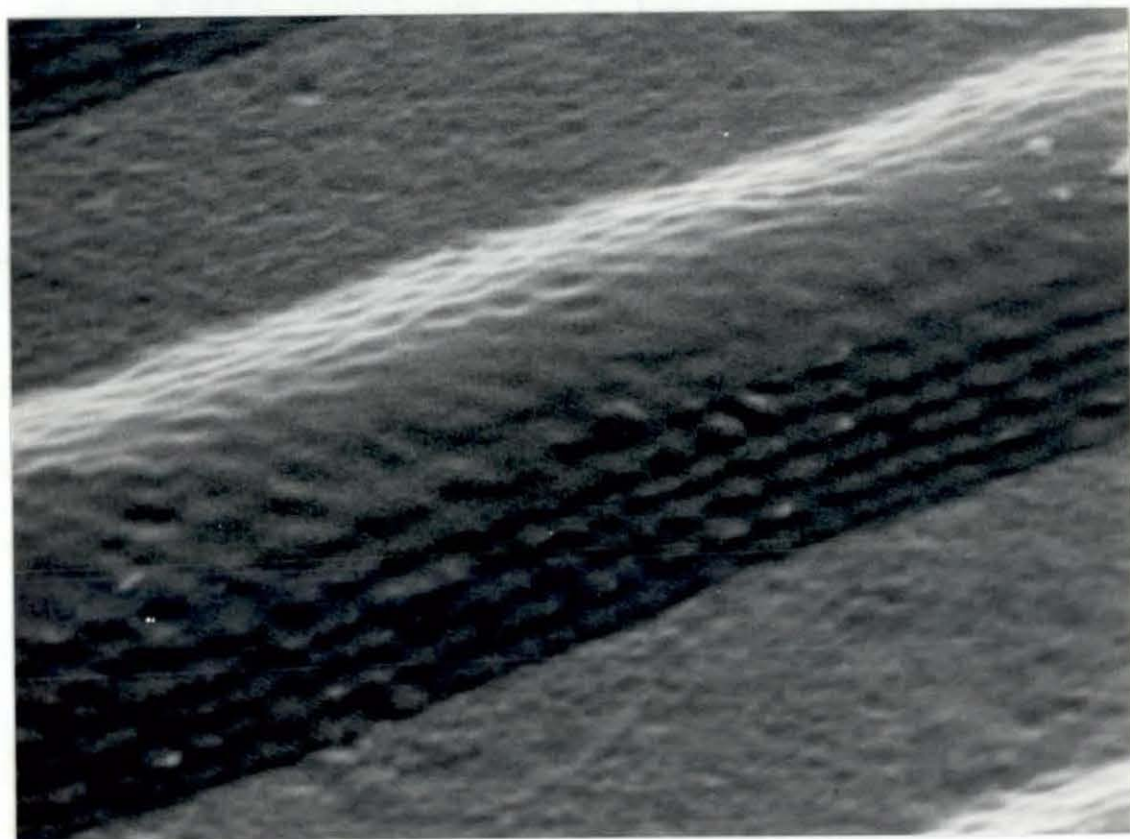


Plate 10.

Investigation of Grating Structures by Scanning Electron Microscope

#### 4.2.1 Assessment of Errors and Experimental Results

##### Scanning Electron Microscopy

No quantitative data has been obtained from this technique but excellent visual assessment has been made. Plate 11 shows a profile from a diffraction grating and the limited depth achieved. Interpretation of the profile edge is difficult to determine.

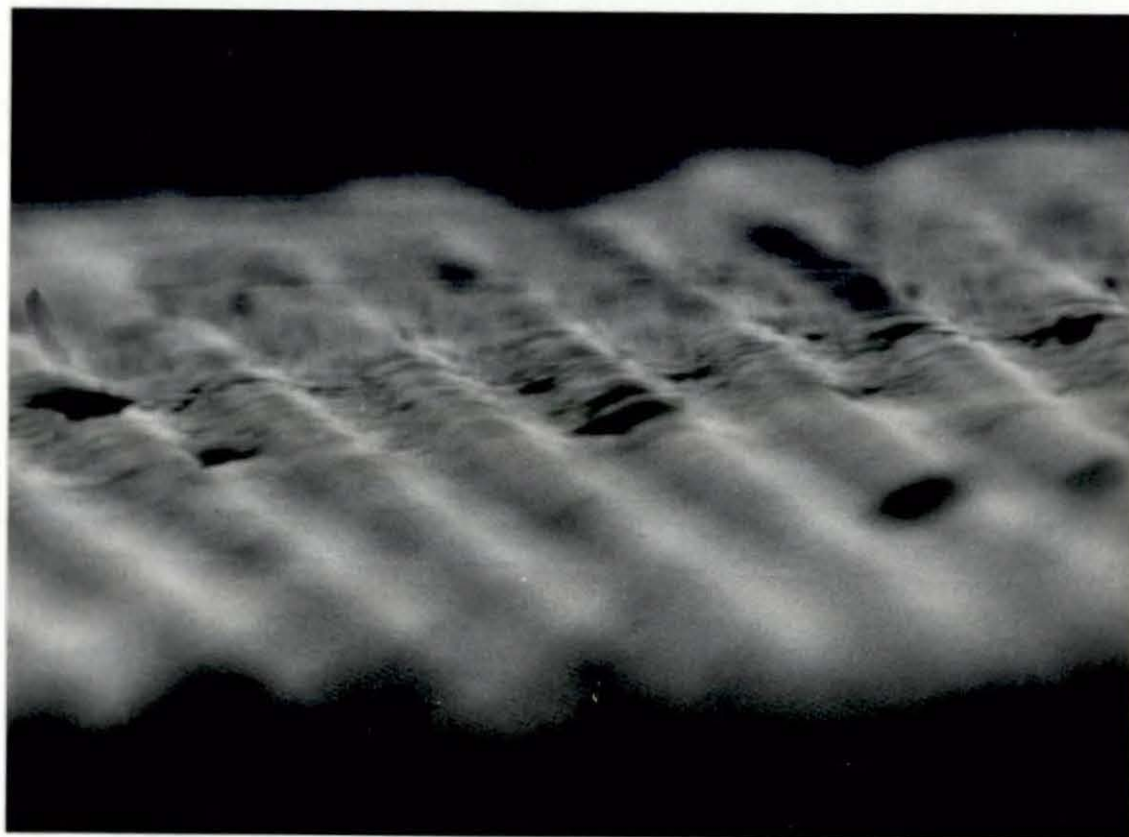


Plate 11. Edge Profile of a Diffraction Grating in Photoresist



Plate 12 shows an alternative approach to profile assessment, a metal diffraction grating was mounted in epoxy resin and sectioned. An aerial view was attempted to show grating profile but this can not be quantified. The excellent magnification and resolution of the SEM has allowed examination of a wide range of results.

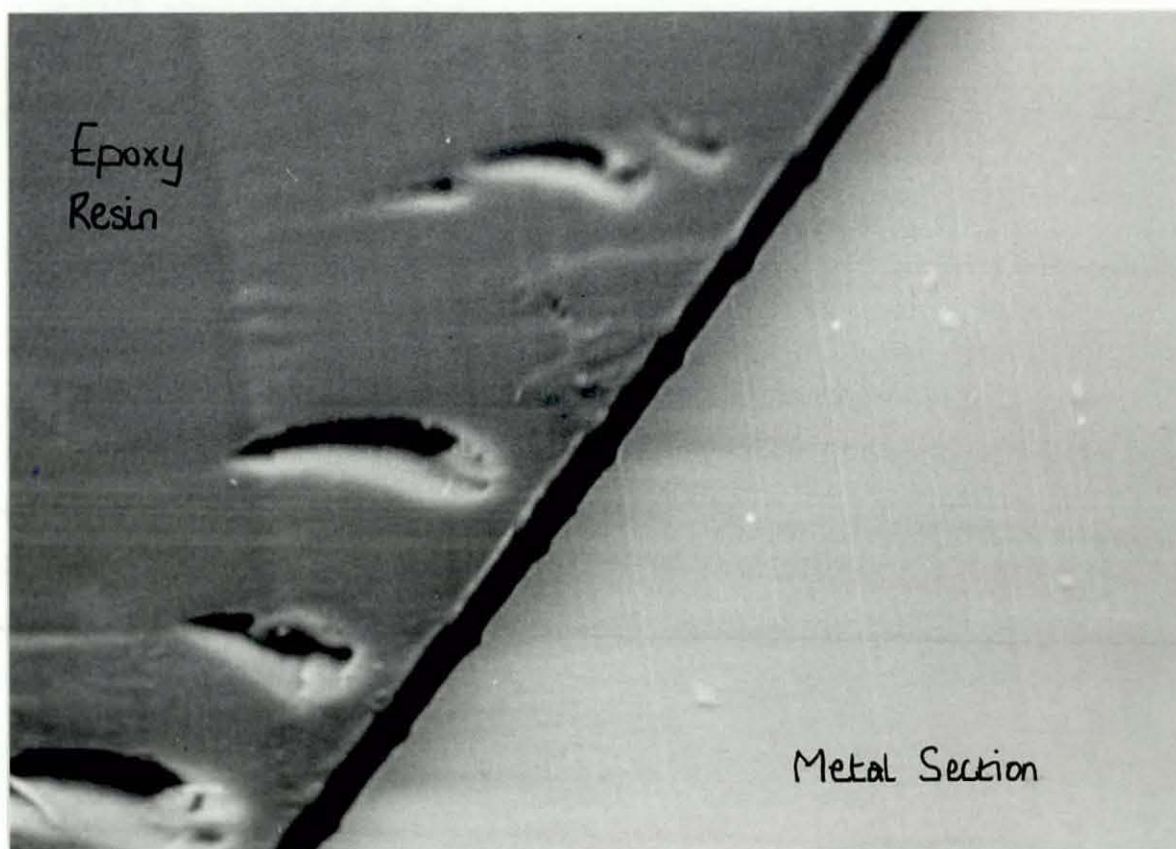


Plate 12. SEM Photomicrograph of Metal Section Mounted in Epoxy Resin



### 4.3 Optical Microscopy

State-of-the-art optical microscopes allow extremely accurate measurements over greater ranges than ever. Specialised techniques of polarized light, phase contrast and interference microscopy can help with the measurement of groove depth and the impression of groove profile. The limitation of such techniques is resolution whereby the instrument may be capable of measuring depths from  $0.01\mu\text{m}$ - $1.0\mu\text{m}$ , but only for coarse gratings upto a limit of  $>1000$   $1/\text{mm}$ .

A successful technique used in this work was that of double and multiple beam interference systems. The principles of which are illustrated in Figure 4.3

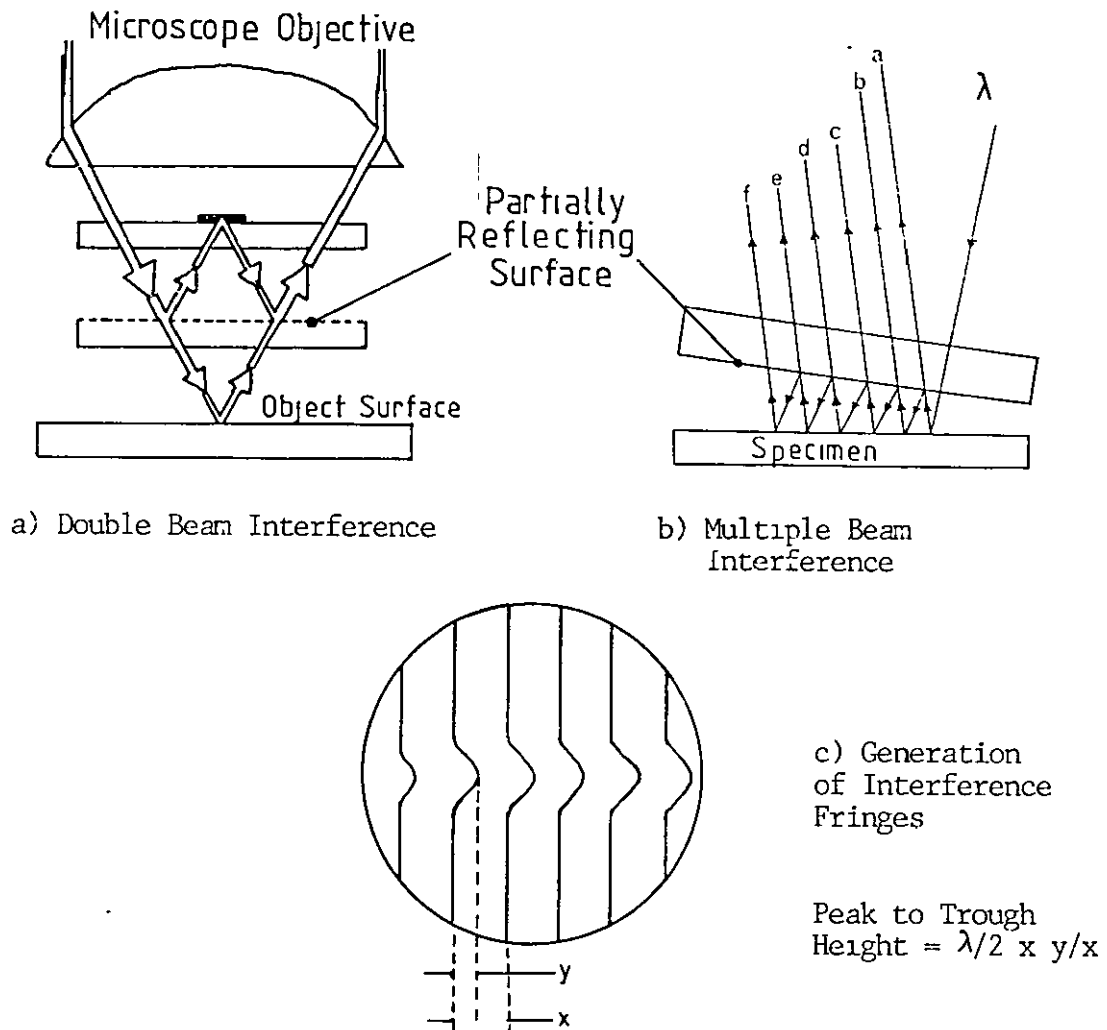


Figure 4.3 Double and Multiple Beam Interference Systems

#### 4.3.1 Double Beam Interferometry

The double beam or Mirau technique generates interference fringes across the surface of the specimen in a non-contact technique. Height differences on the surface are revealed by changes in the interference patterns and can be determined as fractions and multiples of half the wavelength of light used. Monochromatic or white light can be used, Monochromatic illumination makes quantitative assessment easier as white light produces coloured fringes across the surface. Height differences of 3-5 $\mu\text{m}$  can be detected with a minimum resolvable difference of 0.025 $\mu\text{m}$  [46]. Figure 4.3 a) illustrates the use of a modified microscope objective for double beam interferometry work.

#### 4.3.2 Multiple Beam Interferometry

Multiple beam Tolansky methods utilize Fizeau fringes produced between the reflecting surfaces as illustrated in Figure 4.3 b) The reflected beams interfere and are focussed by the microscope objective. The greater the number of fringes, the sharper and narrower the interference pattern appears, making quantitative analysis easier. Each fringe spacing represents a difference of  $\lambda/2$ . The fringe pattern appears as in Figure 4.3 c). If the readout from an eyepiece micrometer is  $x$ , and the value of the disorder of the wavelength is  $y$ , the value of the difference in level or roughness is  $N = \lambda/2 \times y/x$ . The measuring range covers 0.01 $\mu\text{m}$ -0.1 $\mu\text{m}$  depending upon surface reflectivity and shape. [47] The multiple beam system offers advantages in the quality of fringes seen across the sample. In practice the fringes are generated by a reference mirror fitted to the microscope objective that lightly rests upon the sample. The mirror is tilted to produce an extremely small wedge angle over the sample creating contour fringes over that area. Each fringe spacing represents a separation difference of half a wavelength, the deflection and spacing can be measured by eyepiece micrometers for monochromatic or white light. The technique has been used to confirm the accuracy of Talysurf measurements and has achieved accuracies of  $\pm 0.01\mu\text{m}$ . The technique is somewhat slow to use and difficult to measure at times when deep profiles or fine gratings are used. The method has been used as a 'batch' type check, taking samples that have been measured using

Talysurf and comparing results with measurements from multiple beam interference microscopy.

Merits of the system as given below,

<u>Advantages</u>	<u>Disadvantages</u>
Good visual technique for quality of sample.	Some operator skill required.
No sample preparation necessary	Fringes can be difficult to interpret/measure.

#### 4.3.3 Experimental Results

Optical interference microscopy proved successful in assessing groove nature and depth. Whilst limited to a maximum magnification of X1000, with measuring inaccuracy for each technique, interferometric assessment confirmed other system results. A Nikon Optiphot metallurgical microscope with additional features was used for double beam and multiple beam interference techniques.

#### 4.3.3.1 Double Beam Interference

This technique used a simplified non-contacting system producing fringes across the surface of the photoresist or metal shim as seen in Plate 13.

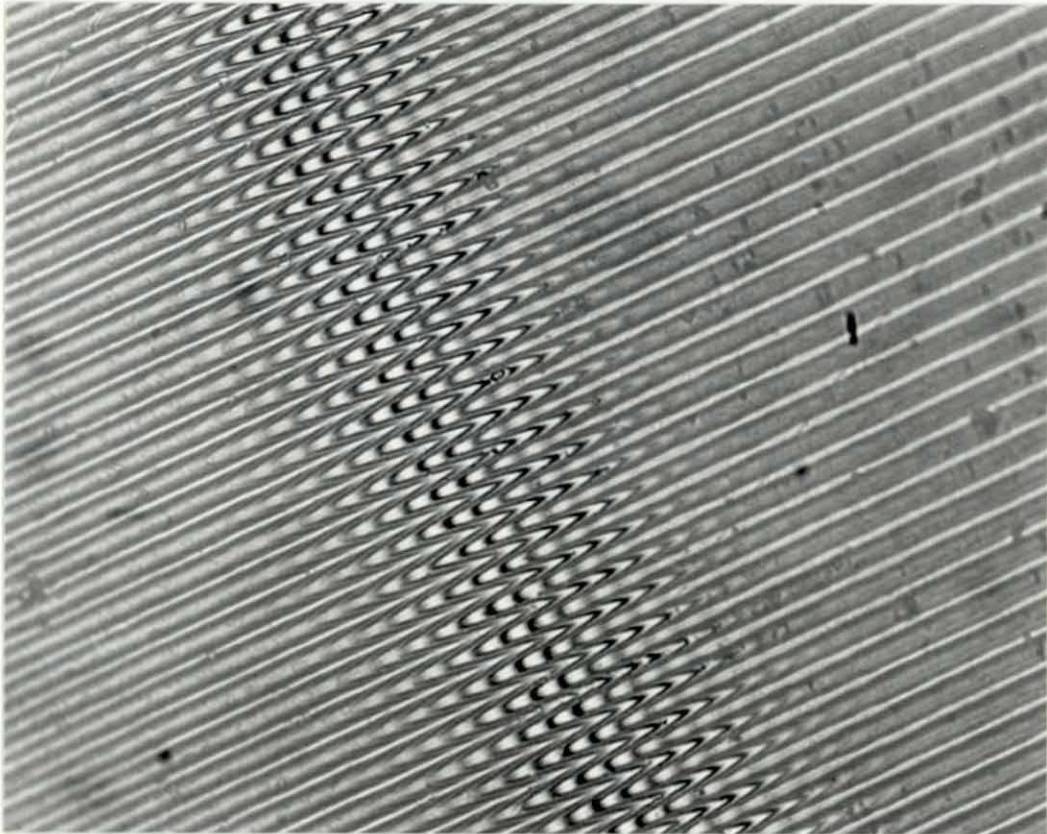
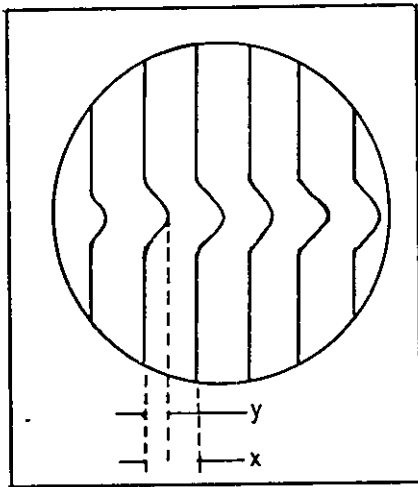


Plate 13 Double Beam Interference Fringes

Fringes appear across the central area only as these were produced using white light without a narrow band filter. Measurements were made using the narrow band filter with  $\lambda=546\text{nm}$ . The fringes are coarse in nature and were extremely sensitive to vibration necessitating mounting the microscope on an isolated table for fringe measurement. The eyepiece micrometer was calibrated for the optics in use and estimated accuracy was  $\pm 0.01\mu\text{m}$ . Calculation of grating depth was made as follows;



Disturbance =  $y$

Readout =  $x$

Level of roughness  $N = \lambda/2 \times y/x$  mm

Level of roughness  $N = \lambda/2 \times y/x$

From eyepiece measurements  $x = 8.75 \times 10^{-3} \text{ mm}$

$y = 12 \times 10^{-3} \text{ mm}$

$\lambda/2 = \frac{0.546 \times 10^{-3} \text{ mm}}{2}$

2

$N = 3.74 \times 10^{-4} \text{ mm}$

Peak to Trough Height =  $0.374 \mu\text{m}$

Surface finish measurement by a Talysurf instrument for this same sample (2b4 First generation metal shim) gave height difference  $0.42 \mu\text{m}$  with an accuracy of  $\pm 0.04 \mu\text{m}$ . Results are tabulated in Table C.

A further sample, first generation metal, grating 2a3 was also assessed by double beam interference microscopy.

From eyepiece measurements:  $x = 1.25 \times 10^{-3} \text{mm}$

$$y = 1.02 \times 10^{-3} \text{mm}$$

$$\lambda/2 = \frac{0.564 \times 10^{-3} \text{mm}}{2}$$

2

$$N = 2.23 \times 10^{-4} \text{mm}$$

$$\text{Peak to Trough Height} = 0.223 \mu\text{m}$$

Talysurf measurement of the same sample gave a height difference of  $0.16 \mu\text{m} \pm 0.04 \mu\text{m}$ .

#### 4.3.3.2 Multiple Beam Interference

This technique relies upon matching the reflectance of the sample under examination to that of a reference mirror attached to the microscope objective. The reference mirror rests lightly upon the sample to create a small wedge angle and generate fringes across the sample. Plate 14 shows fringes from multiple beam interference microscopy.

The fringes are considerably sharper and finer making quantitative assessment easier. Eyepiece micrometer accuracy was limited to  $0.01 \mu\text{m}$ .

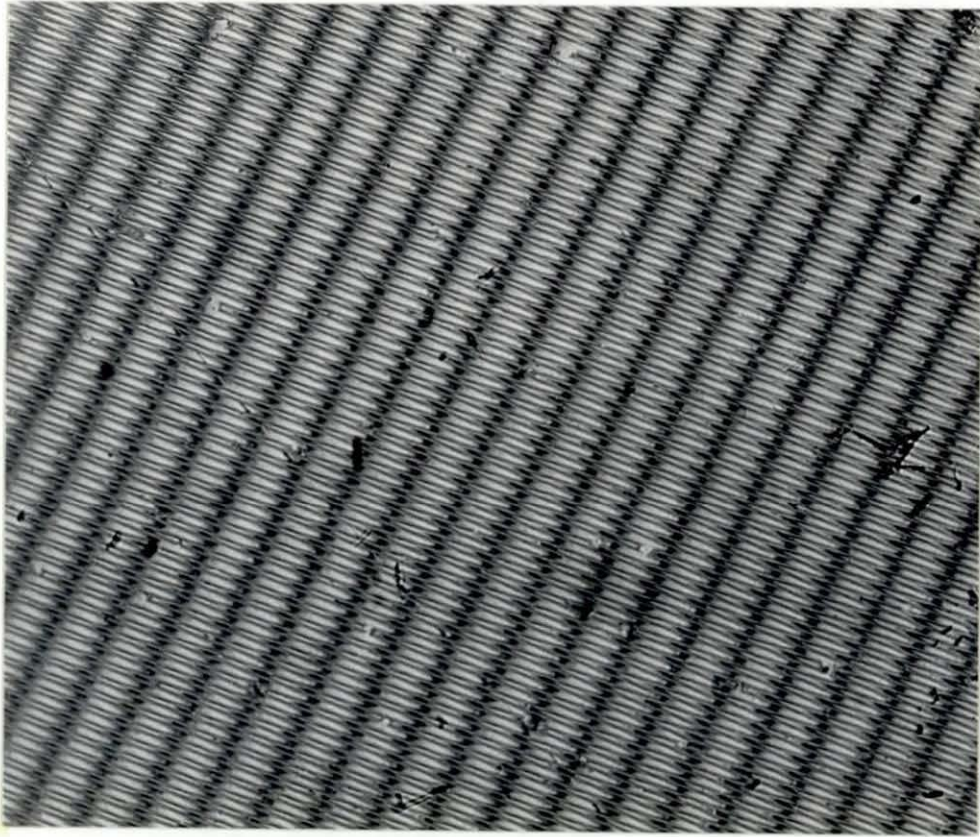
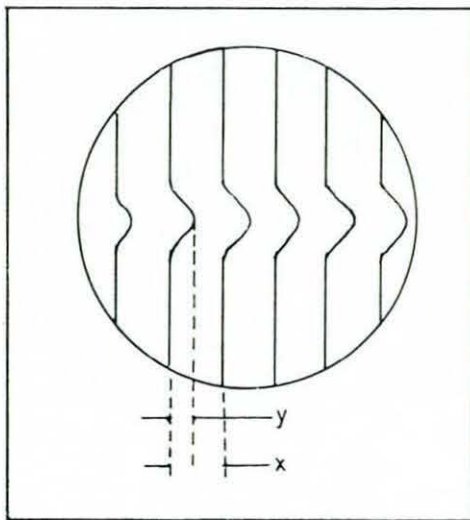


Plate 14 Multiple Beam Interference Fringes

Calculation of height differences was made as follows;



Disturbance =  $y$

Readout =  $x$

Level of roughness  $N = \lambda/2 \times y/x$

From eyepiece measurements for first generation metal, grating 2b4.

$$y = 1.75 \times 10^{-3} \text{mm}$$

$$x = 1.15 \times 10^{-3} \text{mm}$$

$$\lambda/2 = \frac{0.564 \times 10^{-3} \text{mm}}{2}$$

$$N = 4.15 \times 10^{-3} \text{mm}$$

Peak to Trough Height = 0.415  $\mu\text{m}$

A further sample, first generation metal, grating 2a3 was also measured.

From eyepiece measurements;

$$y = 1.15 \times 10^{-3} \text{mm}$$

$$x = 1.5 \times 10^{-3} \text{mm}$$

$$\lambda/2 = \frac{0.546 \times 10^{-3} \text{mm}}{2}$$

$$N = 2.09 \times 10^{-3} \text{mm}$$

Peak to Trough Height = 0.209  $\mu\text{m}$

Table C summarises the results from Double and Multiple Beam interference techniques and compares them with measurements taken from a Talysurf instrument.

Sample	Double Beam	Multiple Beam	Talysurf
2a3	0.223 $\mu\text{m}$	0.209 $\mu\text{m}$	0.16 $\pm 0.04 \mu\text{m}$
<u>1st. Metal</u>			
2b4	0.374 $\mu\text{m}$	0.415 $\mu\text{m}$	0.42 $\pm 0.04 \mu\text{m}$
<u>1st. Metal</u>			

Table C Comparison of Microscopy and Talysurf Measurements  
The multiple beam technique shows better correlation with the Talysurf measurements and lies within experimental accuracy. The improved



quality of fringes from the multiple beam technique reduced the inaccuracy of measuring broad fringe patterns. Whilst the double beam technique was simpler in operation the correlation with Talysurf results lies at the limits of experimental accuracy

#### Image Processing

An investigation into the possibility of using fringe analysis techniques was carried out on video tape images of the double beam interference fringes. The Nikon microscope allowed video camera recording of the samples under investigation. The double beam interference fringes were recorded and processed using a Kontron Bildanalase image processor using a Microvax 11 computer. Plates 15, 16 and 17 show the monitor output for metal samples 2b4 and 2a3. The composite picture shows the video input of the recorded grating. A grey level slice was taken through the sample, running at 90° to the direction of the grating. The final output shows the grating with the profile section beneath. It can be seen that the profile from each sample is significantly different. The results are compared with the Talysurf traces for each. Whilst the technique shows great promise it has not been fully verified, the associated errors of the technique include those of the microscope, the television camera and computer. The results show excellent correlation with those from the Talysurf traces and it would be hoped that quantitative as well as groove profile data could be obtained from this technique.

#### Optical Microscopy on Metal Sections

A further optical microscopy technique used to study grating profiles was investigated by producing cross section samples of the gratings. Only metal shims could be investigated due to preparation methods. A small sliver of the metal was cast into epoxy resin and allowed to set over a period of 24 hours. The pellet was sectioned using a diamond tipped cleaver to remove slices of the sample. The tip of the pellet was then examined under a microscope. Plates 18 and 19 show the section mounted into epoxy resin and detail taken from a magnified area of the metal section. The profile of the shim is clearly visible.

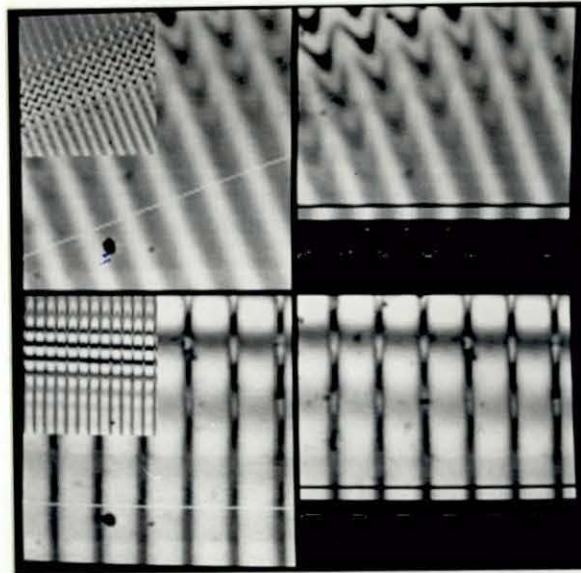


Plate 15. Composite Image Showing Grating Video Image and Grey Level Slice Section.

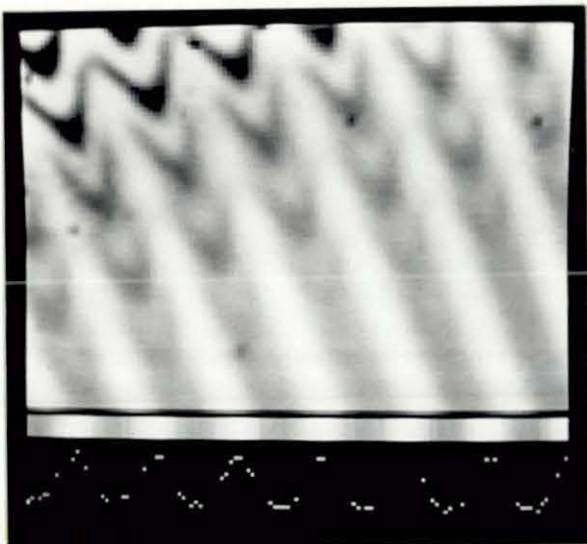


Plate 16. Profile Output from  
Grey Level Slice  
Grating 2a3

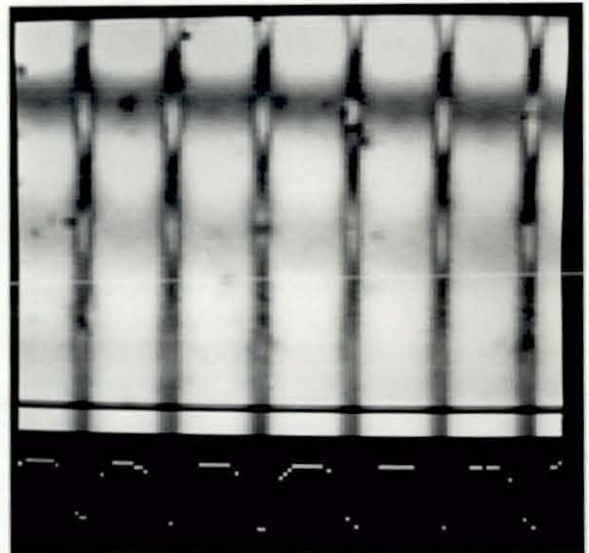
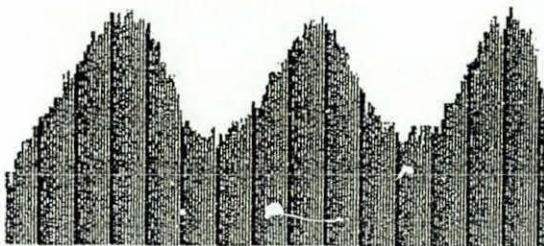
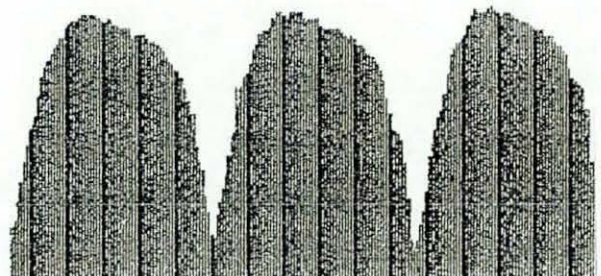


Plate 17. Profile Output from  
Grey Level Slice  
Grating 2b4



Talysurf Profile Trace  
Grating 2a3



Talysurf Profile Trace  
Grating 2b4



Plate 18. Metal Section Mounted into Epoxy Resin

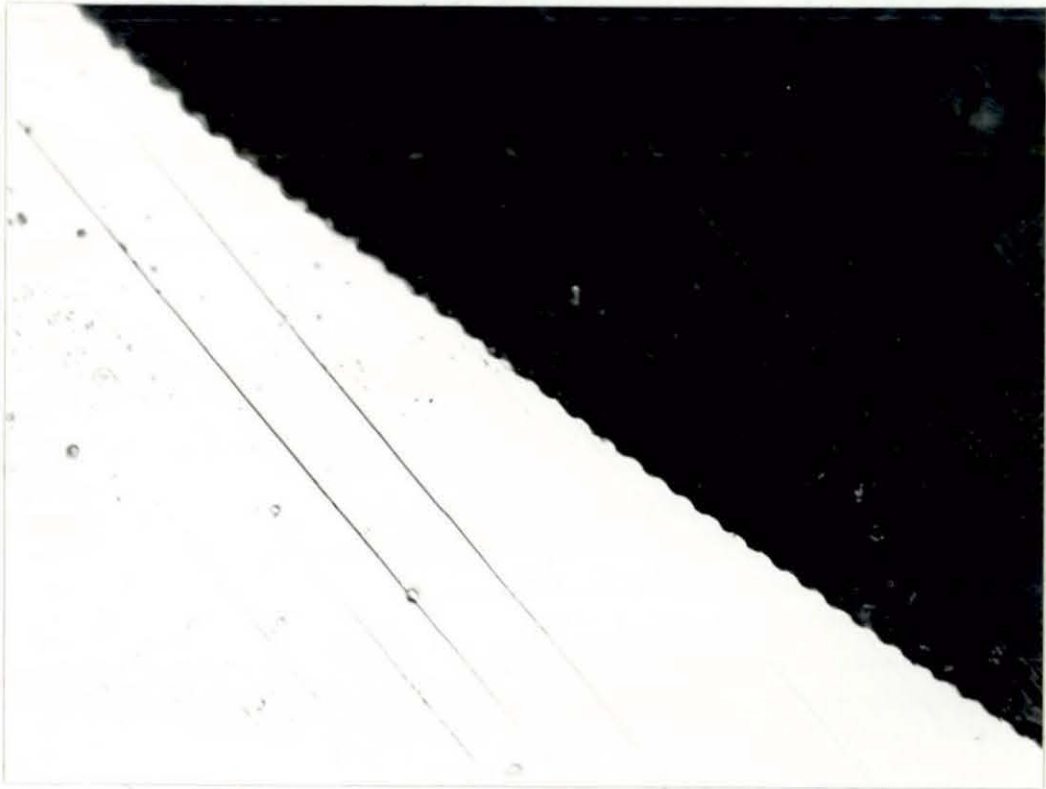


Plate 19. Area from Metal Section Showing Grating Profile



The limitation of the technique was the measuring accuracy of the optical microscope. Although a magnification of x1000 was possible on some of the instruments, the eyepiece micrometers limited measuring accuracy to  $\pm 1\mu\text{m}$ . The technique was therefore used as a visual inspection of profile nature. Considerable skill was required in mounting the samples into the liquid resin to present the correct facet to the diamond cleaver once resin had set. Several samples were repeated because despite cleaving at various angles a direct view of the profile could not be obtained. Examination by scanning electron microscope did not offer any advantage because desired angle of view could not be obtained. A direct plan view was easier to achieve with an optical microscope. Plate 20 shows an SEM image of the profile but from a slanted viewpoint making interpretation difficult.

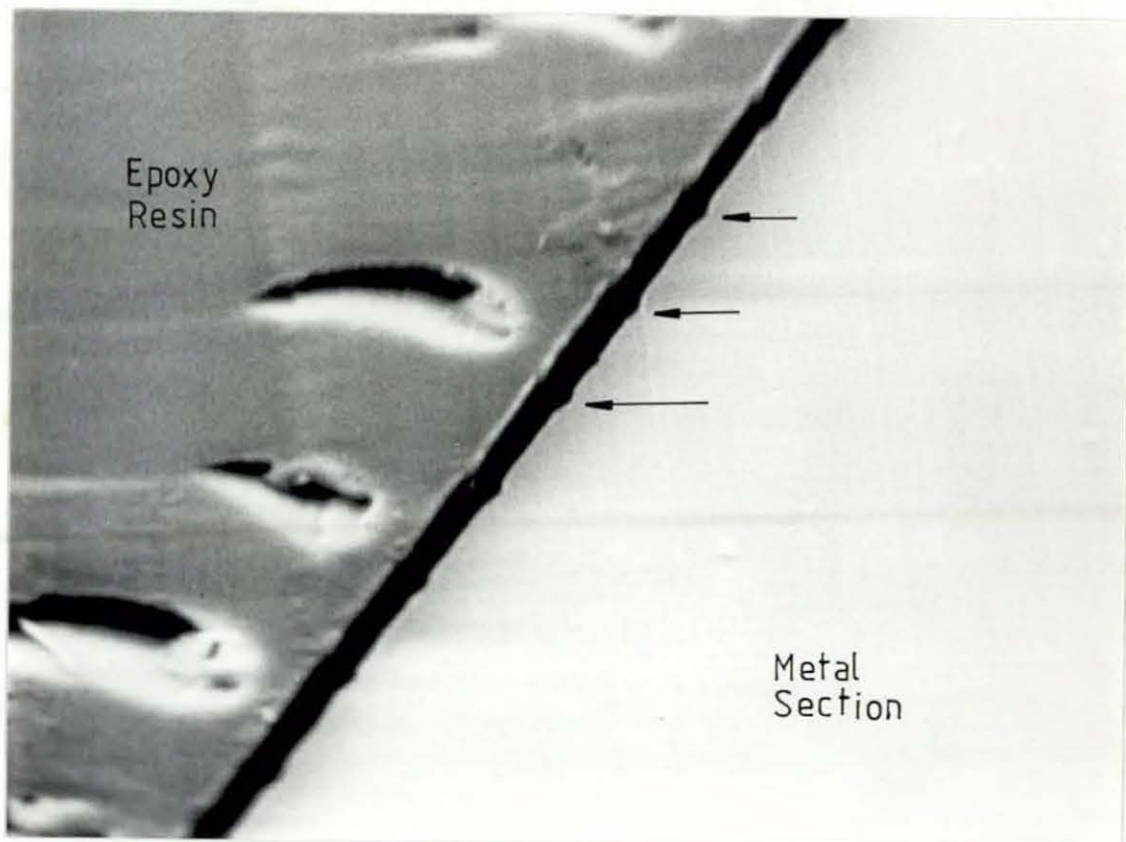


Plate 20 Profile Assessment Using Scanning Electron Microscopy

#### 4.4 Talysurf Instrument

The Talysurf (or Talystep) instrument is typically found in mechanical and production engineering departments and workshops for measurement of surface roughness and surface finish. It is well suited to the measurement of groove height as it gives direct information about a surface finish. The principle involves moving a lightly loaded (approx. 100mg force on surface) diamond tipped stylus across the sample. Figure 4.4 a) illustrates the apparatus.[48] The skid nosepiece arrangement fits down over the stylus as illustrated in Figure 4.4 b).

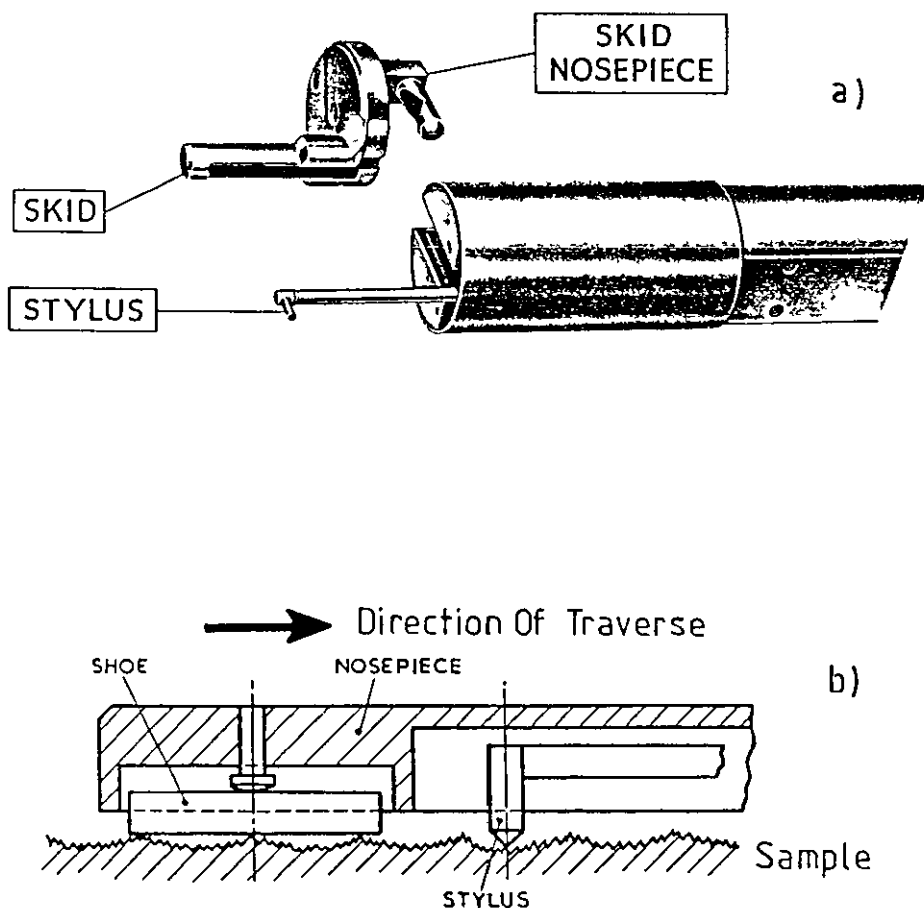


Figure 4.4 Talysurf Stylus and Skid Arrangement

The deflections in a vertical direction are detected electronically and output as a trace of peaks and troughs. Vertical resolution is extremely good, to within  $\pm 20$  nanometres, horizontal resolution is more limited and stylus dependent. Care must be taken with use of the instrument as the shape and size of the stylus can affect the result. Figure 4.5 shows how the stylus may incorrectly measure a groove profile. The use of an angled stylus would more accurately follow the grating profile and overcome this problem.

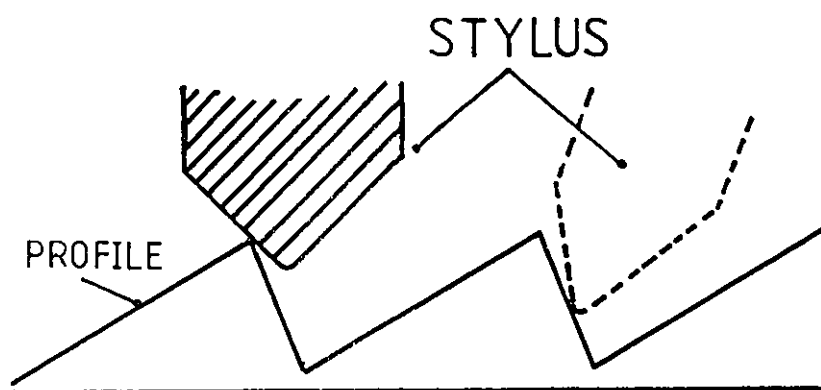
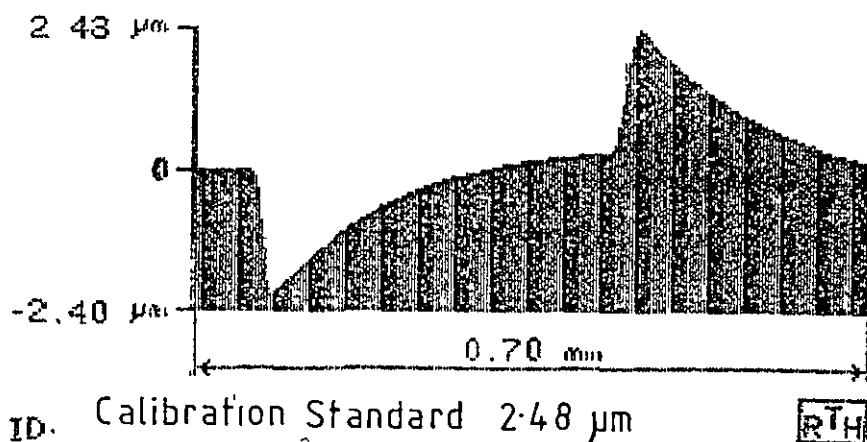


Figure 4.5 Use of An Angled Stylus to Measure Profiles

The stylus is typically chisel shaped,  $1.0\mu\text{m}$  long and  $0.1\mu\text{m}$  or less wide. A skid or shoe is used in conjunction with the diamond stylus depending on the nature of the surface. When using the Talysurf instrument it was found that the stylus and skid arrangement damaged the photoresist surface. Whilst this would normally be undesirable it proved an advantage for the accurate measurement of diffraction efficiency and profile from exactly the same area of the sample for

each assessment. The mark left by the apparatus was seen to transfer through each stage of the copying process providing an additional reference area for study. Postbaking of the photoresist improved the hardness of the material and limited the damage to the surface. (It is possible to measure the grooves without the skid to prevent surface scratching, set-up times for the instrument then took in excess of 40 minutes and offered no real advantage.) The mark of the stylus and skid has been used as a reference point for all subsequent measurements of profile and efficiency. Plates 21 and 22 show the stylus/skid damage to the measured diffraction gratings.

A further advantage of using the Talysurf has been its suitability for measurement of all substrates regardless of substrate reflectivity. (Optical microscopy techniques required matched surface reflectivity.) Provided the substrate could be held rigid and flat the Talysurf was capable of measuring surface detail. The interpretation of results was straightforward presenting data in graphical form. It was a very fast technique requiring little operator skill. The data below shows the standard used for instrument calibration. The trace outputs the result as a plot of plus and minus deviations about zero.



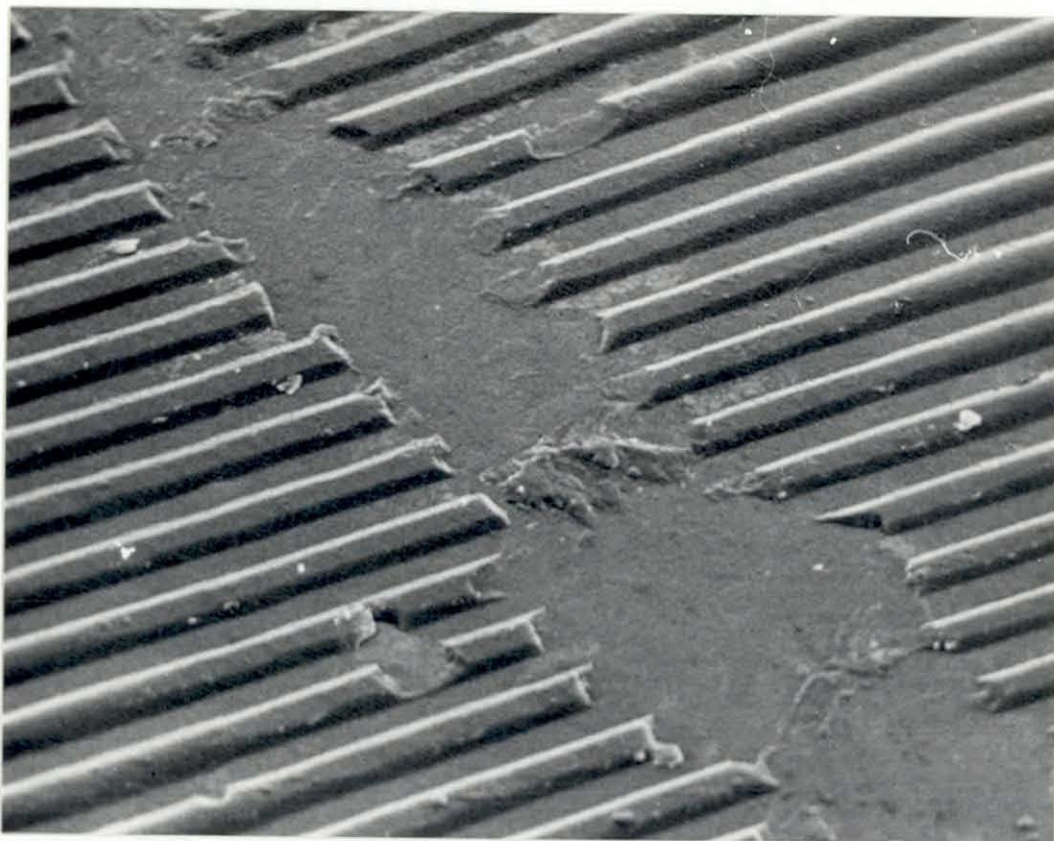


Plate 21.

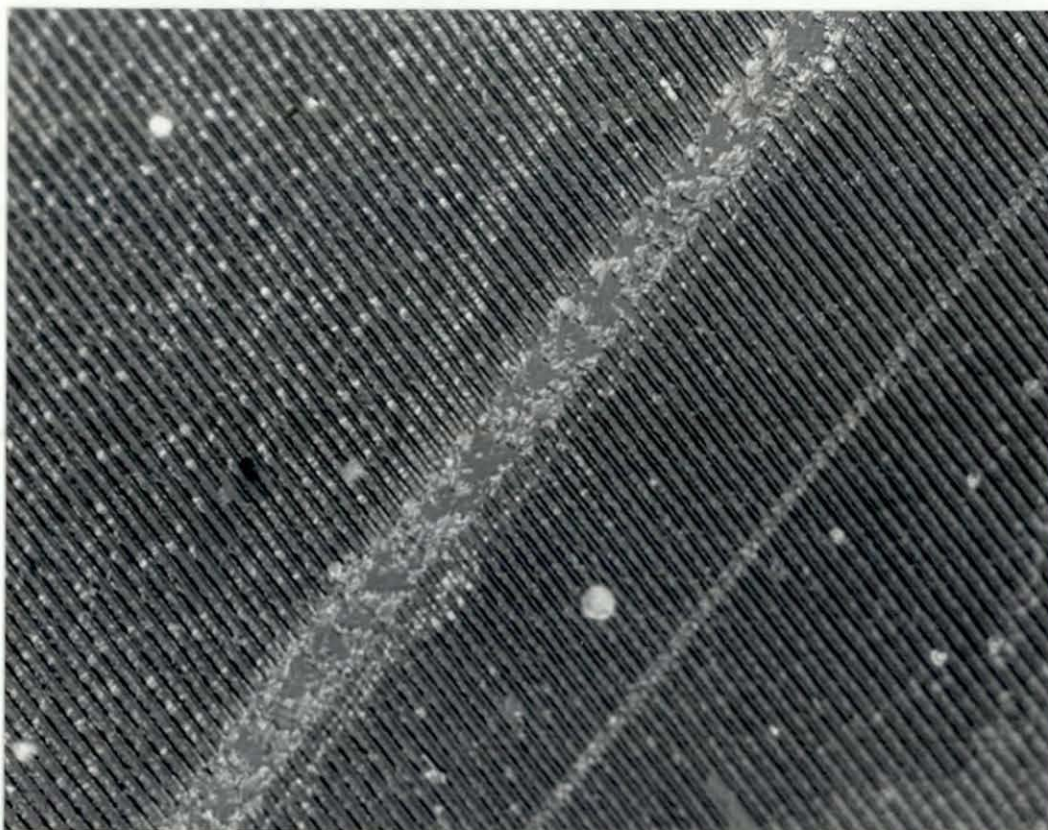


Plate 22.

Damage To the Grating Surface by the Stylus/Skid Assembly



A summary of merits for the Talysurf measuring technique is given below;

<u>Advantages</u>	<u>Disadvantages</u>
Fast, simple method	Contacting method with surface damage
Results presented in graphical peak/trough	Horizontal resolution limited
Excellent vertical resolution	Deep, fine gratings unsuitable for measurement
Capable of measuring transparent or reflective substrates	

#### 4.4.1 Experimental Results

Talysurf measurement was the principal technique used for groove depth measurement. The instrument, a Talysurf 4 with computer analysis, was fast and effective to use on all sample substrates with direct quantitative output. The advantage of speed and accuracy negated any damage caused to the sample by the skid. The accuracy of the instrument was  $\pm 0.02\mu\text{m}$  at the highest magnification, which has proved satisfactory for the gratings used in this work. The pitch of gratings measured was kept to 100 l/mm to facilitate accurate assessment. Gratings recorded at 1000 l/mm were not successfully measured using the Talysurf instrument due to the limited horizontal resolution. The length of the traverse was 11mm which adequately covered the grating. Each grating was traversed several times to ensure that the stylus was measuring at 90° to the grating and to detect any obvious variations across the samples. Before each assessment the instrument was allowed sufficient warm-up time and calibrated standards were traced to monitor measuring accuracy.

None of the above methods is complete in itself for the assessment of groove profile or depth measurement. All three used in conjunction have made a fuller analysis possible. The Talysurf technique has been used extensively and provided the basis for the depth measurements presented in this thesis. Optical microscopy has been used to measure line spacings and quality of gratings with electron microscopy used for some analysis of groove profile and visual inspection.

#### 4.5 Measurement of Diffraction Efficiency

It has been described how two features have been studied to assess the accuracy and efficiency of the Information Transfer Process. These are; groove depth and diffraction efficiency. Measurement of these two features through each stage of the copying process allows quantitative assessment of the accuracy of the system which represents a unique aspect of the study of the embossing sequence.

The diffraction gratings measured for groove depth by the Talysurf instrument were marked by the stylus/skid assembly at the precise point of measurement. These marks acted as the reference points from which to measure diffraction efficiency. The use of a laser for point interrogation greatly facilitated this assessment. An indication of the accuracy of the transfer process will be given by a matching of diffraction efficiency for photoresist, metal and plastic copies without the introduction of higher orders which indicate noise and distortion to groove depth or profile.

Chapter 2 described the measurement of diffraction efficiency and anomalies that may arise. In order to offer a useful expression of true efficiency this study has measured gratings with an optical layout using a configuration whereby the diffracted beam returns along the path of the incident beam as closely as possible (known as a Littrow mounting). Plate 23 shows the system for measurement of a nickel copy of a grating.

The system was designed along an optical rail to ensure accurate alignment of the laser beam onto the diffraction gratings. A 6mW Helium Neon laser was incident upon the grating, used in the S polarization regime. The laser could be introduced at any given angle of incidence onto the grating by rotation of the mounting unit for the grating. The mounting unit allowed accurate rotation through 360° with micrometer adjustment for final positioning. Initial alignment was assured by the return of the diffracted zero order along the axis of the laser beam for normal incidence. The diffracted orders were measured using a

power meter (Coherent 212). All measurements were made in reflection. The incident intensity of the laser output was measured and divided by the diffracted energy output to be expressed as a percentage for Absolute Efficiency. By this method of reflected light readings for a known angle of incidence, plane of polarization and wavelength, the most accurate assessment of diffraction efficiency has been possible.

All of the gratings, in photoresist, metal and plastic have been measured this way with surface reflectivity matched to ensure consistent results. The laser was an excellent point source for interrogation of the surface using the small scratch left by the Talysurf instrument as a reference point. This ensured that any variations across the surface in depth or finish could be avoided and that the same area was studied throughout the transfer process. In order to assess the accuracy over the entire surface of the diffraction gratings the laser was scanned across the surface and variation in diffraction efficiency noted.

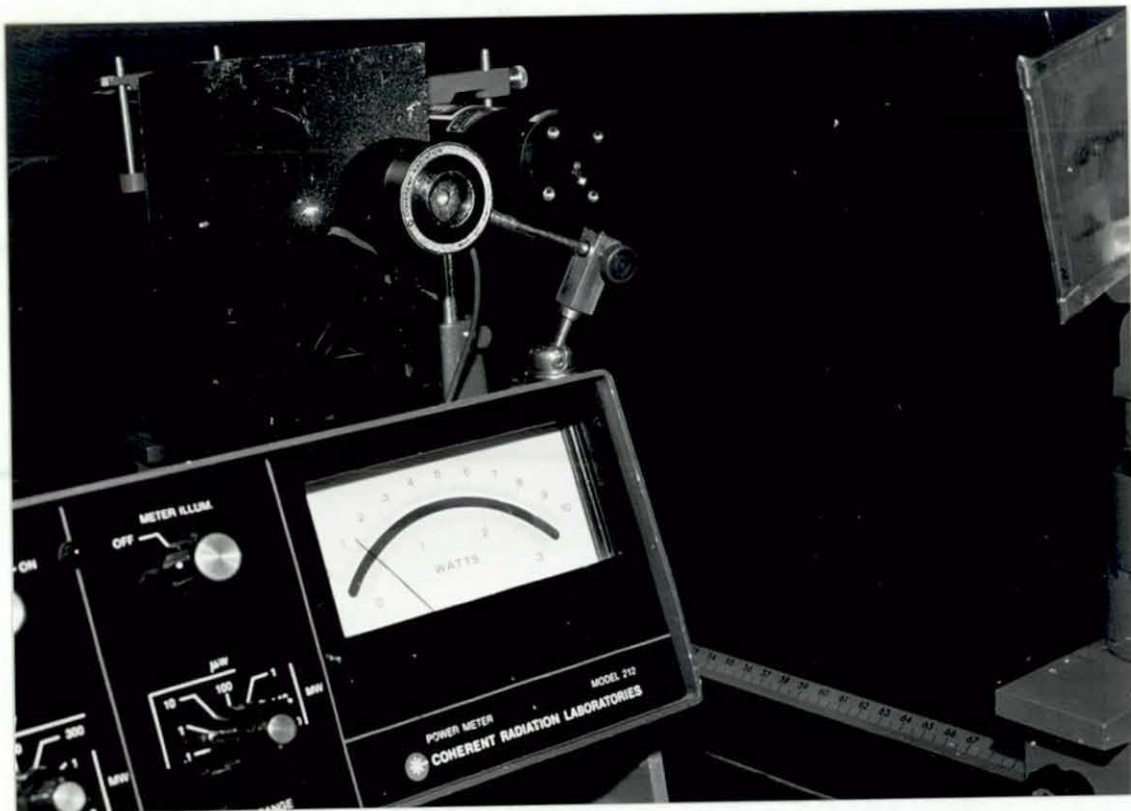


Plate 23 Experimental Arrangement for the Measurement  
of Diffraction Efficiency

#### 4.5.1 Assessment of Errors and Experimental Results

A large number of diffraction efficiency measurements were made upon silver halide and photoresist diffraction gratings. Efficiency is a widely used measurement that is rarely properly expressed and studies were made to assess the errors involved in the process. The study of the anomalies found in grating efficiency was made by considering a silver halide grating of 114 l/mm for different measuring regimes. A He-Ne laser of known input was used and efficiency was calculated over a range of 0-40° angle of incidence, for both vertical and horizontal polarisation planes over plus and minus six diffracted orders. The measuring accuracy of the power meter system was  $\pm 0.01 \mu\text{W}/\text{cm}^2$ . The grating and laser measuring arrangements are illustrated in Figure 4.6.

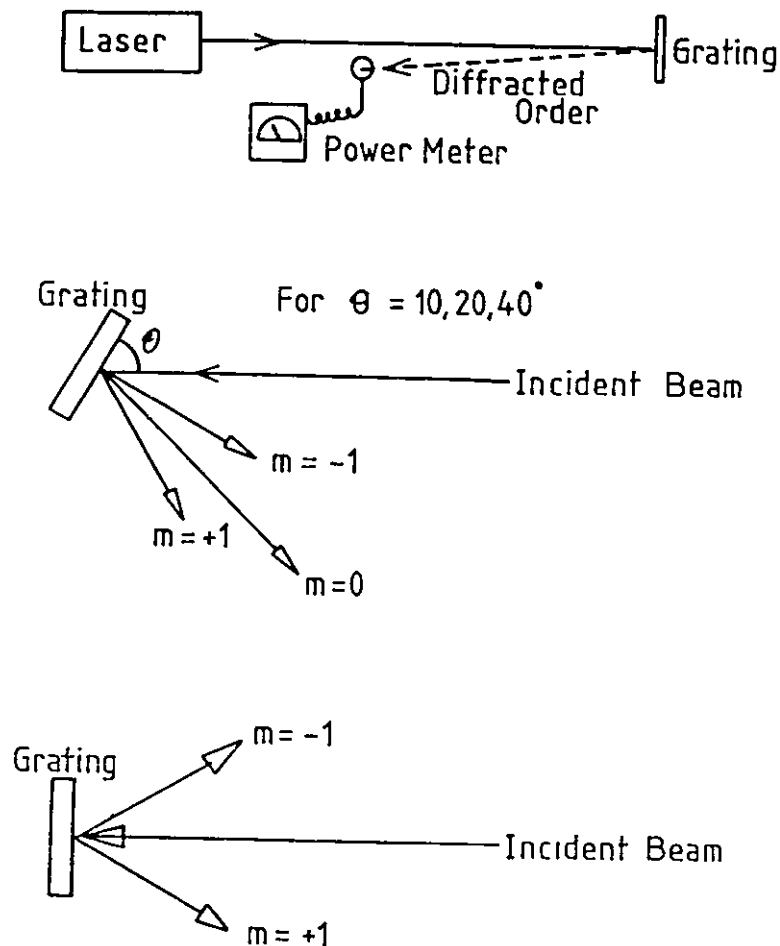


Figure 4 6 Reflection Measurement of Diffraction Efficiency

The results from the measurement of the initial silver halides gratings have been plotted in Graph 4.7. The measurements were taken over a range of laser incident angles, for both polarisation planes over plus and minus six orders. In this way the presence of grating anomalies could be detected. This study was undertaken during early work on diffraction efficiency to fully understand the measurement systems and the difficult nature of recording results. Thanks are given to Mr.M.Hutley for help and suggestions in this area

The results plotted in Graph 4.7 highlight the difficulty of accurately expressing a figure for diffraction efficiency. The graph illustrates a number of features:

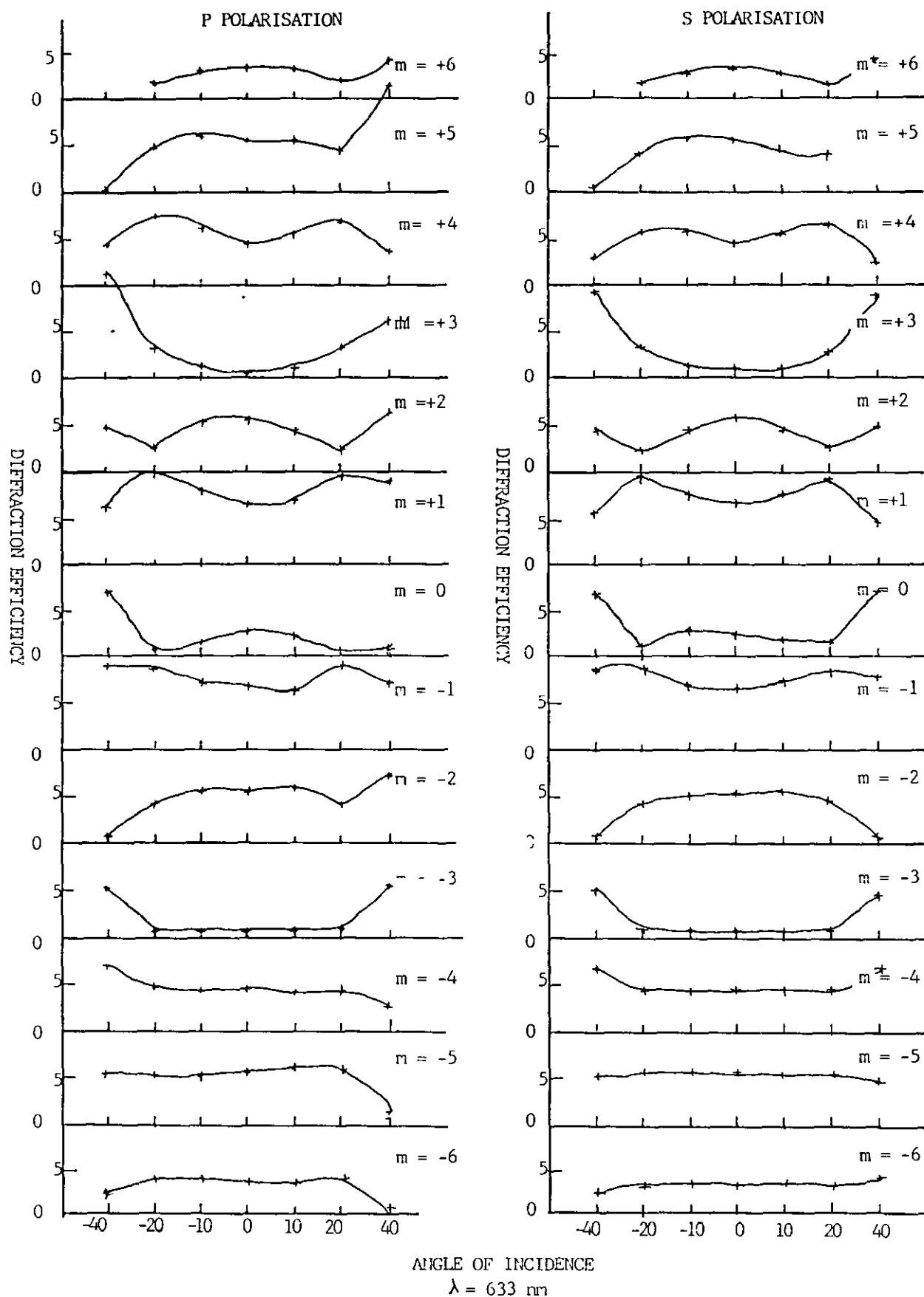
- 1) The plane of polarisation used to interrogate the grating has an effect upon measured efficiency. Efficiency is overall higher for the S polarisation (the electric vector being perpendicular to groove profile.)
- 11) The loss in efficiency for a particular point is expressed as a high point for the corresponding plus or minus order.
- 111) The precise angle of incidence should be detailed to provide a meaningful expression.

From this initial work, measurement of the photoresist, metal and plastic gratings was modified to include only the first three diffracted orders where present. The high number of diffracted orders indicated poor quality gratings with imperfect sinusoid features. Ideally all energy should be diffracted into only the plus and minus first order. The results obtained for photoresist, metal and plastic copies of the diffraction gratings are presented in Chapter 7.

#### 4.5.2 Diffraction Efficiency Versus Groove Depth

An important aspect in quantifying the accuracy and efficiency of the Information Transfer Process has been the study of groove depth and diffraction efficiency and the way in which they may be used as indicators for an optimised transfer system. For each diffraction grating produced, in photoresist, metal and plastic, the groove depth and measured efficiency as a result of that groove depth has been



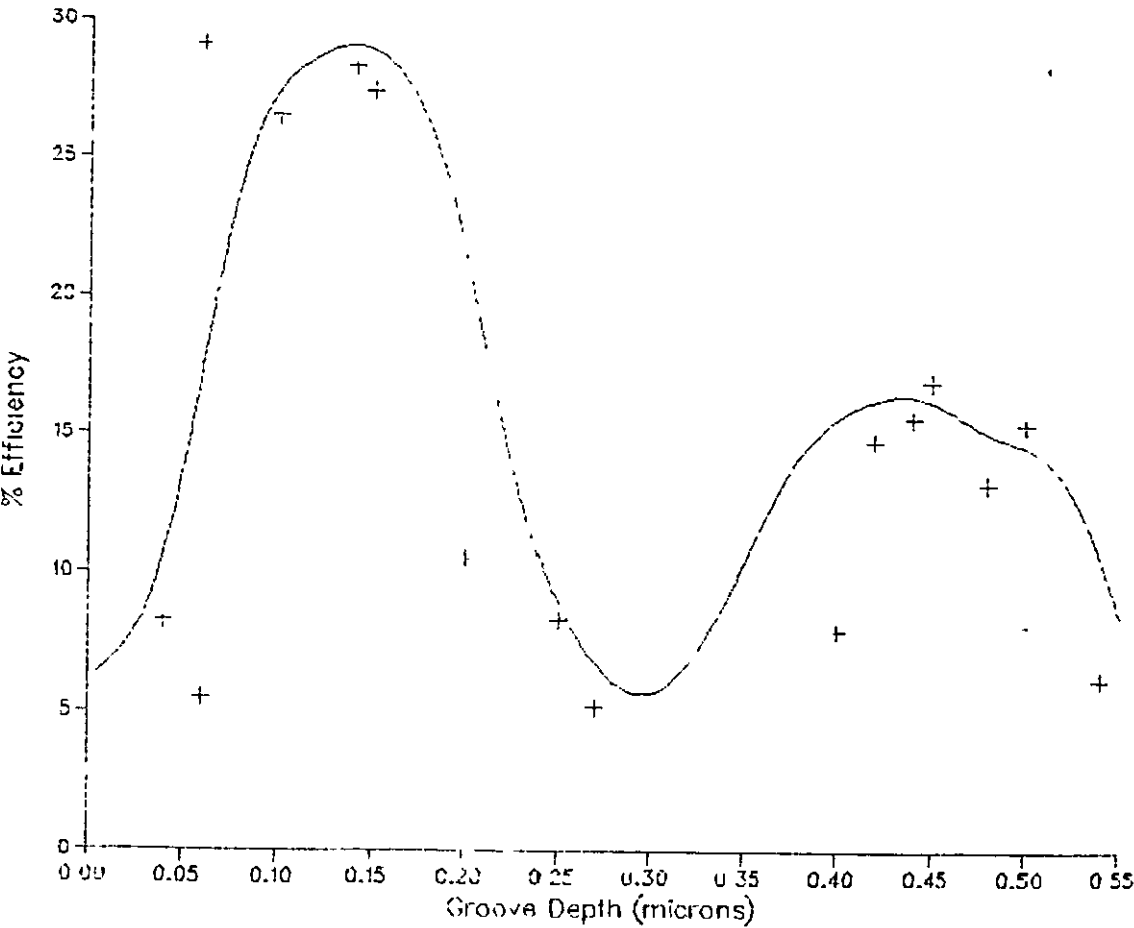


Graph 4.7 Diffraction Efficiency Measurement of a Silver Halide Grating

recorded. This has allowed the visualisation of the overall efficiency of the process to be assessed.

Graph 4.8 shows the plot of diffraction efficiency versus measured groove depth for photoresist. Results are computer plotted using a Multics Computer. The data shows best fit curves for Spline smoothing using a delta value of 0.4.

Results are for the first order diffracted beam, at 0° angle of incidence, measured with a He-Ne laser in the S polarisation regime. The peak efficiency at shallow groove depth (0.10µm) is shown at ≈30% with a second peak at a depth of approximately 0.45µm. This result is compared with those for metal and plastic copies to assess the accuracy of the embossing process. The function should appear as a uniform series of peaks but the deeper groove depths show reduced diffraction efficiency indicating a distortion away from sinusoid profile at the deeper depths. These results are discussed more fully in Chapter 8.



Graph 4.8 Diffraction Efficiency Versus Groove Depth for Photoresist Diffraction Gratings

#### 4.6 Discussion and Conclusions

The measurement of the surface relief pattern for assessment of the information transfer function is fundamental to this study. The complex nature of the holographic surface pattern necessitated the recording of uniform, simplified surface patterns from diffraction gratings. The patterns allowed measurement of groove depth using a variety of optical and surface finish techniques. The measurement regimes for an accurate description of diffraction efficiency has been described. By monitoring both of these features through the transfer process from photoresist, to metal and finally into plastic, a quantitative assessment of the accuracy of transfer has been made.

Optical and surface finish techniques of measuring groove depth and profile have been successfully applied to the range of diffraction gratings. The techniques used in conjunction with each other have provided a more complete analysis than any one technique alone could offer. Measurement of diffraction efficiency has been undertaken on silver halide gratings to assess errors and limitations and on the photoresist, metal and plastic copies of the diffraction gratings. Analysis of the results and associated experimental error has also been included. From the work undertaken the following conclusions may be summarised.

- Assessment by electron and optical microscopy produced visual and quantitative data. Surface finish measurements were successfully used on photoresist, metal and plastic copies of diffraction gratings.
- Study of groove profile by image processing techniques yielded positive results offering an interesting area for further work and study.
- Investigation of the measurement of diffraction efficiency has highlighted limitations of the technique.
- Experimental error of measuring systems has been considered to obtain meaningful data from the results.
- Successful data has been obtained from the measurement of groove depth and diffraction efficiency to assess the accuracy of the Information Transfer Process.



## CHAPTER 5

### REPLICATION OF SURFACE DETAIL BY ELECTROFORMING TECHNIQUES

#### 5.0 Introduction

The sequence of work discussed thus far has covered diffraction gratings and holograms, photosensitive materials and the measurement of features for the assessment of the transfer process. Figure 5.1 outlines the overall Information Transfer Process and it can be seen that the surface relief image must be copied into metal to be used as a stamper for the embossing into plastic.

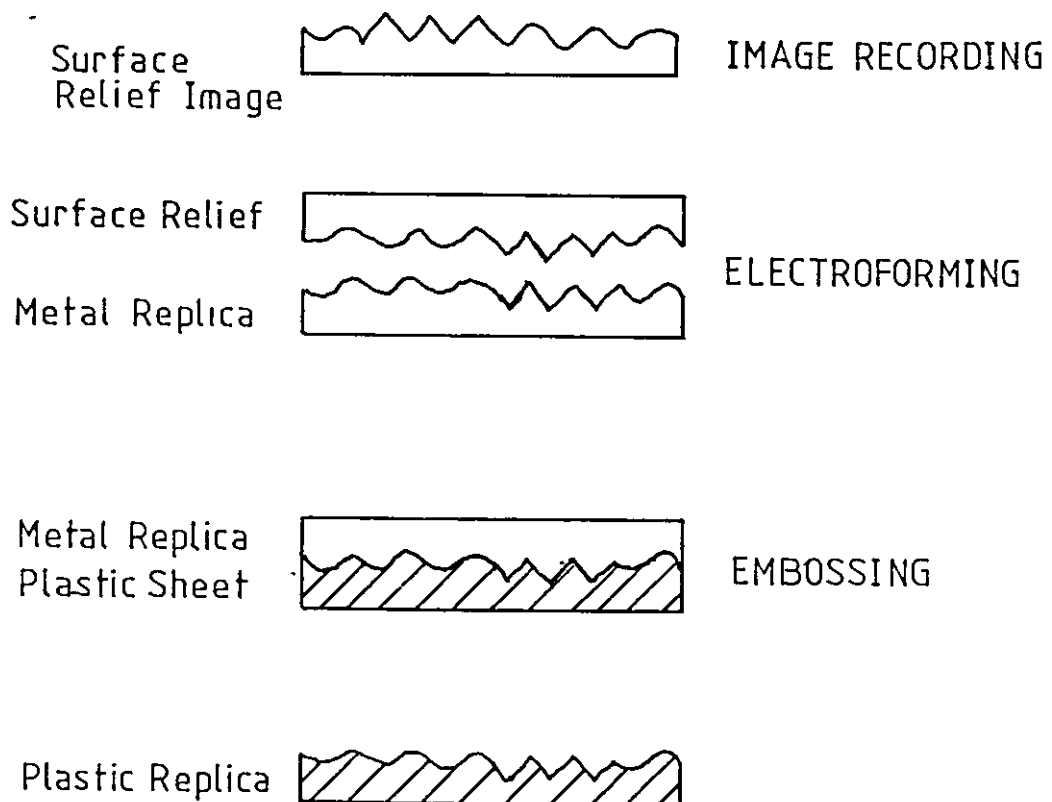


Figure 5.1 Overall Scheme of the Information Transfer Process

It would theoretically be possible to emboss into plastic directly from a stable photoresist profile but this would severely limit the life of the original and would not be sensible for large numbers of embossed images. Consequently a metal copy of the photoresist original is used, capable of withstanding heat and pressure to allow repeated embossings to be made. The reproduction of an exact metal replica is achieved by electroforming techniques. Over 80 metal replicas were produced by electroforming by careful design and consideration of experimental work. Modification to plating tanks and bath formulation resulted in excellent quality metal shims which allowed further metal copies or second generation platings to be taken from those shims.

Electroforming is a specialised technique of electrodeposition or electroplating of metals. Electroplating is the deposition of metal coatings onto a part for decoration or protection whereby the deposited coating becomes a permanent feature designed to remain on the plated object. Electroforming differs in that the metal finish is not designed to be permanently attached to the part but can be removed to serve as a copy of that part. A further important difference between electroplating and electroforming is that electroforming is concerned with reproduction and the deposit must possess structural properties such as low stress, hardness and brittleness characteristics.

The art of electroforming is an old one. As early as 1848 articles had been reproduced in nickel by electroforming. Initial interest arose from the desire to copy art objects followed by the production of printing plates in the mid 19th century and the preparation of phonograph stampers. Electroforming is still used for the reproduction of complicated fine detail parts, video discs, wave guides, parts both large and small. This chapter will consider the application of electroforming to the reproduction of diffraction gratings and holograms. The record, video and compact disc are the most closely allied industries to embossed holographic elements and currently use electroforming techniques for the production of stampers and masters.

### 5.1 Electroforming Process

Figure 5.2 illustrates the process of electroplating which is the deposition of a metal layer by electrolysis. (Electrolysis is the production of a chemical change by passing current through an electrolyte.) Two electrodes (cathode and anode) connected via an external current are immersed in an electrolyte (conducting solution). A potential difference between the two electrodes causes the metal of the positively charged anode to be deposited upon the negatively charged cathode. Consequently the anode slowly dissolves away as the cathode builds up.

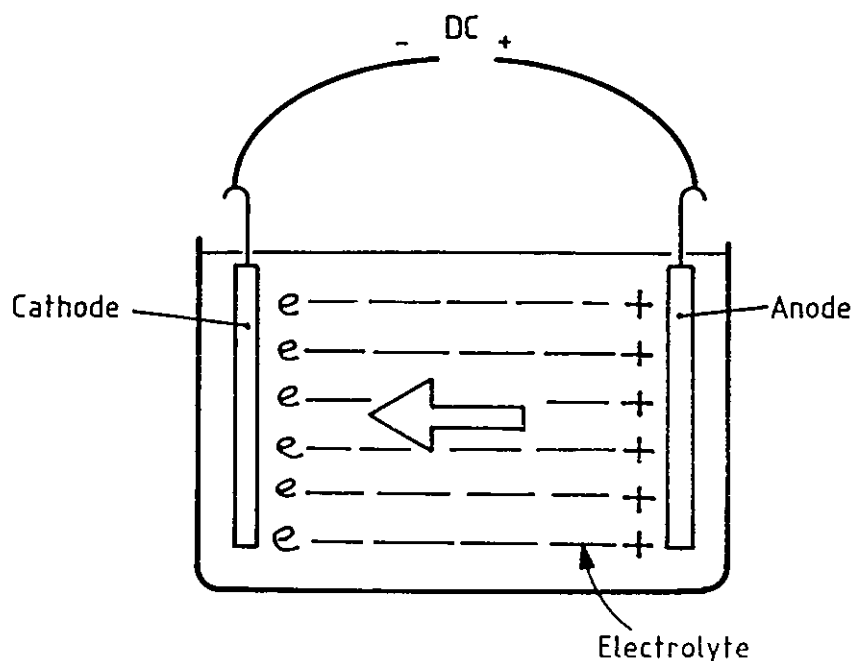


Figure 5.2 The Process of Electrolysis.

To produce metal copies of the diffraction gratings the metal deposited from the anode must build up and contour the surface of the photoresist. The deposited metal layer can then be separated from the

photoresist to produce a durable, accurate copy of the surface profile. For electrolysis to occur both anode and cathode must conduct a current and the photoresist had to be rendered conductive before the metal copies could be produced by electroforming. This was achieved by the deposition of a thin, metallic layer. The conductive layer a few atoms thick, completed the electric circuit between the cathode and anode of the plating tank. The deposition of the initial layer was as critical as the actual electroforming process as this intermediate layer became the front surface for subsequent re-platings when separated from the original photoresist.

The latter section of this chapter will discuss the electroforming of the photoresist after consideration of the deposition of the initial conductive layer.

Possible techniques for rendering the photoresist surface conductive are shown below;

1. Vacuum evaporation of silver/gold.
2. Electroless deposition of nickel.
3. Mirroring process by reduction of silver.
4. Application of conductive laquers.
5. Firing on of metal deposits.

Of these techniques three processes were identified as viable methods for treating photoresist to produce the initial conductive layer:

- i) Vacuum evaporation of silver.
- ii) Electroless deposition of nickel.
- iii) Silver reduction.

## 5.2 Vacuum Evaporation of Silver

Figure 5.3 shows a schematic of the vacuum evaporation process. The silver, 99.99% pure in the form of small balls, was heated by passing a current through the tungsten boat in which it was held. The substrate held above the molten silver was not heated and consequently at a lower temperature. Evaporation deposition occurred by the silver atoms or

molecules travelling away from the source to condense on the cooler surface of the photoresist.

The evaporation source, (almost any metal or alloy or mixture), in this instance silver, can be in the form of filaments or wires or held in foils or boats for quantities of a few grams. Crucibles are used for quantities of a few grams or more. Heating of the metals or alloys can be by resistance heating, high frequency (HF), electron beam bombardment or explosion heatup.

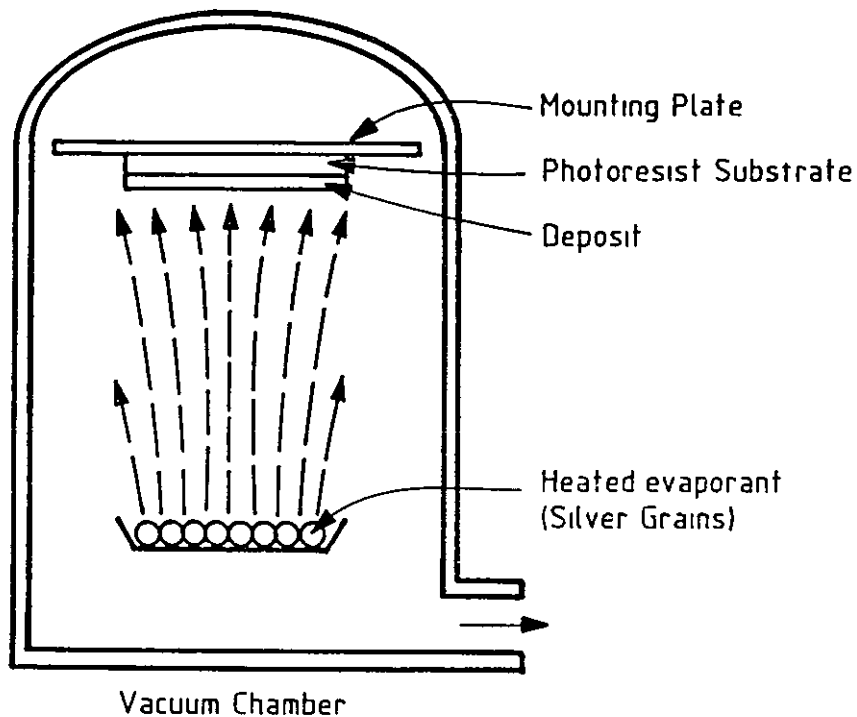
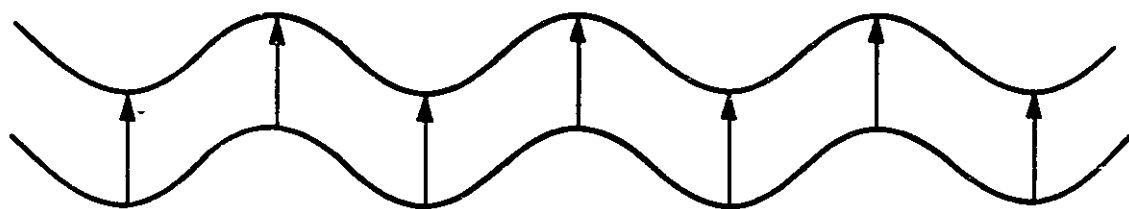


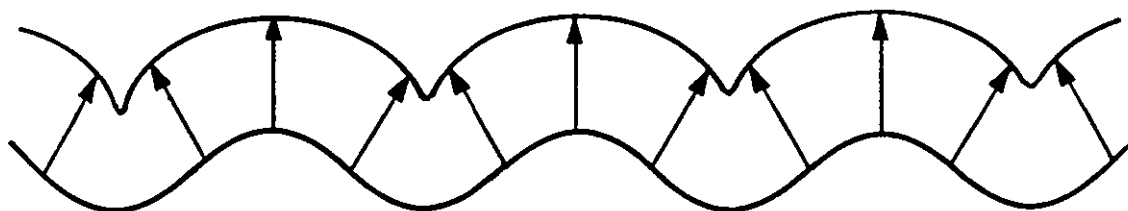
Figure 5.3 Vacuum Evaporation Process.

The coating process occurs on an atomic scale and it could be argued that atoms of silver will more likely deposit evenly over troughs and peaks than other methods of deposition. Gratings of 2000 l/mm are

still macroscopic compared to the number of silver atoms that could be deposited between the grooves. With vacuum evaporation the evaporation source is small and placed a relatively long distance from the resist surface. The metal atoms striking the (macroscopic) surface are assumed to do so at near normal incidence, in which case the thickness of the metallic layer will be constant across the surface. If the thickness is constant the groove shape must match that of the original. Lindau [51] has considered this problem and proposed models to describe the coating process as illustrated in Figure 5.4.



A) LAYER GROWS VERTICALLY - SHAPE UNAFFECTED



B) LAYER GROWS ORTHOGONALLY - SHAPE DISTORTED

Figure 5.4 Model for Growth of Metal for Vacuum Evaporation

Limiting factors of the vacuum deposition process are;

- The material must be suitable for evaporation in a given vacuum and temperature
- A critical level vacuum is necessary to avoid collision of evaporated atoms with residual gas molecules.
- Stress development within the deposit can limit deposited thickness.
- Substrate shape - should be parallel and flat to evaporant.
- Substrate size is limited to vacuum chamber dimensions.

#### 5.2.1 Experimental Results - Vacuum Evaporation of Silver

This technique proved the most straightforward and effective method of producing the initial conductive layer and was used exclusively once other methods had been tried and eliminated.

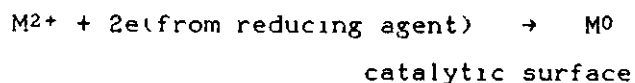
An Edwards High Vacuum, model E500 vacuum coater was used for deposition of silver onto the photoresist gratings. The samples, soaked and cleaned in a proprietary cleaning agent (Microclean) and rinsed in pure water were mounted onto a purpose built plate holder to take up to four samples at a time. The samples did not extend to the edges of the chamber as uneven deposition would have occurred. The plate holder was loaded into the vacuum chamber with the resist surfaces towards the silver source in the tungsten boat. The boat was connected between the heater filaments and a shutter held over the silver until ready for evaporation. The chamber was lowered and evacuated. Deposition could occur once the correct chamber pressure was reached. A current was applied to the filament to melt the silver. Once the silver was fully molten the shutter was opened to allow the silver to evaporate toward the resist surfaces and deposit sufficient film thickness. 0.5-0.8  $\mu\text{m}$  thickness of silver was satisfactory to ensure good conductivity and surface uniformity during electroforming.

It was important that the chamber temperature did not exceed 100°C during evaporation as the resist surfaces would flow and distort at such temperatures. After evaporation the chamber was allowed to cool and air admitted to release the chamber to allow removal of the samples.

Cleanliness of the resist samples was extremely important in achieving quality coatings. Surface dust, fingerprints or marks were clearly visible after coating and handling of the resist was reduced to a minimum prior to vacuum evaporation. To improve the electroforming process by ensuring uniform conductivity across the sample, adhesive lead tape was attached around the edges of the resist samples. (See Section 5.5.1 Design of Cathode.) This was adhered before silver evaporation such that silver covered the whole sample including the tape.

### 5.3 Electroless Deposition of Nickel

Electroless plating is also known as 'chemical plating'. Deposition is based on chemical reduction reactions that do not require an external electric current. Plating occurs by autocatalytic reduction of the metal cations, for example nickel ( $\text{Ni}^{++}$ ), onto the surface to be plated by the presence of hypophosphite anions ( $\text{H}_2\text{PO}_2^-$ ) in aqueous solution. The chemical reducing agent in solution thus provides the electrons for converting metal ions to the elemental form, eg.



The advantage of electroless plating is that it may be carried out on non-conducting surfaces after suitable surface preparation, it does not require an external current and plating is of uniform thickness regardless of the surface shape or geometry. Once deposition is initiated on the surface to be plated the metal must itself be catalytic for deposition to continue. The autocatalytic deposition proceeds almost linearly with time and quite thick deposits can be produced. Some important features are;

- Uniform deposits can be produced regardless of part shape
- Thickness of deposit is only limited by the supply of chemicals.
- Coating characteristics are unique to electroless plating and not like those from electroplating
- Deposits can be placed directly on non-conducting surfaces.

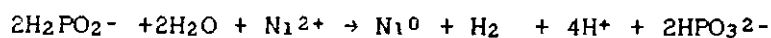


The surface to be plated must be sensitised prior to deposition. This is possible by making the part cathodic for a very short time or by rinsing the part in PdCl<sub>2</sub> (Palladium Chloride) followed by immersion in the plating bath. This leaves a thin immersion deposit of palladium on the surface which initiates electroless plating.

Bath Formulation; an aqueous or non-aqueous bath would contain;

- i) The source of metal for plating, ie. nickel chloride
- ii) A reducing agent, ie. formaldehyde, hypophosphite, which affects the deposit properties. Reaction products are codeposited depending on which reducing agent is used.
- iii) A complexing agent that is the source of the metal.
- iv) Buffer agent for pH control.
- v) A stabilizing agent to control deposition rate.
- vi) Agents such as brighteners, exaltants, chelating agents.

The formulation used in this study was a hypophosphite based bath and the overall reaction may be summarised in the following equation,



Bath temperature and pH are important factors influencing deposition. The deposition rate increases almost exponentially with temperature and most baths operate at high temperatures to take advantage of this. Deposition rate in an acid bath decreases with solution pH and baths are typically kept between pH 4-6 (to compromise on speed of plating and prevention of precipitation). The plating reaction produces hydrogen ions and the inclusion of buffering agents (sodium citrate) prevents rapid pH changes. Agitation is necessary with autocatalytic plating to dislodge gas bubbles generated and to replenish solution in crevices and holes.

The limiting features of the autocatalytic plating process are;

- It cannot be used on parts susceptible to phosphorus or boron which are codeposited with autocatalytic coatings.
- Deposited coatings have little shock or stress resistance
- Electroless nickel coatings are brittle and lack ductility making them unsuitable for flexing around printing rollers for embossing.
- Formulations are limited to fewer deposited metals than for electrolytic deposition.

#### 5.3.1 Experimental Results - Electroless Deposition of Nickel

This technique was tried as an alternative to vacuum deposition for the initial conductive layer using an acidic bath for electroless nickel plating.

The formulation was as follows;

Nickel Chloride	30.0 g/l
Sodium Hypophosphite	10.0 g/l
Sodium Citrate	12.6 g/l
pH	4-6
Temperature	90-100°C

Before successful plating could be achieved, pre-treatment of the resist was necessary using Palladium Chloride sensitization.

Rinse:	De-ionised water with wetting agents
Sensitize:	Sensitizing solution at 25°C
	Stannous chloride 70g/l
	Hydrochloric acid 90 g/l
Activate.	Acid solution palladium chloride 0.1 g/l
Rinse	De-ionised water

The sensitizing solution produced an absorbed layer of tin on the surface. The activation step then formed palladium nuclei on the surface by reduction with the absorbed tin ions. These nuclei provide the catalytic sites for initiation of the electroless nickel deposition. The plating solution was contained within a glass beaker.

heated within a water jacket. Electrical contact with the resist was not necessary and the resist was simply held within the solution on a glass rack. The temperature of the solution was monitored and maintained because plating would increase exponentially with temperature. The solution was not taken above 90°C for fear of damaging the resist. Plating was slow to build up and after four hours the resultant foil was extremely thin at 0.02mm thickness. The initial plating was very poor with the thin nickel coating lifting from the surface. Improved resist surface preparation produced a separate foil that was still extremely thin and too fragile for subsequent plating.

Electroless deposition of nickel for the first conductive layer was found to be slow and surface pre-treatments made repeatability difficult. The initial film of palladium produced on the surface for plating to begin was obviously crucial in maintaining a continuous metal film. One advantage of the method was that the resist did not require complicated jiggling or connection to external circuits although the initial sensitization and activation introduced additional handling stages. The techniques could have been improved to obtain additional results but the alternative methods investigated offered advantages over electroless plating. The use of electroless nickel deposition is an area that would be considered in future work.

#### 5.4 Reduction of Silver

The last method described the process of autocatalytic deposition as part of the electroless chemical regime. A further method of rendering the photoresist surface conductive prior to electroforming can be achieved by chemical reduction of silver. The process is also part of electroless deposition (necatalytic displacement plating). Deposits are produced on non-catalytic substrates in the presence of a reducer in a solution of the metal chemical compound. The surface of the part may or may not require sensitising. In this study, the resist surface was sensitized with tin salts before being sprayed with a solution of silver nitrate and a formaldehyde reducing agent. The two solutions mixed on the surface to produce a thin film of metallic silver. Deposition stopped once the surface was covered and very thin deposits

are typical, 10-200 $\mu$ m. It is a relatively cheap and straightforward method but indiscriminately covers all surfaces in contact with the solutions. Limiting features of the process are;

- Only thin deposits are possible.
- Complicated parts are not easily sprayed.
- Uniformity of coating is variable.
- Nonconducting surfaces can be treated but with limited range of deposited metals.

#### 5.4.1 Experimental Results - Reduction of Silver

This technique for rendering the resist surface conductive is not widely reported. It is known to be used in the production of electroforms for decorative stamping purposes and the process has been studied in this capacity. The technique has not been reported for use with holographic gratings or images and is believed to be unique in this application.

Equipment, No pre-treatment of the resist surface was necessary other than to ensure it was clean and dust and grease free. A spray gun consisting of two nozzles very close together directed two solutions onto the surface of the resist for the period of only a few seconds. The two solutions were ammoniacal silver nitrate and formaldehyde which reacted in the spray droplets to produce a thin film of silver on the resist. The plate was then quickly transferred to an electrolytic plating bath to prevent the oxidation of the silver film. The deposited thickness was controlled by length of spraying but deposition stopped as soon as the surface was covered. As soon as the surface appeared visually bright the spraying was stopped and the gun directed away from the surface to prevent stray droplets falling onto the surface.

The technique is known to work well for electroforms of large scale decorative patterns and did produce holograms which after electrolytic plating were stable and visually bright. No visual defects were seen on the silver surface and it plated and adhered well to the resist. Upon separating the original resist from the overplated copy the resist was lifted from its substrate and retained on the silver. It could be

removed by rinsing in acetone. The method did rely upon the skill of the operator in directing the spray nozzle with the correct distance and speed across the surface in much the same way as for spray painting. Delay in placing the sprayed plate into the electroforming tank produced an oxidised layer on the surface which dulled the silver appearance. The technique was considered as the best alternative to vacuum deposition

Summary The three outlined methods for the deposition of the first conductive layer have been used on photoresist gratings.

The first, vacuum evaporation of silver, was found to be the fastest and easiest method since equipment was available in-house and was reliable and efficient. Deposition of silver, by vacuum evaporation is considered to be the best choice for meeting the requirements of optical disc systems [22,23]. This technique was used consistently for the work undertaken

The electroless deposition of nickel was more time consuming and exacting than silver evaporation. The use of nickel for the initial layer was not a disadvantage as it would have provided a nickel/nickel interface for the next stage. Problems were encountered with inadequate adhesion of the deposited layer due to cleaning and sensitization of the resist surface. The metal copies were extremely delicate and uneven and inferior to those from evaporated silver.

Reduction of silver by spraying the surface of the resist was a fast technique which produced a thin metallic layer that had to be immediately electroformed to prevent oxidation of the metallic silver. The technique had to be used under clean conditions within spray booths with adequate ventilation. Overspray of silver solution makes the technique more expensive than vacuum evaporation of silver but would be ideal for large specimens that could not be mounted in a vacuum chamber. Evenness of coating was acquired with practice by steady and smooth handling of the spray gun.

### 5.5 Electroforming the Conductive Layer - Deposition by Electrolysis

Having rendered the surface of the photoresist conductive it could then be used as the cathode in the process of building up a thick metal deposit by electroforming. As mentioned previously electroplating is an electrochemical process using an electrolyte (conducting solution) to deposit one or more relatively thin adherent layers of metal. The deposited layers may then have different physical or chemical properties from that of the original surface. Electrolysis is the production of a chemical change by passing current through an electrolyte as illustrated in Figure 5.5.

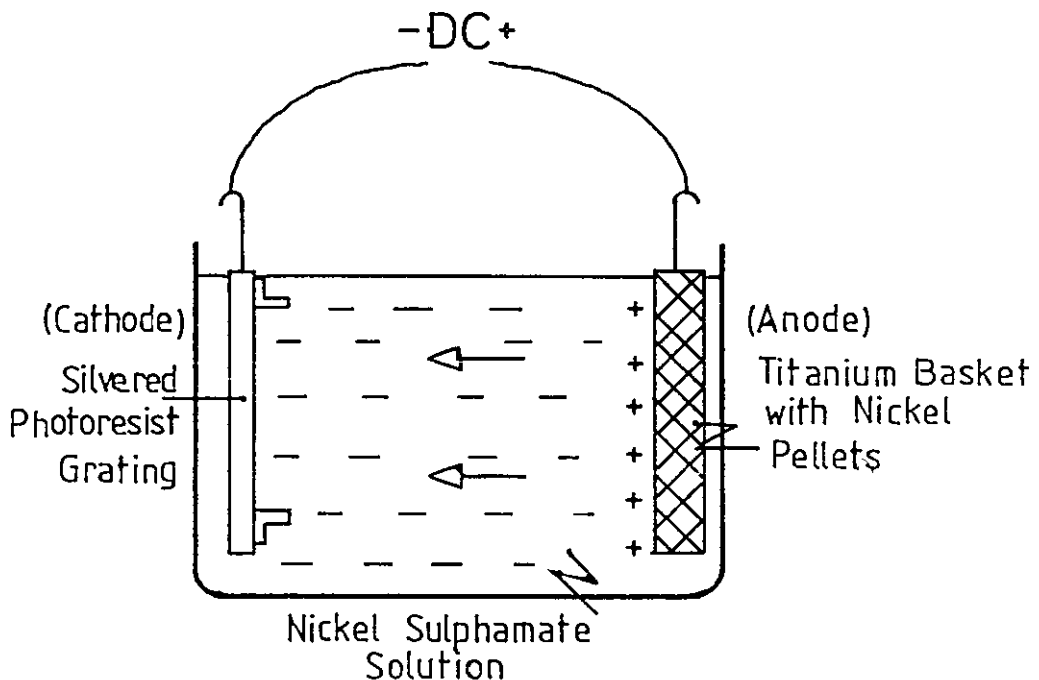


Figure 5 5 Electrolytic Deposition of Nickel

Figure 5.5 shows the anode as a titanium basket containing nickel pellets. The silvered photoresist grating is the cathode. The two are connected via an external current. The electrolyte was nickel sulphamate solution. The potential difference that arises between the anode and cathode when current is applied causes the cathode to become more negatively charged. The surface atoms in the nickel lattice structure become hydrated and dissolve into the solution which contains its ions. At the same time, the metal ions in the solution are attracted to the negatively charged silver cathode and become deposited over its surface. The nickel pellets slowly dissolve away as the nickel deposit built up over the surface of the silver gratings.

There are many complex reactions associated with the process and factors such as stress of the deposit, coverage, efficiency, construction of cathode and anode, bath formulation, uneven charge distribution in cathode and electrolyte all affect the quality of deposition.

Theoretically all metals and alloys which did not directly react with photoresist, used in aqueous or non-aqueous electrolytes could be deposited by electroforming. In practice, a number of limitations are placed upon the electroforming process. These are;

- i) The substrate (photoresist plus the support) must not react with the electrolyte. It must be thermally stable in order to retain the fine dimensional detail during the plating process. Heated solutions and fused salts electrolytes should be carefully monitored.
- ii) The surface profile of the resist influences the accuracy of the metal replica. Very narrow recesses or deep grooves (hence the problems with gratings) can cause unevenness of coating.
- iii) The electroform is separated from the photoresist after plating and has to be rigid and stable. High internal stresses can develop during electroforming and cause cracking of the coating. The thickness of deposit is a function of time and electroforming is a slow process, usually taking days to plate some larger parts. Additionally the bath formulations are more critical in terms of pH, purity, stability etc. than for the equivalent in electroplating terms.

Discussions held with Dr.P.Mitchell of the Chemistry Department, LUT and Mr.T. Hart of Hart Coating Technology indicate that the precision of electroforming required in replicating diffraction gratings goes beyond present commercial and academic interests. A discussion of accuracy of metal distribution is presented in Appendix 4.

A consequence of this work was the design and construction of a high precision, stress-free, micro-deposition, electroforming system. The features of this equipment are discussed in the following section.

#### 5.5.1 Design of Equipment and Bath Formulations

Plating Tank Commercial plating tanks are usually large steel vats. A heavy duty glass tank was used for experimental work. The tank dimensions were chosen to house the anode and cathode in close proximity with optimum solution usage. The glass vessel was easy to clean and allowed observation of the plating process and build-up of any sludge. The plating tank was held within a water jacket to maintain solution temperature. A fish tank was found ideal for this purpose and a small photographic submersible heater operated within  $\pm 1^{\circ}\text{C}$  to maintain constant plating temperature. (An early problem was encountered with the quality of fish tanks used as water jackets' Several leaked and caused the heaters to burn out leaving the plating solution cold.) Maintaining the solution at a temperature of  $40^{\circ}\text{C}$  ensured a reasonable rate of metal deposition. Agitation of the solution was not necessary within the small plating tank although a magnetic stirrer was used when plating larger parts in a larger tank

Power Supply An external direct current supply was necessary to produce the circuit between anode and cathode. A small 15V/30A unit was used which was adequate but not ideal as it did not allow precise adjustment of current to the cathode. The cathode was immersed into the solution live at 1V. The current had to be limited to  $0.5 \text{ A/ft}^2$  (amperes per square foot are the plater standard unit) when the photoresist was first immersed to prevent flaking of the silver. As the nickel deposit built up over the silver the current could be gradually increased until the maximum current of  $2 \text{ A/ft}^2$  could be maintained. A



stabilised, purpose built power supply would be used for future work as it is believed that initial current conditions are crucial in achieving quality platings.

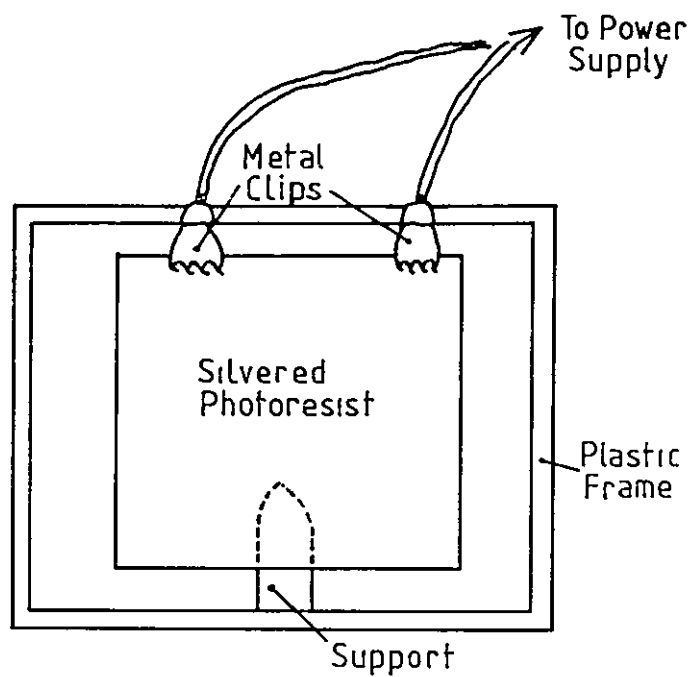
Water Supply. The water used for bath solutions must obviously be ultra pure so as not to contaminate any part of the process. Hard water was avoided as this could leave thin films on the silvered photoresist when rinsing before plating. Modern water plant assures high quality volume output and the water used for rinsing and solution dilution was taken from Chemistry Department plant as ultra pure, particulate free.

Design of Anode: The anode is the positive electrode of the plating tank and that which provides the metal for deposition. This work used a titanium anode basket containing nickel pellets immersed in a solution of nickel sulphamate. The titanium basket was purpose built to match dimensions of the glass tank. The basket was enclosed within a calico anode bag, (calico is not attacked by the slightly acidic nickel solutions.) The anode bag was essential for retaining the sludge produced as the nickel pellets dissolved. By using this design of anode cheaper nickel pellets and scraps could be used and easily replenished. Even though the purest materials are used for the anode a certain amount of sludge is produced and should not be allowed to drop into the plating solution. Choice of material for the anode is critical when considering that it must conduct a current but not react in the plating process. Titanium was chosen since it was capable of forming a passive layer over its surface to limit reaction with the plating solution. However, the passive layer was not insulating and still allowed the conduction of a current through the nickel pellets held within the basket. Connection from the power supply onto the anode was made by clips onto the arms of the unit. Excellent results were achieved with this anode arrangement, the whole unit could be easily replenished during plating and removed for rinsing and replacement of the anode calico bag when necessary.

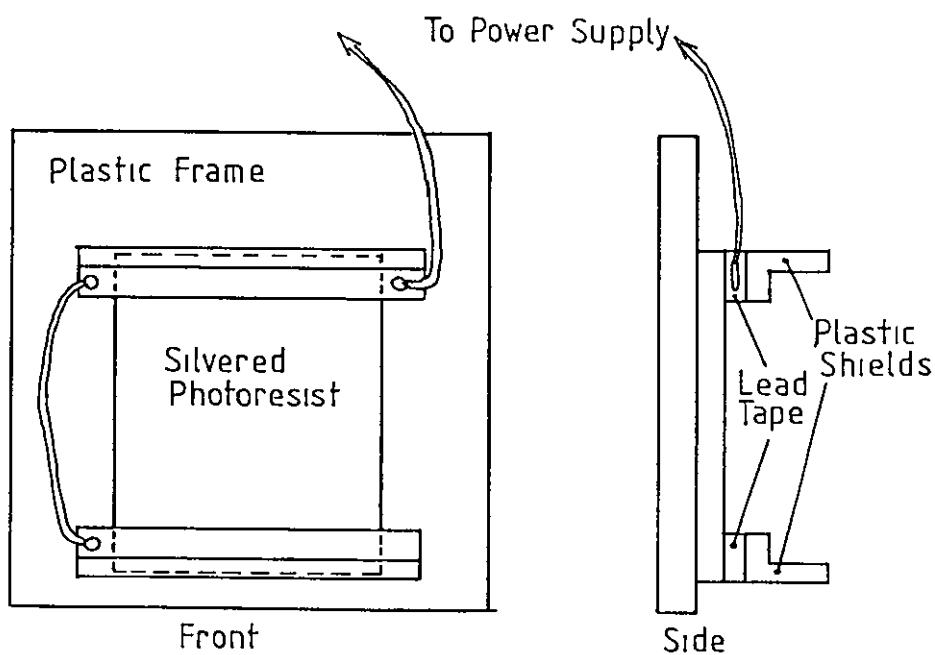
Design of Cathode. The cathode is the negative electrode in the plating process, that to be plated by the deposition of metal. In this instance the silver photoresist gratings served as the cathode. Rendered conductive by the silver layer, nickel could be deposited by completing

the electrical circuit between anode and cathode in the plating tank. From an understanding of the theory of metal deposition it was clear that the even conduction of current across the cathode greatly influenced the quality and evenness of coating. It was therefore necessary to design a plating jig to hold the cathode within the tank and maintain electrical connection to the power supply. In commercial practices where a number of similar articles are plated at one time a rack, or frame is constructed, usually of brass or copper and PVC insulated, to lower any number of parts into the tanks. In this way the parts can be handled from one treatment to the next with greater ease. This principle was adopted for the initial plating trials and a frame, (similar to that designed to hold sheet film) held the glass substrate by top corners with clips connected to the power supply. This arrangement is illustrated in Figure 5.6 a). This method had the advantage of leaving all the image area clear to be plated but the clips dug into the silver and only provided point contact onto the surface and only at the top of the plate. After plating the deposited nickel was seen to have built up over the clips preferentially to the rest of the cathode.

An alternative method for jiggling the cathode was used with greater success. The intention was to provide an almost continuous contact along the silvered photoresist edges. This was achieved by modification to computer edge connectors designed for computer boards. Two edge connectors, for top and bottom of the photoresist plate were connected via a wire soldered onto the end copper pins of the connectors. Connection between the top and bottom connectors ensured a more even current flow across the surface of the photoresist which would improve the uniformity of metal deposition. A second wire was soldered onto the pins for connection to the power supply. The photoresist plate could then be pushed into the connectors, firmly making contact with the row of copper pins on its silvered front surface. To prevent metal deposition over the soldered wires a protective lacquer was sprayed onto the connectors. Exposed parts such as the solder points would 'steal' the metal from the plating solution and hinder the deposition onto the silvered photoresist. A large number of platings were



5 6 a)



5 6 b)

Figure 5.6 Experimental Designs of Cathode Fixings

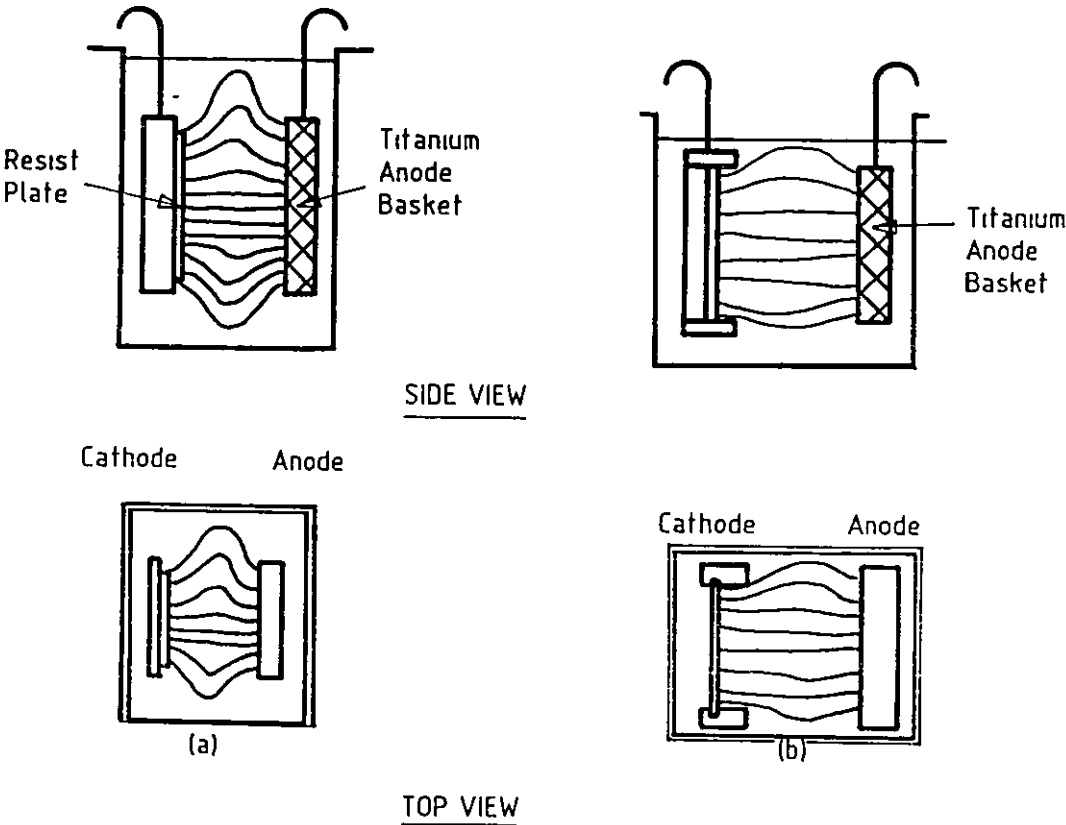
successfully achieved by this method. The edge connectors are seen in Plate 24 showing the experimental apparatus including plating tank, titanium basket and anode bag and power supply. The disadvantages of this method were that some image area was lost by the edge connectors fitting over the surface and that only one sample could be plated at a time. Additionally the connectors would not rest against the side of the plating tank to remain parallel to the anode which was considered desirable.

A further refinement to the jigging was made and used most successfully for the number of platings made. The edge connectors had shown that current flow from top to bottom across the photoresist improved uniformity of metal deposition. However, small pits could be seen on the plated surface appearing to run from top to bottom of the sample. Turning the entire sample plus connectors through 90 degrees in the plating bath showed that the pits still ran between the two edge connectors indicating they were a feature of the electrical connection across the sample. It was believed that conduction of a current along all four edges of the sample should improve deposition further and should alter the nature of the marks on the plating. Adhesive lead tape, (as used for decorative strip on window panes) was applied along all four edges of the photoresist before it was silver coated. Vacuum evaporated silver was then deposited over the entire surface including the tape. Trials were undertaken using the edge connectors as before connecting top and bottom edges of the sample. This time the current was bound to conduct around all the edges of the sample. An improvement was seen in the smoothness of the plating finish although the pits still appeared to run preferentially from top to bottom but less pronounced than previously. The use of the lead tape was applied to all subsequent platings. A jig was still required that would hold more than one sample and a purpose built plastic frame was made designed. When using the frame the edge connectors become cumbersome and further alterations were made to the design of the cathode unit. Figure 5 6 b) illustrates the final arrangement. The plastic unit held two samples, flat and parallel, side by side within the tank. Plastic fixtures were used instead of metal to prevent unwanted plating. A



Plate 24. Experimental Plating Apparatus  
Power Supply, Plating Tank, Titanium Basket and Anode Bag  
and Edge Connectors for the Silvered Photoresist

further refinement was made by the use of 'shields' holding the samples. Consideration of plating theory indicated that current distribution around the sample and through the electrolyte influenced quality of plating. Figure 5.7 illustrates the current distributions for two plating bath arrangements.



(a) SIMPLE JIG ARRANGEMENT SHOWING CURRENT DISTRIBUTION  
 (b) IMPROVED DISTRIBUTION USING SIDE SHIELDS AND RESIST CLOSE TO SOLUTION SURFACE

Figure 5.7 Current Distribution for Two Arrangements of Plating Jigs

Figure 5.7 a) shows how the current distribution runs directly between cathode and anode at the centres of the electrodes but deflects outwards at the extremes of the electrodes. It was considered that the use of 'shields or deflectors as in Figure 5.7 b) could improve current distribution.

The final jig therefore used shaped plastic shields at the top and bottom of samples. On the underside of the shields lead tape was applied which contacted onto the silvered lead tape around the edges of the photoresist Figure 5.6 a) This ensured a full surface contact, not point contact, along the length of the sample. Electrical contact was achieved by soldering a wire to the lead tape on the shield for connection to the power supply. A further wire could then be linked between the top and bottom shields ensuring conduction around all edges of the samples. When excessive metal became deposited on the lead on the shields it could easily be peeled off and replaced. The whole unit could be immersed into the plating tanks and stood upright and parallel to the anode. Different size samples could easily be accommodated by slots for increasing or decreasing the sample holding area. It is believed that this unit encompassed the best designs possible to match plating theory with practical requirements.

Bath Formulation: Sulphamic acid, the basis of the bath used in this work, has been commercially available since the 1930's and is used almost exclusively for electroforming applications. The stress values of such baths can be lowered by reducing the chloride concentration and sulphamate baths are now generally used chloride-free. This bath gives deposits with low stress and good ductility, indeed the lowest stress of any commonly used nickel electrolyte is possible from baths which have been thoroughly treated to remove inorganic and organic impurities. Nickel sulphamate is much more soluble than nickel sulphate and high concentration sulphamate solutions allow high deposition rates with consistently low internal stress. The formulations given are known to be used in the commercial replication of large, low stress, metal shims for decorative patterning of items. Stress in electroforming has been studied by McKinney and Bartle [21], Wearmouth and Bishop [22], and Spiro [52]

## 5.6 Experimental Detail and Results

### 5.6.1 Electrolytic Nickel Deposition

Plate 24 shows the experimental equipment for plating using the edge connectors for holding the silvered photoresist sample.

Nickel sulphamate baths (chloride free) were used exclusively, with the following formulation.

Nickel sulphamate	320 g/l
Boric acid	78 g/l
Nickel pellets	

Temperature 40°C, pH 4.0

Operating current:	Initial	0.5 A/ft <sup>2</sup>
	Final	2.0 A/ft <sup>2</sup>

The experimental design of the equipment has been described in Section 5.5.1. Over 80 diffraction gratings were reproduced by electroforming in this study using nickel sulphamate baths and different jiggging arrangements.

The silvered photoresist gratings were rinsed immediately prior to electroforming in a dilute solution of Microclean. This was found to remove surface grease and marks and improved the quality of deposit. The sample was mounted onto the plastic jig and connected under the lead tape on the shields. The anode and cathode were connected to the power supply and a voltage of 1V applied before immersing in the solution. Solution level was temperature controlled and maintained fractionally over the cathode shields. A current of 0.5A/ft<sup>2</sup> was applied to the cathode on immersion into the plating tank. After a period of one hour the current was increased to 1.0A/ft<sup>2</sup> as the metal deposit built up. After two hours the current was increased to a maximum of 2.0A/ft<sup>2</sup> and the sample was left to build sufficient thickness. Plating was usually achieved overnight, depositing a nickel



thickness of 1.5-2.0mm. This was thicker than would be normally required but the extra thickness provided support for Talysurf measurements and helped in the embossing stage.

When the plating was sufficiently thick the sample was removed from the plating tanks and washed under fast flowing water to remove nickel sulphamate from under the connectors and screws. To separate the metal copy from the photoresist the adhesive lead tape was carefully lifted from the edges of the glass plate. It was essential to remove the plating without buckling or creasing the metal copy. In early trials the resist was removed from the glass substrate when the metal was peeled away leaving resist on the front surface of the metal. Post baking of the resist improved the adhesion to the glass and the metal copy could be separated without removing the resist. Whilst the resist was damaged by this process it was left mostly in tact and proved useful for SEM examination and comparison with the metal versions. The rear surface of the nickel plate was found to vary in quality. If the current was increased too rapidly a rough deposit was laid down leaving pits on the surface. These pits are believed to be a result of hydrogen bubbles, evolved from electroplating, adhering to the surface as plating proceeded. On one occasion when the back surface was ground down to remove the rough spots, plating solution was detected trapped within the pits (the bright green colour was easily spotted). Agitation could have prevented the air bubbles remaining on the surface of the sample. By ensuring the current was increased slowly and carefully once an initial deposit could be seen the level of pits was greatly reduced and the back surface remained smooth. No problems were encountered with the nickel/silver interface and removing the metal shim from the sample always lifted the silver front surface easily away from the photoresist.

Groove depth of the metal shims was assessed by SEM and Talysurf instruments and diffraction efficiency measurements were also made. The original metal shims are referred to as first generation shims and from these other metal copies can be taken to build up a 'family' of shims. This process is detailed in the following section.

### 5.6.2 Second Generation Plating

Embossing into plastic is rarely done using the first generation metal shims. The photoresist original is often lost in the process of electroforming and since the embossing shims have a limited life further shims could only be produced from original photoresist plates, if still available. Consequently the first generation shim is used to produce other metal copies by continuing the process of nickel plating as illustrated in Figure 5.8. The first generation shim is kept secure and used for re-plating as and when the second generation copies become worn.

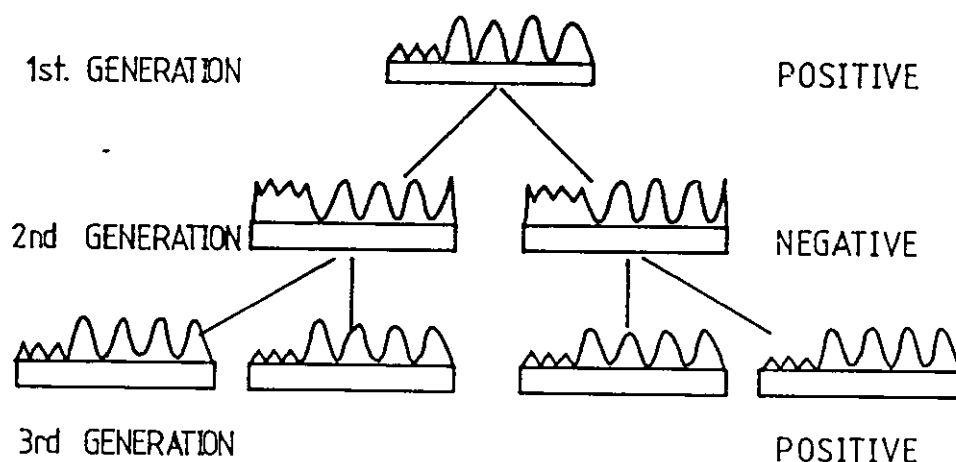


Figure 5.8 Electroforming to Produce a 'Family' of Metal Shims

Further copies are produced by re-plating the original metal shim. A passivating layer must be applied to allow separation of the second generation shim from the first generation shim. Plating the shim

before passivation would simply deposit a new nickel layer upon the old that would be intimately and permanently attached.

#### 5.6.3 Passivation of First Generation Shim

Passivation of the front surface was achieved by immersion in a series of baths designed to leave a uniform oxide layer across the surface. The oxide layer acts as an interface between first and second generation platings

The stages for passivation were as follows;

1. Rinse of original metal shim in pure water.
2. Immersion in Sulphuric acid 10% solution. 1 minute.
3. Immersion in Sodium dichromate 5% solution. 30 seconds.
4. Immersion into nickel sulphamate plating tank.

This initial procedure was not successful. A faint orange film was observed over the surface before re-plating but the second generation shim was difficult to separate from the original and dull and tarnished in appearance. The tarnished appearance of the second generation shim could not be removed. The difficulty in separating first and second generation shims caused some buckling to the thinner shims which made embossing from them unsatisfactory.

A modification to this bath was made by combining the acid and dichromate into one solution. This formulation was discovered to be a proprietary passivating dip for zinc and zinc alloys [49]. When the original metal was placed into the solution an orange film formed across the surface and dulled the appearance. If the metal was then rinsed in clean water and the surface gently wiped, re-immersion into the passivating solution brightened the surface and the orange colour disappeared. After a further rinse in clean water the metal surface was bright and slightly greenish. The metal original could then be jigged ready for immediate immersion into the plating tank. Plating occurred in the same manner as for the original production, a low current of  $0.5 \text{ A/ft}^2$  was applied and gradually increased to  $2.0 \text{ A/ft}^2$ . Plating was left to run overnight to build thick shims. To

separate the two copies the edge of the shim was trimmed with shears and the copies simply fell apart. The need to oversize the original became clear as each copy further reduced the image size when separating by this technique. The surface finish appeared bright and clean without marks or tarnish

The passivation of the first generation shim leaves much scope for further work. This method works by producing an oxide layer across the surface and the homogeneity of that layer is important. Since the embossing process relies upon second and third generation copies from a photoresist original the accuracy of plating and re-plating should be further investigated

Plates 25, 26 and 27 show SEM photomicrographs of photoresist, first generation and second generation metal copies. The mark left by the stylus/skid assembly was used as a reference point to try and ensure that an identical area on each sample was examined. Whilst accurate interpretation is difficult, it can be seen that the unevenness of the side walls of the ridges has copied through from resist to both generation metal shims.

#### 5.6.4 Accuracy of Electroforming

By measurement of the groove depth and diffraction efficiency for each of the photoresist, first and second generation metal shims, an indication of the accuracy of the electroforming process could be acquired. The quantitative analysis of this process is considered a unique feature in this application of electroforming

Graphs 5.9-5.10 show the plots of diffraction efficiency against groove depth for the first and second generation shims. (A similar graph was plotted for original photoresist in Chapter 4) All gratings were measured in reflection at  $0^\circ$  angle of incidence measuring the first diffracted order using a He-Ne laser at S polarisation. The results show that diffraction efficiency and groove depth does not remain constant between the two subsequent platings

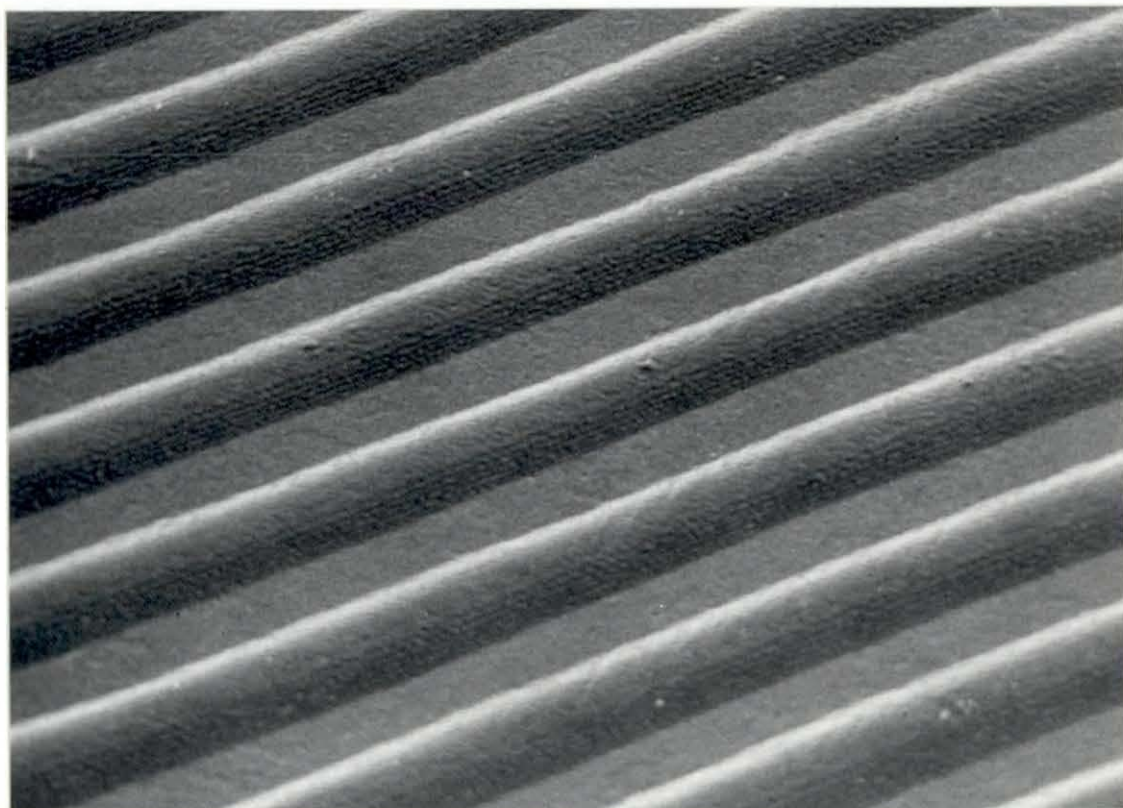


Plate 25. Diffraction Grating Recorded in Photoresist

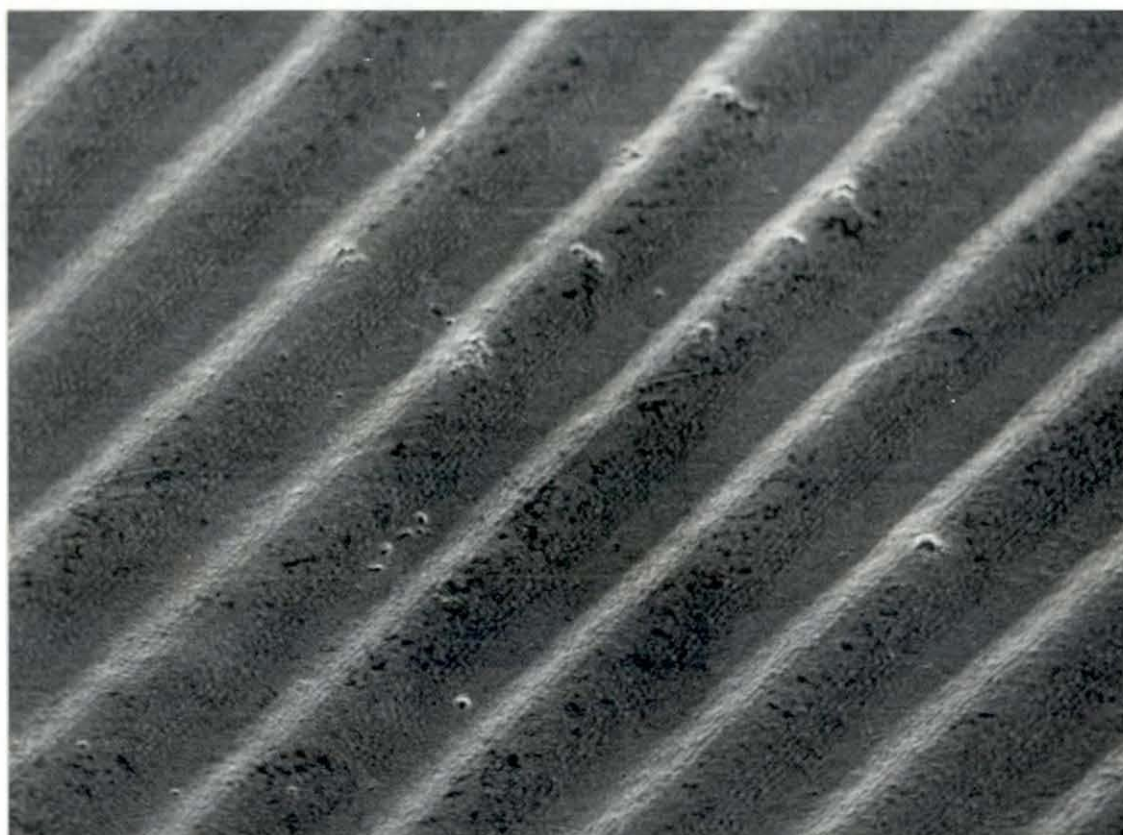


Plate 26. Diffraction Grating Copied into First Generation Metal

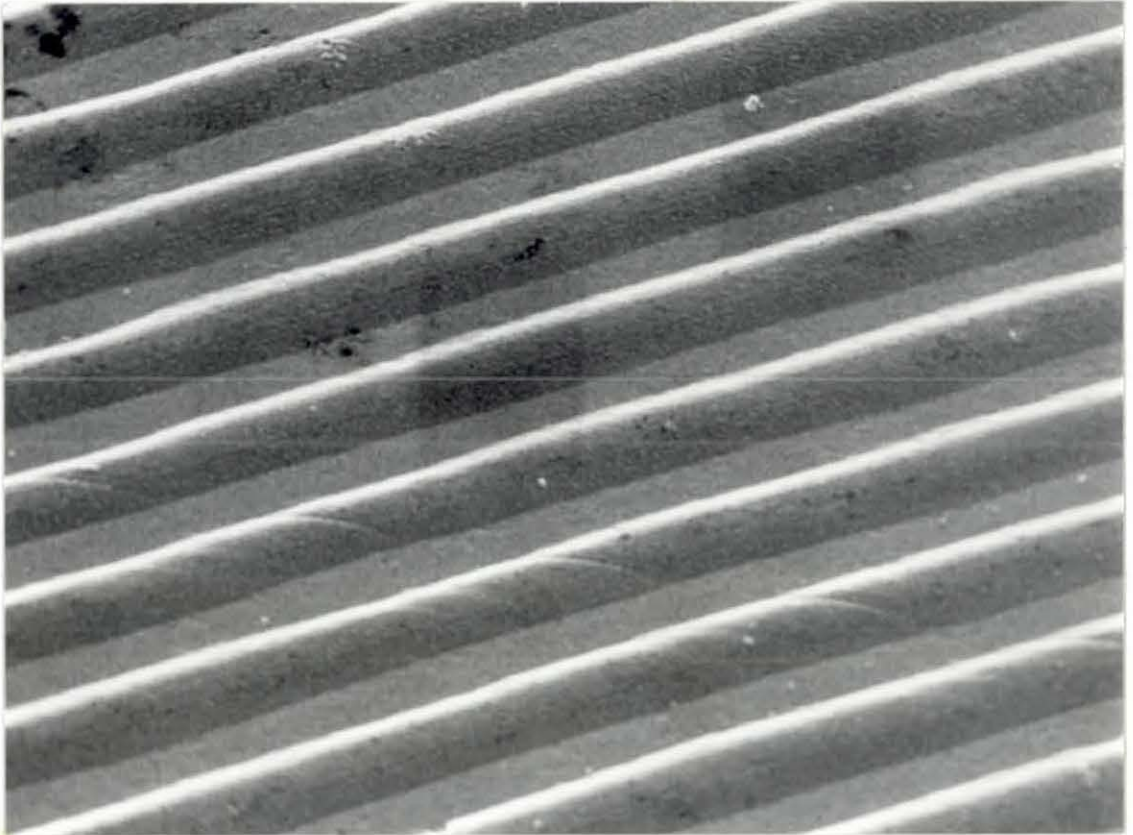
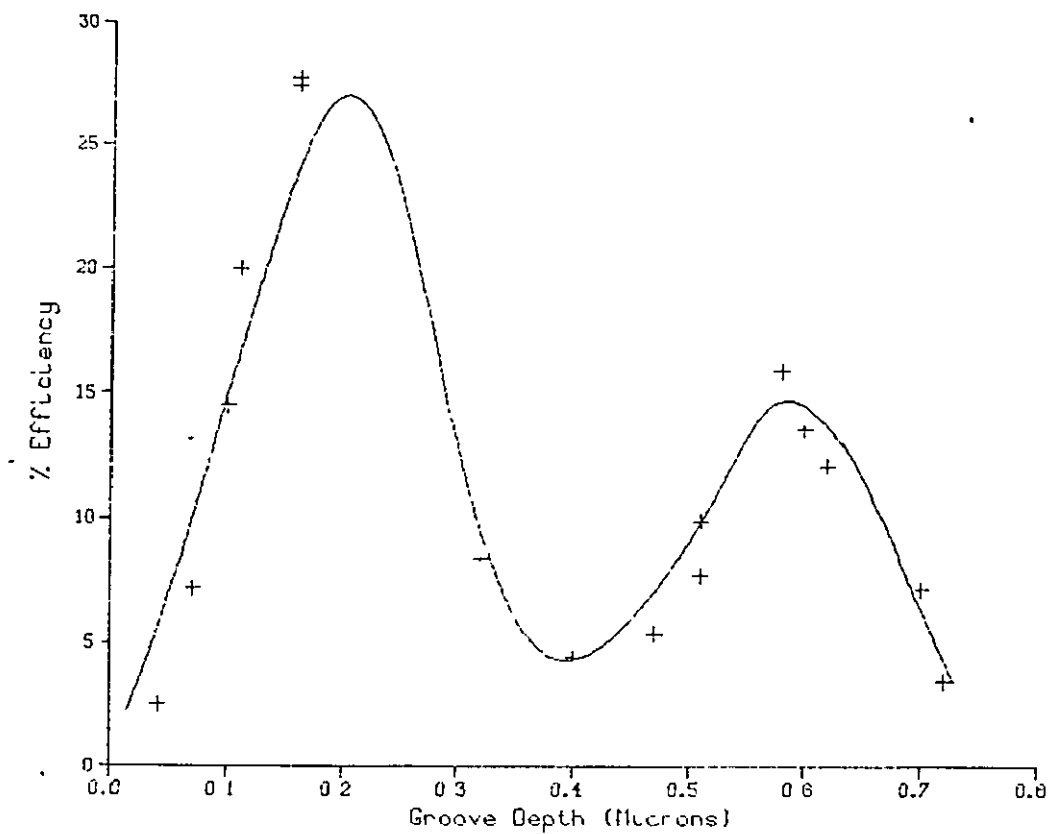
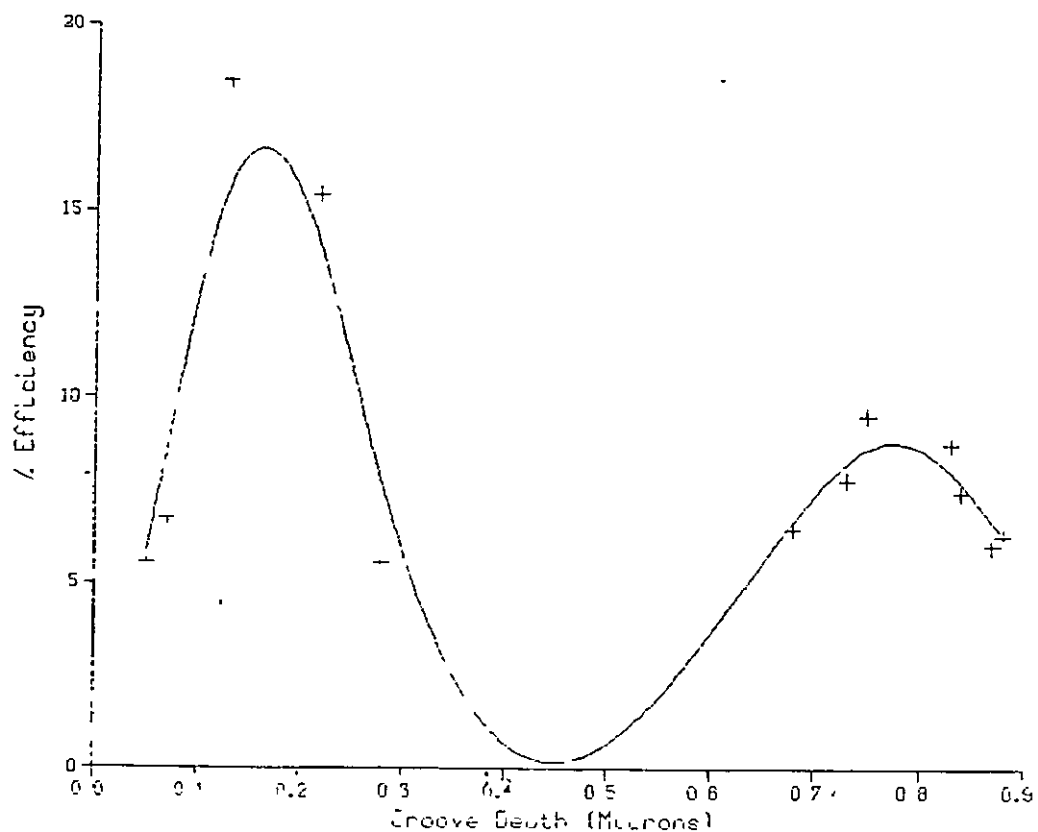


Plate 27. Diffraction Grating Copied into Second Generation Metal



Graph 5.9 Plot of Diffraction Efficiency Versus Groove Depth  
for First Generation Metal Shim



Graph 5.10 Plot of Diffraction Efficiency Versus Groove Depth  
For Second Generation Metal Shim

From the graphs it may be noted;

- i) The peak diffraction efficiency at shallow groove depths ( $\approx 0.18\mu\text{m}$ ) is higher for the first generation metal shim (27.8%) than for the second generation metal (18.46%). The value for photoresist efficiency was found to be 29.1%.
- ii) The second peak efficiency appears at a depth of  $\approx 0.58\mu\text{m}$  for the first generation metal but has shifted to  $\approx 0.78\mu\text{m}$  for the second generation metal.
- iii) The second generation metal shim does not accurately follow the original profile, consequently the noise terms, i.e. higher diffracted orders, reduce the available first order efficiency such that instead of producing a sinusoid function with uniform brightness peaks a decaying function is seen as in Figure 5.11. (Detailed comparison between photoresist, metal and plastic copies is given in Chapter 8)

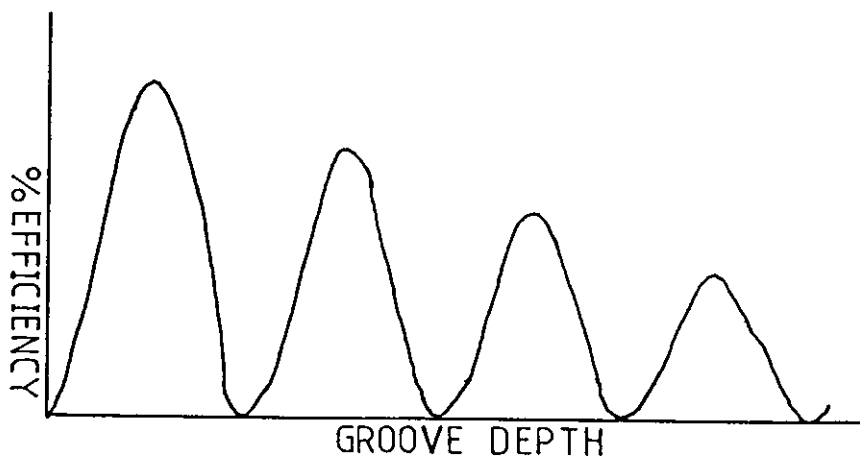


Figure 5.11 Function of Diffraction Efficiency Versus  
Groove Depth



### 5.7 Discussion and Conclusions

An important factor in the process of electroforming is the deposition of the initial conductive layer and the profile it adopts from the original photoresist. This profile, whether accurate or not dictates the profiles that follow in the electroforming process. If the profile of the initial layer is distorted or inaccurate the subsequent platings can only compound matters and result in a profile significantly altered from that of the photoresist. The random nature of the holographic image without regular profiles would be considered 'forgiving' since variation in the surface profile may not produce changes in overall image brightness or clarity. The same could not be true for audio or optical discs where distortions would reveal themselves more clearly. Similarly in spectroscopy, variation in grating profile would change the spectroscopic properties of the grating.

This chapter has considered alternative methods for producing the initial conductive layer and presented experimental detail for each technique. The process of electroforming has been studied in theory and by experimentation. The design of plating tanks and jiggging has been extensively researched to produce high quality, accurate, stress-free electroforms. Second generation plating has been successfully achieved after modification to passivation baths. The measurement of groove depth and diffraction efficiency has allowed quantitative analysis of electroforming accuracy. Conclusions reached from the study of metal replication may be summarised,

- Vacuum evaporation of silver onto photoresist yielded accurate and repeatable results
- Electrolytic plating of nickel onto silvered photoresist could be achieved and repeated.
- Design and maintenance of electroforming tanks and jigs influenced quality of plating
- Subsequent re-platings could be produced by use of modified passivation baths.
- Groove depth and profile did not remain constant during the electroforming process.

- Preferential plating occurred in the production of second generation nickel shims.
- The original groove depth and profile influenced accuracy of electroplating.

The area of electroforming and accuracy of metal to metal copies offers the largest area for future work. Results of electroforming accuracy and aspects of future work are discussed in Chapter 8. The following chapter considers the final stage of the Information Transfer Process which is the embossing of the metal shim into plastic.

## CHAPTER 6

### EMBOSSING THE METAL REPLICA INTO PLASTIC FILM

#### 6.0 Introduction

Embossing is the final stage in the information transfer process. The metal shim that has been produced by electroforming is used as a stamper which, under heat and pressure transfers the surface relief pattern into suitable plastics. The process of embossing is illustrated in Figure 6.1. Electroforming is an established technology dating from 1848. Embossing predates this; the earliest example being official seals in wax. Applying pressure to an engraved plate into heated wax for a period of time is identical to the techniques of embossing used today for both functional and decorative purposes.

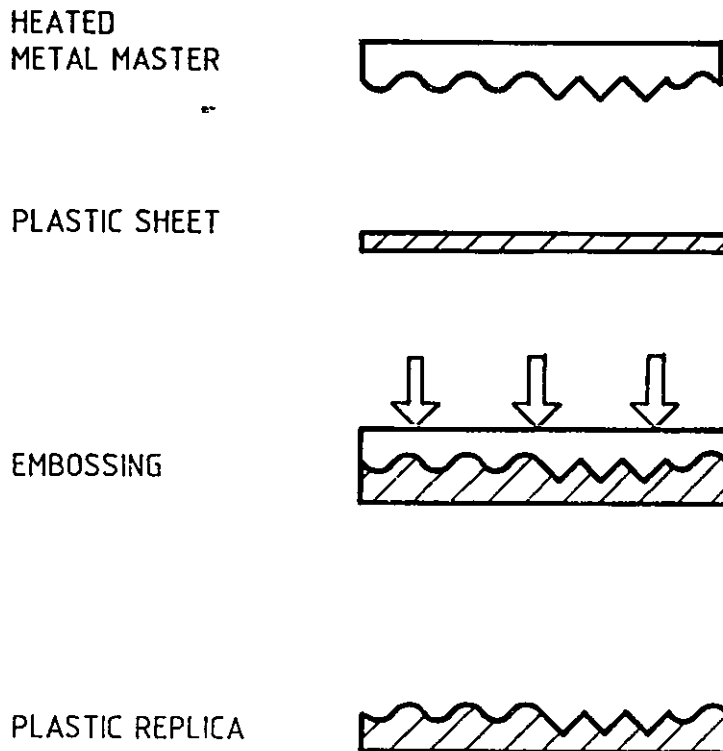
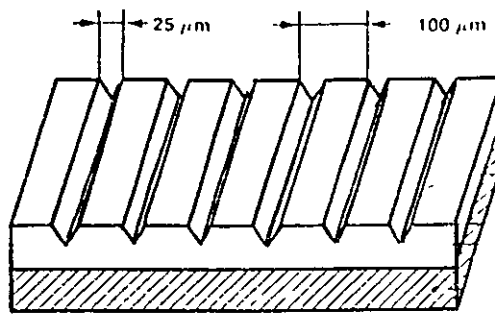


Figure 6.1 Embossing Into Plastic - The Final Stage  
of the Information Transfer Process

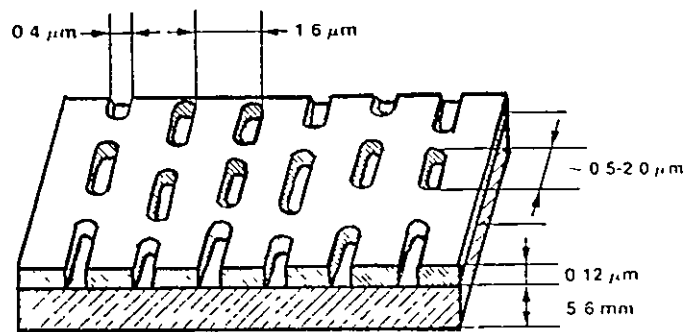
The record industry, decorative printing, optical and compact disc manufacture all transfer information by application of heat and pressure into plastic or vinyl. The heated plastic moulds to the shape of the stamper or die to produce flexible or rigid lightweight plastic copies of the original stamper. The information storage capacity and capture of fine detail has advanced such that features of  $1\mu\text{m}$  can be repeatably stamped and replicated for hundreds of thousands of copies.

The hand engraved seal has been replaced with laser cut dies or ion etched stampers and the sealing wax replaced by polymers with known and controllable thermosoftening behaviour. Clear thermoplastic films such as vinyl, polyester, acetate, polycarbonate and polyolefin are all suitable materials. Figure 6.2 illustrates the detail of features currently used for the production of records, optical discs and gratings.

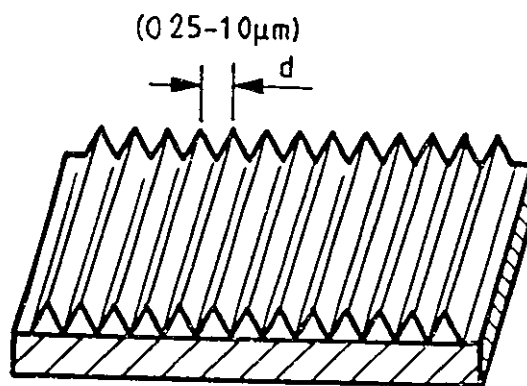
This chapter considers two aspects of embossing. Firstly, the plastics used for embossing are detailed. Secondly, the physical process of embossing using roller and platen techniques is discussed. The experimental detail and results for the embossing of the metal shims is also given. A more detailed account of physical properties and characteristics of polymers and plastics is presented in Appendix 5.



Record Disk



Optical Disc



Optical Element

Figure 6.2 Comparison of the Level of Detail for Record Disk, Optical Disc and Optical Element

### 6.1. Plastics for Embossing

The plastics used for embossing must be capable of resolving the fine detail applied to the plastic under heat and pressure. The plastics most commonly embossed are polyvinyl chloride, polyester, acetates or polycarbonate. Full details of these plastics will be found in Appendix 5, the section below presents a brief description of the structure and uses of the plastics.

#### 6.1.1 Polyvinyl Chloride (PVC)

The chemical structure is shown in Figure 6.3

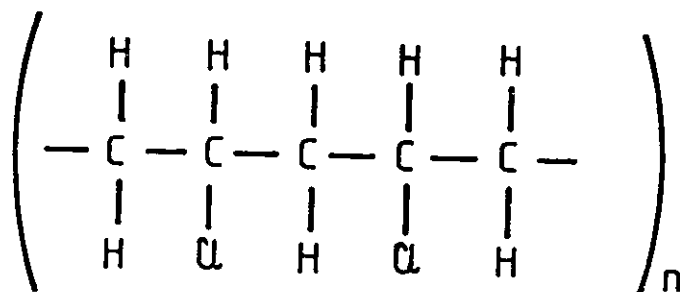


Figure 6.3 Chemical Structure of Polyvinyl Chloride

The general properties of PVC are good chemical resistance and good mechanical strength. In the manufacture of PVC, plasticizer is added to improve flexibility but highly plasticized film and sheet can become brittle at low temperatures. The range of PVC usage and products is vast, from shower curtains to meat wrapping, toys to gramophone records. The versatility of the product depends much upon its processing, make-up and manufacture. The essential feature of PVC film for embossing is that it is able to be embossed by platten or roller techniques.

### 6.1.2 Polyester

Polyester films show great strength and aging characteristics. The chemical structure for polyethylene terephthalate, ("Mylar") is shown in Figure 6.4

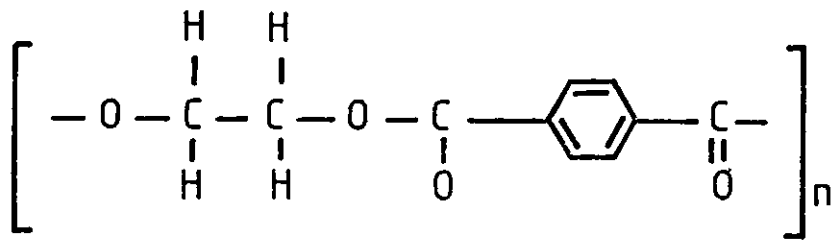


Figure 6.4 Chemical Structure of Polyester

Most typically, polyesters are used for vacuum packaging, boil-in-the-bag products, and laminations with PVC films for packaging. Use as photographic film substrate illustrates the toughness of polyester and the ability to withstand high temperatures is demonstrated in the use of polyester as a carrier for pigments and metal leaf in hot stamping foils.

### 6.1.3 Polycarbonate

Polycarbonates are produced from a wide range of polyfunctional hydroxyl compounds. Figure 6.5 Polycarbonate is exceptionally tough with good transparency and temperature resistance. The largest application area is in electronics, where its electrical insulation properties, flame resistance and durability are essential. Sheet glazing is mostly polycarbonate used for light weight, transparency and toughness.

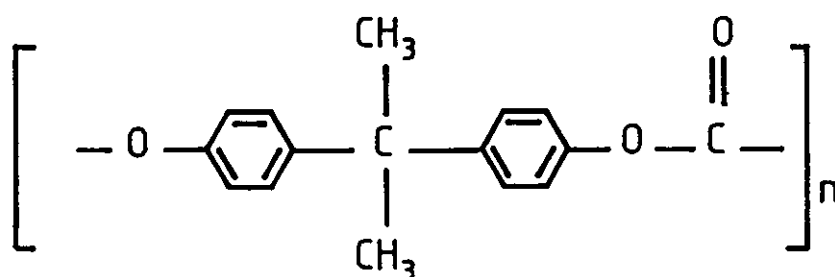


Figure 6.5 Chemical Structure of Polycarbonate



#### 6.1.4 Cellulose Acetate

Cellulose acetate is derived from the acetylation of cellulose. The chemical structure of cellulose is shown in Figure 6.6.

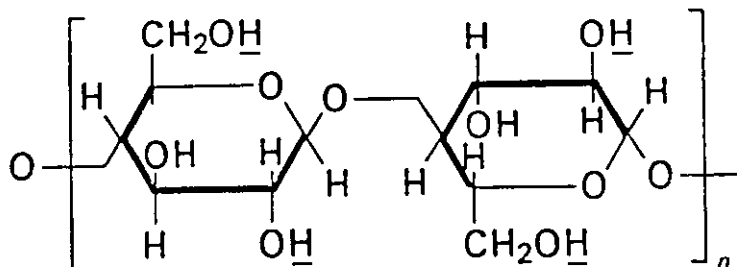


Figure 6.6 Chemical Structure of Cellulose

In cellulose acetate the underlined hydrogens ( $\underline{\text{H}}$ ) are replaced by acetate groups ( $-\text{OCCH}_3$ ). Cellulose acetate has high clarity, good toughness and impact strength. It is suitable for display packaging due to its heat formability, clarity and toughness. It is also used in graphics arts and for photographic substrates.

The following section will detail the nature of embossing for roller and embossing techniques before considering some alternative embossing methods and presenting experimental detail and results.

6.2 The Nature of Embossing

Whilst embossed holograms are relatively new, embossed products are not. Luggage, furniture coverings, book bindings, vehicle upholstery are all examples of decorative embossing. Apart from decorative finishes an embossed surface can mask imperfections in sheeting produced by calendering or extrusion processes. Projection screens are embossed with lenticular arrays for even light distribution. Embossing relies upon three factors, heat, pressure and dwell time (length of time of applied pressure). Two different embossing methods will be considered, roller and platen embossing. Figure 6.7 illustrates two roller embossing designs. [53]

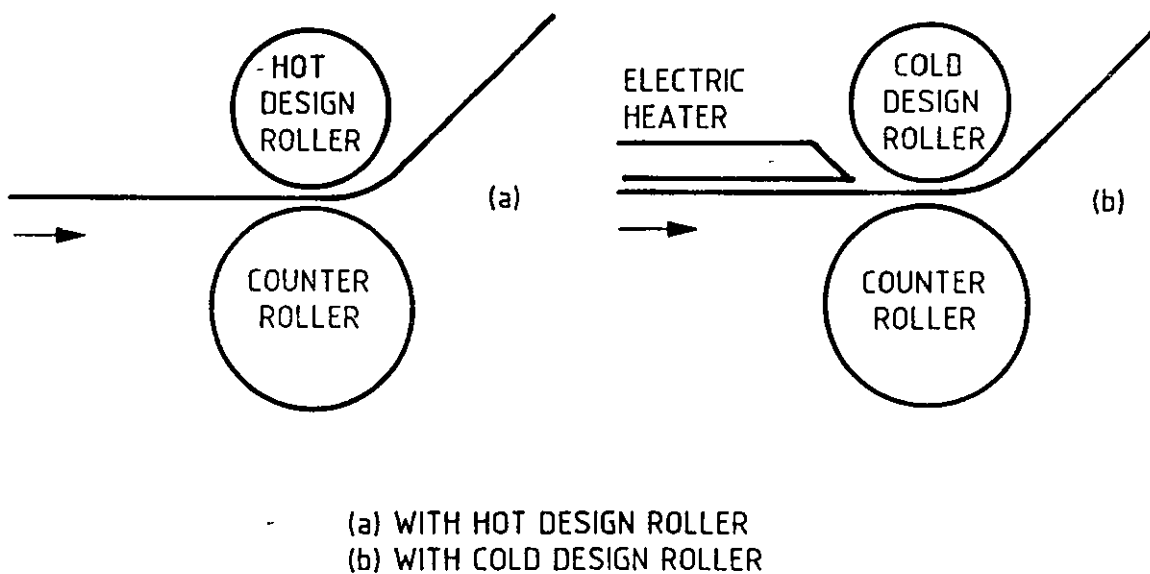


Figure 6 7 Roller Embossing Designs

### 6.2.1 Roller Embossing

The metal shim produced by electroforming must be sufficiently thin (2mm) and flexible to 'wrap' around large rollers. In practice, multiple shims would be adhered over the entire surface of the roller to provide a continuous embossing area in the same fashion as printing rollers. This becomes the design roller. Variations in shim thickness must be avoided in order to maintain constant pressure over the roller surface in contact with the plastic. The hot design roller, Figure 6.7 a) is the most simple technique. A continuous plastic sheet at ambient temperature is fed between the hot design roller and the cold counter roller. The plastic sheet is simultaneously heated and stressed by the rollers. As the plastic sheet becomes hotter stress is relieved by molecular re-arrangement of the polymer chains and the plastic assumes the patterns transferred from the design roller. Until the dwell time stops, i.e. the sheet leaves the rollers, the stress continues to be relieved and the plastic sheet reaches the same temperature as the design roller. The embossed pattern will still flow after this time due to the relief of residual stresses within the plastic. Consequently, machines using hot design rollers tend to give depth of embossing approximately half that of the design on the embossing roller. The loss of depth occurs rapidly at the end of the dwell time and forced cooling of the sheet on removal from the roller offers only slight improvement to the process. However, this hot technique gives higher retention temperatures because the embossed sheet is virtual stress-free as a result of the heating allowing continued stress relief.

The alternative method, Figure 6.7 b) uses a cold design roller aimed at improving the depth and hence quality of embossing. The plastic sheet is fed between cold rollers but heated prior to reaching them. The sheet must be sufficiently hot on reaching the rollers to emboss upon contact before it cools and resets. The sheet leaves the rollers below the temperature at which it can flow, so no residual stress relief occurs and more accurate embossing is achieved. Both designs are used in industry for embossed products, the choice being dictated

by the finish desired. Even the so-called 'cold' process may use rollers heated to 25-60°C depending on the plastics in use.

Figure 6 8 illustrates the embossing process used in the production of embossed motion pictures for television playback [19]. In this instance the metal shim is a continuous metal tape replicated from a photoresist tape. Photoresist was deposited onto a 16mm polyester substrate for use with motion picture recording equipment.

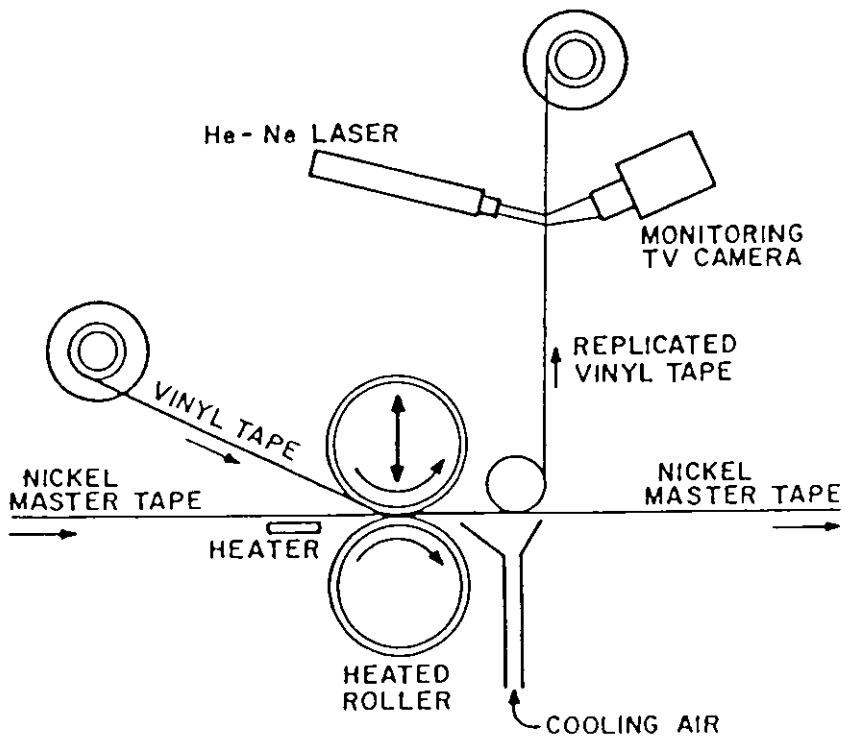


Figure 6 8 Replication of Embossed Motion Pictures

### 6.2.2 Platen Embossing

Unlike roller embossing where a thin metal shim is required, platen embossing can use thick, flat shims. For large format embossing, 12" square, shims as thick as 40mm may be necessary [17]. The platen embosser consists of two flat metal plates, upper and lower, the shim being attached to the upper heated plate. The plastic sheet is fed between the two plates, the upper plate lowered and 'pressed' onto the plastic. Variations in the technique use two heated plates and rapid air or water cooling of the plastic or plates after sufficient dwell time. Internal heating and cooling of the plates ensures even plastic flow similar for roller embossing methods. Production rate is considerably slower than for roller embossing and a comparison of the techniques is given in Table C.

The most obvious application of platen embossing is the record industry and the 'stamping' of records. From similar technology of metal masters and shims, electroformed nickel stampers are pressed into a mass of heated thermoplastic material. The pressing is rapidly cooled until rigid, removed from the press and trimmed.

Table C Comparison of Roller and Platen Embossing

<u>Roller embossing</u>	<u>Platen embossing</u>
High production rates	Lower production rate
-30 m/minute	-Seconds/impression
Thin, flexible shim $\approx 2\text{mm}$	Rigid, thick shim $\approx 20\text{-}40\text{mm}$
High equipment cost	Lower equipment cost
<u>High production numbers only</u>	<u>Single embossings possible</u>

### 6.2 3 Alternative Embossing Techniques

Injection, blow and vacuum moulding techniques are well established and future trends suggest products with holograms as an integral part of a moulded items. Figure 6.9 illustrates injection and compression moulding for optical disc production. The resolution requirements for holography could well be met by advances in this technology.

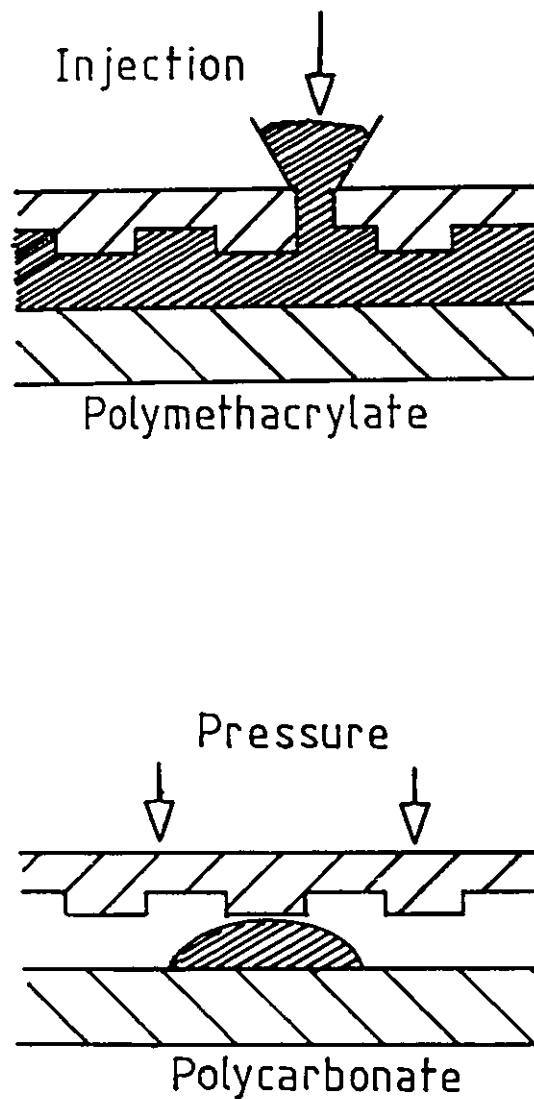


Figure 6 9 Injection and Compression Moulding  
for Optical Disc Production

#### 6.2.4 Hot Foil Printing

Hot foil printing is not a new technique of decorative printing. Greetings cards, business cards and decorative finishes of silver, gold or coloured foils are all examples of hot foil printing. Metallic or coloured foils are transferred to a surface by application of heat and pressure. The interest in hot foil printing for holography developed when the metallic or coloured layer in the printing foil was replaced with a hologram. The holographic image is transferred by heat and pressure with the image being an integral part of the printing 'foil'. Figure 6.10 illustrates a cross-section of a foil showing the incorporation of the holographic image. Platen type embossers are used to transfer the image whereby the foil is held in contact with a heated metal plate to transfer the image to almost any surface. High quality, large production output is possible with this method.

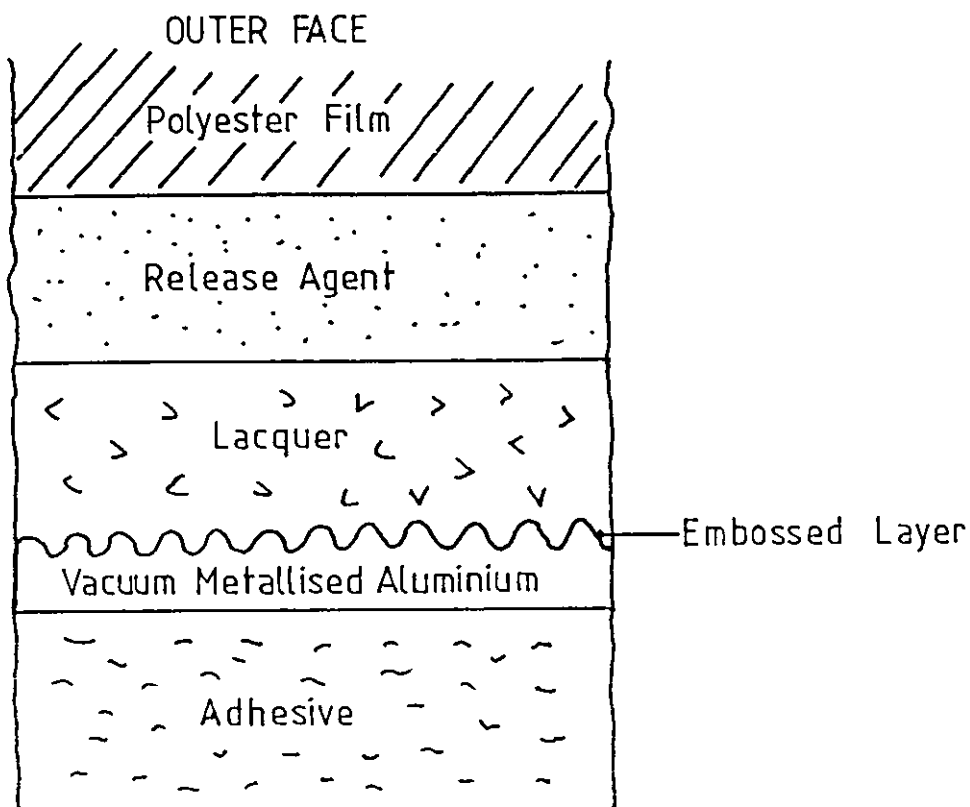


Figure 6 9 Cross Section of a Printing Foil

The carrier material is typically polyester,  $\approx 25\mu\text{m}$  thickness. The hologram is embossed into the thermoplastic varnish or lacquer as shown in Figure 6 10. The release agent between the polyester carrier and the embossed varnish allows separation of the hologram from the carrier under heat and pressure. An adhesive coating may also be applied allowing hot foil printing onto a variety of surface finishes. Registration of hot foil printed holograms is very critical and registration marks are usually incorporated into the foil runs. Printing is achieved by placing the holographic foil between the platen plates, the adhesive toward the surface to be printed. The heated platen presses the foil onto the surface simultaneously releasing the printed lacquer layer from the polyester carrier.. The hologram is printed onto the surface as the polyester carrier is advanced by rollers to present a fresh area for printing.

Hot foil printing offers an alternative technique to holograms embossed into thermoplastics. It offers advantages of speed and transfer of images onto almost any flat surface including paper, fabric, metal, polished wood, etc. The stages required to produce the initial foil for printing follow those for the production of embossed holograms and this research is also applicable to hot foil printing. The transfer of information from surface relief original through to metal replicas is identical. The metal shims are then used to emboss the lacquer used in the foils as opposed to embossing plastic sheet. An interesting aspect for further work would be the comparison of techniques between embossing the lacquer for the foil and embossing thermoplastics.



### 6.3 Experimental Detail and Results

The experimental investigation into embossing selected a number of plastics, embossed using a platen embosser.

#### 6.3.1 Choice of Plastic

Details of the embosser and embossing parameters will be found in a latter section of this chapter. The following details the plastics used for trial embossing.

- a) Polyester Gloss Clear film: a transparent gloss polyester film typically used for photograph reproduction layouts, receptive to pen, pencil, marker and typewriter
  - b) Milmar Bright Silver Polyester: a metallized polyester film designed for decorative metallic finishes for appliances, name plates, etc. The film is top coated for ink receptivity, claiming excellent dimensional stability, weathering resistance and good ageing characteristics.
  - c) Embossable Polyester Gloss Silver: a metallized polyester film designed for embossing emblems and signs with a metallic finish. Top coated for ink receptivity
  - d) Dumar Bright Silver Polyester: a metallized polyester film with similar uses and characteristics as b) above.
- All the above samples were produced by ADP Ltd (Adhesive and Display Products Ltd.).
- e) Chrome Dart Flight: a metallized polyester film designed for decorative finishes. Produced by CSL (Coated Specialities Ltd.).
  - f) Acetate Overlay Foil: a transparent acetate sheet designed to impart gloss finish for heat sealed mounting Produced by Ademco Ltd
  - g) Silver Mirror Polyester: a metallized polyester designed for decorative finishes. 200µm and 400µm thickness.
  - h) Silver Mirror PVC a 400µm PVC sheet designed for decorative finishes.

All of the polyester films were embossed under a range of conditions. (Section 6 3 3) The Chrome Dart Flight material (CSL Ltd.) yielded the best results for embossing at 16kg/cm<sup>2</sup> for dwell times of 10-15 seconds

at 120°C. Unfortunately this material is no longer available. The embossable polyester film produced by ADP Ltd. showed a very definite surface structure from the manufacturing process that obscured detail from the embossed gratings as seen in Plate 28.

The acetate film (Ademco Ltd.) was used extensively for a number of trials and those for assessing embossing variability. Plate 29 shows an SEM photomicrograph of a grating embossed into this material.

Observations and Discussion The range of material available for embossing is limited to polyesters, acetates, PVC or polycarbonates. In this study, polyester, acetate and PVC have all been used for embossed gratings. The choice of plastic has been determined by cost, availability and supply of material (minimum orders typically far beyond that required for assessment). The Chrome Dart Flight material (metallized polyester CSL Ltd ) was the first choice in this instance because of the range of embossing conditions over which results could be obtained, cost effectiveness and small sheet size availability. The ceased production of this material meant that the subsequent results were produced on acetate sheet. The sheet was cheap, available in small roll quantities and already in use for other purposes. The film was not metallized and consequently viewing of the gratings or hologram was by mounting against mirrors or mirror foil.

Commercially produced holograms were obtained for assessment over the different plastics. Plates 30 and 31 show detail from two identical images embossed onto PVC and polyester.

The depth of impression obtained in PVC is very much greater than for the polyester material. The surface finish quality is also enhanced and the PVC holograms appear visually brighter. Results were photographed using DIC (differential interference contrast) techniques

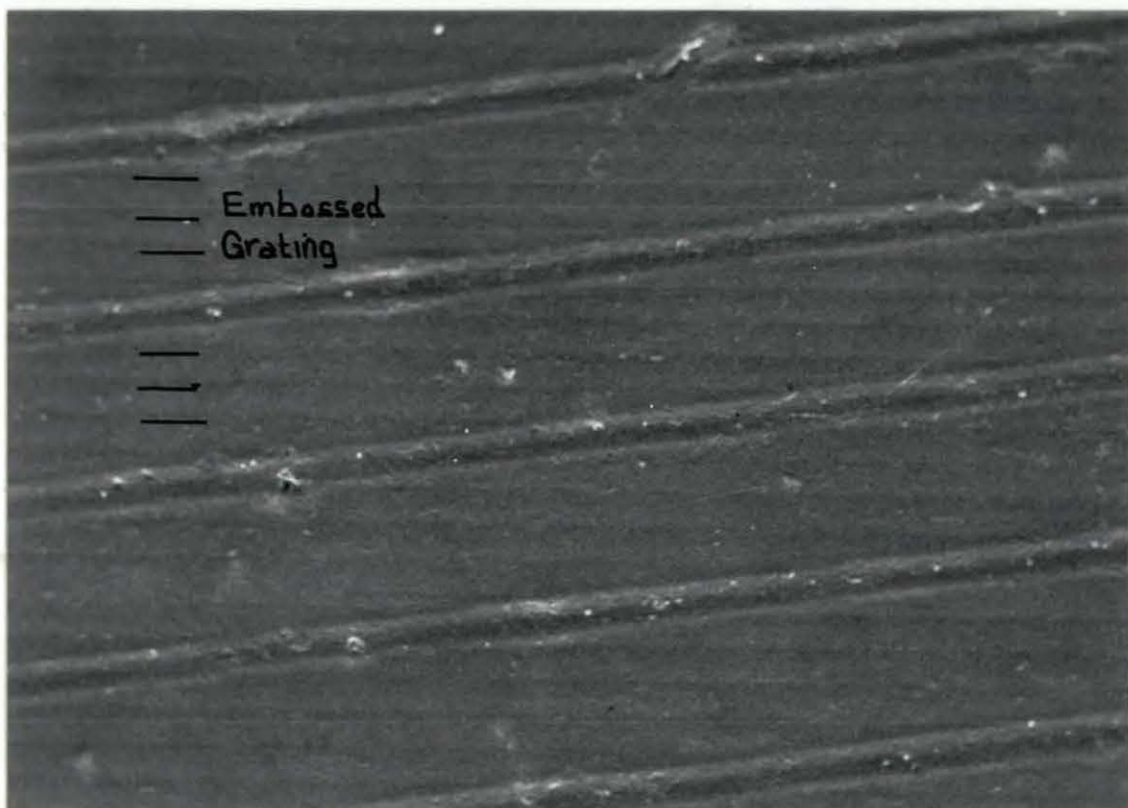


Plate 28. Embossable Polyester Film Showing Manufacturing Process Marks

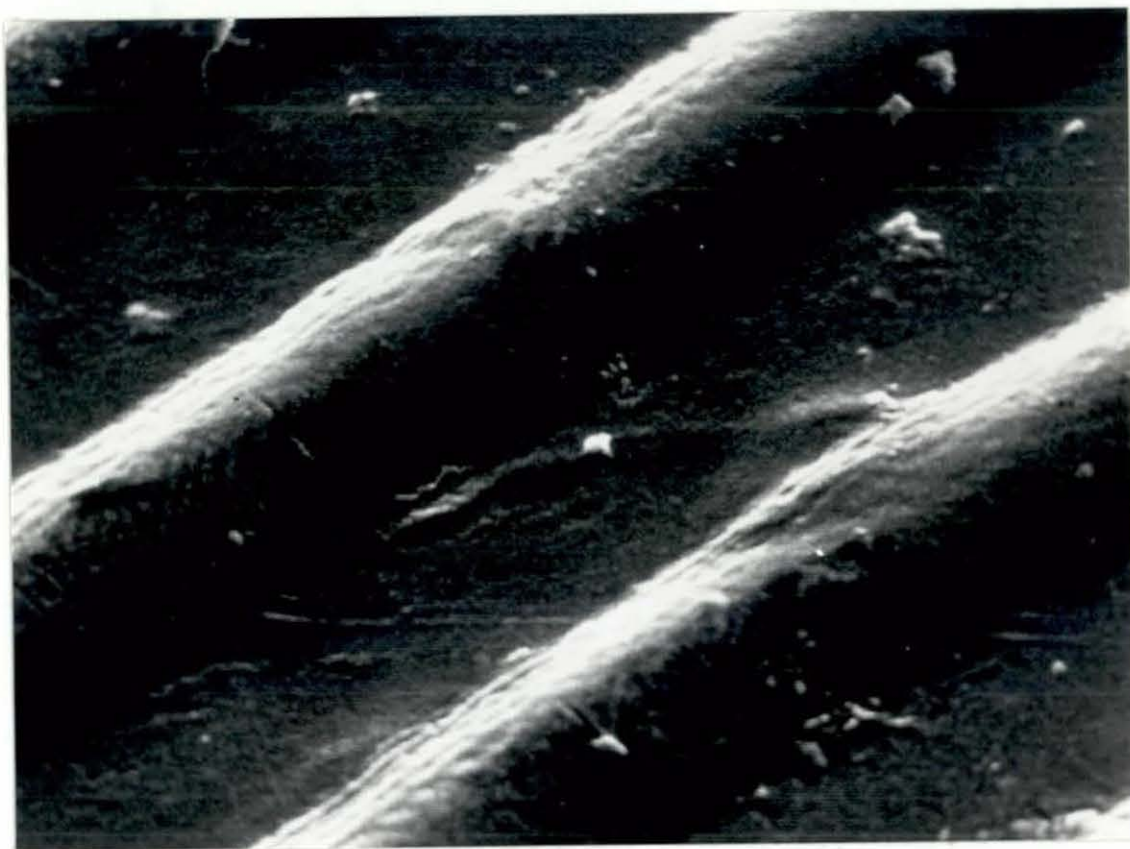


Plate 29. Embossed Acetate Sheet



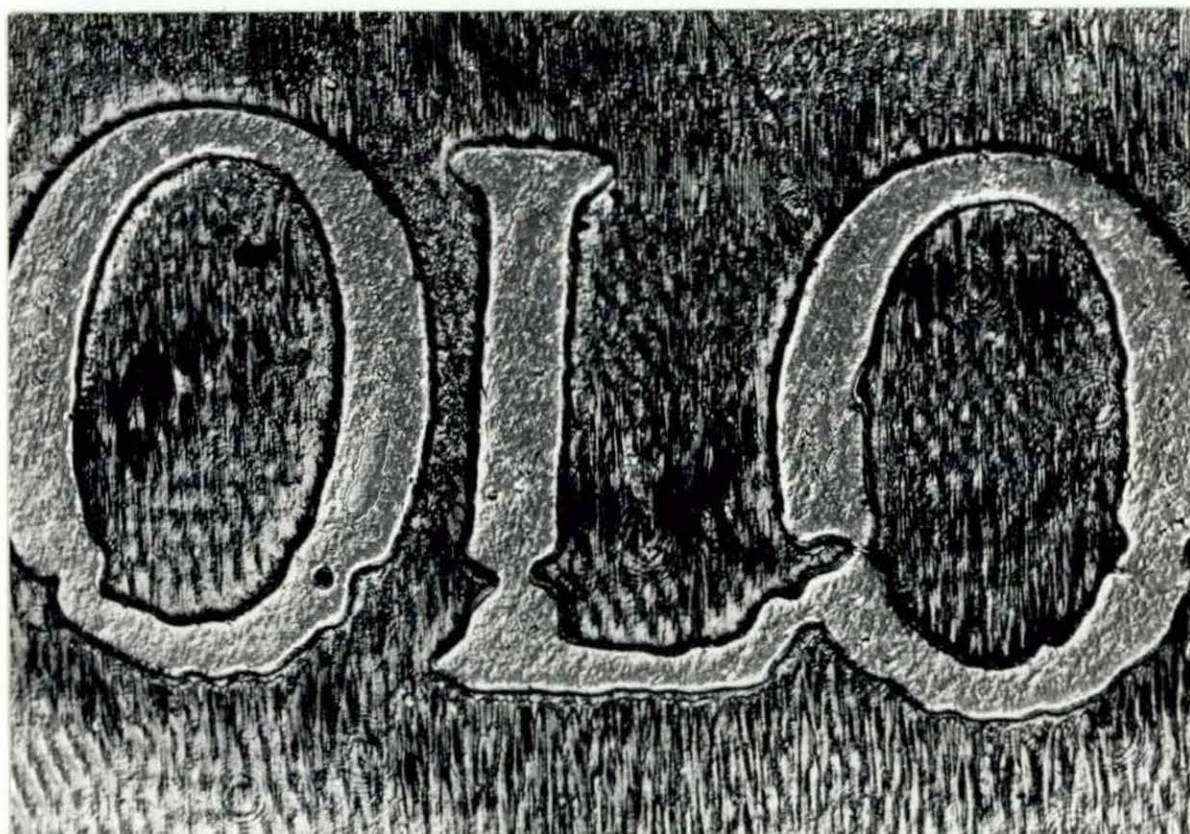


Plate 30. Detail from Hologram Embossed Into PVC

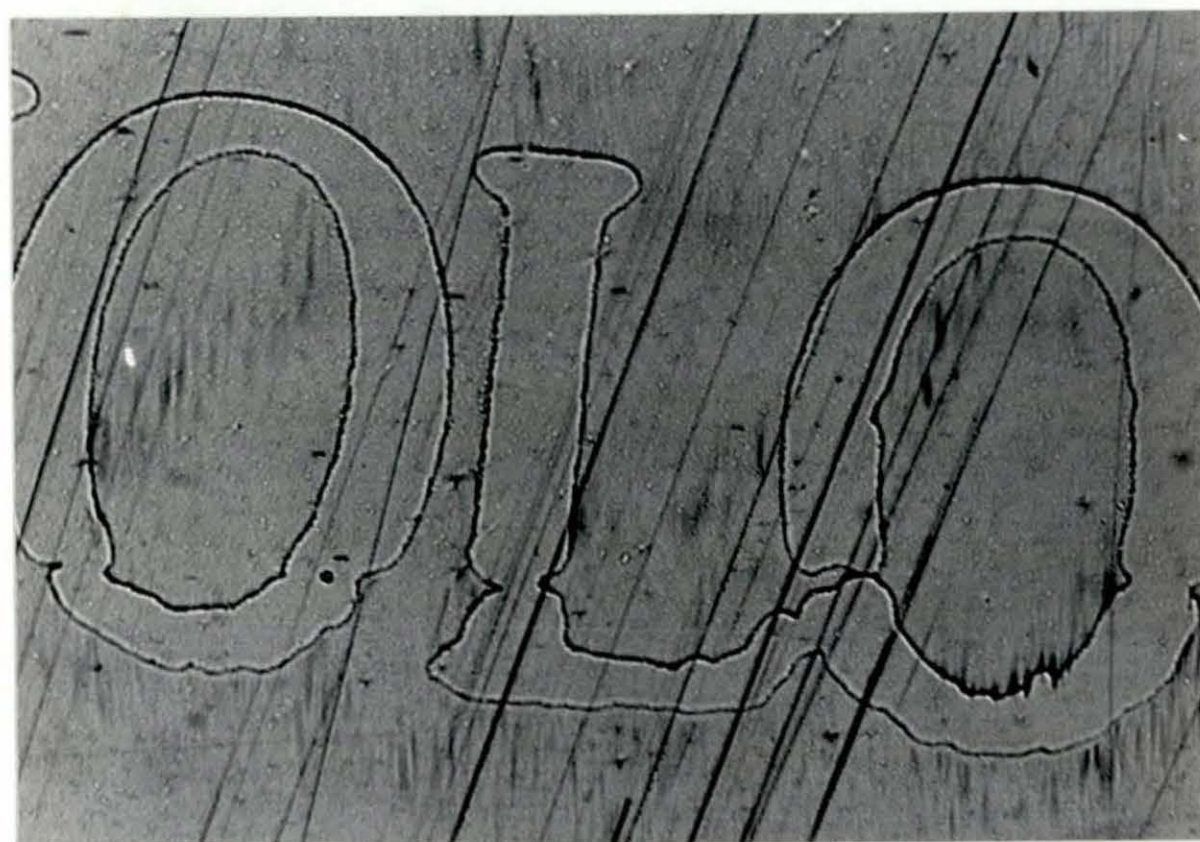


Plate 31. Detail from Hologram Embossed into Polyester

### 6.3.2 Modification of A Platen Embosser

A unique feature of this research has been the quantitative analysis of the accuracy and efficiency of the embossing process through all of the image transfer stages. The process of embossing was identified as the greatest influencing factor in determining the accuracy of the process. In order to obtain meaningful and accurate results the embosser required modification to measure applied pressure, temperature and dwell time.

A hand operated platen embosser, designed for small scale hot foil printing, Hot Printer 1000, was acquired to perform embossing experiments. The unit had no indication of applied pressure or accurate temperature monitoring on the platen face. Accurate measurement of temperature of the metal shim and applied pressure into the plastic was required. Plate 32 shows the platen embosser with detail of the upper plate.

A polished steel die block was constructed to fit into the upper unit of the embosser. The upper unit was heated and heat conducted through the die block to the front face. The metal shims produced by electroforming were attached to the front face of the block by a thermal adhesive. In order to accurately monitor the temperature of the block a thermocouple was clamped between the block and mounting bars. Close proximity to the face of the metal shim ensured an accurate reading of the shim temperature. The thermocouple unit is seen beside the embosser in Plate 32. The unit took 10-15 minutes to warm-up and the thermostatic heater allowed temperature operation between 103° and 203°C. The temperature of the metal block would vary during operation and after four to five embossings a short break was required to allow the temperature of block to stabilize. By modification of the unit in this way it was possible to monitor the 5-6°C temperature drop that occurred across the metal shim on contact with the plastic when embossing.



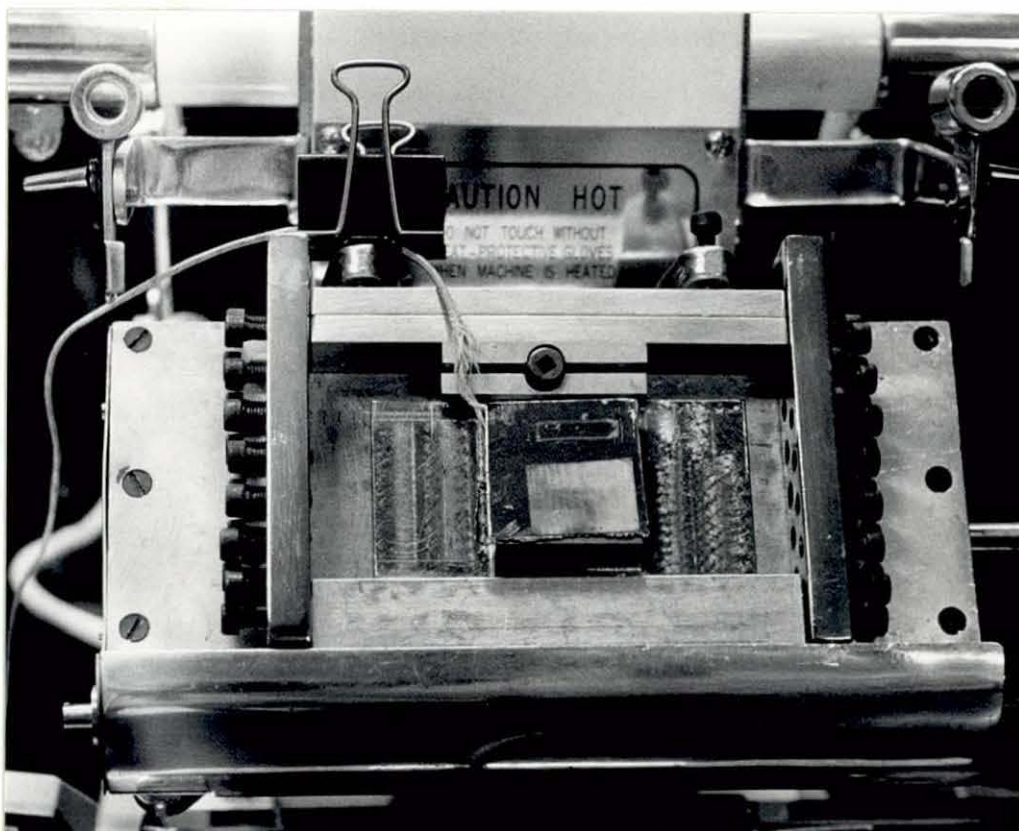


Plate 32. Modified Platen Embosser - Detail of Heated Upper Plate

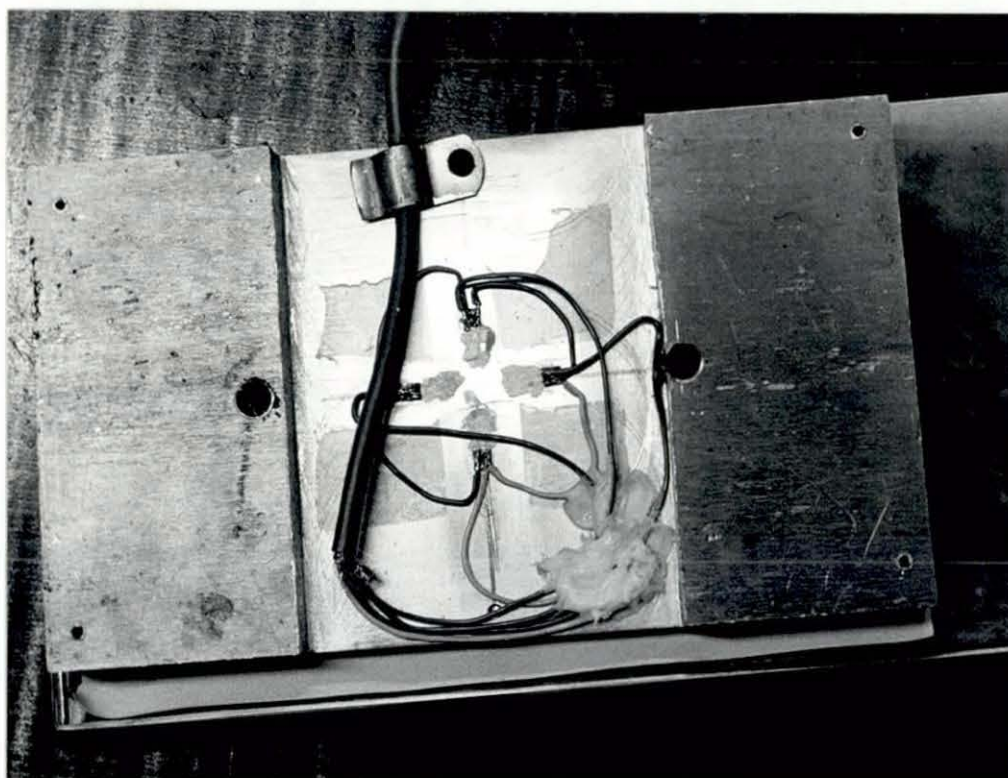


Plate 33. Modified Platen Embosser - Detail of Load Cells Attached to Lower Plate to Calibrate Applied Pressure

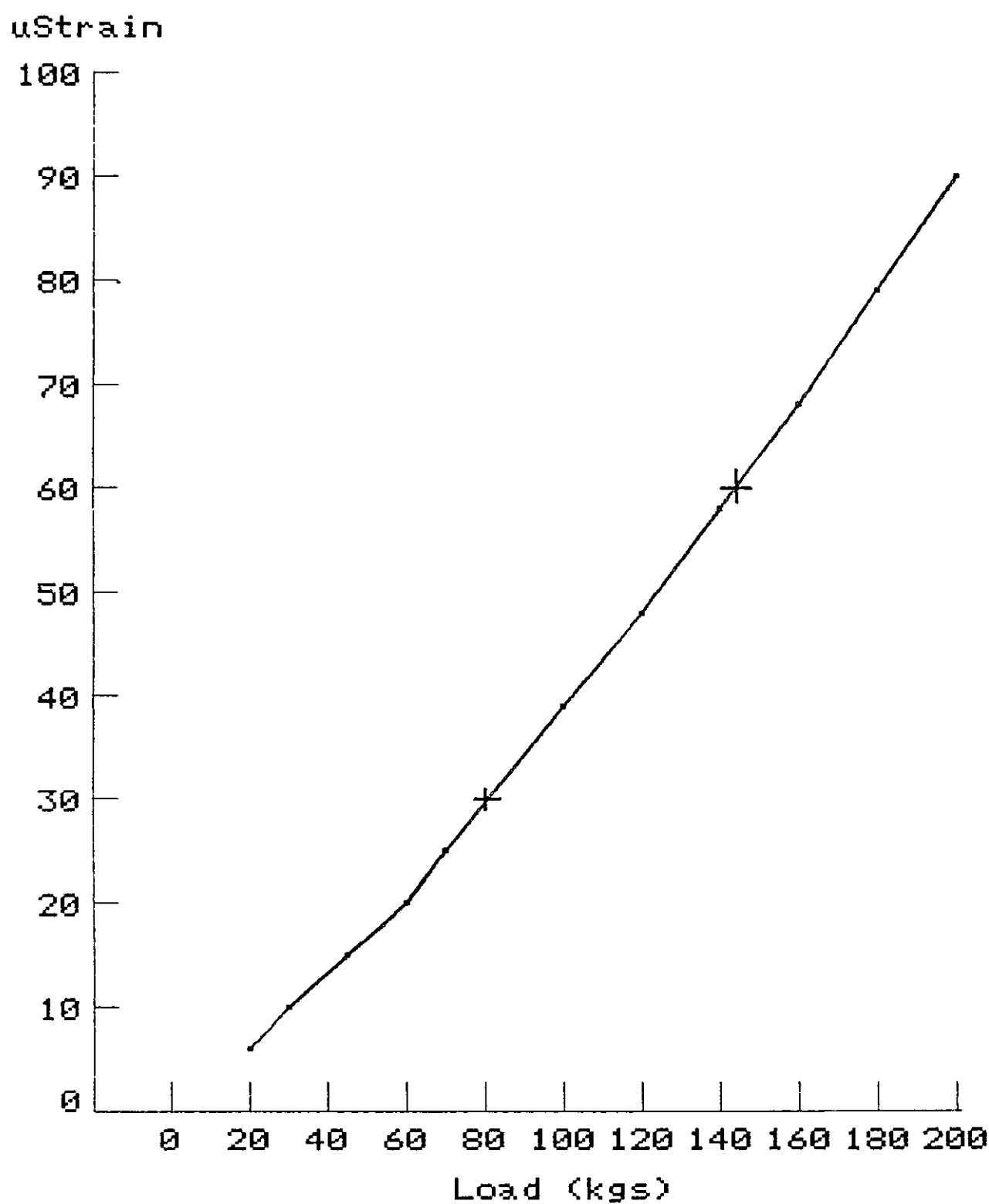
The second modification to the platen embosser was to allow accurate measurement of applied pressure to the metal shim into the plastic. Plate 33 shows detail of the underside of the lower plate of the embosser. Attached to the plate are load cells arranged in a half bridge. The bottom plate was purpose built and designed to spread the applied load in a controlled manner.

The platen embosser was calibrated using an Instron machine. The design of the heated die block presented an imprint area of 9cm<sup>2</sup> onto the lower plate fitted with load cells. The upper and lower plates were rigged upon the Instron machine in an identical fashion as when embossing to calibrate the applied load to the unit. The attached load cells produced a resistance change output as  $\mu$ strain deflections on a bridge meter. (Temperature corrected.) The calibration curve in Graph 6.11 shows a plot of applied load in kilograms against  $\mu$ strain. Highlighted on the graph are two embossing pressures of 30 and 60  $\mu$ strain. From the calibration curve these values relate to applied pressure in kg/cm<sup>2</sup>.

Meter	Equivalent Pressure
$\mu$ Strain	kg/cm <sup>2</sup>
30	10
60	16

These pressures were chosen to produce results over a range of embossing pressures. Using only a small hand-operated platen embosser, pressures above 80  $\mu$ strain, representing 20kg/cm<sup>2</sup> were difficult to apply and maintain. Hydraulically operated presses can apply in excess of 30kg/cm<sup>2</sup> at the lower range of embossing pressures.

The accurate measurement of dwell time was achieved by a stop watch started as the heated upper plate and metal shim contacted the plastic sheet beneath. A range of embossing temperatures, pressure and time was investigated as detailed in the following section.



Graph 6.11 Calibration of Embosser  
Applied Load Versus  $\mu$ Strain



### 6.3.3 Trial Embossing

The calibrated embossing unit, capable of accurately monitoring temperature, pressure and time permitted a number of trial embossings to be made to identify variables of the process. The plastic copies embossed from the metal shims could be quantitatively measured for groove depth and diffraction efficiency and compared to the values obtained for the photoresist and metal originals.

An initial metal shim was used for early embossings. This was a second generation metal shim, 1b4 as detailed.

Grating 1b4	Incidence	Zero / 1st Order		Grating Depth
	Angle	Efficiency		$\mu\text{m}$
Resist	0°	58.3%	5.5%	0.06
1st Gen Metal	0°	47.61%	7.14%	0.07
2nd Gen Metal	0°	31.25%	4.84%	0.15

The second generation metal shim showed a groove depth over twice that of the photoresist or first generation metal. The Talysurf traces of the profile show the reason for this anomaly. (Section 6.4) The profiles are far from sinusoidal showing flat tops to the peaks. The distorted profile accounts for the low first order diffraction efficiency. This choice of shim was made to assess the accuracy of embossing over best and worst profiles. This shim offered the worse case likely to be encountered.

A first generation shim with a more sinusoidal profile was also embossed. This was metal shim 1a2 as detailed below;

Grating 1a2	Incidence	Zero / 1st Order		Grating Depth
	Angle	Efficiency		$\mu\text{m}$
Resist	0°	2.50%	28.3%	0.15
1st Gen Metal	0°	2.58%	27.40%	0.16
2nd Gen Metal	0°	3.07%	13.33%	0.15

This metal shim showed high first order diffraction efficiency and small variation between resist and first metal shim groove depth. The profiles of the grating structures are shown in Section 6.4

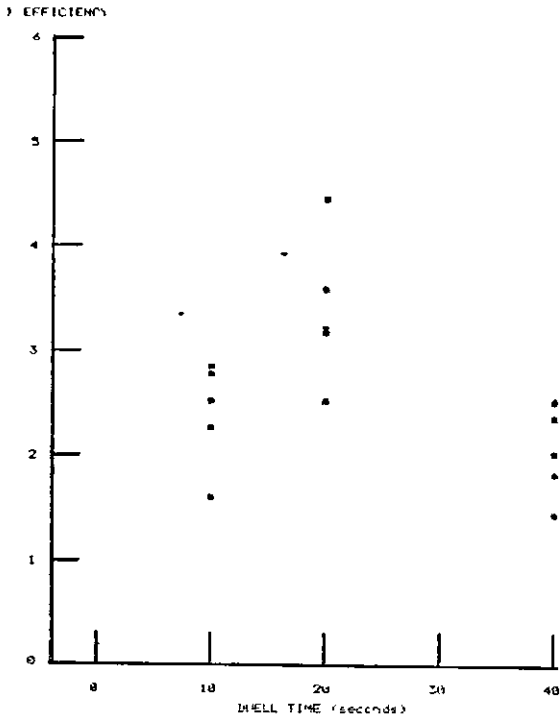
After difficulty in acquiring metallized polyester film all embossed results were produced in acetate sheet. The acetate sheet was laid against smooth vinyl to ensure a flat, even surface for embossing into. The nature of the surface under the acetate sheet was important for quality embossings. Initial experiments used card and rubber surfaces under the acetate sheet. The heat from the metal shim caused the rough texture of the card to impart into the plastic sheet making measurement of the diffraction gratings difficult. Similarly with the rubber matt used to absorb the heat, the fine pattern on its surface transferred to the embossing. The use of the vinyl sheet overcame these problems and presented a smooth surface, capable of absorbing heat from the metal shim without interfering with the embossing.

Results are presented for trial embossings made to establish optimum temperature, pressure and dwell time for embossing a second generation shim into acetate sheet.

TEMPERATURE °C	PRESSURE kg/cm <sup>2</sup>	DWELL TIME seconds	% EFFICIENCY-FIRST ORDER				
			A	B	C	D	E
120	10	10	2.24	1.58	2.83	2.50	2.76
		20	2.50	4.44	3.16	3.20	3.57
		40	2.34	1.42	2.00	1.80	2.48
120	16	10	1.63	3.49	2.66	2.10	2.22
		20	2.33	4.76	3.33	2.80	3.16
		40	3.66	4.03	2.16	2.50	2.84
130	10	10	2.66	3.44	2.16	3.00	2.40
		20	4.16	3.44	2.50	3.50	3.98
		40	3.33	4.65	2.66	3.00	3.67
130	16	10	2.50	4.82	3.20	4.10	4.50
		20	3.50	5.68	2.80	3.10	4.41
		40	2.16	4.12	3.50	2.80	3.00
145	10	10	2.16	4.48	3.70	2.90	3.14
		20	2.83	5.00	4.10	3.20	3.50
		40	2.16	5.34	4.60	3.33	4.05
145	16	10	2.50	6.55	5.20	3.76	3.22
		20	3.50	4.31	2.90	4.32	4.13
		40	2.16	5.34	3.70	4.22	3.33

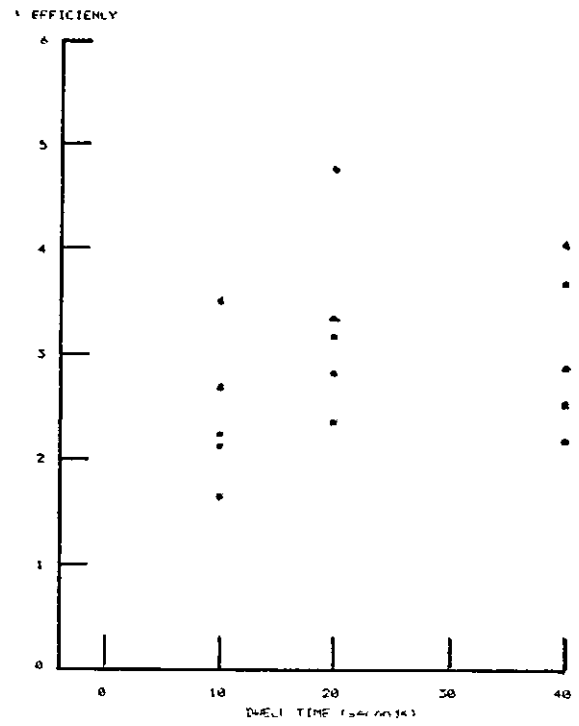
Graphs 6.12-6.17 plot dwell time versus diffraction efficiency for the two embossing pressures for temperatures of 120°, 130° and 145°C. The embossing temperatures were chosen as those best suited for acetate sheet.

Trial Emboss. 120C 10kg/cm<sup>2</sup>



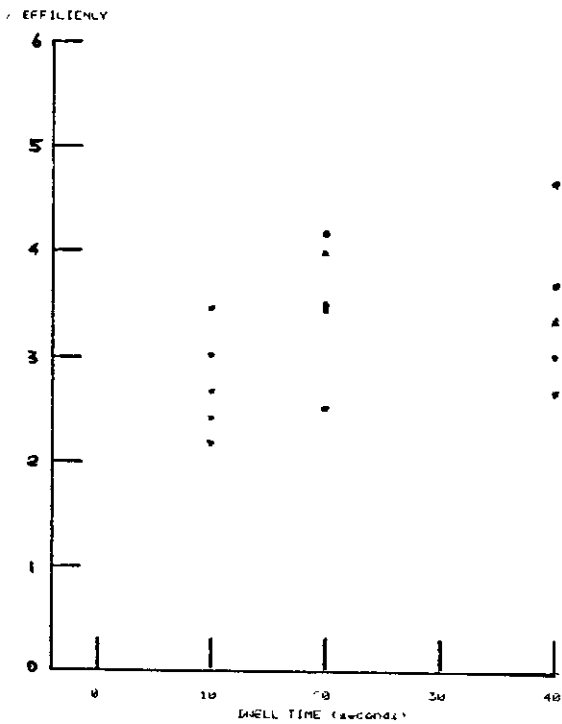
Graph 6.12

Trial Emboss. 120C 16kg/cm<sup>2</sup>



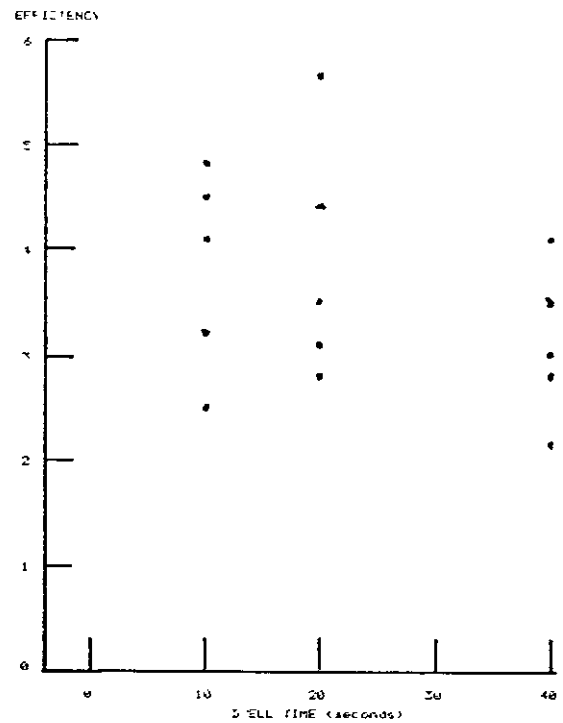
Graph 6.13

Trial Emboss. 130C 10kg/cm<sup>2</sup>



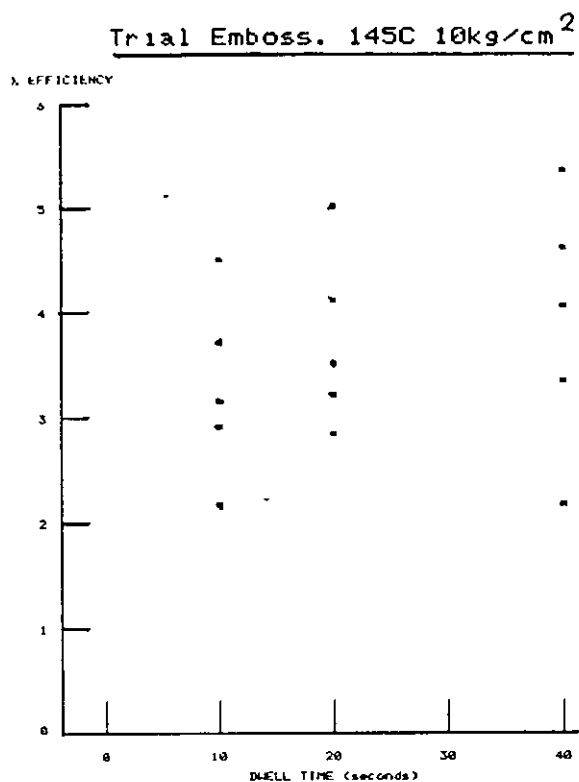
Graph 6.14

Trial emboss. 130C 16kg/cm<sup>2</sup>

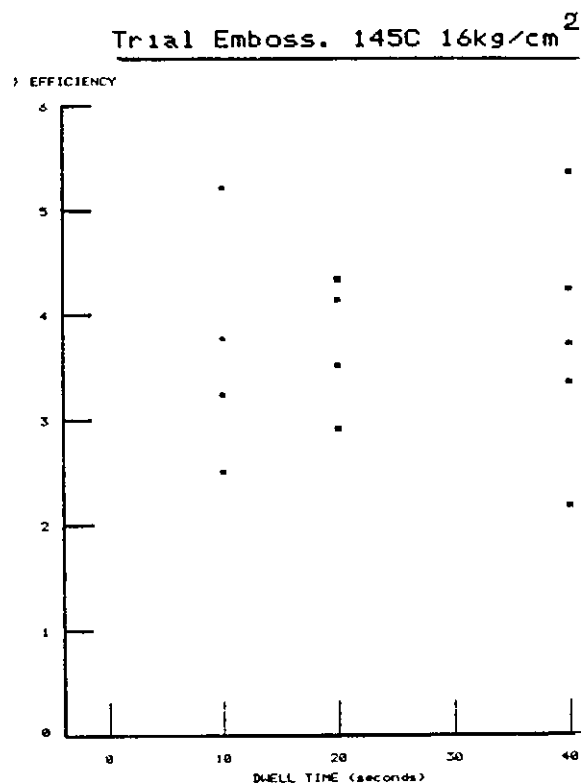


Graph 6.15

Graphs 6.12-6.15 Diffraction Efficiency Versus Dwell Time  
For Different Temperatures and Pressures



Graph 6.16



Graph 6.17

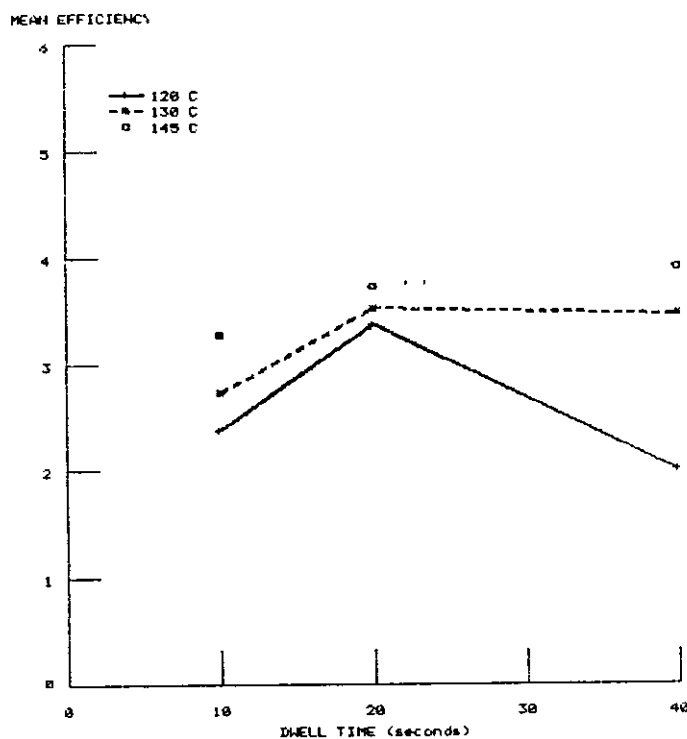
Diffraction Efficiency Versus Dwell Time For Different Embossing Pressures

From the data collected it was possible to combine results to obtain an indication of the optimum embossing conditions. Results in Graph 6.18 show dwell time versus diffraction efficiency for the two pressures over the three temperatures plotted from the data presented below.

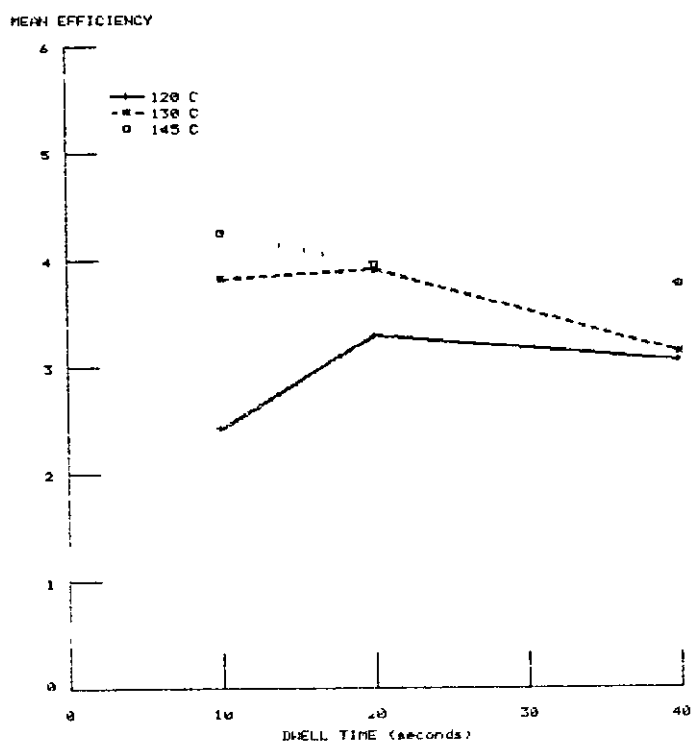
TEMPERATURE	PRESSURE	DWELL TIME	MEAN 1st ORDER	S.D.
$^{\circ}\text{C}$	$\text{kg/cm}^2$	seconds	$\bar{x}$	$\sigma$
120	10	10	2.38	0.45
		20	3.37	0.63
		40	2.00	0.38
120	16	10	2.42	0.63
		20	3.28	0.82
		40	3.04	0.70
130	10	10	2.73	0.45
		20	3.52	0.58
		40	3.46	0.68
130	16	10	3.82	0.86
		20	3.90	1.04
		40	3.12	0.66
145	10	10	3.28	0.78
		20	3.73	0.76
		40	3.90	1.10
145	16	10	4.25	1.45
		20	3.95	0.55
		40	3.75	1.04

After the identification of the optimum embossing conditions for the unit and plastic in use, all embossed results were produced under identical conditions. A number of selective shims were embossed offering a range of groove depths and efficiencies for comparison with metal originals. In this way a quantitative analysis of the accuracy of the embossing process has been possible. Results of these selective shims are presented in Chapter 7. A discussion of the results obtained from the initial trial embossings follows.

# MEAN EFFICIENCY FOR THREE EMBOSSING TEMPERATURES AT 10kg/cm PRESSURE



# MEAN EFFICIENCY FOR THREE EMBOSSING TEMPERATURES AT 16kg/cm PRESSURE



Graph 6.18

#### 6.4 Discussion and Conclusions

The experimental work undertaken attempted to identify suitable plastics and determine variables in the embossing process. Modification to the embosser unit allowed accurate monitoring of temperature, pressure and time during embossing.

Graphs 6.12-6.17 from the embossing trials showed definite trends in the increase of efficiency from 10kg/cm<sup>2</sup> to 16kg/cm<sup>2</sup> applied pressure and from 120°C to 145°C. The high scatter seen in the graphs can be attributed to a number of causes:

- a) Applied pressure; the applied pressure over the metal shims during embossing was achieved by lever action of the embossing unit. Embossing at the higher pressure required full body weight on the unit to achieve desired pressures. This action was difficult to maintain over the longer dwell times and pressure was seen to drop after the initial high pressures to less than the maximum 16kg/cm<sup>2</sup>.
- b) Temperature; the temperature of the metal shim was seen to drop by 5-6°C on contact with the acetate sheet. Consequently an embossing temperature of 130°C would actually be ~125°C over the period of embossing. Raising the temperature of the metal shim to account for this instantaneous loss in temperature allowed an actual embossing temperature of 130°C to be achieved.
- c) Dwell time; the measurement of dwell time was achieved by timing starting on contact of the metal shim with the plastic and ending when the shim was raised from the plastic. On many occasions the acetate sheet stayed adhered to the metal shim when the upper plate was released. This meant that the sheet still experienced heat but no pressure for longer than intended. It is possible that the plastic sheet would continue to stress relieve or flow at this point.

The relationship between dwell time, applied pressure and embossing temperature is a complex one. A point will exist whereby increased temperature will cause the plastic to flow or melt and increased dwell time at higher temperatures would increase the likelihood of this occurrence. For accurate reproductions of detail the plastic must rise above its glass transition temperature (see Appendix 5) and this



temperature must penetrate through the thickness of the plastic to retain the embossed information. If only the upper surface of the plastic receives sufficient heating the embossing will not be recorded to its full depth. Hence the importance of correct pressure and temperature for accurate reproduction.

It is believed that variability in embossed depth occurs as a result of trapped air and stretching as illustrated in Figure 6.19.

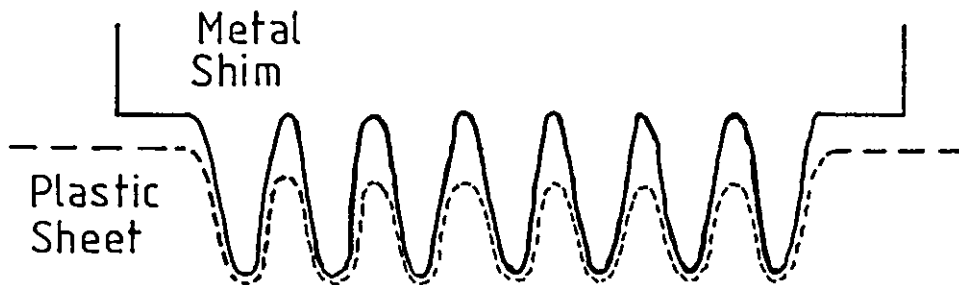


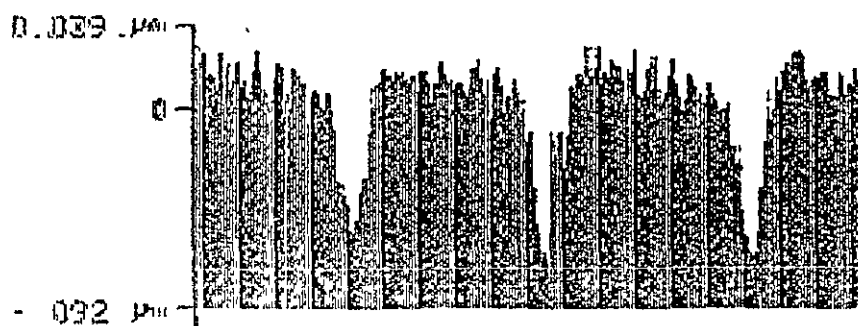
Figure 6.19 Illustration of Inaccuracy of Embossing Process

The summation of the data from the graphs shown in Graph 6.18 illustrated a peak efficiency for the two applied pressures with an upward trend seen toward peak efficiency for a dwell time of 20 seconds in each case. For both applied pressures higher efficiencies have been obtained with increasing embossing temperatures, the peak in each instance being 145°C. Increasing the range of dwell times and

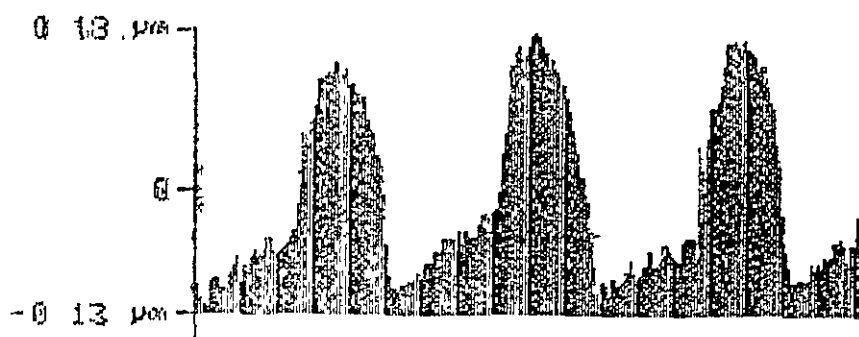
embossing temperatures would have provided more data points but it is believed acceptable that the trend illustrated is accurate.

Results from the embossed shims are shown in the following pages. The Talysurf traces show the profiles for first and second generation metal shims for grating 1b4.

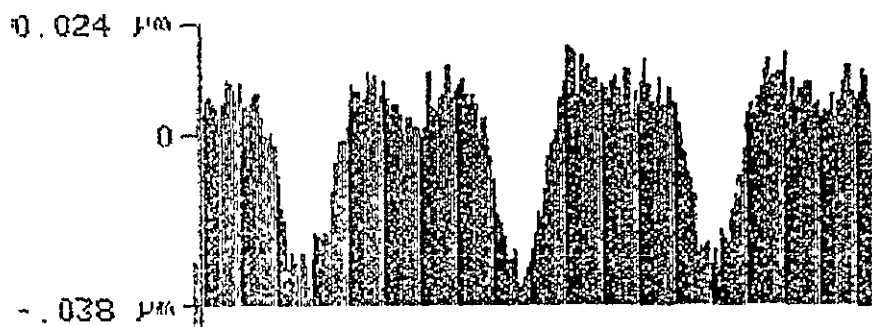
GRATING 1b4



FIRST GENERATION METAL Av. 0.07 $\mu m$



SECOND GENERATION METAL Av. 0.15 $\mu m$



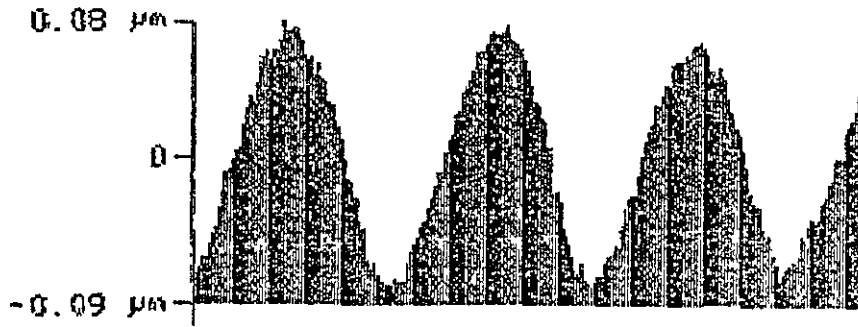
PLASTIC EMBOSSED FROM SECOND GENERATION METAL Av. 0.06 $\mu m$

COMMENTS Grating 1b4. This series shows distorted non-sinusoidal profiles and the diffraction efficiency measurements show high noise, low efficiency as a result of this. The interesting feature of the profiles is the 'mirror-image' type appearance of the traces. The photoresist shows wide bottoms between the peaks which are mirrored in the first generation metal trace showing flat tops to the peaks. The period between the peaks appears sharp and narrow. The second generation metal again shows the mirror image of the first generation metal. The distorted curve now shows sharp narrow peaks with large areas between and this non-flat spacing may account for the apparent increase in groove depth from 0.07 $\mu$ m to 0.15 $\mu$ m (2nd.gen.) This poor quality grating was embossed to illustrate a worst case example.

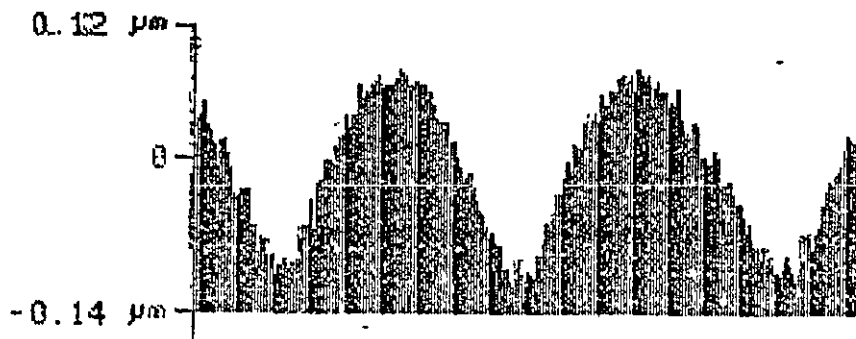
	<u>DEPTH (<math>\mu</math>m)</u>	<u>ZERO / 1st ORDER EFFICIENCY</u>	
Photoresist	0.06	58.3%	5.50%
1st Gen Metal	0.06	47.61%	7.14%
2nd Gen Metal	0.15	31.25%	4.48%
Plastic	0.06	36.45%	2.56%

The resist shows the high zero order associated with the distorted profiles seen in the Talysurf traces. However, the metal shims show lower zero efficiencies arising from the emergence of many higher orders >10. The high number of diffracted orders produced by the grating reduced the available energy available for first and second orders and indicated a non-sinusoid, very inefficient grating.

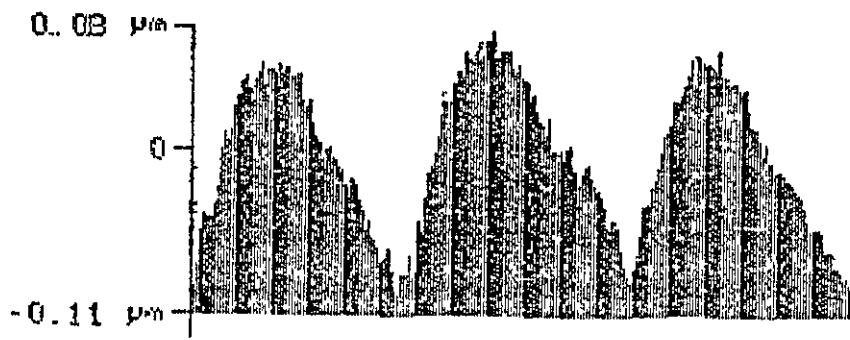
GRATING 1a2



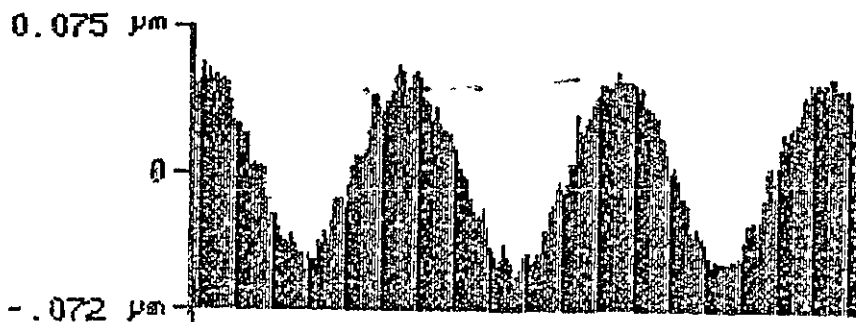
PHOTORESIST Av. peak to trough height 0.15 $\mu\text{m}$



FIRST GENERATION METAL Av. 0.16 $\mu\text{m}$



SECOND GENERATION METAL Av. 0.15 $\mu\text{m}$



PLASTIC, EMBOSSED FROM FIRST GENERATION METAL Av. 0.10 $\mu\text{m}$

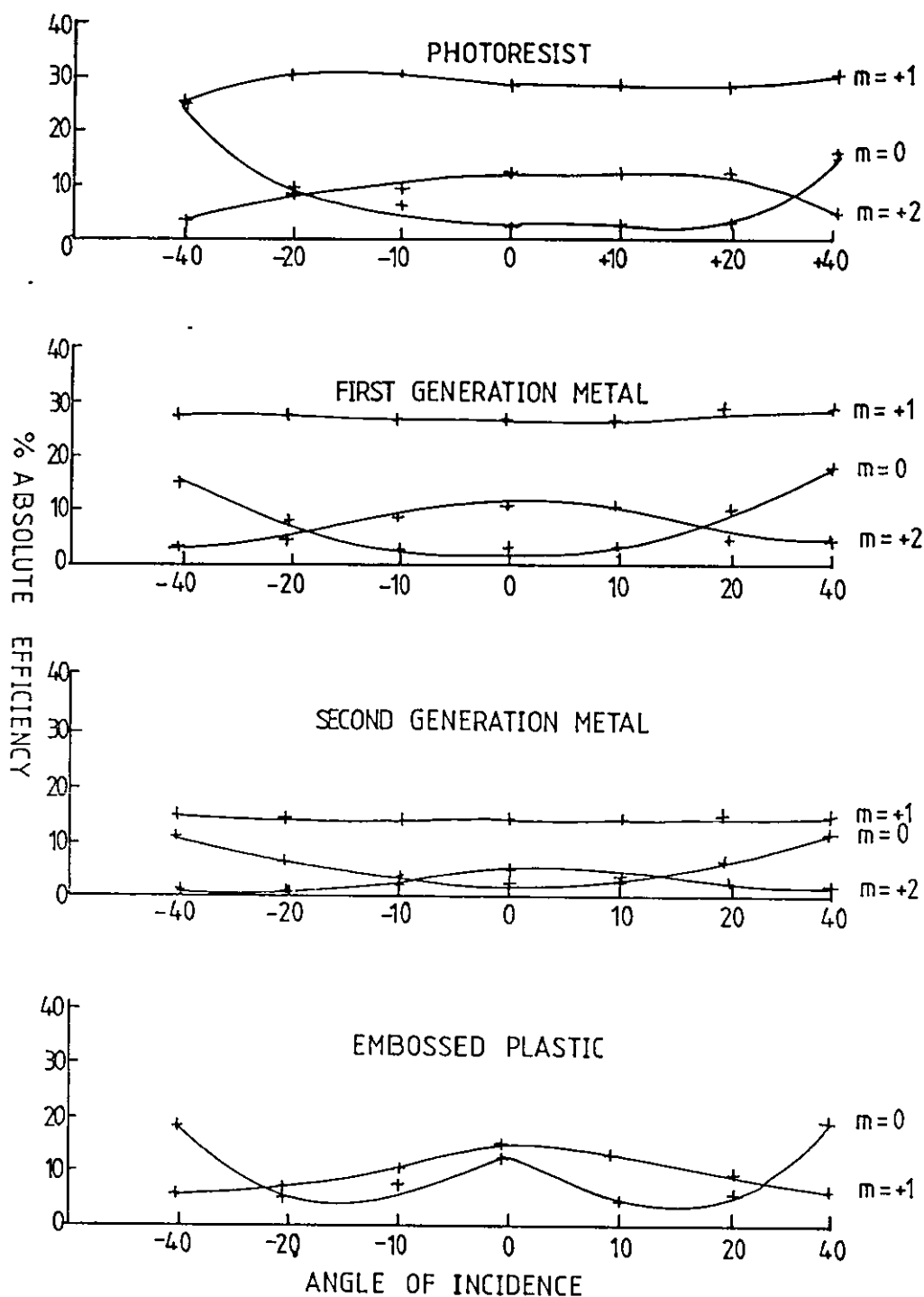
COMMENTS Grating 1a2. This series shows good sinusoidal resist and first metal profiles with a slight increase in groove depth between resist and first metal. (Talysurf accuracy limited to  $\pm 0.02\mu\text{m}$ ).

	DEPTH ( $\mu\text{m}$ )	ZERO / 1st ORDER EFFICIENCY	
Photoresist	0.15	2.50%	28.30%
1st Gen Metal	0.16	2.58%	27.40%
2nd Gen Metal	0.15	3.07%	14.46%
Plastic	0.10	11.35%	13.33%

The profile for second generation metal has distorted away from a true sinusoid so increasing the noise which is seen as diffracted higher orders in the measurement of diffraction efficiency. The plastic grating was embossed from the first generation metal shim and shows good sinusoidal profile. The peak to trough height for each has varied from  $0.16\mu\text{m}$  (1st.gen.metal) to a mean of  $0.10\mu\text{m}$  for the plastic. The first order diffraction efficiency has fallen from 27.4% to 18.3%. The zero order efficiency for the plastic has increased dramatically from 2.58% to 18.0% due to profile reduction away from the optimum depth.

Graph 6.20 shows the variation in diffraction efficiency versus angle of incidence for photoresist, first and second generation metal shims and embossed plastic. The photoresist and first generation metal show excellent correlation between zero and first orders. Comparing resist and second generation figures shows how the first order efficiency has fallen for the second generation shim. The plastic grating was embossed from first generation metal and shows the dramatic increase in zero order efficiency reducing available energy for the more important first and second orders.

Plate 34 shows a photomicrograph of the diffraction grating embossed from the first generation metal shim. The input depth from the shim was  $0.16\mu\text{m}$  consequently the plastic shows very little surface relief measured at  $0.10\mu\text{m}$ . The compares with the embossed image seen in Plate 35 showing an embossed depth of  $0.47\mu\text{m}$  from an input depth of  $0.58\mu\text{m}$  (3b2, first generation metal shim).



Graph 6.20 Variation in Diffraction Efficiency Versus Angle of Incidence for Photoresist, First and Second Metals and Embossed Plastic for Grating 1a2



Plate 34. Photomicrograph of the Surface of Embossed Plastic  
Metal Input  $0.16\mu\text{m}$  - Plastic Groove Depth  $0.10\mu\text{m}$



Plate 35. Photomicrograph of the Surface of Embossed Plastic  
Metal Input  $0.58\mu\text{m}$  - Plastic Groove Depth  $0.47\mu\text{m}$

Details of additional shims embossed into plastic are given in Chapter 7.

Summary Embossing has been described as the final stage in the transfer process under study. The plastic replica of the original photoresist surface pattern is reproduced by application of heat and pressure to a metal stamper in contact with a thermoplastic.

An investigation into a selected number of thermoplastics has been conducted using a hand operated platten embosser. Successful modification to the embosser unit has allowed the accurate measurement of temperature, pressure and time whilst embossing occurred. Conclusions may be summarised;

- Polyester, acetate and polyvinyl-chloride (PVC) materials have been embossed.
- A temperature drop of 5-6°C occurred on contact of the metal shim with the plastic necessitating a higher operating temperature to ensure consistent input temperature into plastic.
- The applied pressure to the metal shim was limited between 10-16kg/cm<sup>2</sup> for the embossing unit available.
- Applied pressure of the embossing unit could not be accurately maintained over long dwell times.
- The relationship between temperature, pressure and dwell time has been investigated by the trial embossing of selected shims.
- Over 200 individual embossings of diffraction gratings have been made to quantify the accuracy and efficiency of embossing as part of the information transfer process.



## CHAPTER 7

### EXPERIMENTAL RESULTS

#### 7.0 Introduction

The information transfer process has been identified as the transfer of a surface relief profiles from a photosensitive recording medium to a metal copy of the pattern, to stamping of the pattern into thermoplastic. This overall scheme is illustrated in Figure 7.1. One unique aspect of this work has been the quantitative analysis of the individual processes involved in the production of embossed elements. The measurement of each stage has facilitated the development of a 'feedback' system to gain the greatest accuracy and efficiency from the process. Results from the research are intended to be applicable to the commercial production of embossed holographic elements and images.

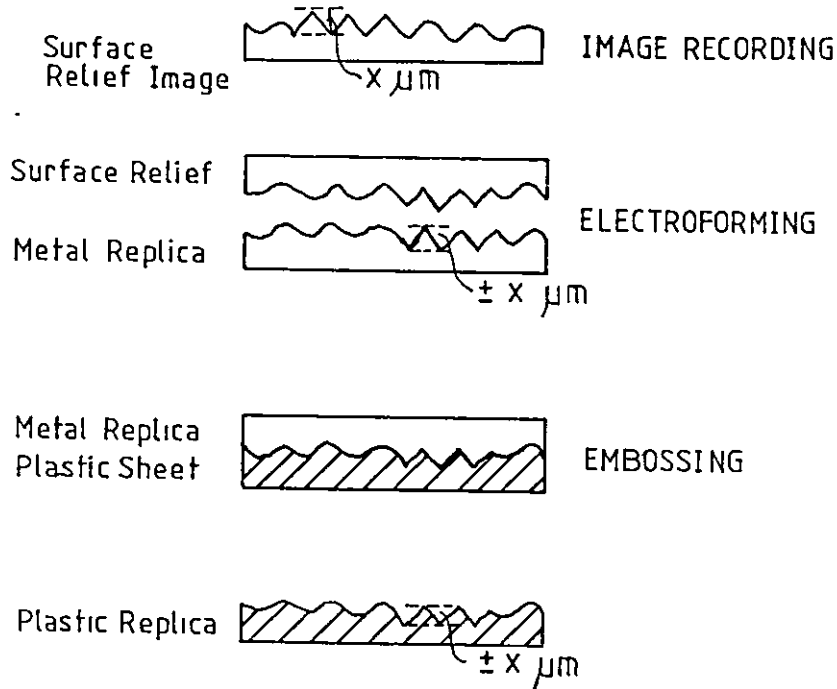


Figure 7.1 Overall Scheme of the Information Transfer Process

### 7.1 Review of the Information Transfer Process

Quantitative analysis of the information transfer process has been possible by the manufacture, study and measurement of diffraction gratings which possessed uniform surface profiles compared to those of holographic images. Two specific features of diffraction gratings were identified, groove depth and diffraction efficiency, that would facilitate accurate measurement of the level of distortion or change that occurred through each stage of the optical and mechanical copying process. Different measurement techniques were utilised; surface finish measurement, scanning electron microscopy, optical interference microscopy and image processing analysis.

The optical recording stage of the information transfer process began with the manufacture of diffraction gratings. Diffraction gratings were recorded into positive working photoresist. Full understanding and characterisation of photoresist properties was achieved by theoretical study and experimentation. Optical arrangements, exposure and development regimes were investigated and refined to produce the optimum quality diffraction gratings with ideal surface relief profiles. Consideration was given to material type, image recording and development in order to achieve reproducible results.

The mechanical copying stages involved electroforming of the surface relief photoresist to produce metal shims. Deposition of an initial conductive layer was necessary prior to the electroforming stage. Comparison between techniques identified vacuum evaporated silver as an ideal option before the metal replicas were produced by electrolytic deposition of nickel. Subsequent re-plating of the nickel shim to create a series of positive and negative metal copies was achieved after passivation of the original surface to allow the new copies to be easily separated. Quantitative analysis of groove depth and diffraction efficiency for original photoresist and subsequent metal copies identified levels of distortion and change.

The final mechanical copying stage of the information transfer process was embossing. Embossing the metal shims into suitable thermoplastics was achieved by modification of a platen embosser designed for small scale hot foil printing. Control over temperature, pressure and embossing time allowed accurate multiple embossings from a selective range of metal shims. The choice of plastics for embossing dictated the operating conditions of the embosser. Choice of two different embossing pressures combined with a range of embossing temperatures and times allowed sufficient experimental data to be acquired. Comparison of plastic groove depths and diffraction efficiencies with those of original photoresist and metal shims illustrated the degree of losses and distortions.

The production of holographic images using the data acquired completed the experimental work undertaken. These images were electroformed and embossed using the same experimental methods and constraints as described in this work.

## 7.2 Experimental Detail

The experimental results presented in the following section will be considered in a number of separate areas.

1. Grating Manufacture. Tabulation of results showing the groove depths for photoresist, first and second generation metal copies and selected embossed plastic. Variation in groove depth between the copying stages is shown.

2. The results from the variation in groove depths for the photoresist to metal and metal to metal copying stages are plotted as plus and minus variations to allow quantitative analysis of the repeatability of the electroforming process.

3. Talysurf profile and depth results are presented for the selected shims used for embossing to quantify the accuracy of the transfer process. The diffraction efficiency curves for the embossed plastic showing the wide variation in embossing are included.

Analysis of the results and calculation of the efficiency of the information transfer process will be found in Chapter 8.

### 7.2.1 Manufacture of Diffraction Gratings

The individual areas of research for optical arrangements, exposure and development times are detailed within the relevant chapters. This section presents the results from the quantitative analysis of the information transfer process for the measurement of selected diffraction gratings. Results are given for the measurement of groove depth and diffraction efficiency for photoresist, first and second generation metal shims and selected plastic embossings in order to determine the accuracy and efficiency of the process.

Results are tabulated below for the exposure and measured groove depths for the series of diffraction gratings produced for the original photoresist, first and second generation metal shims and plastic embossings where given. Groove depth was measured using a Talysurf instrument.

GRATING	E mJ/cm <sup>2</sup>	MEAN GROOVE DEPTH $\mu\text{m}$ ( $\pm 0.02\mu\text{m}$ )				GROOVE DEPTH VARIATION $\mu\text{m}$	
		Resist	1st.Metal	2nd.Metal	Plastic	Resist/ Metal	Metal/ Metal

Series 1

1+4 dev

1a1	3	0.06	0.10	0.07		0.04	-0.03
1a2	6	0.15	0.16	0.15	0.10	0.01	-0.01
1a3	12	0.27	0.40	0.29		0.17	-0.11
1a4	18	0.25	0.32	0.39		0.07	0.07
1b1	24	0.18	0.19	0.19		0.01	0.00
1b2	30	0.10	0.12	0.21		0.02	0.09
1b3	36	0.12	0.08	0.28		-0.04	0.20
1b4	42	0.06	0.07	0.15	0.06*	0.01	0.08

Series 2 1+5 dev

2a1	9	0.04	-		0.05		
2a2	18	0.10	0.13	0.13	0.08	0.03	0.00
2a3	27	0.15	0.16	0.212		0.01	0.05
2a4	36	0.18	0.28	0.23	0.18	0.10	-0.05
2b1	45	0.32	0.55	0.48		0.23	-0.07
2b2	54	0.42	0.51	0.72		0.09	0.21
2b3	63	0.48	0.58	0.79	0.47	0.10	0.21
2b4	72	0.50	0.42	0.80		-0.08	0.38
2c1	81	0.46	0.70	0.73		0.24	0.03
2c2	90	0.54	0.73	0.78		0.19	0.05
2c3	99	0.48	0.72	0.76	0.38	0.14	0.14
2c4	108	0.44	0.60	0.63		0.16	0.03

GRATING	E	MEAN GROOVE DEPTH $\mu\text{m}$ ( $\pm 0.02\mu\text{m}$ )				GROOVE DEPTH VARIATION $\mu\text{m}$		
		mJ/cm <sup>2</sup>	Resist	1st.Metal	2nd.Metal	Plastic	Resist/	Metal/
							Metal	Metal
<u>Series 3</u>								
<u>1+6 dev</u>								
3a1	36		0.05	0.07	0.09		0.02	0.02
3a2	54		0.20	0.27	0.30		0.07	0.03
3a3	72		0.31	0.48	0.29		0.17	-0.19
3a4	81		0.37	-	0.71			
3b1	90		0.47	0.80	0.87		0.33	0.07
3b2	99		0.47	0.63	0.83	0.42	0.16	0.20
3b3	108		0.43	0.47	0.87		0.04	0.40
3b4	126		0.40	0.45	0.79		0.05	0.34

- Sample was damaged before measurement was made.

Shipley Positive working resist, AZ1450B.  $1\mu\text{m}$  thickness.

25 minutes softbake at  $90^{\circ}\text{C}$ .

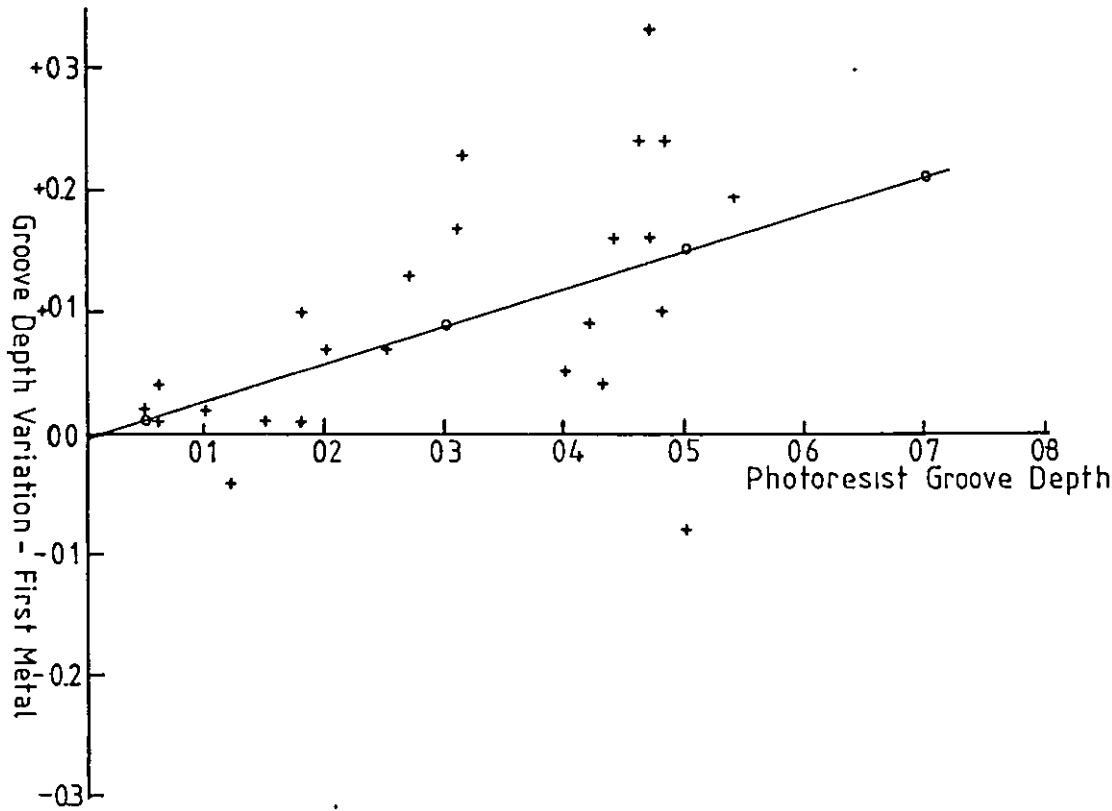
Development; Shipley AZ303, 1 minute at  $20^{\circ}\text{C}$ .

All plastic embossings were made from first generation metal shims with the exception of that marked \*. Shims were embossed at  $145^{\circ}\text{C}$  for 10 seconds dwell times at  $10\text{kg}/\text{cm}^2$  pressure. An average of 40 embossings was made from each metal shim to take account of embossing variables to present a mean value for groove depth.

#### 7.2.2 Variation In Groove Depth from Electroforming Process

The experimental detail for the electroforming of the diffraction gratings has been presented in Chapter 5. The measurement of groove depth and diffraction efficiency for the photoresist and first and second generation metal shims has allowed the efficiency of the transfer to be assessed. Two separate stages are considered; the groove profile variation in photoresist to first generation metal copying and variation in first generation to second generation metal copying.

Graph 7.1 plots the variation in groove depth for the first generation metal shim against the input photoresist groove depth.



Graph 7.1 Variation In Groove Depth Between Photoresist and First Generation Metal Copy

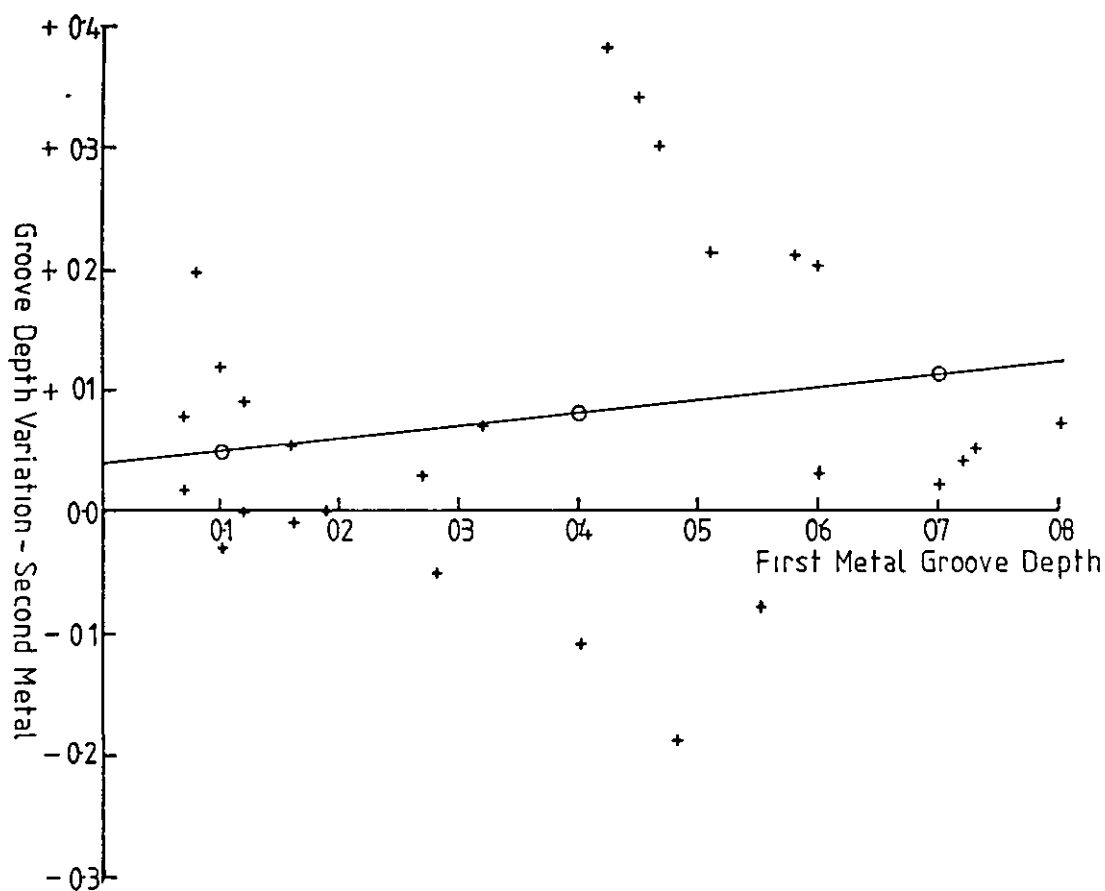
A linear regression has been carried on the data to plot the best line fit which has allowed the variation in groove depth between photoresist and metal to be factored in the determination of the feedback system. It can be seen that variation between resist and first metal groove depths is less at shallow input depths upto  $0.25\mu\text{m}$  than for the large variation in groove depths between  $0.4\text{--}0.5\mu\text{m}$ .

Anomalies appear with the minus groove depth variation seen when the photoresist input of  $0.5\mu\text{m}$  shows a decrease in groove depth of  $0.08\mu\text{m}$ . Conversely, a photoresist input groove depth of  $0.47\mu\text{m}$  has produced an increase in groove depth in metal of  $0.33\mu\text{m}$ .

Graph 7.2 plots the variation in groove depth of the second generation metal shim against the input depth of the first metal shim input. A similar linear regression has been used for the best fit line. The experimental data is used to determine the efficiency of the electroforming process.

The high number of anomalies in this data make the quantitative analysis of the percentage groove depth increase less precise than for the photoresist to first metal electroforming process.





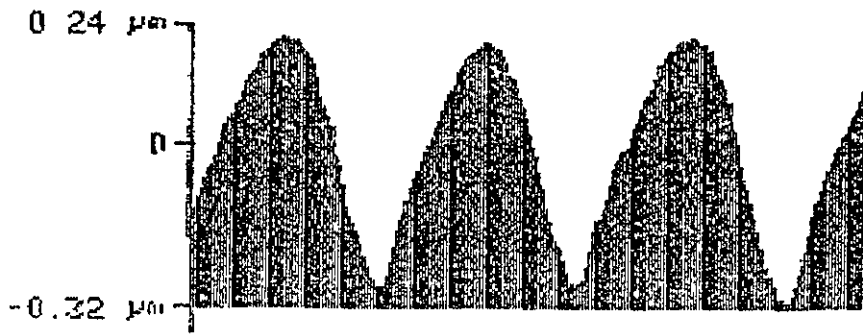
Graph 7.2 Variation in Groove Depth Between First  
and Second Generation Metal Copies

These experimental results are discussed in full in the concluding chapter for the assessment of the efficiency of the information transfer process.

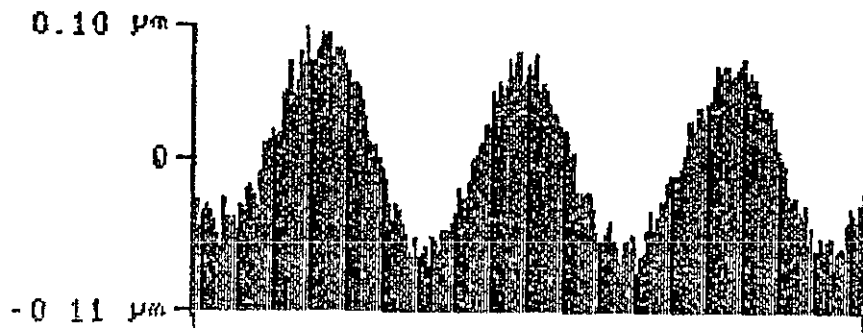
### 7.2.3 Presentation of Selected Embossed Metal Shims

The following Talysurf results are taken from four selected first generation metal shims used for multiple embossings. The Talysurf traces show the grating profile as a plus and minus deviation about a zero axis. Calculation of the grating depth is taken from this axis. The series was chosen to quantify the accuracy of embossing over a range of original input depths. Results are presented as profile traces for each of the photoresist, first and second generation metal shims and the embossed plastic. Over 20 embossings were made from each shim and the mean diffraction efficiency for zero and first orders are presented with the results. Discussion and analysis of the results given in this section will be found in Chapter 8.

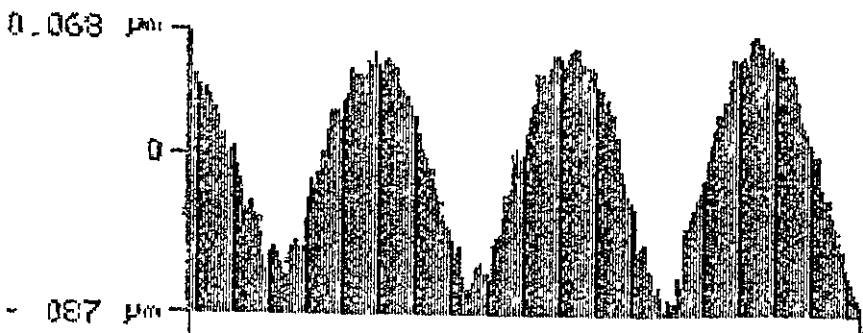
GRATING 2a2



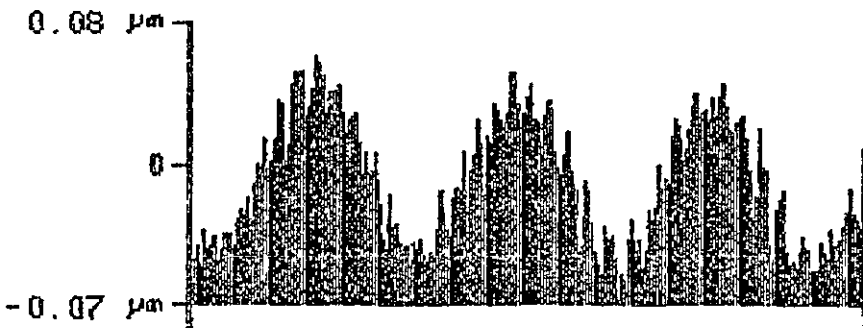
PHOTORESIST Av. peak to trough height 0.10 $\mu\text{m}$



FIRST GENERATION METAL Av. 0.13 $\mu\text{m}$



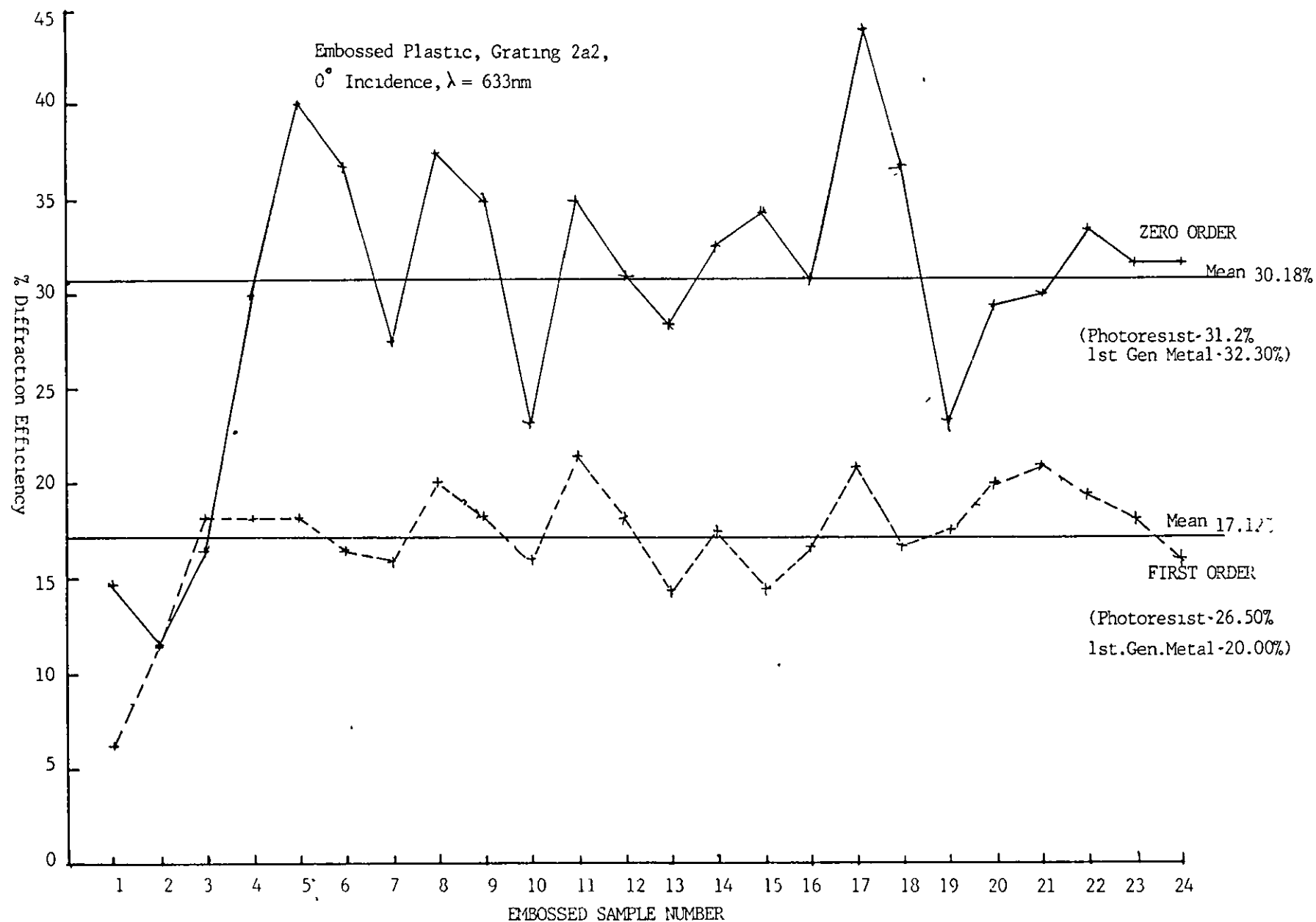
SECOND GENERATION METAL Av. 0.123 $\mu\text{m}$



PLASTIC. EMBOSSED FROM FIRST GENERATION METAL. Av.0.08 $\mu\text{m}$

Prof.7.1. Profile of Grating 2a2, Embossing Family

Graph 7.3 Variation in Diffraction Efficiency for Embossed Plastic Grating, 2a2

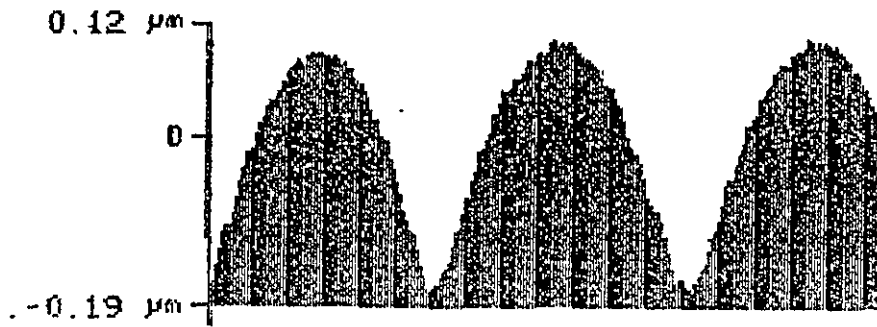


COMMENTS Grating 2a2. This series of traces shows a good sinusoidal resist profile. The trace for the embossed plastic shows spikes superimposed upon the main sinusoid which has distorted the true nature of the profile. This error may have arisen from a damaged surface or from dirt on the Talysurf stylus.

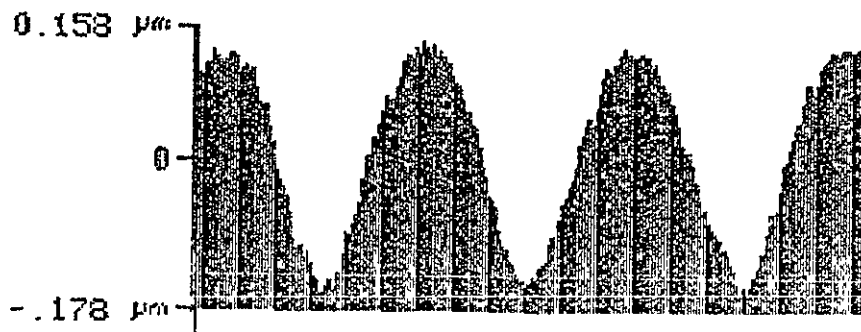
	MEAN	MEAN	
	DEPTH ( $\mu\text{m}$ )	ZERO / 1st ORDER EFFICIENCY	
- Photoresist	0.10	31.20%	26.50%
1st Gen Metal	0.13	32.30%	20.00%
2nd Gen Metal	0.13	20.00%	18.46%
Plastic	0.08	30.18%	17.12%

Graph 7.3 shows the variation in diffraction efficiency for the embossed plastic over the 24 embossed samples. The mean diffraction efficiency for photoresist and first generation metal shim is included on the plot. These results demonstrate the accuracy of information transfer process for gratings of shallow groove depth. The variation in groove depth and diffraction efficiency all lie within experimental measuring limits.

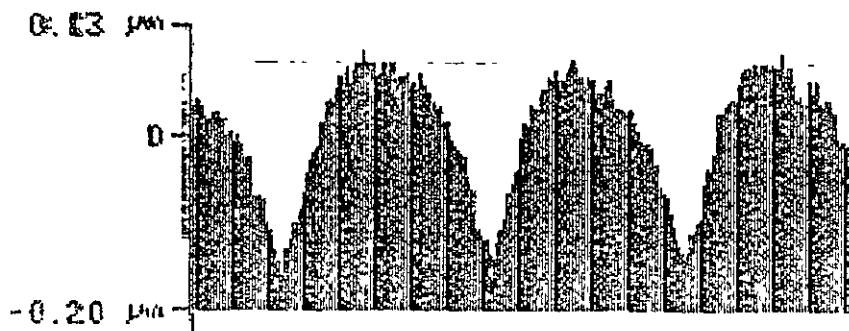
GRATING 2a4



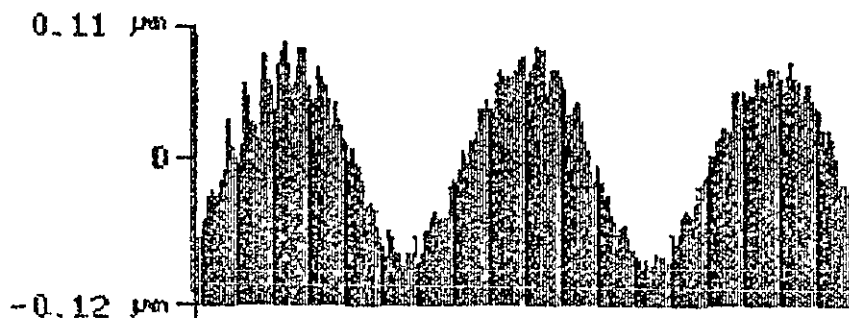
PHOTORESIST Av. peak to trough height  $0.18\ \mu\text{m}$



FIRST GENERATION METAL Av.  $0.28\ \mu\text{m}$



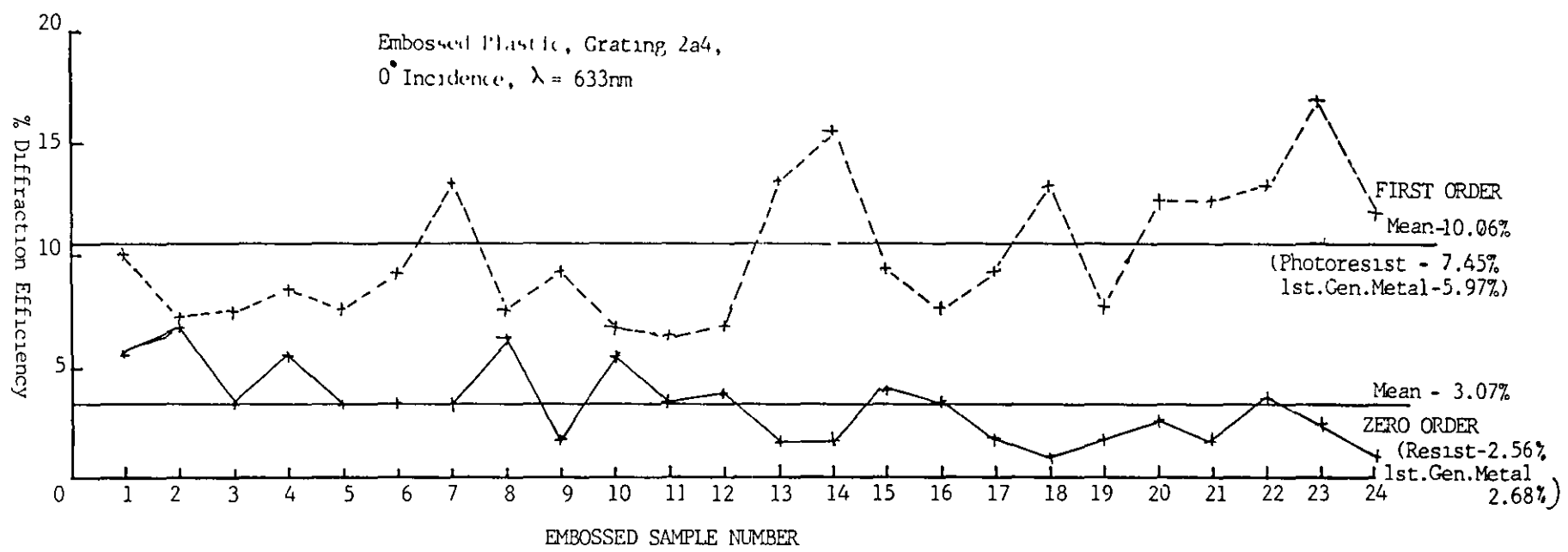
SECOND GENERATION METAL Av.  $0.23\ \mu\text{m}$



PLASTIC EMBOSSED FROM SECOND GENERATION METAL Av.  $0.18\ \mu\text{m}$

Prof.7.2. Profile of Grating, Embossing Family

Graph 7.4 Variation in Diffraction Efficiency for Embossed Plastic Grating, 2a4



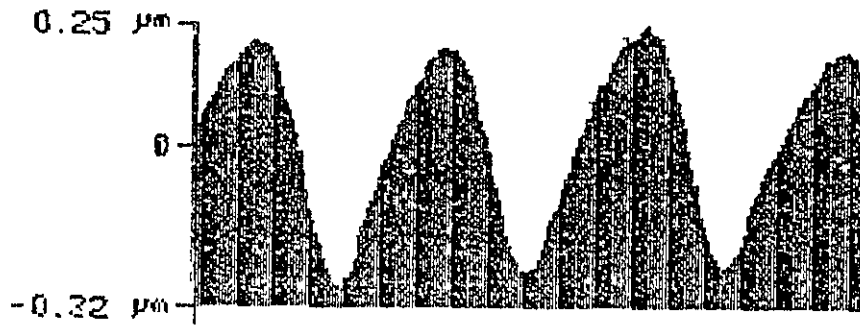
COMMENTS Grating 2a4. This series again shows good sinusoidal profiles. Results are tabulated below:

	MEAN		MEAN
	DEPTH ( $\mu\text{m}$ )	ZERO / 1st ORDER EFFICIENCY	
Photoresist	0.18	2.56%	7.45%
1st Gen Metal	0.28	2.68%	5.97%
2nd Gen Metal	0.23	3.37%	8.30%
Plastic	0.18	3.07%	10.06%

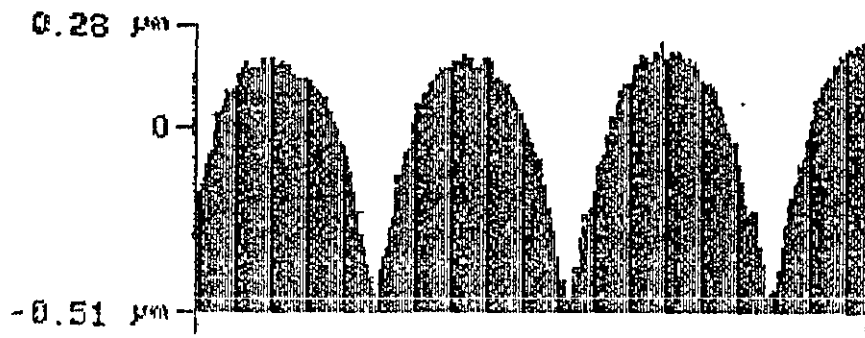
The embossed plastic from the first generation metal shows a groove depth reduction of  $0.10\mu\text{m}$ . It does however show higher zero and first order diffraction efficiencies. This series shows the discrepancy associated with the transfer process since the groove depth between first and second generation metal shims shows a reduction of  $0.05\mu$ . The gratings still produced in excess of seven diffracted orders suggesting the introduction of noise or distortion to the surface. Graph 7.4 plots the variation in diffraction efficiency for the embossed plastic and presents the mean values for photoresist and first generation metal shim.



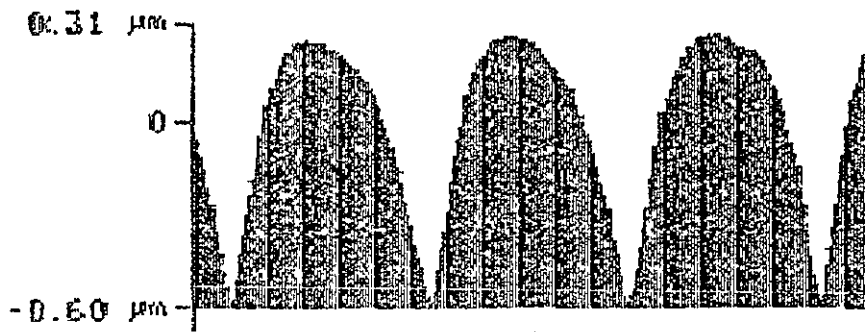
GRATING 2c3



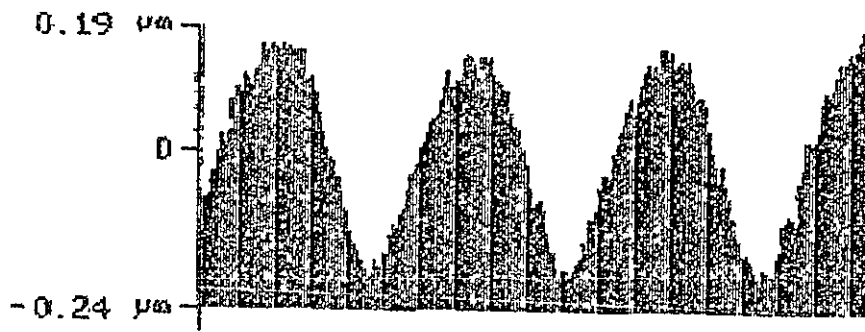
PHOTORESIST Av. peak to trough height 0.48 $\mu\text{m}$



FIRST GENERATION METAL Av. 0.62 $\mu\text{m}$

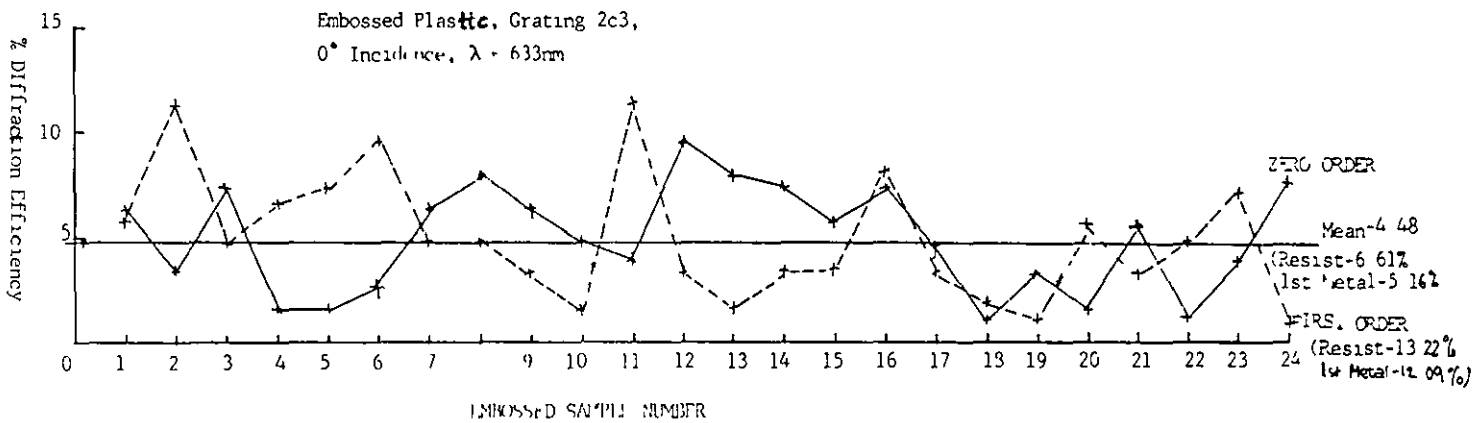


SECOND GENERATION METAL Av. 0.76 $\mu\text{m}$



PLASTIC EMBOSSED FROM SECOND GENERATION METAL Av. 0.38 $\mu\text{m}$

Prof.7.3. Profile of Grating 2c3, Embossing Family



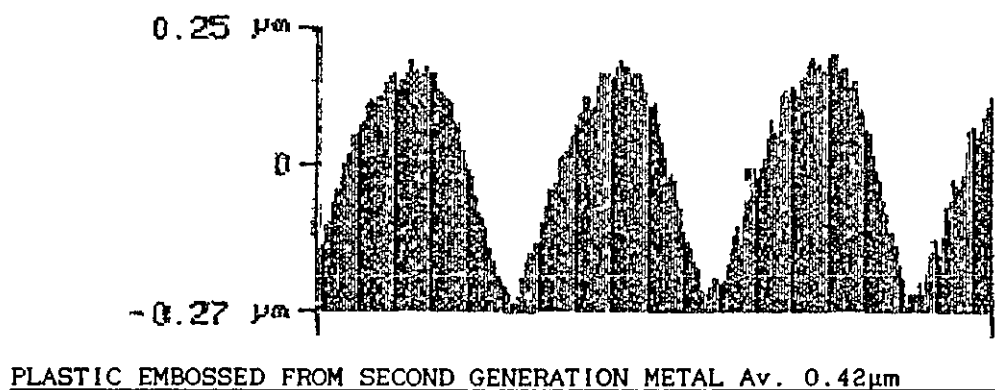
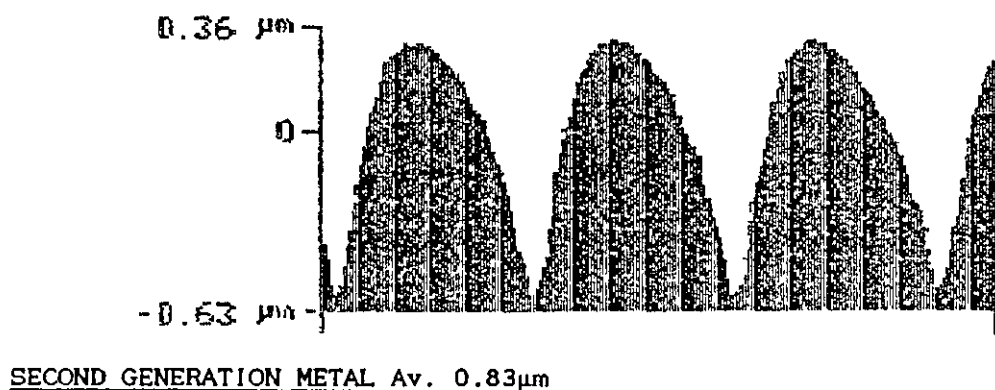
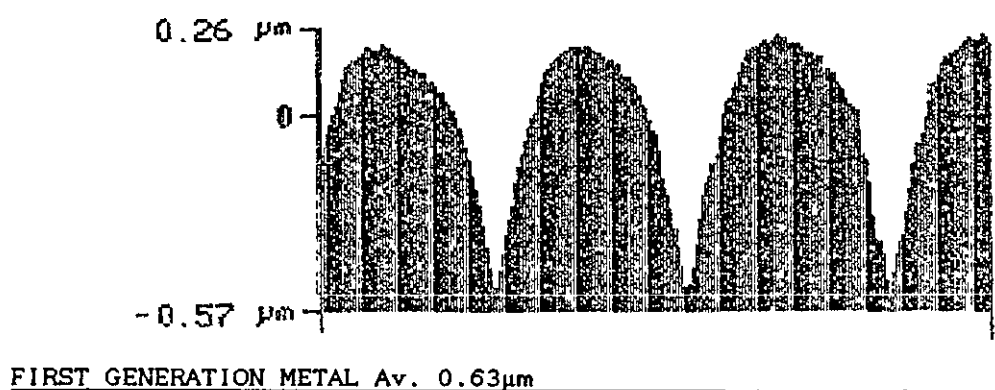
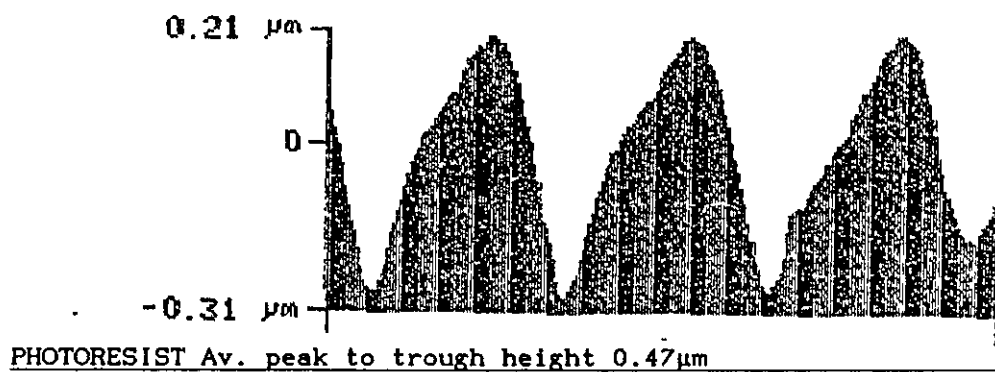
Graph 7.5 Variation in Diffraction Efficiency for  
 Embossed Plastic, Grating 2c3

COMMENTS Grating 2c3. This series of profiles shows more rounded peaks than have been presented before. The sharp troughs show a distortion away from sinusoidal form. The results obtained as are follows:

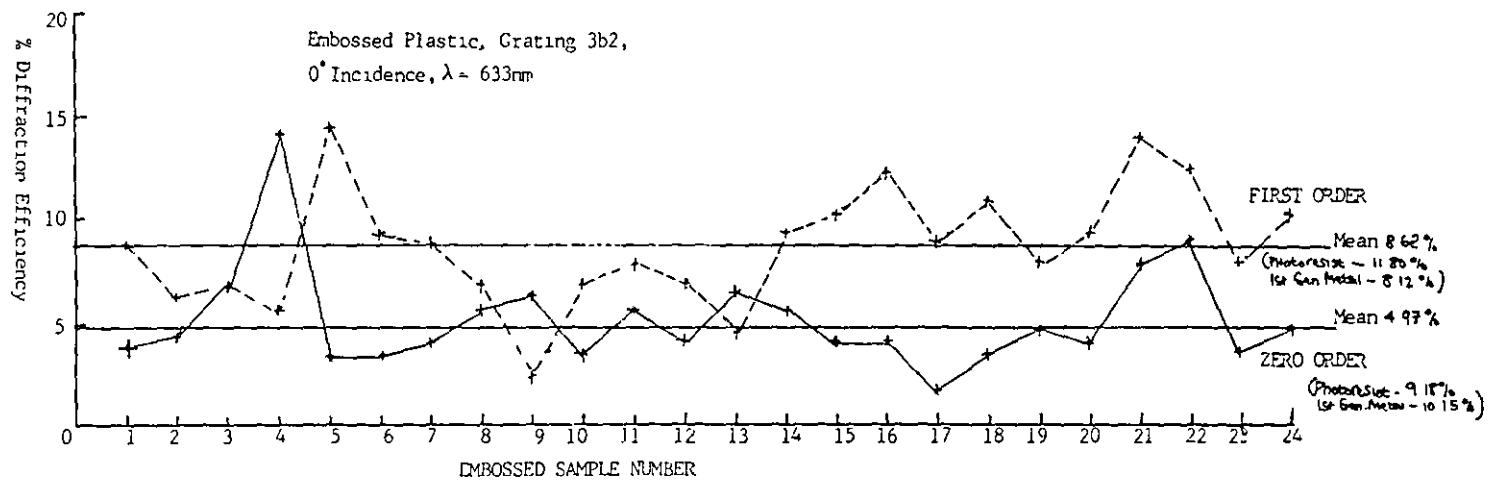
	MEAN	MEAN	
	DEPTH ( $\mu\text{m}$ )	ZERO / 1st ORDER EFFICIENCY	
Photoresist	0.48	6.61%	13.22%
- 1st Gen Metal	0.62	5.16%	12.09%
2nd Gen Metal	0.76	2.81%	8.12%
Plastic	0.38	4.48%	4.89%

The embossed plastic samples were taken from the first generation metal and have only reproduced half the input depth. The inaccuracy of reproducing metal shims from deep groove depths is becoming evident with an increase of 0.14 $\mu\text{m}$  groove depth between photoresist and first generation metal. The first order diffraction efficiency has consequently fallen to one third that of the metal shim indicating distortion and noise and the introduction of higher diffraction orders. Graph 7.5 plots the variation in diffraction efficiency for the embossed plastic and shows the mean efficiency for the photoresist and first generation metal.

GRATING 3b2



Graph 7.6 Variation in Diffraction Efficiency for Embossed Plastic, Grating 3b2



COMMENTS Grating 3b2. This series shows the form of a slanted sinusoidal profile. The peaks of the profiles have distorted and this profile is mirrored through the photoresist and metal copying stages. The plastic samples were embossed from the first generation metal shim and does not share this distorted profile but presents an almost true sinusoid form. Results are tabulated below:

	MEAN	MEAN	
	DEPTH ( $\mu\text{m}$ )	ZERO / 1st ORDER EFFICIENCY	
Photoresist	0.47	9.18%	11.80%
1st Gen Metal	0.63	10.15%	8.12%
2nd Gen Metal	0.83	5.93%	6.25%
Plastic	0.42	4.97%	8.62%

The embossed plastic shows a loss of groove depth of  $0.21\mu\text{m}$  from the input of the first generation metal shim. The first order diffraction efficiency has remained high but the zero order has halved compared to that of its metal counterpart. The variation in first order diffraction efficiency for the embossed plastic samples is shown in Graph 7.6.

### 7.3 Summary

This concludes the presentation of experimental work and results. A selective number of results have been given from those produced during the course of this study. The examples have shown the necessary desired features such as good sinusoidal profiles, distorted profiles, deep and shallow groove depths through the entire information transfer process. Results not presented simply replicate the various profiles and have been used to establish confidence in the process and identify any anomalies.

This chapter has shown the visual differences between groove profile for photoresist, metal and plastic diffraction gratings in the form of Talysurf outputs. Variation in diffraction efficiency has been tabulated and plotted and an analysis of the accuracy and efficiency of the information transfer process is presented in Chapter 8.

## CHAPTER 8

### DISCUSSION AND CONCLUSIONS

#### 8.0 Introduction

This concluding chapter will discuss the experimental results obtained in the study of the information transfer process. The objective of the research has been to quantify the accuracy and efficiency of the overall process in the production of embossed elements. The research is considered unique in this approach. No quantitative data has previously been available that relates the initial input profile in photoresist to the output profile in embossed plastic. Initially groove depth had been considered the only important transfer parameter. It now appears that to fully determine the transfer process the diffraction efficiency and groove depth must be considered together. The diffraction efficiency can act as an indication of noise in the system as well as signal strength. Measurement of these features has permitted the development of a 'feedback' system to optimise the overall information transfer efficiency of the optical and mechanical copying stages.

The development of a feedback system dictates that the groove depth necessary in photoresist to produce the final required groove depth in plastic can only be calculated once the accuracy and efficiency of the transfer process has been quantified. In this way the initial groove depth in photoresist is correctly factored by the actual groove depths that occur through the copying stages.

The discussion and conclusions will centre on two major aspects of the information transfer process that have introduced distortions and inefficiency to the process. These are; the Electroforming and Embossing stages.

#### 8.1 Accuracy of Electroforming

The electroforming process has been described in Chapter 5. The photoresist diffraction gratings were electroformed by electrolytic

nickel deposition to produce durable metal replicas that could be used for embossing. The first copy of the photoresist produces a first generation metal shim. These shims were re-plated by electrolytic nickel deposition to produce second generation shims. There is no limit to how many times this copying process can occur and third and four generation shims may be used for large scale roller embossing. The production of metal shims by electroforming has occurred in two stages:

- photoresist to first generation metal copy,
- first generation metal copy to second generation metal copy.

As can be seen from Graph 7.1 for the transfer between photoresist and first generation metal and Graphs 7.2 for the transfer between first and second generation metal the information transfer accuracy is not identical for both processes.

These graphs were plotted using a linear regression fit assuming the general form,  $y = A + Bx$ . B describes the slope and A describes the intercept value. The calculation of regression of y on x yields an average value of y being scattered on either side. A level of confidence of this fit can be obtained by considering the standard deviation of the data values relative to the calculated regression.

Calculated values for Graph 7.1 and 7.2 respectively;

$A = 9.44 \times 10^{-4}$ ,  $B = 0.306$ ,  $x\sigma_n = 0.16$ ,  $y\sigma_n = 0.09$ .

$A = 0.042$ ,  $B = 0.105$ ,  $x\sigma_n = 0.22$ ,  $y\sigma_n = 0.141$ .

#### 8.1.1 Photoresist To First Generation Metal Copy

The scatter and standard deviation of the photoresist to first generation metal electroforming process (Graph 7.1) indicates good correlation suggesting control of the plating to be satisfactory. The slope indicates that with increasing input profile depth the process will further increase the groove depth.



One explanation for this would be preferential deposition of the initial conductive layer of evaporated silver. The effect of preferential deposition upon gratings over a range of depth to pitch ratios would lead to a relative variation in plated groove across the grating or hologram, ie. the higher frequency components of a holographic element would not receive the same increase in groove depth as the lower frequency information. If this assumption were applied to the white light 'rainbow' hologram it would imply that the final embossed high frequency terms would be reduced (assuming the rest of the process to be near linear) with a loss of high frequency information. High frequency information is responsible for perception of image depth in holograms. A low resolution silver halide emulsion (eg. Agfa 10E56) can transfer information with a narrow angle of view compared to that recorded on high resolution emulsion (eg. Agfa 8E56) which can transfer a greater angle of view with increased image depth. Limited image depth has always been associated with embossed holograms,  $\approx 1-2"$  compared to the depth of  $10-12"$  for silver halide materials.

#### 8.1.2 First Generation to Second Generation Metal Copy

The subsequent re-plating of the first metal copy (Graph 7.2) shows a higher scatter and standard deviation than for the photoresist to metal stage. The slope of the graph suggest the alteration to the input groove depth is not as great as for the photoresist to metal transfer. The higher deviation merits consideration and two aspects may be introduced; i) oxidation of the front silver face of the first generation metal shim prior to re-plating and ii) an inhomogenous passivation layer on the front face of the initial metal shim.

The metal to metal electroformed was undertaken on individual diffraction gratings over a period of time. Whilst all initial electroforms were stored in a dessicator and soak cleaned in detergent prior to second generation plating, the period between first and second generation plating varied from days to weeks. This was not deemed important at the time although there is the possibility that oxidation of the front silver face of the first metal shim could have a minor influence on the accuracy of the second generation plating process.

Prior to second generation electroforming a uniform parting layer must be applied to the front surface of the first metal shim to prevent permanent adhesion of the second plating. The technique of chemical passivation described in Chapter 5 relied upon producing a uniform oxide layer of dichromate across the surface. This is the essential difference between the first and second generation electroforming processes. The composition and operating conditions of the electroforming tanks was identical for every metal shim produced. Variability in passivation of the front metal surface is regarded as having contributed to the large deviation seen in the results. This conclusion has implications for embossing operations that use second, third and even fourth generation metal shims on embossing rollers.

#### 8.1.3 Diffraction Efficiency Versus Groove Depth

The changes in groove depth between photoresist and the first generation metal copy have affected the diffraction efficiency of the gratings. Distortion away from sinusoidal profiles introduce noise terms and higher diffracted orders that reduce available energy for first order diffraction. The measuring regime for diffraction efficiency used a He-Ne laser of wavelength  $0.633\mu\text{m}$ . Assuming constructive interference for a reflected light measuring system, peak efficiency would appear at  $\lambda/4$  phase shifts as illustrated in Figure 8.1. This highlights the peak efficiencies occurring at groove depths of  $0.16\mu\text{m}$ ,  $0.47\mu\text{m}$ ,  $0.79\mu\text{m}$  etc.

The introduction of noise and distortion into the copied profiles alters the function to that seen in Figure 8.2. Diffraction efficiency is reduced as groove depth increases due to variability in the electroforming process. Experimental verification of this has been illustrated in Graphs 4.8, 5.9 and 5.10 which plotted diffraction versus groove depth for photoresist, first and second generation metal shims.

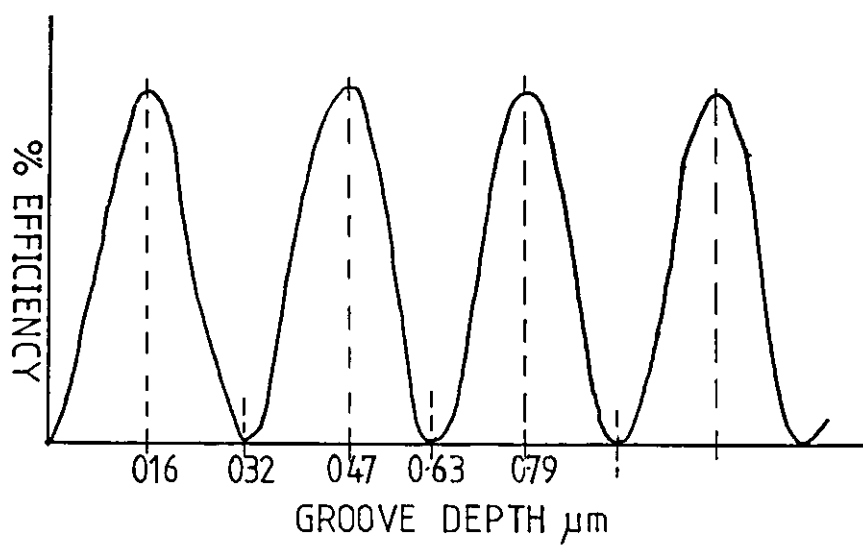


Figure 8.1 Idealised Function of Diffraction  
Efficiency Versus Groove Depth

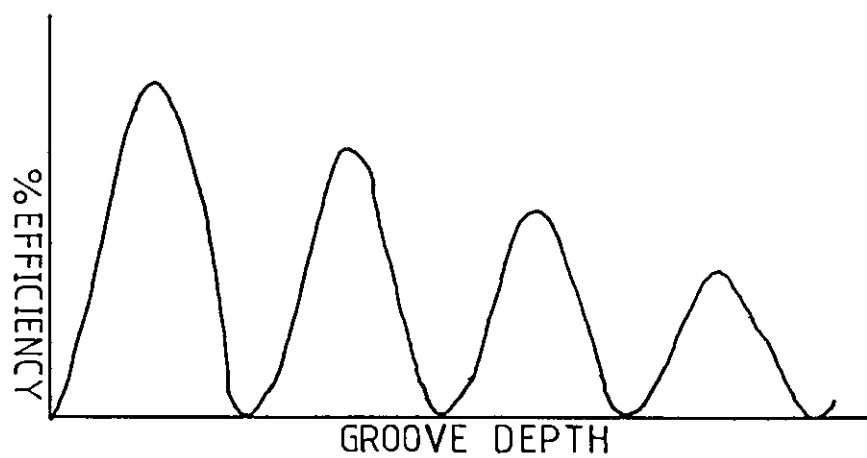


Figure 8.2 General Form of the Experimental Diffraction  
Efficiency Versus Groove Depth

## 8.2 Accuracy of Embossing

The embossing process has been described in Chapter 6 and detailed the modification to a hand operated platen embosser. Results for the determination of the accuracy of embossing have been taken by the selective embossing of a number of first generation metal shims as detailed in Chapter 7. The first generation shims have been used for comparison with the original photoresist groove depths and diffraction efficiencies.

To ensure a useful range of results over 24 embossings were made from each metal shim for measurement of groove depth and diffraction efficiency. The plots showing the variation in diffraction efficiency for the selected embossed shims have been shown in Chapter 7.

### 8.2.1 Variation In Groove Depth

The results from measurement of the embossed plastic gratings are tabulated in Table D.

TABLE D. Percentage Transfer for Embossing Efficiency

GRATING NUMBER	METAL INPUT $\mu\text{m}$	PLASTIC OUTPUT $\mu\text{m}$	PERCENTAGE TRANSFER
2a2	0.13	0.08	61.5%
2a4	0.28	0.18	64.28%
2c3	0.62	0.38	61.29%
3b2	0.63	0.42	66.66%

This percentage transfer value gives an indication of the transfer depth of the embossing process only.

The percentage figures for the embossing into acetate sheet from the first generation metal shim show mean values of ~ 63% over a range of input depths (0.13-0.63 $\mu\text{m}$ ). It is surprising that this transfer depth efficiency remains consistent irrespective of the range of input

depths. It was expected that shallow profiles would transfer more completely than would deeper groove depths.

The overall embossed transfer efficiency allows calculation of the required groove depth in metal that would be necessary to achieve a desired groove depth in plastic. For example;

A groove depth in plastic of  $0.16\mu\text{m}$  is required to optimise peak efficiency. See Figure 8.1. What first metal groove depth would be necessary for this optimal embossing assuming a percentage transfer of ~ 63% ?

If  $d$  is the metal depth required,  $d \times 63\% = 0.16\mu\text{m}$

$$\therefore d = \frac{0.16}{0.63}$$

$$\therefore \text{Required depth in metal shim} = 0.25\mu\text{m}$$

This figure is confirmed from the experimental result of embossed grating number 2a4. An input metal groove depth of  $0.28\mu\text{m}$  yielded an embossed depth of  $0.18\mu\text{m}$ . The measuring accuracy of the Talysurf instrument was  $\pm 0.02\mu\text{m}$  so these figures lie within experimental error.

It is possible therefore with a priori knowledge of the illuminating wavelength of the diffraction efficiency measuring system to plot optical diffraction efficiency against groove depth to determine the required plastic profile. Factoring of this profile by the embossing transfer function can determine the required metal shim depth.

### 8.2.2 Diffraction Efficiency Versus Groove Depth

It has been described how distortion of groove depth affects the diffraction efficiency of first generation metal shim and embossed plastic from that of the original photoresist efficiency. The results in Table E show the first order diffraction efficiency for photoresist, metal and embossed plastic from the four metal shims used for the embossing trials. (See Section 7.2.3 of Chapter 7).

TABLE E. % Diffraction Efficiency Transfer for Embossed Shims

% Diffraction Efficiency (1st Order)				% Transfer	
Grating	Resist	Metal	Plastic	Resist/Metal	Metal/Plastic
1	2	3	4	5	6
2a2	26.50%	20.00%	17.12%	-24.5%	-14.4%
2a4	8.00%	7.50%	10.06%	- 6.3%	+34.0%
2c3	13.22%	12.07%	4.89%	- 8.7%	-59.5%
3b2	11.80%	8.12%	8.62%	-31.8%	+ 6.2%

KEY: Column 1 - Grating sample number.

Column 2,3,4 Measured diffraction efficiency, 1st Order.

Column 5 - Change in efficiency between columns 2 and 3

Resist % - Metal %

Resist %                      x 100%

Column 6 - Change in efficiency between columns 3 and 4

Metal % - Plastic %

Metal %                      x 100%

The change in the figures for the percentage transfer from resist to metal and metal to plastic may be explained by considering Figure 8.1 which shows the function of diffraction efficiency versus groove depth for perfect transfer profiles.

The figures for grating 2a4 show that for metal to plastic transfer an increase efficiency of 34% has occurred. The input depth of the metal was 0.28 $\mu$ m which represents a low point in the curve above. The embossed plastic showed a depth of 0.18 $\mu$ m taking the efficiency back to the peak of the curve. From this it would appear that an increase in diffraction efficiency has been achieved despite embossing ~ 63% of the metal input.

Consider grating 3b2. The groove depth in photoresist was 0.47 $\mu$ m indicating a peak on the efficiency versus groove depth curve. The metal copy increased the groove depth to 0.63 $\mu$ m, moving off the peak

efficiency curve reducing the measured diffraction efficiency by 32%. Embossing the metal shim gave a groove depth in plastic of  $0.42\mu\text{m}$  moving the efficiency back up the curve. This is confirmed experimentally by an increase in diffraction efficiency of 6%.

These results illustrate that with an embossing transfer of ~63% of the input information an apparent increase in diffraction efficiency can result. In practice the distortions and noise introduced into the gratings through the copying process would reduce the quality of the surface profile.

The information transfer process has been studied and quantified by the measurement of diffraction gratings. The uniform surface profile of gratings offer a model of the transfer process for holographic images. The 'feedback' system developed through this work by the quantitative analysis of the electroforming and embossing processes allows the information transfer process to be illustrated as in Figure 8.3

The desired groove depth and efficiency of the embossed element should be calculated prior to exposure in photoresist. The desired groove depth can be achieved by optimised exposure and development sequences. Calculation of the required groove depth in photoresist could be made by reference to Graph 8.2 which indicates the optimum embossed depth for  $\lambda=633\text{nm}$  to be  $0.16\mu\text{m}$  groove depth.

Assuming the embossing is made from the second generation metal shim;

1. An embossed groove depth  
in plastic of ..... $0.16\mu\text{m}$
2. Would require a second  
generation metal shim depth of ..... $0.25\mu\text{m}$  assuming a 63%  
transfer efficiency
3. Which would require a first  
generation metal shim depth of ..... $0.19\mu\text{m}$
4. Which would require a  
groove depth in photoresist of ..... $0.15\mu\text{m}$

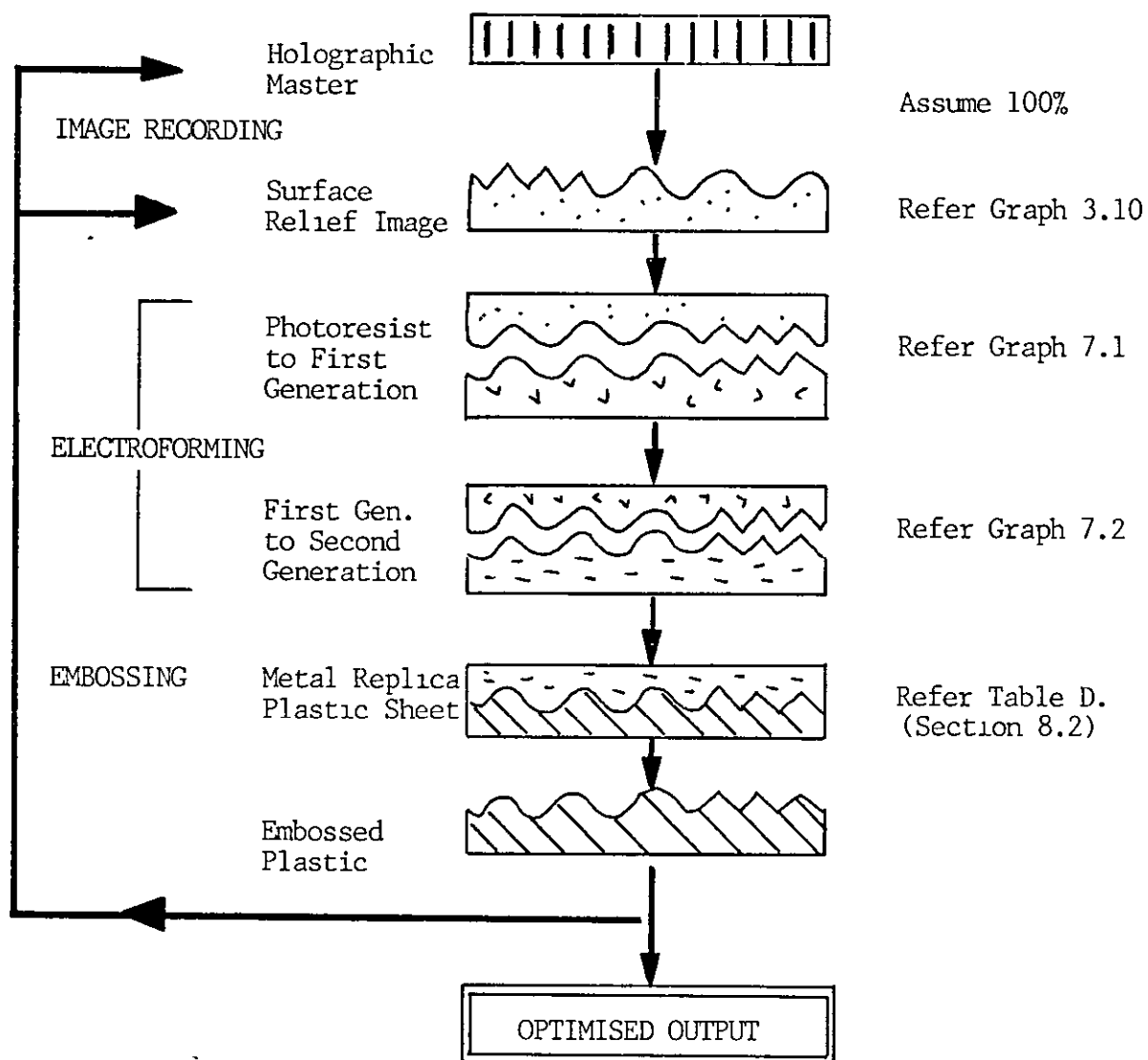


Figure 8.3 The Development of a Feedback System for the Determination of Optimum Groove Depths for Maximum Embossed Efficiency.



For embossing from third or fourth generation shims similar factoring of the groove depth would be necessary.

For the experimental results achieved by the embossing of the first generation shim similar calculations can be made by reference to Graphs 4.8 and 7.1.

1. An embossed groove depth  
in plastic of .....0.16 $\mu$ m
2. Would require a first  
generation metal shim depth of .....0.25 $\mu$ m
3. Which would require a  
groove depth in photoresist of .....0.195 $\mu$ m
4. Which by reference to  
Graph 3.10 for a 1+5 developer  
dilution would require an  
exposure E of .....23mJ/cm<sup>2</sup>

It is felt that the objective of this research has been met in assessing the information transfer process for accuracy and efficiency. Whilst many questions have been answered in the pursuit of this objective still more have been raised that could not be answered during this research. These areas are briefly discussed in the Further Work Section that follows.

In-line assessment of the quality of images used for embossed holograms could be developed by the inclusion of a diffraction grating on the original master plate in photoresist. Quantitative assessment of the accuracy of the transfer process would be possible by measurement of grating profile. A distortion of the grating would indicate distortion to the holographic profile. This technique could be applied in the same way as photographic test strips used in development tanks. Operational controls for the acceptable level of distortion could be established and would highlight changes in the transfer process before a poor result is produced at the final stage of embossing.

### 8.3 Further Work

In assessing the information transfer function it has become clear that the largest area for further work is that of electroforming. However, future work would also seek to study the following areas;

1. An improvement in the application of photoresist by spinner. A spinner unit to allow larger format substrates to be coated would be advantageous. Re-design of the existing spinner for higher speeds with controlled ramp features would be necessary and desirable.
2. The refinement of photoresist processing techniques using spray development would be useful to improve processing repeatability and uniformity.
3. The development of image processing techniques for profile assessment incorporating whole field, non-contacting phase stepping fringe analysis techniques. Inclusion of these techniques with multiple beam interference microscopy could provide whole field quantitative surface analysis.
4. Investigation into alternative techniques and materials for the deposition of the initial conductive layer in electroforming. Quantitative analysis of the surface profiles using various techniques should be made.
5. Alternative passivation techniques and formulations should be sought to identify the variables seen in metal to metal electroforming. Study of the nature of the passivating oxide layer by whole field interferometric techniques before and after passivation would highlight changes in surface profile.
6. Refinements to the plating tanks and cathode fixings in the electroforming process could improve the repeatability of plating.
7. Investigation into roller embossing techniques and the comparison with platen embossing efficiency should be undertaken. A wider range of embossing materials should be sought to extend the research area.

This concludes the final chapter of this thesis. The references and appendices will be found in the following pages.

## REFERENCES

- [1] JARREL,R.F                      Grating Manufacture; New Advances in Grating Ruling and Replication.  
Appl.Opt.3,(11),p1258,1964
- [2] GOLDBERG,B                      Electroformed Precision Optics.  
J.Opt.Soc.Am.38,(4),p409,1948
- [3] DEW,G                              On Preparing Plastic Copies of Diffraction Gratings: An extension to the Merton NPL Process.                      J.Sci.Instrum.33,p348,1956
- [4] LEITH,E  
    UPATNIEKS,J                      Wavefront Reconstruction with Continuous-Tone Objects.                      J.Opt.Soc.Am.53,(12),p1377,1963
- [5] HARRIS,F                           Copying Holograms.  
Appl.Opt.5,(4),p665,1966
- [6] LANDRY,M                           Effect of Two Hologram Copying Parameters on the Quality of Copies.                      Appl.Opt.6,(11),p1947,1967
- [7] PALAIS,J                           Improving the Efficiency of Very Low Efficiency Holograms by Copying.  
Appl.Opt.10,(3),p667,1971
- [8] PUECH,C                           Copying Holograms on Photoresist.  
Opt.Comm.4,(4),p279,1970
- [9] NAKAJIMA,J  
    et al                                  Copied Phase Hologram of Photoresist.  
FUJITSU Sci.& Tech.J.6,(3),p69,1970
- [10] NAKANO,M  
    ISHIDA,N                           Contact Printing Method Utilizing Heated Photoresist Adhesive Property for Hologram Copying.                      Appl.Opt.18,(18),p3073,1979
- [11] BEESLEY,M  
    CASTLEDINE,J                      The Use of Photoresist as a Holographic Recording Medium.                      Appl.Opt.9,(12),p2720,1970
- [12] BARTOLINI,R                      Characteristics of Relief Phase Holograms Recorded in Photoresist.  
Appl.Opt.13,(1),p129,1974
- [13] NORMAN,S  
    SINGH,M                              Spectral Sensitivity and Linearity of Shipley AZ1350J Photoresist.  
Appl.Opt.14,(4),p818,1975
- [14] NEUREUTHER,A  
    DILL,F                                  Photoresist Modelling and Device Fabrication Applications.  
Opt.& Acoustical Micro.Elect.April,p233,1974

- [15] DILL,F  
et al Characterisation of Positive Photoresist.  
IEEE Trans.ED22,(7),p445,1975
- [16] KIM,D  
et al Development of Positive Photoresist.  
IEEE Trans.ED31,(12),p1730,1984
- [17] BURNS,J Large Format Embossed Holograms.  
SPIE,523,Appl.of Holography, 1985
- [18] IWATA,F  
TSUJIUCHI,J Characteristics of a Photoresist Hologram and its  
Replica. Appl.Opt.13,(6),p1327,1974
- [19] BARTOLINI,R  
et al Embossed Hologram Motion Pictures for Television  
Playback. Appl.Opt.9,(10),p2283,1970
- [20] HAMMOND,R Stress In Electrodeposits.  
Trans.Inst.Metal Finishing.30,p145,1954
- [21] MCKINNEY,W  
BARTLE,L Development in Replicated Nickel Gratings.  
SPIE,315,Reflecting Optics for Synch.Radiation  
p170,1981
- [22] WEARMOUTH,W  
BISHOP,R Hard, Smooth,Stress-free Electroformed Nickel  
for Video Discs. Trans.IMF.62,(1),p32,1984
- [23] LEGIERSE,P Mastering Technology and Electroforming For  
Optical Disc Systems.  
Trans.Inst.Metal Finishing.65,p13,1987
- [24] KUHN,A  
DAVIES,E Accuracy and Detail Capture in One-Off  
Electroforms and The Role of Metallising Powders.  
Trans.Inst.Metal Finishing.62,(1),p1,1984
- [25] BARTOLINI,R  
et al Replication of Relief-Phase Holograms for Pre-  
Recorded Video. J.Electrochem.Soc.Solid State  
Science & Tech.120,p1408,1973
- [26] GALE,M  
et al Surface Relief Microimages.  
J.Micrographics.11,(3),p155,1978
- [27] GALE,M Sinusoidal Relief Gratings for Zero-Order  
Reconstruction of Black & White Images.  
Opt.Comm.18,(3),p292,1976
- [28] KNOP,K  
GALE,M ZOD Micor-Images:Colour and Black & White Image  
Reproduction from Surface Relief Gratings.  
J.Phot.Sci.26,p120,1978
- [29] HUTLEY,M Diffraction Gratings.  
Techniques of Physics Series. Academic Press,1982.

- [30] BRAININ,Y                      Controlling the Groove Depth of a Hologram Grating.    Sov.J.Opt.Technol.54,(11),p686,1987
- [31] BENTON,S                      Hologram Reconstruction With Extended Coherent Sources.    J.Opt.Soc.Am.59,p1545,1969.
- [32] ROGERS,G                      Experiments in Diffraction Microscopy.    Proc.RoyalSoc.Edin.A63-64,p193,1952.
- [33] COLLIER,                      Optical Holography.    Academic Press, 1971.
- [34] MEYERHOFER,D                  Dichromated Gelatin. Holographic Recording Materials.    Topics In Appl.Phys.Springer-Verlag 20,p75,1977
- [35] CURRAN,R                      The Mechanism of Hologram Formation in SHANKOFF,T                  Dichromated Gelatin.    Appl.Opt.9,(7),p1651,1970
- [36] BRANDES,E                      Preparation of Dichromated Gelatin Films for et al                      Holography.    Appl.Opt.8,p2346,1969
- [37] CURRAN,R                      Efficient, High Resolution, Phase Diffraction SHANKOFF,T                  Gratings.    Appl.Phys.Letts.13,p239,1968
- [38] DEFOREST,W.S                  Photoresist, Materials and Processes.    McGraw Hill Book Co. 1975
- [39] LEVINE,H                      Positive Photoresist Materials. Polymer Preprints, Polymer Chem,ACS,10,(1),p377,1969
- [40] BARTOLINI,R                      Holographic Recording Materials. Editor. H.M.Smith. Springer Verlag.1977
- [41] BROYDE,D                      Exposure of Photoresists.    J.Electrochem.Soc.117,p1555,1970
- [42] HEFLINGER,D                      Submicron Grating Fabrication on GaAs by et al                      Holographic Exposure. Opt.Eng.21,(3),p537,1982
- [43] ELLIOT, D                      One Micron Range Photoresist Imaging: A Practical HOCKEY,M                      Approach.    Solid State Tech.22,(6),p53,1979
- [44] DECKERT,C                      Processing Latitude In Photoresist Patterning. PETERS,D                      Solid State Tech.23,(1),p76,1980

- [45] LEONARD,R  
et al Automated In-Line Puddle Development Of Positive  
Photoresists. Solid State Tech.21,(6),p99,1981
- [46] ZEISS. Technical Information Literature. 1989
- [47] NIKON.Technical Information Literature.  
Optiphot.1989
- [48] RANK,TAYLOR,HOBSON. Technical Information  
Literature. Talysurf 4.
- [49] OLLARD,E  
SMITH,E Handbook of Industrial Electroplating.  
Iliffe Books, 1964
- [50] BRUGGER,R Nickel Plating.  
Robert Draper Ltd. Teddington, 1970
- [51] LINDAU,S The Groove Profile Formation of Holographic  
Gratings. Optica Acta,92,(10),p1371,1982
- [52] SPIRO,P Electroforming.  
Robert Draper Ltd. Teddington.1968
- [53] PINNER,S  
SIMPSON,W Plastics: Surface and Finish.  
Butterworth Co. 1971
- [54] HARIHARAN,P Optical Holography. Principles, Techniques &  
Applications. Cambridge Press. 1984
- [55] KOZMA,A Photographic Recording of Spatially Modulated  
Coherent Light. J.Opt.Soc.Am.56,(4),p428,1966
- [56] MASCHEV,L  
TONCHEV,S Formation Of Holographic Diffraction Gratings  
in Photoresist. Appl.Phys.A26,p143,1981
- [57] GRAHAM,K  
(Ed) Electroplating ,Engineering Handbook.  
Van Nostrand Reinhold,1971

## APPENDIX 1

### Mathematical Description of The Holographic Recording Process

Holography is a two beam recording process using an object and reference beam. The object beam illuminates the object and light is reflected and scattered back from the object to impinge upon a holographic plate. The reference beam falls directly upon the holographic plate and is a uniform even intensity beam not modulated in any way. The essential feature of the holographic recording process is the ability to record phase information from the interfering wavefronts of object and reference beam. Phase information is not recorded directly (photosensitive emulsions can only record intensity) but phase information is encoded within the interference pattern as intensity distributions across the holographic emulsion. Figure A1.1 illustrates a recording regime with an off-axis reference beam.

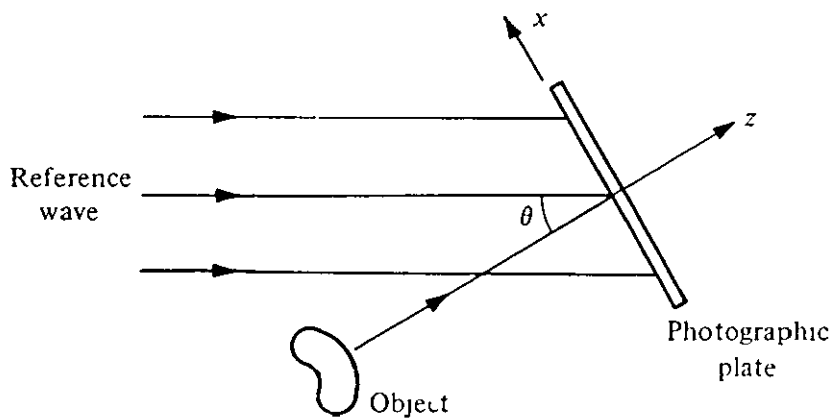


Figure A1 1 Image Recording with an Off-Axis Reference Beam

Let  $o$  represent a monochromatic wave from the object and  $r$  a reference wavefront, coherent with  $o$ . The object wavefront is modulated and the phase relationships of the scattered wavefronts unknown. The reference wavefront is a plane wavefront, not modulated, with uniform intensity and a known phase relationship. The functions are expressed in terms of complex amplitudes such that the object beam can be written;

$$o(x,y) = |o(x,y)| \exp[-i\phi] \quad \dots\dots\dots 1$$

and the reference beam,

$$r(x,y) = |r| \exp(i2\pi\zeta_r x) \quad \dots\dots\dots 2$$

The phase information for the object wavefront is unknown and is expressed as the complex value  $\phi$ . From Hariharan [54].

The phase information for the reference beam can be determined as  $\zeta_r = (\sin \theta / \lambda)$  since the beam intensity is uniform and unmodulated and only the phase of the wavefronts should vary across the emulsion.

The complex interference of the two beams at the emulsion is recorded as intensity, expressed as the square of the amplitude of the two beams.

$$\begin{aligned} I(x,y) &= |r(x,y) + o(x,y)|^2 \\ &= |r(x,y)|^2 + |o(x,y)|^2 \\ &\quad + r|o(x,y)|\exp[-i\phi(x,y)]\exp(-i2\pi\zeta_r x) \\ &\quad + r^*|o(x,y)|\exp[i\phi(x,y)]\exp(i2\pi\zeta_r x), \\ &= r^2 + |o(x,y)|^2 + 2r|o(x,y)|\cos[2\pi\zeta_r x + \phi(x,y)] \quad \dots\dots 3 \end{aligned}$$

This expression shows the intensity of both the reference beam and the object beam and importantly, the amplitude and phase of the object wave are encoded, respectively, as amplitude and phase modulation of a set of interference fringes equivalent to a spatial carrier with a spatial frequency equal to  $\zeta_r$



(The importance of coherent laser light is seen since without a phase relationship between the two beams, the final part of the expression above would not exist. Without phase encoded, only the intensity of the beams is recorded and the hologram would not reconstruct an image of the original object.)

It is assumed that the amplitude transmittance of a correctly exposed and processed plate is linearly related to the intensity in the interference pattern. The amplitude transmittance of the hologram can be written as;

$$\begin{aligned}
 t(x,y) = & t_0 + \beta T \{ |o(x,y)|^2 \\
 & + r |o(x,y)| \exp[-i\phi(x,y)] \exp(-i2\pi\zeta_r x) \\
 & + r |o(x,y)| \exp[i\phi(x,y)] \exp(i2\pi\zeta_r x) \} \quad \dots 4
 \end{aligned}$$

where  $\beta$  is the slope of the amplitude transmittance versus the exposure characteristic of the photographic material,  $T$  is the exposure time and  $t_0$  is a constant background transmittance.

In order to reconstruct the image, as shown in Figure A1.2, the hologram must be illuminated with the same reference beam as used to record it

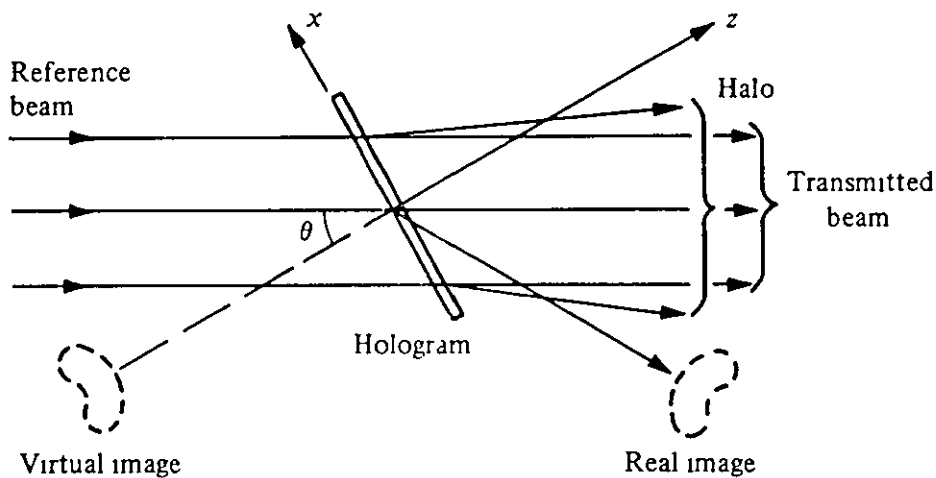


Figure A1 2 Image Reconstruction for an Off-Axis Hologram

The complex amplitude  $u(x,y)$  of the transmitted wave is the sum of four terms, each corresponding to one of the terms of equation 4 and can be written;

$$u(x,y) = r(x,y)t(x,y),$$

$$= u_1(x,y) + u_2(x,y) + u_3(x,y) + u_4(x,y) \quad \text{.....5}$$

where

$$u_1(x,y) = t_o \exp(i2\pi\zeta_r x) \quad \text{.....5.1}$$

$$u_2(x,y) = \beta Tr |o(x,y)|^2 \exp(i2\pi\zeta_r x) \quad \text{.....5.2}$$

$$u_3(x,y) = \beta Tr^2 o(x,y) \quad \text{.....5.3}$$

$$u_4(x,y) = \beta Tr^2 o^*(x,y) \exp(i4\pi\zeta_r x) \quad \text{.....5.4}$$

The first term of equation 5,  $u_1(x,y)$ , is the attenuated reference beam transmitted directly through the plate. The transmitted beam is surrounded by a halo due to the second term,  $u_2(x,y)$ , which is spatially varying. The angular spread of the halo is determined by the angular extent of the object.

The third term,  $u_3(x,y)$  is identical with the object wave, except for a constant factor and generates a virtual image of the object in its original position. This wave makes an angle  $\theta$  with the directly transmitted wave. The fourth term,  $u_4(x,y)$  generates the conjugate real image, the term  $\exp(i4\pi\zeta_r x)$  indicates that the conjugate wave is deflected off the axis at an angle approximately twice that which the reference wave makes with it. Thus two images, real and virtual are generated from the replay of the original hologram, angularly separated from the directly transmitted wave and from each other. This off-axis technique eliminates the problem associated with the Gabor type hologram of replay and viewing. The generation of the real image allows the copying to produce white light viewable holograms. The real image can be focussed onto a second holographic plate, which with the introduction of a second reference beam can allow display copies to be recorded. Figure A1 3 illustrates the generation of the real and virtual images by use of conjugate reference beams.

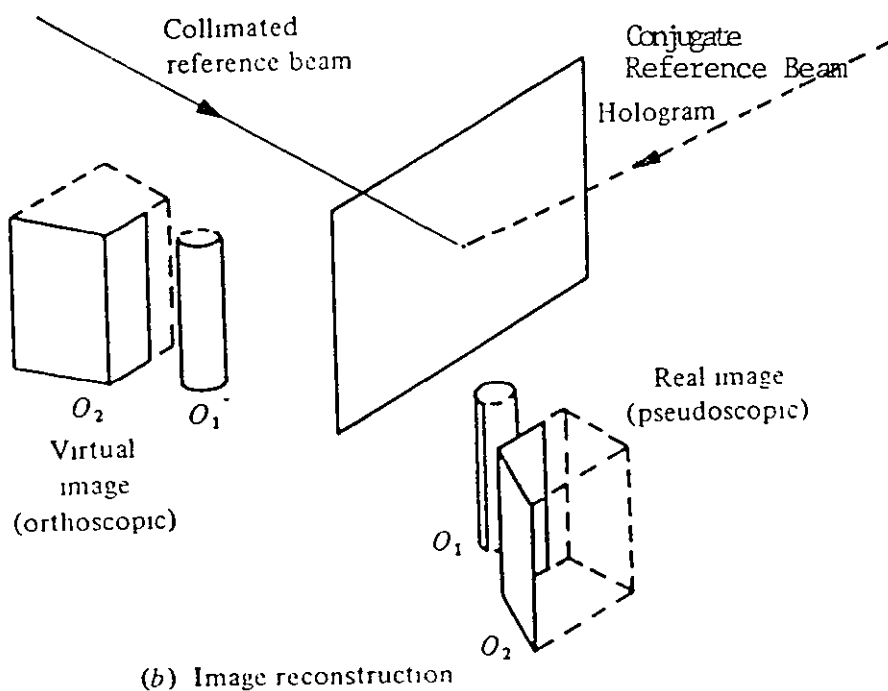
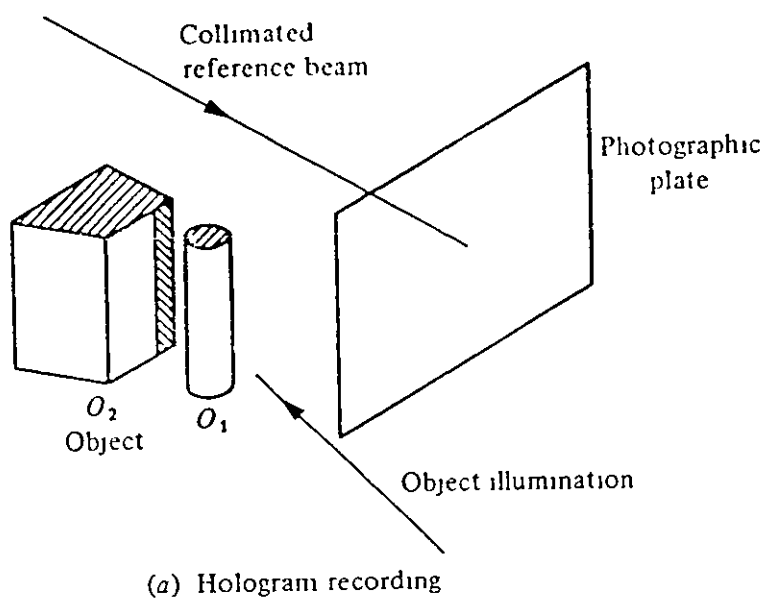


Figure A1.3 The Formation of Real and Virtual Images

## APPENDIX 2

### The Development of Diffraction Gratings

The earliest recorded investigation of diffraction gratings was in 1786, when D.Rittenhouse produced diffracted orders by diffracting light around small apertures made from hair wound onto nails. The name more renowned for the study of gratings however is that of Joseph von Fraunhofer who repeated the earlier work of Rittenhouse and in 1821 produced a grating 12mm wide containing 9600 grooves. From this grating the nature of diffracted orders, measurement of wavelength of light and grating equations were derived. Limitations in the use of early gratings lay in the difficulty of manufacture. Traditionally watch makers had produced fine wire gratings and it was not until the introduction of ruled gratings in the 1880's that further progress was made. Lord Raleigh (1874) proved theoretically that a grating could resolve more spectral lines than the prisms used up to that time and the first diamond ruled grating supported this theory. The 'ruling engine' as it was known, literally cut grooves into the surface of a mirror or glass blank and the engineering precision required made the ruling engine the finest form of machine tool available. The advancement to gratings ruled onto the surface of a concave spherical mirror extended the type and ability of instruments to study the nature of light. The re-design and use of ruling engines continued into the 1950's and the use of casting and plastic replicas meant the replacement of prisms with gratings in the majority of spectroscopic instruments. The ability to 'tune' gratings by shaping or 'blazing' (profiles with a slanted or shaped nature) to control the distribution of light among diffracted orders led to even wider usage.

The invention of the laser producing monochromatic, single phase light, renewed interest and placed greater demands on the production of quality gratings. The laser helped further in this respect with the generation of gratings by interference techniques. Interference between two beams of monochromatic, coherent light produces fringes of light

and dark bands that can be recorded by photographic materials. The spacing of the bands and optical properties of these gratings can be controlled by the wavelength of light used,  $\lambda$  and the angles,  $\theta$  formed between the interfering beams. See Figure A2.1

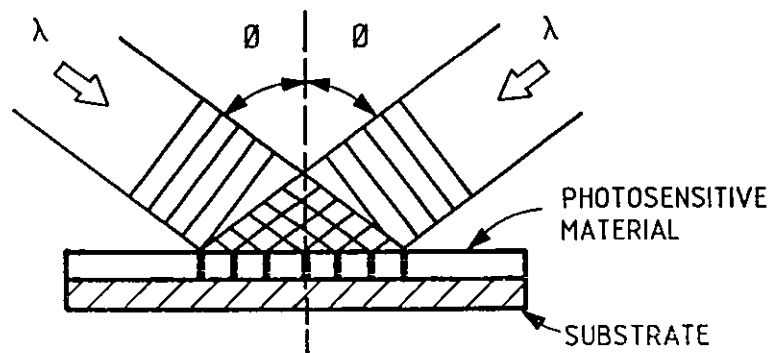


Figure A2.1 Interference Fringes Generated by Collimated Coherent Beams of Light

With correct processing 'interference gratings' can be made almost perfect without stray light or ghosts associated with ruled gratings due to the engineering and mechanical limitations. Whilst the gratings are cheaper and easier to produce, control over the groove profile is more difficult since sinusoidal or quasi-sinusoidal profiles typically result from two-beam interference. Advances are now being seen with the production of two and three-dimensional gratings recorded in photoresist materials and cheaply mass produced by embossing techniques.

### Diffraction and Wave Propagation

The action of splitting light into orders by a grating is known as 'diffraction'. The effect is a general characteristic of wave phenomena occurring whenever a portion of a wavefront encounters an obstacle, (transparent or opaque) and the resultant wavefront is altered in either amplitude or phase. The wavefronts which propagate beyond the obstacle interfere and result in a particular energy density distribution known as a diffraction pattern.

The diffraction grating is a repetitive array of obstacles or apertures, around which diffraction occurs to produce periodic alterations in phase, amplitude or both. The simplest diffraction grating would consist of a single slit, (a rectangular aperture whose length is large compared to its breadth) as illustrated in Figure A2.2

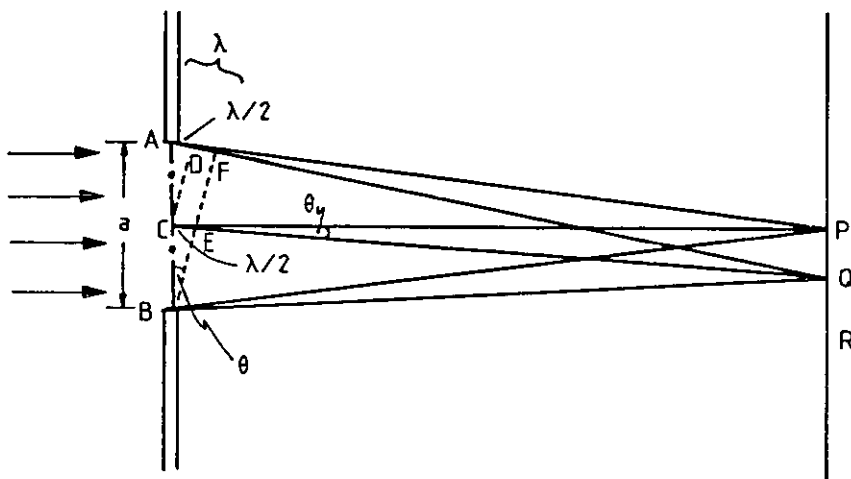


Figure A2 2 Diffraction at a Single Slit

Parallel light is incident on the slit AB. The irradiance falling at any point, eg. P or Q, can be found by vector addition of the amplitude of the distribution of the wavefronts at that point. Consider the general effect of the two halves, AC, CB of the wavefront, AB. The wavelets (according to Huygen's principle) arriving at P will all be in phase. If the size of the slit is the order of a few wavelengths of light, the amplitude at P of the whole wavefront AB is large and a bright band will be seen at P. Away from P the wavefronts reaching the screen are more and more out of phase and the brightness diminishes. Considering the point, Q, the wavefront AQ is half a wavefront larger than CQ such that a disturbance from C would be out of phase by  $180^\circ$  at point Q. Thus Q corresponds to the edge of minimum intensity around the central band of brightness, P. Out towards R, the intensity rises again but to a much smaller maximum where  $AR-AB=3\lambda/2$ . If the slit is very narrow other maxima and minima diffraction bands will be observed.

The angular width of the bright central band shown in Figure A2.3 is  $2\theta$ . From Figure A2.2 the line CQ makes an angle  $\theta$  to the direction CP of the incident light, given by;

$$\sin \theta = \lambda/d \quad \text{where } d = \text{slit width AB}$$

Hence the period,  $d$  of the grating is equal to the width of the slit and becomes;

$$d = \lambda/\sin \theta \quad \text{or} \quad \lambda = d \sin \theta$$

When the slit width is widened and  $d$  becomes large compared with  $\lambda$ ,  $\sin \theta$  is very small, hence  $\theta$  is small. In this case the directions of the maximum and minimum intensity of the central band are very close to each other and practically the whole of the light is confined to a direction immediately in front of the incident direction so no spreading occurs.

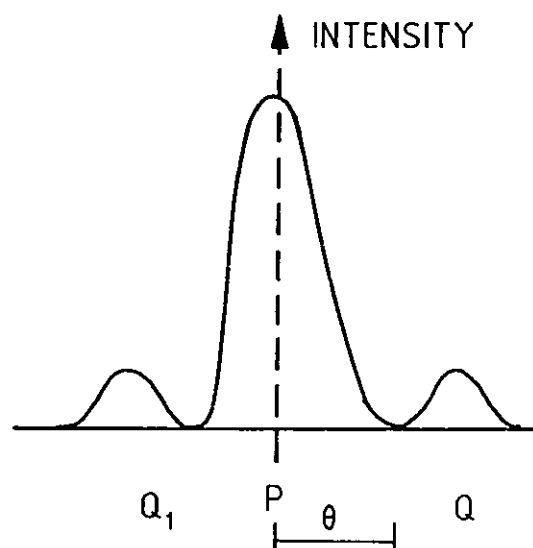


Figure A2.3 Variation in Intensity Across a Single Slit

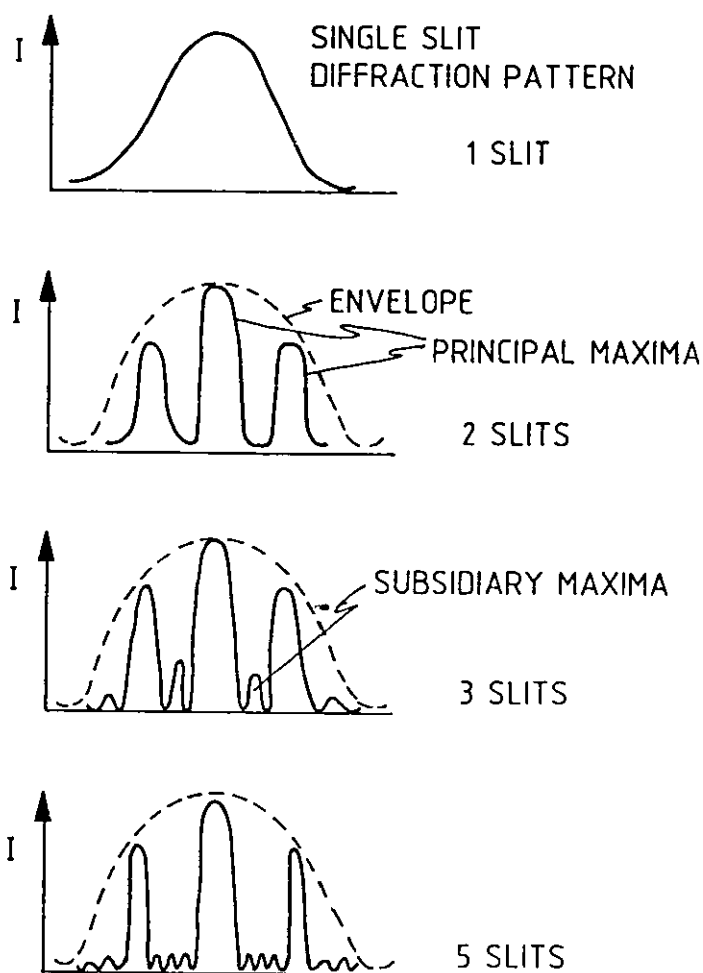


Figure A2.4 Effect of Increasing Slit Numbers



A true diffraction grating contains many slits, each producing a diffraction pattern. As the number of slits is increased, the intensity and sharpness of the principal maximum as found at point P in Figure A2.3 increases and that of the subsidiary maxima decreases. The effect is illustrated in Figure A2.4

Replacing the single slit by an arrangement of closely placed parallel slits, only a few sharp principal maxima are seen. The angular separation depends upon the distance between the slits whereas the width of the slits affects the intensity of the higher order principal maxima, the narrower the slits, the greater the diffraction of light into the higher orders.

The position at which the maxima are seen can be determined. Consider Figure A2.5 for normal incidence of a grating.

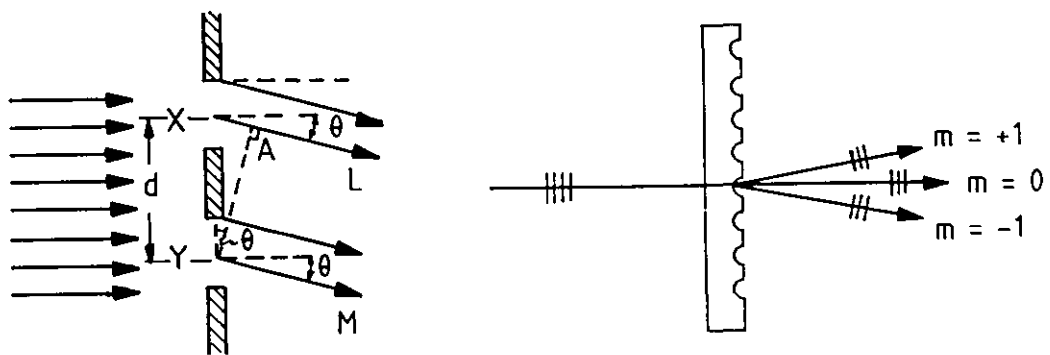


Figure A2 5 Normal Incidence-Determination of Maxima Position

For normal incidence the bright or principal maximum are obtained when;

$$d \sin \theta = m\lambda$$

$m$  an integer = diffracted order

The images corresponding to  $m = 0, 1, 2$ , are respectively zero, first and second orders. The zero order image is the image where the path difference of diffracted rays is zero.

A more general case is found with oblique incidence illustrated in Figure A2.6 when a bright diffraction image is seen when;

$$d (\sin i \pm \sin \theta) = m\lambda.$$

$m$  is an integer known as the order number which can be positive, negative or zero - zero corresponding to the undeviated beam. The precise form of the grating equation depends upon sign conventions for angles of incidence and diffraction. It is important for calculations of grating properties and describing the formation of the spectrum and diffracted orders.

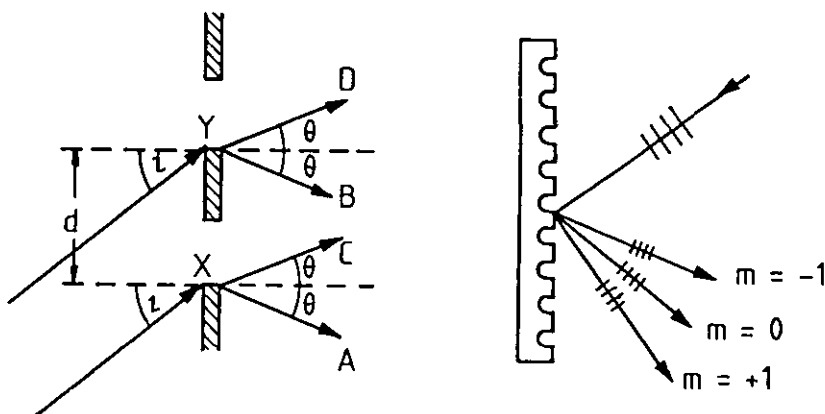


Figure A2.6 Oblique Incidence-Determination of Maxima Position

## Types of Diffraction Gratings

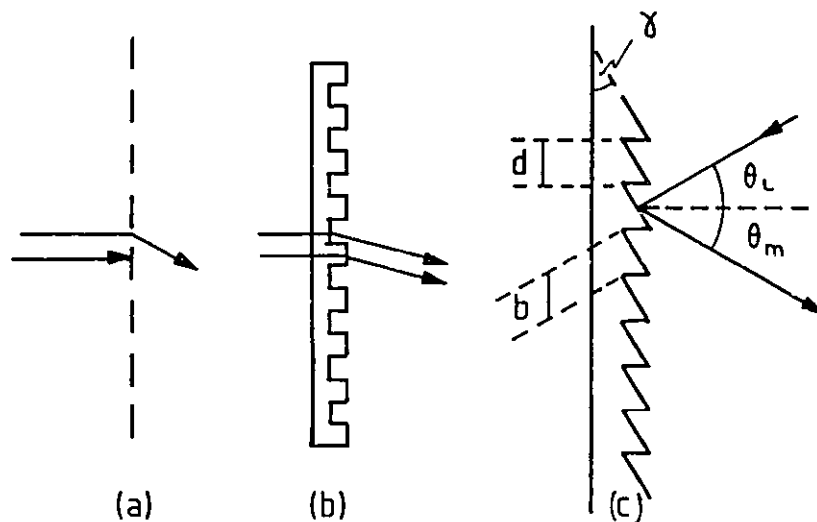


Figure A2.7 Three Grating Structures

Figure A2.7 a) **Amplitude grating.** The grating consists of clear and dark stripes which modulate the amplitude of the incident wavefront. The irradiance for such would be  $I_0 \frac{1}{4\pi^2}$

Figure A2.7 b) **Phase Grating.** The optical thickness of the grating varies, (physical thickness  $\times$  refractive index) and yields a phase modulation. This has the effect of doubling the amplitude and the irradiance would be  $I_0 \frac{1}{\pi^2}$ .

Figure A2.7 c) **Blazed Grating.** The advantage of the blazed grating is that most of the incident light undergoes specular reflection acting as a plane mirror with irradiance in the zero order effectively wasted. By controlling the shape of the groove, the angular positions of the various orders and  $\theta_m$  values are determined by  $\lambda$ ,  $d$  and  $\theta_i$ . As the phase varies across each groove, each contribution is in phase and the amplitude of the diffracted wave is increased by a factor of  $\pi$  and the efficiency of the grating by  $\pi^2$ . Most gratings are of this shaped or blazed variety and used in reflection.

### APPENDIX 3

#### Positive Photoresist, Formulation and Image Models

A brief description of the relevant details of composition and image formation models for positive photoresist are given below.

##### Sensitizers for Positive Resist

Hundreds of possible sensitizers can be used within resist formulations, the majority being found only in patent literature. Most are derivatives of the diazo oxides or orthoquinone diazide compounds, typically; yellow in colour, stable and resistant to decomposition, soluble in solvents of low polarity and insoluble in water. Examples of the structure of the quinone diazides are shown in Figure A3.1 [38]

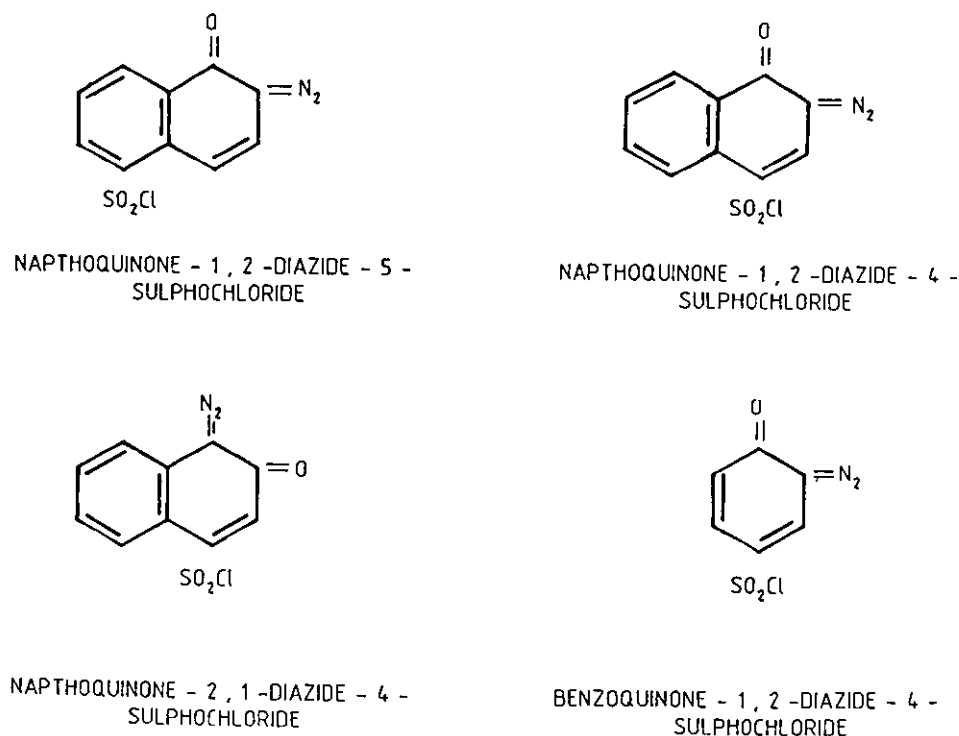


Figure A3.1 Positive Resist Sensitizers

All the elements possess a sulfochloride ( $-SO_2Cl$ ), important in forming the ester or amide linkage that joins the sensitizers to the central groupings. The sulfochloride is reacted with hydroxy ( $-OH$ ) or amine ( $-NH_2$ ) on the central group. The central group affects the overall properties of the resist characteristics although it may not be in itself photo-sensitive. It may affect the solubility of the sensitizer in certain solvents, along with film-forming properties, crystallization tendencies and development characteristics.

#### Resins for Positive Resist

The sensitizer in positive resist does not react with the resin in the formulation. Typically a positive resist may contain 2 to 4 times as much resin as sensitizer whereas negative resists contain 50 to 70 times as much resin as sensitizer - this is because the sensitizer does not have to react with the resin.

The function of the resin is as follows;

- to improve the adhesion of the coating to the substrate,
- to lessen the tendency for the sensitizer to crystallise out of the solution,
- to increase the coating viscosity and enhance coating characteristics,
- to reduce the cost of the system by acting as a partial substitute for the resin-like sensitizer.

The resin is typically of low molecular weight to ensure good aqueous developing characteristics - it should be soluble in alkaline solutions and be resistant to acids. It is important the resin is not too soluble in alkaline solutions otherwise it could be leached from the coating in the unexposed areas and leave no useful image.

The resin most commonly used for positive resists is the phenol formaldehyde novolak, accounting for the characteristic reddish amber colour of the resist formulations. The resin is soluble in alkaline solutions and many common solvents. Derivatives of phenol may be used

to prepare novolak resins, an illustration of which can be found in Figure A3.2

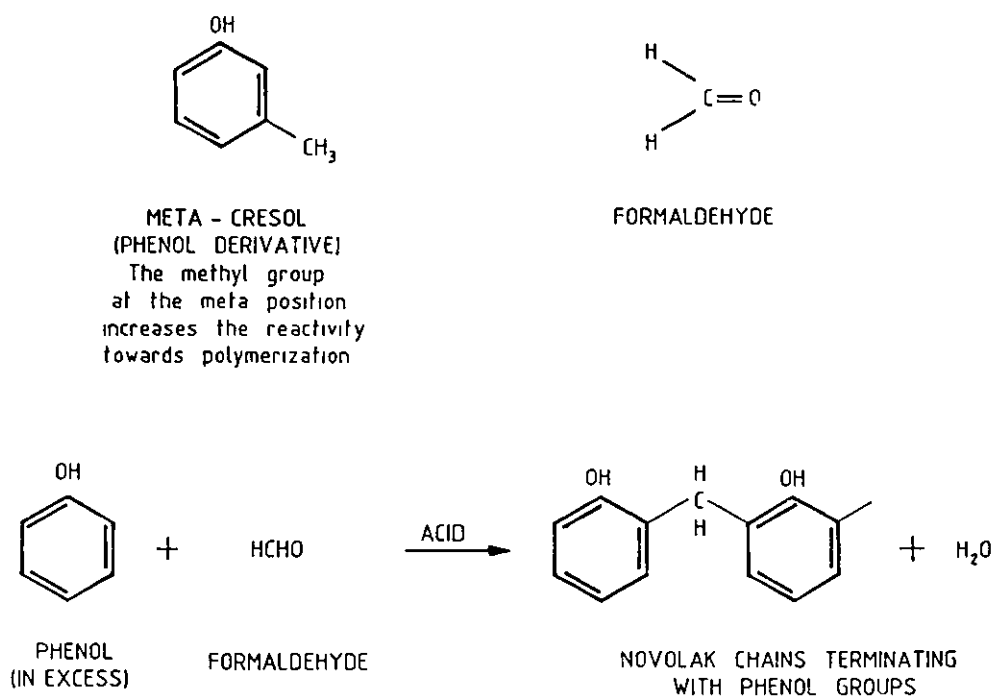


Figure A3.2 Preparation of a Novolak Resin from Phenol and Phenol Derivatives

#### Solvents for Positive Resist

During preparation of the resins and constituents of the resists, solvents are used to hold them in solution for storage or application and for the development procedures. Solvents in positive resists must be chosen carefully to avoid crystallization of the large amount of sensitizer present in the formulation. This may occur due to sheer quantity maintained in solution or incompatibility with the type of

resin used. The solvent, sensitizer and resin combinations are critically bound, the type and amount of resin being determined by the quantity that can be maintained in solution. In turn the amount and type of solvent used affects the characteristics of the film-forming and coating properties. When applying the resist to the substrate it is important that the solvent in the system does not evaporate too quickly, this would prevent the resist from flowing and causes unevenness of coating. Unlike negative resists, the positive resists are less likely to form "skins" on the surface during drying and do allow for the film to flow before the baking stages. Typically a combination of solvents may be used, some of which are illustrated in Figure A3.3

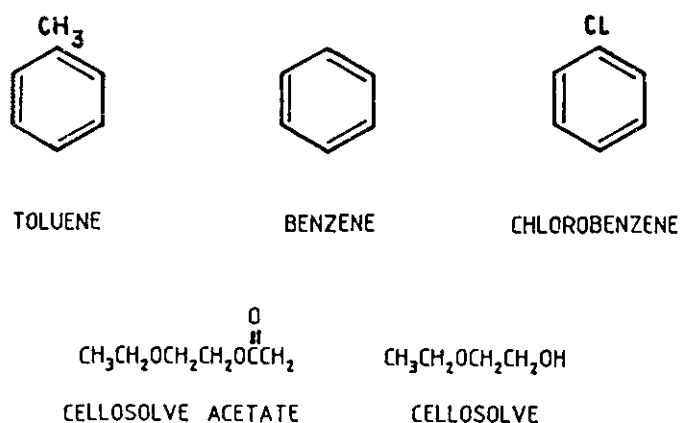


Figure A3 3 Common Photoresist Solvents

Film formation may occur by virtue of the size of the polymer molecules within the solvent system upon evaporation - referred to as "physical film formation". Paints and enamels form films by chemical combination of smaller molecules into larger ones - a method known as "chemical film formation" This is not desirable for a photoresist because the

resultant film would literally become too hard and hinder development. A compromise is needed to allow the polymer molecules to arrange themselves into a film, i.e. the transition from a liquid solution phase to produce a coherent layer of resist. A rapidly evaporating film would not facilitate this process, equally a slowly evaporating solvent may remain within the emulsion and interfere with subsequent exposure and development procedures.

#### Additives for Positive Resist

Positive resists using diazo oxides or orthoquinone diazide compounds as sensitizers have an inherent disadvantage in that such compounds are unstable and stabilizing additives are included in the formulations to overcome this. Dyes and resin plasticisers may also be included.

The stabilizers for diazo compounds are typically reducing agents or antioxidants, such as thiourea, sugar and related compounds. The dyes are used sparingly because of possible effects upon the exposure characteristics of the resist. The sensitizer and basic resin (novolak) are both coloured, the sensitizer (quinone diazide) being strongly yellow and the novolak amber red. This is the colour that pre-dominates the resist formulation. Resin plasticisers may be added to function as a cross-linking agent to give a harder coating with good chemical resistance - hexamethylenetetramine can be used to harden novolak resins

#### Image Formation Models

Image formation occurs by chemical reactions within the resist layer initiated by the absorption of radiation. In summary, the functional groups within the sensitizer of the resist change from hydrophobic diazides to groups soluble in alkaline solutions. These changes result in the removal of resist by the process of development as a consequence of differential reactions to the absorbed radiation.

The mechanism of image formation must be modelled as a part of the entire exposure and development procedure. The development procedure is considered an integral part of the total mechanism



Neureuther and Dill [14] consider the mechanism for positive photoresist films and base their model upon the two major constituents of the formulation; the resin and the sensitizer. The resist is modelled as a bleachable absorber during exposure and a surface rate limited etching process during development. Exposure is described by the photodecomposition of the light sensitive inhibitor compound whereby the diazo ring structure absorbs a photon and breaks a bond. The change in light intensity with depth for exposure at a given wavelength is expressed by;

$$\frac{dI(x,t)}{dx} = -I(x,t)[A M(x,t) + B]$$

where  $I$  = optical intensity within the resist  
 $M$  = relative inhibitor concentration  
 $A$  = inhibitor related optical absorption  
 $B$  = base resin related optical absorption

The "bleaching" of the inhibitor with time is given by;

$$\frac{dM(x,t)}{dt} = -I(x,t)M(x,t)C$$

where  $C$  = optical sensitivity term.

The development process described by Neureuther and Dill is of a developer physically etching the surface layer as a function of the local inhibitor concentration after exposure. Exposure causes photodecomposition of the inhibitor, therefore the final etched image is a function of the exposure in that the developer can remove certain areas that have undergone photodecomposition. It is assumed that the reaction is surface limited in that the developer must not penetrate the photoresist before etching begins and that as etching occurs the developer by-products do not interfere with the process. With these assumptions, Neureuther and Dill base the development model upon a single curve of etch rate versus inhibitor concentration. The model

requires in-situ thickness measurements of the remaining photoresist during the etching process.

Neureuther and Dill use the model to simulate the interference process in grating manufacture with some major simplifying assumptions using electric field effect,  $E(x,z)$  and absorption values of resist  $M(0.7)$ . The net exposure and resulting bleaching of  $M(x,z)$  is found from  $|E(x,z)|^2$  and the exposure time. Having calculated  $M(x,z)$  the development can be simulated. The theory of image formation was applied to gratings manufactured on glass and aluminium substrates. The determination of the value of  $M$ , the relative inhibitor concentration is not defined making the model difficult to evaluate experimentally. However, the basis of the model, (exposure-bleaching, development-etching) does form ideas used by other workers in this same area.

A later work by Dill et al [15] still uses the value  $M$  for relative inhibitor concentration and the relationship with the etch rate (rate of removal) for positive resist. In this later model the exposure process is extended by consideration of the three further parameters,  $A'$ ,  $B'$  and  $C'$  where,

$A'$  = exposure absorption dependent term

$B'$  = exposure independent absorption term

$C'$  = optical sensitivity term.

These three terms are exposure wavelength dependent. The development process is described by the function  $RIM1$ , where  $R$  is the etching or removal rate as before. The theory relies upon a single positive photoresist and developer type and concentration being held constant, although it does acknowledge that etch removal rate is weakly dependant on developer flow-rate or agitation.

The validation of the theory relies upon optical absorption measurements for photoresist films on optically matched substrates, the Beer Lambert law can be used for light passing through the resist without reflections. The model expands the Beer Lambert law as follows;

$$\frac{dI}{dx} = -I \sum a_i m_i$$

where  $I$  = light intensity  
 $x$  = distance from resist/air interface  
 $m_i$  = molar concentration of  $i$ th component  
 $a_i$  = molar absorption coefficient of the  $i$ th component

Expanded to the following to include the three absorbing species of inhibitor, base resin and reaction products.

$$\frac{dI(x,t)}{dx} = -I(x,t)[a_1 m_1(x,t) + a_2 m_2(x,t) + a_3 m_3(x,t)]$$

where  $I(x,t)$  = light intensity at any depth  $x$ , in the film with exposure time  $t$   
 $a_1$  = molar absorption coefficient of inhibitor  
 $a_2$  = molar absorption coefficient of base resin  
 $a_3$  = molar absorption coefficient of reaction products  
 $m_1(x,t)$  = molar concentration of inhibitor  
 $m_2(x,t)$  = molar concentration of base resin  
 $m_3(x,t)$  = molar concentration of reaction products

The model relies upon having factors such as constant lamp intensity ( $I$ ), uniformity of inhibitor and resin distribution and a linear relationship between the exposure given and destruction of the inhibitor, ie. resist thickness after development as a function of exposure energy for different values of illumination intensity

The model by Dill et al [15] was applied to several photoresist materials under constant processing chemistry. The results showed good tie-up between measured etch rate curves and analytical fits. The difficulty of using the model is the measurement of inhibitor concentration in the resist formulation and the need for in-situ thickness measurements during processing. Additionally no account is taken of the developer chemistry or surface rate reactions in the overall model.

This factor was subsequently studied in the work by Kim et al [16]. Their model was derived to describe the development behaviour for positive resists as a function of depth and concentration of inhibitor (M) but over the full range of exposures. Kim et al recognized that the development of the resist can be surface rate limited and hence described by a kinetic function affected by development chemistry and temperature. In addition, Kim et al have retained a product formulation in which the retardation of the development rate near the surface is used as a multiplier  $f(z,M)$  to the overall bulk development rate,  $R_{BULK}$

$$\text{Rate}(z,M) = f(z,M)R_{BULK}(M)$$

Their model for the bulk development rate considers the physical processes which result from exposure and development, these are;

- 1) the dissolution of the base resin modified by the presence of the photoactive compound (PAC) and
- 2) the dissolution of base resin modified by the presence of the reacted PAC - mostly carboxylic acid - termed PPA (photoproduct acid) by Kim

The parameter M is a measure of the relative concentration of PAC remaining whilst  $1-M$  is the relative concentration of PPA. Using these definitions, the model compares the development rates of resist with PAC (which slows development compared to pure base resin) to that of exposed resist possessing PPA (which enhances the development rate). Hence the development is considered as the dissolution of the various reactions of resin-PAC and resin-PPA system.

Kim et al recognize that they have limited their bulk development equations to the minimum set of parameters for a two component mixture and that if additives or processing resulted in a mixture of organic acid and ketenes, further parameters would be needed. For the experimental verification, Kim et al have closely followed the work of Dill using development cells for in-situ monitoring during processing. The exposed substrate is back illuminated using a He-Ne laser and directed to a detector to measure the variation in reflectivity from the substrate. Developer temperature and flow rate across the substrate are controlled parameters and the effects of soft bake, developer type and concentration are also considered. The conclusions and observed data fit well with the model proposed by Kim et al and cover resist/developer combinations and exposure ranges from 0 mJ/cm<sup>2</sup> to 300 mJ/cm<sup>2</sup>.

The notion of etch rates of exposed and unexposed photoresist was used by Bartolini [12] in his study of the characteristics of relief phase holograms recorded in photoresists. Though not strictly offering a model for grating formation, Bartolini does propose a "design procedure" for high efficiency, low noise, high sensitivity grating structures. The holograms produced are identified as being limited by two non-linearities, the inherent non-linearity of the phase recording process and the material non-linearity associated with the exposure characteristics of the photoresist. Bartolini is the first to include the non-linearity of a phase recording process to the study of photoresist. Kozma [55] investigated this phenomena much earlier in 1966.

The two non-linearities are considered by Bartolini as follows;

Inherent non-linearity;

$$t(x,y) = \exp j\phi(x,y)$$

where the transmittance function  $t(x,y)$  is a non-linear function of the recorded phase shifts.

Material non-linearity;

$$\Delta d = T[r_1 - \Delta r \exp(-\alpha E)]$$

where the relief depth,  $\Delta d$  is a non-linear function of exposure  $E$  and

$T$  = development time (secs)

$r_1$  = photoresist removal rate

$\alpha$  = a constant

Bartolini offers practical recording parameter definitions by considering the effects of exposure values, reference to object beam ratios and development processing. It is shown that the material non-linearities can be overcome by suitable processing. Bartolini suggests control of the inherent non-linearity in the following way;

By consideration of the Bessel function within the expression for the intensity  $I_p$  of the primary hologram image  $U_p$ ;

$$I_p = |U_p|^2 = |U_R|^2 J_1^2[(4\pi/\lambda_R)(n-1)ge|U_o||U_r|]$$

where  $U_R$  = readout beam

$J_1$  = Bessel function of first kind, order 1

$U_o$  = complex field amplitude of object beam

$U_r$  = complex field amplitude of reference beam

Bartolini states that if the following approximation is made;

$$J_1(a) \sim \frac{1}{2}a \quad \text{where } a \text{ is small and given by;}$$

$$a = 2 \cdot 2\pi/\lambda_R (n-1)ge|U_o||U_r| = 4\pi/\lambda_R (n-1)ge/|U_o||U_r|$$

The parameters given are;

$n = 1.7$  R.I of photoresist       $I_0 \sim 10 I_{U_0} I^2$  = Hologram irradiance.  
 $\lambda R = 632.8 \text{ nm}$  He-Ne laser.       $I_{UR} I \sim (10) * I_{U_0} I$  Beam ratio 10:1.  
 $\Delta d = g_e = 0.1 \mu\text{m}$  Typical exposure value.

With the parameters given Bartolini's expression calculates;

$$a = 0.44$$

which would support  $J_1(a) \sim \frac{1}{2}a$  as a valid approximation.

In using this approximation, the inherent non-linearity has been overcome. In practical terms this would mean the elimination of noise effects in the images from the holograms, eg. harmonic and intermodulation (IM) distortion. IM distortion often appears as a ghost image in the background of the hologram reducing the overall image contrast. The measure and acceptable level of IM distortion is a value that finds disagreement between other workers as detailed in Bartolini's discussion.

The problem of material non-linearity as mentioned earlier is overcome by proper development procedures. Bartolini discusses this relationship in detail and this model for photoresist behaviour forms the basis of experiments undertaken for this work.

Bartolini's model was published in 1974 and following his studies, several workers applied his techniques to the updated resist formulations available. In particular the work of Norman and Singh [13] use later resists to confirm the linear development behaviour possible with correct processing.

The work of Mashev and Tonchev [56] combines a number of elements from all the previous models and further considers the influence of the reflective substrate upon the grating formation. All previous models have been based upon a sinusoidal profile on a glass substrate. Mashev

and Tonchev use GaAs and metals which produce standing wave effects on the gratings. In addition they consider the effect of recording geometries when interference fringes are perpendicular to the plane of the film or slanted at some angle with respect to the medium boundaries. The modelling for the exposure-development process uses the concentrations of the inhibitor, resin and solvent components and the Beer-Lambert Law for light intensity at a given depth in the resist (after Dill et al) but includes the relationship  $r = dw/dT$  for removal rate and exposure  $E$  to explain the development process. ( $w$  is used to indicate directional normal,  $T$  development time). For experimental verification factors such as soft bake effects on removal rates ( $r$ ) for exposed and unexposed resists are studied. Also the use of different developers on removal rate is included. The model is applied to predicting grating profiles for sinusoidal, rectangular, trapeoidal and quasi-rectangular type.

#### Summary

The image formation models described have been based upon the work of Neureuther and Dill and Kim who have all suggested resist exposure can be described as a bleaching reaction and development as an etching process. The experimental limitations of some models have been highlighted. The development of the Bartolini model for resist image formation has arisen from study of previous models and provides the basis of the theoretical and experimental work described.



## APPENDIX 4

### Accuracy of Electroforming - Metal Distribution

No matter what the application of plating, the nature of metal distribution over the workpiece is important for accurate reproduction of detail. The distribution of the deposit is most greatly affected by the primary current distribution determined by the geometry of the plating tanks, conditions of operation and cathode efficiency. It is independent of solution properties provided they are uniform throughout right up to the cathode surface. Physical or electrochemical phenomena can change the state of this uniformity termed 'polarization'. Any such changes bring about a secondary current distribution which will further influence the metal distribution. If the primary current distribution is uniform the cathode polarization will also be and results in uniform metal deposition. Factors to be considered are the geometry of the bath, size and shape of electrodes, conductivity, relationship of electrodes to each other and the electrolyte boundaries and the inclusion of conducting or non-conducting surfaces such as 'thieves' or 'shields'.

#### Potential Field

When voltage is applied between two electrodes in an electrolyte (electric potential), every point in the electrolyte assumes some potential intermediate between that of the two electrodes. The metal electrodes are significantly more conductive than the electrolyte and so it is assumed that every point on the electrode surface is at the same potential, an equipotential surface. Similarly, equipotential surfaces will be found in the electrolyte surrounding each electrode. The equipotential surface around one electrode will actually resemble the shape of the electrode and changes as it moves further away from the first to take on the shape of the second. Figure A4 1 illustrates this

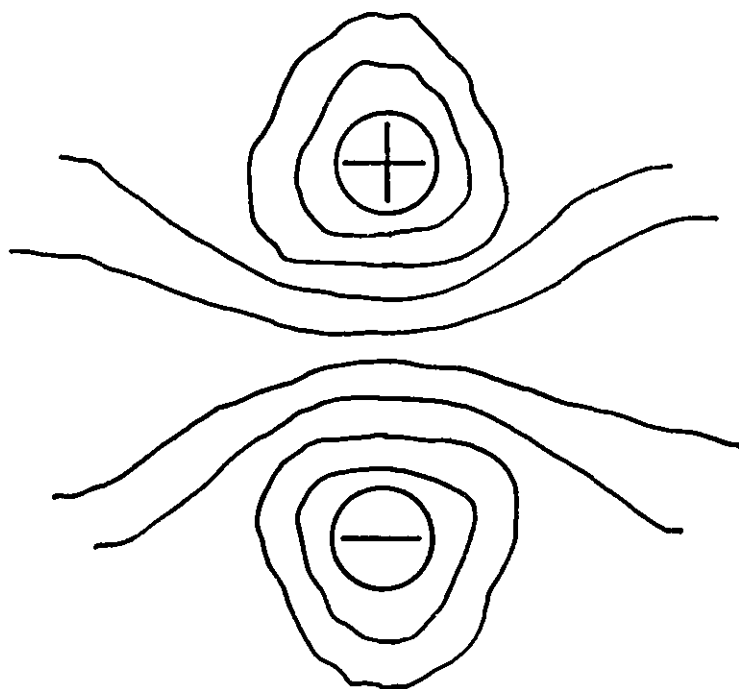


Figure A4 1 Illustration of Equipotential Surface  
Around Electrodes

This may be thought of as a three dimensional contour map with current density the greatest where the equipotential lines are crowded together. The traces of the equipotential surfaces form an orthogonal net crossing each other at right angles. The electrodes are also equipotential surfaces and this means that the current enters or leaves the electrode at any point in a direction perpendicular to the surface at that point. A further point in the theory allows that any equipotential surface may be replaced by a conductor without disturbing the field, similarly for replacement by an insulating boundary for a line of force. The replacement however must be with a perfect substitute, otherwise the imaginary net is disturbed and the field

lines will change altering the metal distribution. The practical consequence of considering this theory is that plating tanks and their contents can be designed to produce the ultimate control over metal distribution. Parts can be 'boxed' in to produce short, parallel plating areas, which is one of the best arrangements for the field lines. A plating rack full of closely spaced flat parts, held equidistant between two rows of anodes in a tank just big enough to hold the rack is an ideal situation. However, for objects and parts that do not represent a uniform current distribution and objects that present recesses or angles, control over metal distribution is still necessary. For a perfect angle with sharp corners, the primary current density is infinite on the sharp external corners and zero on the internal corner. It should then be theoretically impossible to deposit on the internal corner whilst plating on the external corners should be excessive. Plating is not influenced by the size of the angle, only its shape. Figure A4.2 illustrates this feature for different shaped parts.[57]

Even metal distribution is also determined by factors of throwing power and covering power briefly mentioned below.

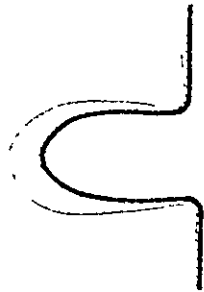
#### Throwing Power

"Throwing power" describes how thick a layer may be deposited, in particular, the difference in thickness of deposit within the peak or trough of a profile. The practical implication of the term arises in that certain plating baths, typically nickel are capable of in-filling micro-pores whilst cyanide baths are not. It is thought that when the dimensions of a recess approach the order of magnitude of the thickness of the cathode, film plating breaks down. Tank geometry and rack design are important in this aspect since widely spaced parts within a tank will not plate as efficiently as parts close together because the field lines become distorted.

#### Covering Power

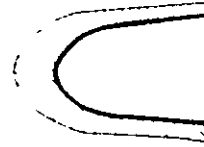
This property of plating baths is concerned with the ability to deposit metal at very low current densities as when plating deep holes or

MAXIMUM 2.2 MILS MINIMUM 0.1 MIL



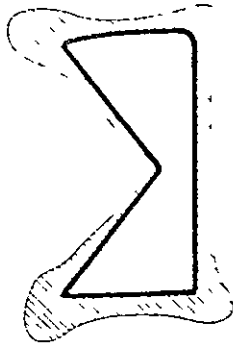
AVERAGE .08 MIL RATIO  $\frac{\text{AVERAGE}}{\text{MINIMUM}} .80$

MAXIMUM 2.7 MILS MINIMUM 0.7 MIL



AVERAGE .14 MILS RATIO  $\frac{\text{AVERAGE}}{\text{MINIMUM}} 2.0$

MAXIMUM 3.8 MILS MINIMUM 0.2 MIL



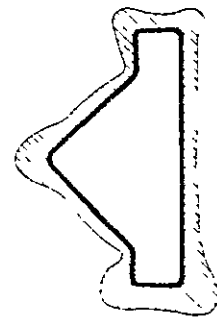
AVERAGE 1.3 MILS RATIO  $\frac{\text{AVERAGE}}{\text{MINIMUM}} 6.5$

MAXIMUM 2.7 MILS

MINIMUM 0.6 MIL

AVERAGE 1.2 MILS

RATIO  $\frac{\text{AVERAGE}}{\text{MINIMUM}} 2.0$



IDEAL RATIO INDICATING  
UNIFORM THICKNESS = 1.0

$$\text{Ratio} = \frac{\text{Av. Thickness}}{\text{Min. Thickness}}$$

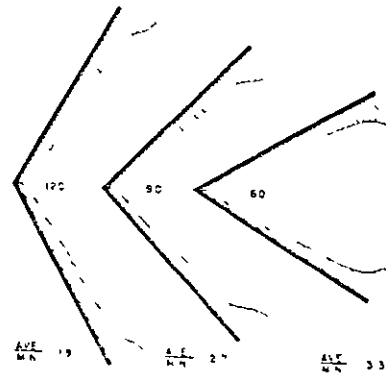


Figure A4.2 Illustrating Uniformity of Plating  
for Different Shaped Parts

cavities. The greater the amount of metal deposited in such areas the better the covering power. Two factors affect this; the bath composition which determines the decomposition potential (the lowest voltage at which metal can be deposited) and the cathode and its surface condition (this affects the voltage in excess of the decomposition voltage necessary to produce a plating). The distribution of current flow to the cathode thus becomes very important.

These ideas illustrate the importance of system design for electroforming. The ideal practical solution is;

- A tank and jigging capable of carrying the current without appreciable voltage drop.

- A pure electrolyte which offers uniform conductivity throughout the solution (uneven temperature or concentration of solution would destroy this).

- The current directly reaching from one electrode to the other without being disturbed by some means (referred to as stray currents).

The experimental tanks used for this work have tried to encompass as many aspects of these points as possible, tanks have been small, solution levels and quality monitored and design of jigging optimised. In this way it has been possible to achieve quality platings with ease and repeatability.

#### Choice of Metals for Electroforming

Nickel need not be the only metal deposited electrolysis but is the most widely used material. A number of alternative choices are considered;

Copper is cheaper than nickel and strong enough for many applications of work, it is deposited quickly and in a reasonably low state of stress. It is not well suited for corrosion resistance parts.

Iron whilst being extremely cheap is deposited in a very high state of stress and brittleness. To overcome this it must be deposited at high temperatures, 195°F, which would be detrimental to the photoresist. The biggest application has been in the production of printing plates.

Silver/gold are deposited in an extremely low state of stress. Their

high cost usually warrants some additional reason for use such as the electrical properties the electroforms then possess

Nickel has the advantage of being extremely well documented in terms of bath formulations, physical properties and characteristics. It can also be deposited over the widest range of parameters. It has been shown to possess suitable wear characteristics and be capable of accurately reproducing the fine detail required from the gratings.

## APPENDIX 5

### Thermoplastics for Embossing

The action of embossing is to transfer detail under heat and pressure into a plastic. The material used for embossing must obviously be capable of reproducing the detail transferred from the metal shim and certain polymers are capable of achieving this. Polymers are composed of many thousands of atoms joined into giant molecules which are composed of repeating units called monomers. The process of linking the monomers to produce long chains is polymerisation, either addition or condensation according to the nature of the bonding process. Figure A5.1 illustrates an addition polymerisation to form polyethylene (polythene) from ethylene gas.

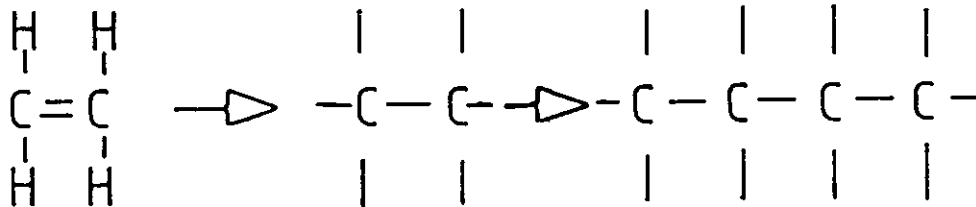


Figure A5.1 Example of Addition Polymerisation

The long chain polymers can be broadly divided into two classes, thermosetting and thermoplastic. The properties of each are determined by the chain structure of the polymer. Thermosetting plastics often

supplied as moulding powders or casting resins, only soften in the initial stage and then harden by further polymerisation to a rigid, brittle material. Heating has the effect of causing chemical change whereby the chain molecules anchor to each other by covalent bonding. Bakelite is an excellent example and scrap material cannot be re-used. Thermoplastic materials can be readily moulded and extruded because of the absence of cross links in their structure and can be repeatedly softened and re-hardened on heating and cooling. The mechanical properties of thermoplastics are; sensitivity to temperature and sunlight and exposure to temperature may cause a thermal degradation, i.e. the breakdown of some bonds. The qualities of thermoplastic films depend upon their manufacture and polymer preparation. The method of fabrication has a marked effect on optical quality and determines surface flatness and parallelism. Polymer chains may be drawn or stretched from a random entanglement into a more orderly arrangement, parallel to the direction of the applied stress. When the chain straightening occurs, the mutual attraction between chains is increased and this determines the tensile strength and elastic modulus of the plastic. This orientation of polymer chains is fundamental to the nature and property of the plastic sheet. Casting of sheet film produces the highest quality material. The polymer used in manufacture should possess a narrow molecular weight distribution and contain no reaction by-products. The properties of scattering and light transmission for clear films are affected by additives used to compound the polymers and these should be known and controlled. The material used for embossing is typically polyvinyl chloride (PVC), polyester or polycarbonate. Properties of plastics may be classified as follows, many of which, such as flatness, transparency, thermal range are important for embossing.

Physical	Mechanical	Chemical	Optical	Thermal
Thickness	Tensile strength	Gas-	Transparency	Range of-
Density	Modulus	perm.	Haze	service-
Flatness	Impact strength		Gloss	temps.
	Coeff. of friction			Shrink heat
				sealing



### Physical States of Polymers

Polymers can exist in three physical states. Consider a polymer at high temperature being cooled:

i) Melts and rubber-like states. At sufficiently high temperatures, some low molecular weight uncross-linked polymers become a viscous liquid allowing amorphous chains to readily flow past each other. Other polymers possess highly flexible, wriggling, mobile molecules and are in a rubber-like state.

ii) Amorphous glassy state. As the temperature is reduced so the flexibility of the molecules reduces because the segmental rotations about the single carbon-carbon bonds are inhibited. Under suitable cooling the polymer will change from the rubber-like state to the amorphous glassy state, which is brittle. The temperature at which this transition occurs is denoted by  $T_g$ , the glass transition temperature.

iii) Partially crystalline state. If the cooling rate is sufficiently low certain molecules can produce crystalline structures whereby molecules can become regular, repeatedly folded structures. Crystallisation causes a dense packing of molecules which increases the inter-molecular forces and produces higher strength, rigidity and brittleness.

The reason these states are important is that during embossing the thermoplastic material will undergo cycles between rapid heating and cooling, the temperatures of which will influence the quality of embossing.

### Comparison of Plastics for Embossing

	PVC	Polyester	Polycarbonate	Cellulose Acetate
Transmittance	Transparent	Transparent	Transparent	Transparent
Crystalline				
Melting Point °C	200	255	230	upto 300
Glass Transition				
Temperature Tg °C	60	69	150	70-180

The table above details some properties of plastics typically used for embossed products. Notice the difference in the values of Tg between the examples. The glass transition is seen as a change in the properties from those of a hard, brittle, glassy substance (at lower temperatures) to those of a soft, flexible material (at higher temperatures). Below the glass transition temperature the polymer chains are rigid and only above this temperature do they gain a degree of freedom allowing stretching under applied stress. Beyond the Tg the polymer becomes firstly tougher and more flexible and then more rubbery in nature. The importance of this should be seen for embossing when plastics are heated and deformed at the same time. Only with correct temperatures and pressures will results be achieved. Three components make up the glass transition process;

a) the instantaneous elastic deformation caused by bond stretching, which is completely recoverable when the stress is removed.

b) the molecular alignment deformation caused by uncoiling, giving a more linear molecular arrangement parallel to the surface and which is retained into the structure when the material is cooled.

c) the non-recoverable viscous flow caused by molecules sliding past each other.

Hence, these three stages can be found in the embossing stage;

- 1) when insufficient heat is applied to impress the surface,
- 11) when correct heat for the correct time is applied and the impress remains in the surface,
- 111) and finally if too much heat is applied the plastic melts.

